PLANKTONIC FORAMINIFERAL DIVERSITY AND ABUNDANCE CHANGES ACROSS CRETACEOUS-PALEOGENE BOUNDARY BEDS IN THE HAYMANA BASIN AND NEW OBSERVATIONS ON THE EXTINCTION HORIZON

A THESIS SUBMITTED TO
THE GRADUATE SCHOOL OF NATURAL AND APPLIED SCIENCES
OF
MIDDLE EAST TECHNICAL UNIVERSITY

BY

ALİ UYGAR KARABEYOĞLU

IN PARTIAL FULFILLMENT OF THE REQUIREMENTS
FOR
THE DEGREE OF MASTER OF SCIENCE
IN
GEOLOGICAL ENGINEERING

AUGUST 2017

Approval of the thesis:

PLANKTONIC FORAMINIFERAL DIVERSITY AND ABUNDANCE CHANGES ACROSS CRETACEOUS-PALEOGENE BOUNDARY BEDS IN THE HAYMANA BASIN AND NEW OBSERVATIONS ON THE EXTINCTION HORIZON

submitted by **ALİ UYGAR KARABEYOĞLU** in partial fulfillment of the requirements for the degree of **Master of Science in Geological Engineering Department, Middle East Technical University** by,

Prof. Dr. Gülbin DURAL _____
Dean, Graduate School of **Natural and Applied Sciences**

Prof. Dr. Erdin BOZKURT _____
Head of Department, **Geological Engineering**

Prof. Dr. Sevinç ÖZKAN ALTINER _____
Supervisor, **Geological Engineering Dept., METU**

Prof. Dr. Demir ALTINER _____
Co-Supervisor, **Geological Engineering Dept., METU**

Examining Committee Members:

Prof. Dr. İsmail Ömer YILMAZ _____
Geological Engineering Dept., METU

Prof. Dr. Sevinç ÖZKAN ALTINER _____
Geological Engineering Dept., METU

Prof. Dr. Cemal TUNOĞLU _____
Geological Engineering Dept., Hacettepe University

Assoc. Prof. Dr. Bilal SARI _____
Geological Engineering Dept., Dokuz Eylül University

Assoc. Prof. Dr. Kaan SAYIT _____
Geological Engineering Dept., METU

Date: 01.08.2017

I hereby declare that all information in this document has been obtained and presented in accordance with academic rules and ethical conduct. I also declare that, as required by these rules and conduct, I have fully cited and referenced all material and results that are not original to this work.

Name, Last Name: Ali Uygar Karabeyoğlu

Signature:

ABSTRACT

PLANKTONIC FORAMINIFERAL DIVERSITY AND ABUNDANCE CHANGES ACROSS CRETACEOUS-PALEOGENE BOUNDARY BEDS IN THE HAYMANA BASIN AND NEW OBSERVATIONS ON THE EXTINCTION HORIZON

KARABEYOĞLU, Ali Uygar

M.Sc., Department of Geological Engineering
Supervisor: Prof. Dr. Sevinç ÖZKAN ALTINER
Co-Supervisor: Prof. Dr. Demir ALTINER

August 2017, 279 pages

Abundance and diversity patterns in planktonic foraminifera are important for paleo-environmental and paleoclimatic interpretations before and after the Cretaceous-Paleogene mass extinction. A 14,53 m-thick section was measured crossing the boundary between the Haymana Formation and the Yeşilyurt Formation in the northern part of the Haymana Basin. In the last 3.75 meters of the Maastrichtian below the K-Pg boundary, a series of quantitative analyses were carried out on planktonic foraminifera found above 63 and 150-micron screen sizes. By using foraminiferal bioevents, biozones were established which are: *Plummerita hantkeninoides* Zone for the uppermost Maastrichtian; P0 and *Parvularugoglobigerina eugubina* zones for the base of the Danian. Additionally, paleobathymetry of the measured section was studied with the help of planktonic-benthic ratios. Calculations indicate approximately 400 m water depth for the depositional environment. Identification of deep water dweller planktonic foraminifers in the studied section, such as *Planoglobulina multicamerata* and *Gublerina cuvillieri* also supports this result.

Quantitative analyses resulted that at the end of Maastrichtian, *Heterohelix* species, which are tolerant to temperature, nutrient, oxygen and salinity fluctuations,

dominated (~40%) the environment while those which are not resilient such as *Globotruncana* species remained low (~10%). On the other hand, *Guembelitria cretacea*, which show opportunistic blooms during environmental crisis and dwell at the surface of the water column, survived from the K-Pg mass extinction. This study, for the first time in Turkey, shows blooms of *Guembelitria cretacea* in the Haymana Basin for the latest Maastrichtian and right after the K-Pg boundary in P0 Zone.

Right after the K-Pg boundary, the first samples of the Danian P0 Zone are characterized by *Thoracosphaera* acme whose diameters are ranging between 10 to 20 microns. In addition to that, another sharp increase was also found in echinoid fecal pellets which peak at 2 cm above the boundary. Previously, the same pellet increment was recognized in the southern part of the basin. These discoveries support the idea of ‘’Echinoid fecal pellet peak as a K-Pg boundary marker’’.

In the Haymana Basin, Maastrichtian mudstones are overlain by marls and calcareous mudstone alternations in the Danian indicating a major change in the depositional regime after the K-Pg boundary. A similar stratigraphy has also been observed in the Mudurnu-Göynük Basin in the K-Pg boundary beds. This similarity in an interval of high chronostratigraphic resolution brings the possibility whether these two basins were connected to each other during end Cretaceous and the beginning of Paleocene.

Keywords: Haymana Basin, Cretaceous-Paleogene boundary, Planktonic foraminifera, Quantitative analysis, *Guembelitria cretacea* bloom, *Thoracosphaera* bloom, Echinoid fecal pellet increase.

ÖZ

HAYMANA HAVZASI'NDA KRETASE-PALEOJEN SINIR TABAKALARINDAKİ PLANKTONİK FORAMİNİFERLERİN BOLLUK VE ÇEŞİTLİLİK DEĞİŞİMLERİ VE KİTLESEL YOKOLUŞ DÜZEYİ ÜZERİNE YENİ GÖZLEMLER

KARABEYOĞLU, Ali Uygar

Yüksek Lisans, Jeoloji Mühendisliği Bölümü

Tez Yöneticisi: Prof. Dr. Sevinç Özkan Altıner

Ortak Tez Yöneticisi: Prof. Dr. Demir Altıner

Ağustos 2017, 279 sayfa

Son büyük kitlesel yok oluş olan Kretase-Paleojen (K-Pg) geçişi öncesi planktonik foraminifer türlerindeki bolluk ve çeşitlilik paleoortamsal ve paleoiklimsel yorumlamalarda son derece önemlidir. Bunun için Haymana Havzası'nın kuzey kesiminde yer alan istifteki Haymana Formasyonu'ndan Yeşilyurt Formasyonu'na geçen 14,53 metrelik kesit ölçülmüş, Paleosen sınırına kadar olan son 3,75 metrelik kısımda ise 63 ve 150 mikronluk eleklerin üzerinde kalan planktonik foraminiferler toplanmış, bunların sayısal bolluk ve çeşitlilik analizleri yapılmıştır. Stratigrafik kesit boyunca belirlenen biyo-olaylara dayanarak Maastrihtiyen'in en üst düzeyi için *Pseudoguembelina hariaensis* zonu*;* Daniyen'in en altı için ise P0 ve *Parvularugoglobigerina eugubina* zonları belirlenmiştir. Ayrıca planktonik-bentik foraminifer birey oranından yola çıkılarak yapılan paleobatimetrik çözümleme çökelme ortamının yaklaşık 400 metrelik bir derinlikte olduğunu ortaya koymuştur. Su kolonunun derin kısmında yaşadığı bilinen *Planoglobulina multicamerata* ve *Gublerina cuvillieri* formlarının bulunması da bu hesaplamayı destekler niteliktedir.

Bu analizler sonucunda Maastrihtiyen sonuna gelindiğinde sıcaklık, besin, oksijen ve tuzluluk değişimlerine dirençli olduğu bilinen *Heterohelix* türlerinin ortamda çok bol

bulunduğu (~%40), bu değişimlere uyum gösteremeyen *Globotruncana* türlerinin bolluk oranlarının çok düşük kaldığı gözlenmiştir (~%10). Bunun yanında, su kolonunun üst kısmında yaşayan ve çevresel kriz koşullarında hızla artış gösteren fırsatçı *Guembelitria cretacea*'nın ise bu kitlesel yok oluş sınırını geçtiği teyit edilmiştir. Yapılan bu çalışma Türkiye'de ilk defa *Guembelitria cretacea* türünün Maastrihtiyen sonunda ve K-Pg sınırından hemen sonra Haymana Havzası'ndaki aşırı bolluğunu ortaya koymaktadır.

K-Pg sınırından hemen sonrasındaki Daniyen P0 zonuna tekabül eden ilk örneklerde çapları 10 ila 20 mikron arasında değişen *Thoracosphaera* formlarının çok büyük orandaki artışı dikkat çekmektedir. Bunun yanında Haymana Havzası'nın güney tarafında yapılan daha önceki çalışmada da tespit edildiği gibi, sınırın 2 cm üzerinde ekinid pelletlerinde ani bir artış kaydedilmiştir. Bu ani artışın dünyadaki Kretase-Paleojen sınırlarının belirlenmesinde yardımcı veri olarak kullanılabileceği görüşü bu çalışmayla beraber daha da önem kazanmıştır.

Kretase sonunda çamurtaşı birimlerinden Paleosen'deki kireçtaşı ve çamurtaşı ardalanmasına ani olarak geçiş Mudurnu-Göynük Havzası'nda da gözlemlenmiştir. Bu stratigrafik benzerlik Haymana Havzası ve Sakarya Havzası'nın Kretase sonundan Paleosen başına kadar olan sürede birbirine bağlı olabileceği olasılığını da akla getirmektedir.

Anahtar Kelimeler: Haymana Havzası, Kretase-Paleojen sınırı, Planktonik foraminifera, Sayısal Analiz, *Guembelitria cretacea* artışı, *Thoracosphaera* artışı, Ekinoid pellet artışı.

to memories of my beloved grandmother Emine Karabeyoğlu and my terrific cat Miu Cappuccino...

ACKNOWLEDGEMENTS

Firstly, I would like to thank to my supervisor Prof. Dr. Sevinç Özkan Altıner for her guidance, continuous support and enthusiasm through each step of the thesis.

I would like to express my gratitude to my co-supervisor Prof. Dr. Demir Altıner for his encouragement and invaluable advises on the thesis progress.

I would like to express my appreciation to Dr. Johan Vellekoop for indication of the thesis area, and his friendship through my stay in Leuven and Utrecht.

I would like to thank specially to Prof. Dr. Robert P. Speijer for his help, advices, and guidance on the thesis topic and sample preparation methods. Without the laboratory practice and microscope analysis that we conducted in KU Leuven, I would not obtain clean fossil specimens from my samples. Also, I would like to thank to Dr. Lineke Woelders for sharing information on benthic foraminifera and for her advices on the thesis topic.

I would like to express my gratitude to Prof. Dr. Jan Smit, Prof. Dr. Gerta Keller, Prof. Dr. Billy P. Glass and Prof. Dr. Christian Koeberl for their help and recommendations on enigmatic spherules that I have recovered from the K-Pg boundary layer.

I am grateful to my dear friend S. Görkem Atasoy for his fellowship, endless support and help at every stage of the thesis. I am indebted to my friends Ezgi Vardar and Gamze Tanık for their support during the field works.

I would like to thank to Tuğrul Bülbül for providing me some rare papers on the Haymana region. It helped me a lot.

I am appreciated to Orhan Karaman for preparing the thin section slides.

I would like to thank to Serkan Yılmaz for capturing Scanning Electron Microscope (SEM) images.

At last but not the least, I would like to thank to my parents Neşenur Karabeyoğlu and Serdar Karabeyoğlu and to my sister Ekinsu Karabeyoğlu for their understanding, patience and endless support.

I would like to thank to my grandfather Ali Karabeyoğlu for his invaluable support and interest on the thesis work.

I am indebted to my grandmother Emine Karabeyoğlu, who passed away May 2017, for her prays, good wishes and support at every stage of my life.

I would like to thank to my cats Miu Cappuccino, who passed away December 2016, and Topik for being outstanding buddies.

Without my family, this thesis would not have been accomplished.

TABLE OF CONTENTS

LIST OF TABLES

TABLES

LIST OF FIGURES

FIGURES

CHAPTER 1

INTRODUCTION

1.1 PURPOSE AND SCOPE

The Cretaceous-Paleogene (K-Pg) boundary corresponds to one of the most devastating mass extinction event in the Earth history (Raup and Sepkoski 1982). During this crisis, planktonic foraminiferal assemblages altered drastically. All large, ornamented, keeled forms, such as globotruncanids, rugoglobigerinids and racemiguembelinids underwent extinction, while small, unornamented forms, such as heterohelicids, guembelitrids, and hedbergellids survived and gave way to evolution of new Paleocene assemblages.

This thesis aims to scrutinize planktonic foraminiferal changes across the late Maastrichtian-early Danian time interval in the Haymana Basin, Central Anatolia/Turkey. For this reason, a variety of studies have been carried out:

- Multiple times of preliminary field works, samplings, and sample washings to decide the study area,
- Two major field campaigns for sample collection,
- Auxiliary field works for additional samplings,
- Sample preparation in laboratory (i.e. sample crushing and washings),
- Detailed planktonic foraminiferal taxonomy,
- Planktonic foraminifera biozonation,
- Comprehensive quantitative micropaleontology in both 63-150 μm and >150 μm size fractions (i.e. foraminifera counting),
- Delineation of the Cretaceous-Paleogene (K-Pg) boundary and its characteristic features,

- Paleobathymetric investigation of the depositional area via P/B ratio,
- Microfacies analysis by means of thin-sections

Overall, this study is the first comprehensive attempt to delineate and demonstrate lithologic features of the K-Pg boundary and planktonic foraminiferal associations across the late Maastrichtian and early Danian time interval focusing on populations from 63-150 μm and >150 μm size fractions. In consequence of these works, new findings were unveiled for the first time in Turkey. Our findings were compared also with other well-known K-Pg boundary localities in the world (see Discussion and Conclusion Chapter).

1.2 GEOGRAPHICAL SETTING

The study area is located about 60 km southwest of Ankara city and 5 km northeast of Haymana town (Figs. 1 and 2). Coordinates of the studied section are 39°27'53N and 32°31'41E. The measured section is approximately 100 m away from the Haymana-Gölbaşı road (Fig. 3).

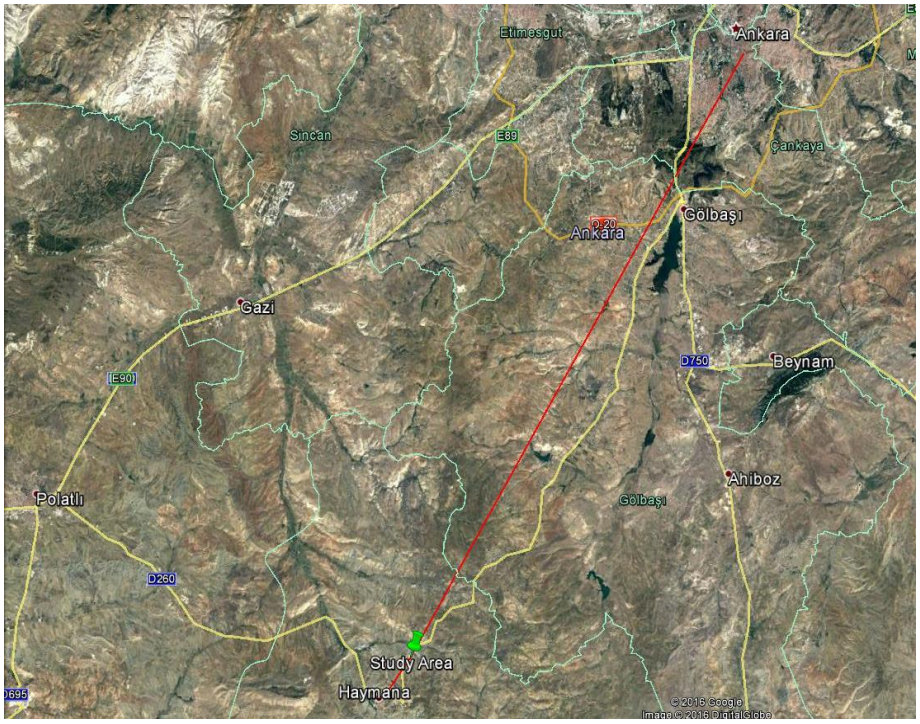

Figure 1. Location of the study area (indicated by green mark. *Image taken from Google Earth*)

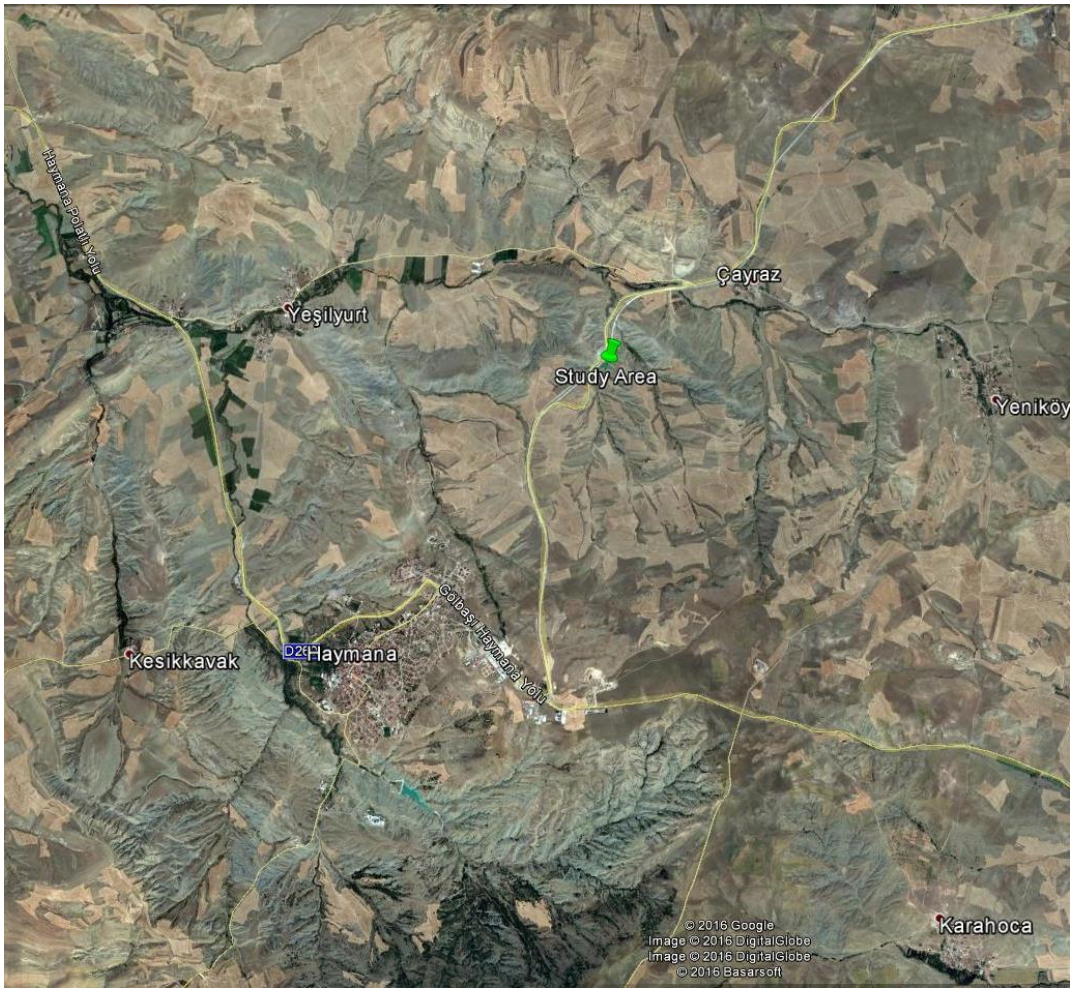

Figure 2. Close-up view of the study area (indicated by green mark. *Image taken from Google Earth*)

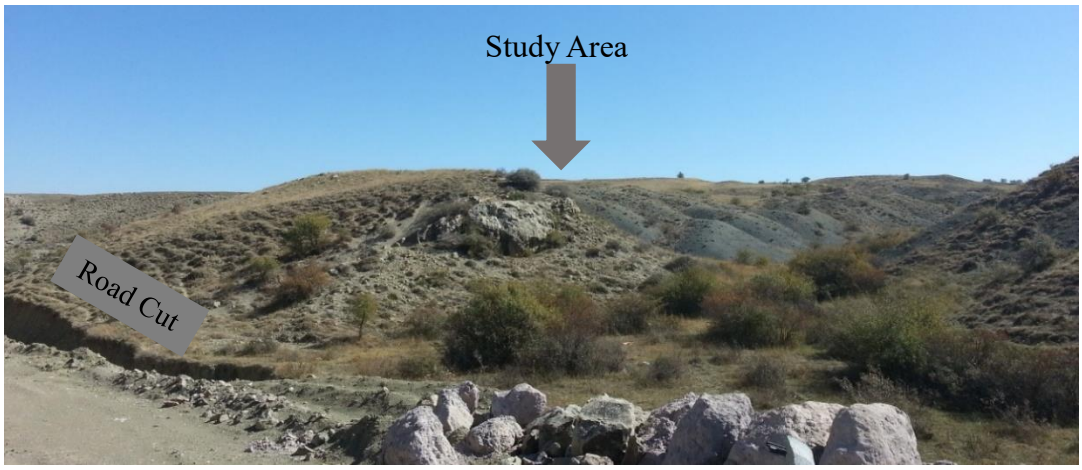

Figure 3. The study area is located approximately 100 m away from the Haymana-Polatlı road.

1.3 METHODS OF STUDY

Samples were collected by two major and one auxiliary field campaigns. For each sampling process, a trench was dug in order to collect rather fresh unaltered rocks and surfaces of the rock samples were carefully cleaned to prevent undesired contamination. During the sampling process, rock lithologies were identified, sample levels were recorded and logged. The study area and the measured sections were photographed as well.

Two sections were measured in the study area: UH and UKHB sections. The UH section is 9.70 m in total. It covers uppermost 9.55 m of the Maastrichtian, the K-Pg boundary, and first 15 cm of the Danian. Sampling interval is 20 cm in stratigraphically lower parts and it narrows into 10 cm and 5 cm as getting closer the K-Pg boundary. Additional samples, such as 2 cm before and after the K-Pg boundary, sampling of the K-Pg boundary itself and samples from important points were collected during the auxiliary field campaign. In total 51 samples, labeled from UH-1 to UH-51, were gathered from the main field campaign; and 10 samples, labeled from E-2 to E+50, collected from the auxiliary field campaign through the UH section.

On the other hand, the UKHB section is 5.14 m in total. It starts from 5 cm below the K-Pg boundary, and ranges 5.09 m through the Danian. Sampling interval is 5 cm above and below the K-Pg boundary and widens (10 to 20 cm) through the up-section in Danian. In total 38 samples, labeled from UKHB-1 to UKHB-38, were gathered from UKHB section.

These two measured sections were calibrated via the position of the K-Pg boundary and paleontological associations of key stratigraphic levels.

The quantitative work was done within the UH section corresponding last 3.75 m of the Maastrichtian and first 15 cm of the Danian. The remaining samples from both UH and UKHB sections were examined for micropaleontological and microfacies analyses.

The quantitative study was carried out in two size fractions: 63-150 μm and >150 μm. For each sample, a representative split of an average of 380 and 394 planktonic

foraminifera individuals were identified, counted and mounted on the cardboards from 63-150 μm and >150 μm size fractions, respectively.

Additionally, for planktonic-benthic ratio (P/B) and eventually for paleobathymetric estimation, benthic foraminifera were also picked and counted from the same splits of the >150 μm size fraction.

Taxonomic identifications were carried out via Nikon SMZ-645 optical microscope in METU micropaleontology laboratory and Scanning Electron Microscope (SEM) photographs were taken and Energy Dispersive X-ray (EDX/EDS) analysis were carried out at METU Metallurgical and Materials Engineering Department. For microfacies analyses, more than 90 thin-sections were prepared (covering all samples from UH and UKHB sections) in METU Geological Engineering Department thin-section preparation laboratory.

1.3.1 Sample Preparation

In the study area, mudstones of late Maastrichtian change to marl and calcareous mudstone alternations in Danian. All rock units are highly friable especially mudstones can easily be broken by hand which eased the rock crushing process.

A single method was used for both rock types in the study area. First, rock samples were put into a transparent nylon bag and crushed with a help of hammer until they become about 2-5 mm^3 in size. Breaking the rocks until this size was also stated in work of Lirer (2000). A couple of clean A4 papers were used for padding between surface and the rock samples. Padding was helpful to recover small samples escaped from ruptured bag during the crushing. It is important to note that one should avoid powdering the rock samples. Excessive crushing not only breaks delicate foraminifers but also hampers general fossil identification. Eventually, this may cause difficulties during taxonomic identification and biozonation. In our study, crushing rock samples less than 1 cm^3 (approximately 2-5 mm^3) created good results and made disintegration process easier when they react with a solvent. This was also mentioned in Lirer (2000) who advised small rock fragments for better results.

After the crushing process, rock fragments were dried in an oven at 50°C for overnight to obtain completely moisture-free samples. After that, 100 gr of sample was treated with 200 ml of 50% diluted hydrogen peroxide (H_2O_2) for 20 minutes. Then, samples were washed under tap water through 825, 150, 63, 38 μm sieves. 825 μm screen, in particularly, was used to eliminate big chunks.

It is important to note that hand-rubbing during wet sieving is highly recommended which led good-clean results in our washings. If specimens are durable enough (it has to be checked in advance), rubbing removes the clay coating on fossils and improves the identification. After we have checked the durability of fossils for rubbing, we have used it and obtained very clean specimens.

After the wet sieving and rubbing, fossils were collected from sieves to petri dishes by means of distilled water and finally oven-dried at 50°C. In this process, it is critical to use distilled water instead of tap water since if tap water is used, small calcium ions start to cover surfaces of fossils as water evaporates in the oven and hence inhibit fossil recognition.

After collection of specimens, each sieve was soaked into blue ink and washed through water jet. Since we obtained clean specimens, no ultrasonic treatment or any further process were needed.

Preservation obtained from mudstones and calcareous mudstones was generally moderate to good. Yet, there are some recrystallization or dissolution (especially on smaller specimens from 63-150 μm fraction) exist.

On the other hand, preservation from marls was moderate to poor. Specimens from some intervals were effected from recrystallization and strong dissolution which hampered fossil recognition. Dissolution was particularly observed on first Danian samples corresponding P0 and Pα biozones which characterized by broken or foliated test walls. Additionally, pyritization of fossils was observed which may have occurred from subaerial alteration (Robert P. Speijer personal commun.) or low O_2 conditions through taphonomy (Keller 2002).

1.4 PREVIOUS WORKS

1.4.1 Previous works on mass extinctions and the K-Pg boundary

The mass extinction concept was first articulated by French anatomist Georges Cuvier (1769-1832) in early 1800s after examining extraordinary presence of fossils of horse-like and dog-like creatures with seashells in the Paris Basin. Cuvier along with his associate Alexander Brongniart (1770-1847), interpreted this juxtaposition as an unprecedented environmental catastrophe had occurred in Earth's distant past. For him, this phenomenon affected both terrestrial and shallow marine environments, dislocated the fauna and deposited them together away from their natural habitats. He concluded that, these ''revolutionary extinctions'' suddenly annihilated whole groups of organisms such that only a few survivors left (MacLeod 2014).

On the contrary, Charles Darwin (1809-1882) considered the extinction phenomenon as a gradual process caused by natural selection and by-product of struggle for existence. He opposed the idea that large numbers of extinctions induced by natural catastrophes (MacLeod 2014).

The first biodiversity diagram was published by John Phillips (1800-1847) in 1860. In his chart, Phillips demonstrated: ascending pattern of life divided by Paleozoic, Mesozoic and Cenozoic; and biodiversity drops whose perpetrators are extinction events. By studying data mainly collected from United Kingdom sections, he could delineate quite accurate portray of the Phanerozoic biodiversity and clearly revealed extinctions in Paleozoic and Mesozoic Era. After Phillips, extinction studies remained unpopular during late 1800s and early 1900s because of Darwin's opinions on extinction as being natural process rather than catastrophic (MacLeod 2014).

In 1963, Norman Newell created biodiversity and percent-extinction-intensity charts in stage-level time intervals. He recognized that total number of families increased over geological time and at certain time intervals, there are much higher rates of disappearances than appearances corresponding extinction events. David Raup and Jack Sepkoski in 1982, updated the Norman Newell's Phanerozoic extinction intensity curves for family and genus levels. By their investigations, there are five major extinction events exist from Cambrian to Recent which are: end-Ordovician, end-

Devonian, end-Permian, end-Triassic and end-Cretaceous. Recently, Phanerozoic biodiversity curve was revised in genus-level by Alroy et al. (2008).

The Cretaceous-Paleogene (K-Pg, formerly K-T) mass extinction is arguably the most contentious event among the big five major catastrophes. It marks the boundary of the Mesozoic and Cenozoic eras corresponding 66 million years before present. Several animal groups annihilated across the K-Pg boundary, such as total demise of nonavian dinosaurs, marine and flying reptiles, ammonites and rudists coupled with large number of extinction within planktonic foraminifera, calcareous nannofossils and land plants; and substantial alteration in assemblages of benthic foraminifera (Schulte et al. 2010 and references therein).

Impact-induced extinction theory was first proposed by Alvarez et al. (1980) after observing Iridium (Ir) and other platinum group elements (PGEs) anomaly at the Cretaceous-Paleogene boundary which corresponds to planktonic foraminifera extinction level both in Italy, Denmark and New Zealand sections. They proposed that an asteroid with a diameter of 10 ± 4 km hit the Earth produced an impact crater and ejected dust-sized material reached the stratosphere and spread across the globe. These dust particles would have prevented sunlight from reaching the surface for several years before they get settled to the Earth. The loss of sunlight shut down photosynthesis which in turn gave way to food chain collapse and eventually extinctions happened.

Shock metamorphism is a credible evidence for detection of an impact site (Kring 2007). Discovery of impact melt spherules and shocked minerals in Haiti by Hildebrand et al. (1990) and later in the Yucatan-6 core by Kring et al. (1991) indicated Chicxulub structure as a prominent candidate for the shocked quartz found in the K-Pg sediments (Kring 2007). Further discovery of ~180 km diameter Chicxulub crater on the Yucatan peninsula (Mexico) by Hildebrand et al. (1991) indicated a product of impact large enough to cause globally distributed Ir and shocked quartz (Kring 2007).

Link between the Chicxulub crater and the K-Pg boundary was found from a variety of features. Analyses of impact melt spherules and Chicxulub melt rock provided similar ages 65.01 ± 0.08 Ma and 64.98 Ma, respectively. Additionally, K-Pg

boundary ejecta deposits become thinner and shocked quartz get sparse farther from the Chicxulub site. In consequence of these findings, the Chicxulub impact has been considered as the cause of the K-Pg mass extinction (Kring 2007).

Several environmental effects of the Chicxulub impact were thoroughly summarized by Kring (2007). Right after the impact, shock waves and air blasts, exceeding velocity of 1000 km/h, would have been radiated and swept across the Gulf of Mexico. These effects may have happened very rapid and intense which would have affected an area of approximately 1500 km radius (Fig. 4). Also, they would have devastated forests and coastlines before tsunamis hit them.

Additionally, temperatures exceeding 10.000 °C would have been produced in core of the plume rising from the crater which may have been hot enough to ignite fires within distances of 1500 to 4000 km (Fig. 4). This thermal pulse would have been lasted 5 to 10 minutes. As impact ejecta fell through the atmosphere it would have exacerbated the heating for 3 to 4 days (Kring 2007 and references therein).

Tsunamis are another element of the devastation. About 100 to 300 meters-high tsunami waves may have arrived 5 to 10 hours after the collision and engulfed whole nearby coastlines of the Gulf of Mexico and radiated across proto-Caribbean and Atlantic basins. These waves may have been invaded more than 300 km inland. In fact, multiple penetrations of waves may have occurred before the finest Ir bearing airborne constituent was settled. Additionally, density currents and seismically-induced slumping of coastal deposits took place in consequence of cataclysmic earthquakes larger than 11 magnitude (Kring 2007 and references therein, Schulte et al. 2010 and references therein).

Short-term period of heating right after the impact substituted by surface cooling resulted from dusts, aerosols and soot (Kring 2007). Especially, about 19°C to 26°C pre-impact Cretaceous temperature was dropped by 9°C (Brugger et al. 2016) to 10°C (Vellekoop et al. 2016) and a series of cooling pulses would have repeated during first 1000 years after the impact around the Tethyan Realm (Vellekoop et al. 2015). Likewise, Galeotti et al. (2004) suggest millennial-scale cooling after the collision which is characterized by expansion of Boreal cyst-forming dinoflagellates and benthic foraminifera into western Tethys (e.g. Tunisia).

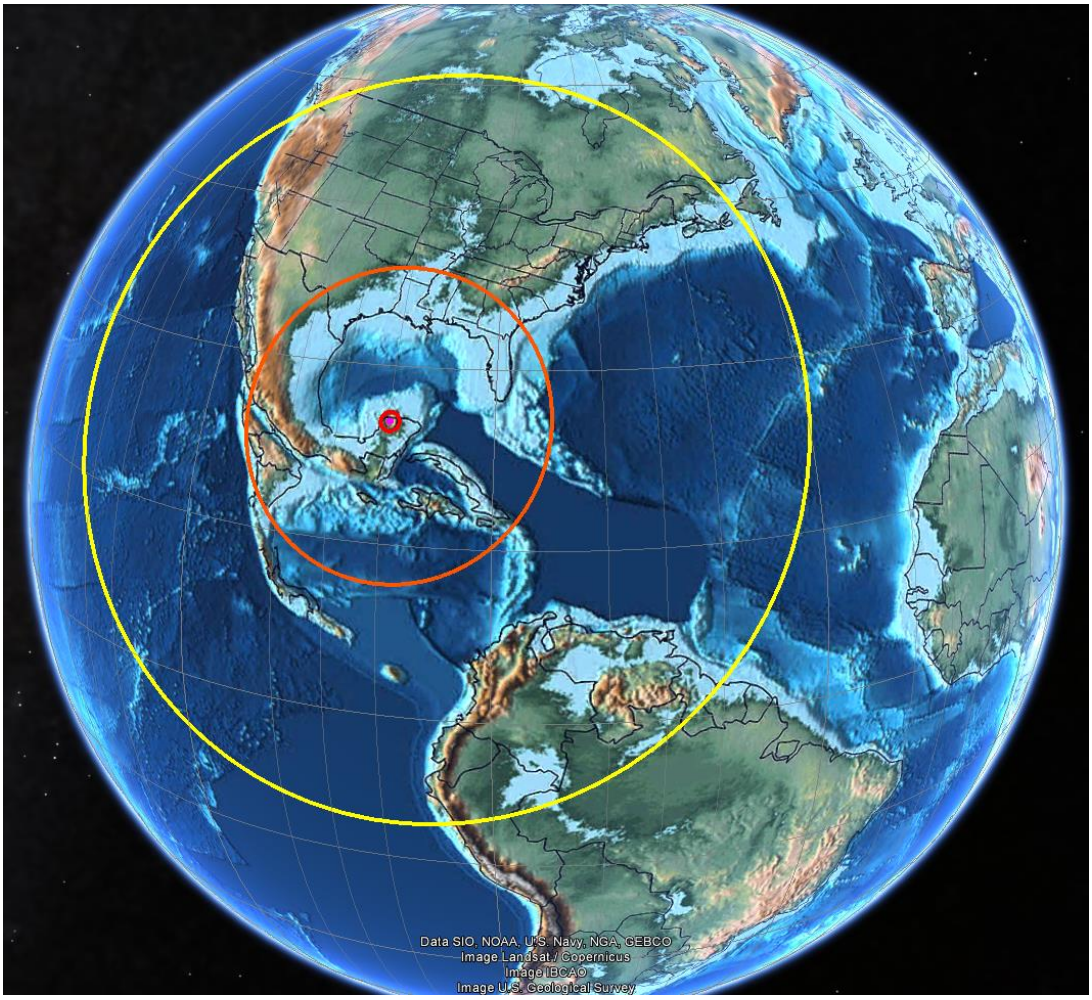

Figure 4. Paleogeography of the Earth at the time of K-Pg boundary and regional-scale effects of the Chicxulub impact. Chicxulub asteroid (innermost purple) apx. 10 km wide, Chicxulub crater created by the impact (small red circle) apx. 180 km in diameter, shock waves might have affected an area of 1500 km (middle orange circle), and fires might have reached distances from 1500 to 4000 km (outer yellow circle). Paleomap created from C.R. Scotese PALEOMAP Project 2013 via Google Earth.

On global scale, effects of the Chicxulub impact differ. By colliding with carbonate and sulfur rich target rocks (e.g. anhydrite), sulfur vapor would have been inserted to the stratosphere (15-50 km above the ground) and eventually turned out sulfuric acid rains (Kring 2007 and references therein). About 100 to 500 Gt of sulfur injected to the atmosphere within minutes after the impact (Schulte et al. 2010 and references therein). Sulfur eventually would have transformed to sunlight absorbing sulfur aerosols capable to cool Earth's surface for years to decades. On the other hand, shock-heated atmosphere may have produced nitric acid rains (Kring 2007 and references therein).

Detection of fusinites, pyrolitic polycyclic aromatic hydrocarbons, carbonized plant debris and charcoals in various K-Pg boundary localities indicate impact-generated wildfires. Although soot from post-impact wildfires is found globally, because of being airborne component, it is poor indicator of where fires were ignited. Therefore, the distribution of those fires is unclear. The globally distributed ejecta may have caused widespread atmospheric heating such that ground temperatures may have risen 100's of °C and resulted spontaneous fires. Yet, if the mass and speed of ejecta was low, then fires may have ignited in the vicinity of the impact (Kring 2007 and references therein).

Other components resulted from the impact event are injection of dusts and aerosols in the atmosphere. Models demonstrated that dust, sulphate aerosols and post-wildfire soot would have blocked the sunlight to reach the surface and the shut down the photosynthesis. Settlement time of these particles from atmosphere is variable due to differential dust-size distribution. Particles about 250 μm in diameter would have precipitated within hours to days. If there are large amounts of nanoparticles, they may have suspended in the atmosphere for months. Soot, on the other hand, is another component. If it was injected to stratosphere, it would take long times to settle. Whereas, if it was able to rise to troposphere (0-15 km above the ground), it would have precipitated quickly by rain (Kring 2007 and references therein).

Ozone destruction is another environmental consequence of the Chicxulub impact. Cl and Br, which are capable to destroy ozone layer, may have been produced from the vaporized projectile, target rocks, and biomass burning. In order of 5 times more Cl

to destroy today's ozone layer coupled with Br, N_2 and other reactants was injected into the stratosphere. Consequences of ozone destruction may have spanned for several years, yet the severity of its effect on surface is unclear. Finally, after dusts, aerosols and soot settled to the ground (which caused period of cooling), greenhouse warming occurred as a function of significant amount of H_2O, CO_2, and CH_4 injected into the atmosphere from target rocks and the projectile (e.g. carbonate target rocks would have vaporized and emitted CO_2) (Kring 2007 and references therein).

Overall, regional and short-term effects of the Chicxulub impact can be summarized as: shock waves and air blast, high-temperatures, seismic effects, shelf collapse around the Yucatan platform and tsunamis around the Gulf of Mexico and nearby areas. On the other hand, global longer-term effects can be categorized as: nitric acid rain, deposition of sulphate aerosols and eventually sulfuric acid rain, dust, wildfires and soot (preventing sunlight to reach surface), destruction of the ozone layer, enhanced erosion and greenhouse warming (Fig. 5). Atmospheric heating generated by Chicxulub impact was followed by a cooling period then substituted by again a warming period (Kring 2007 and references therein).

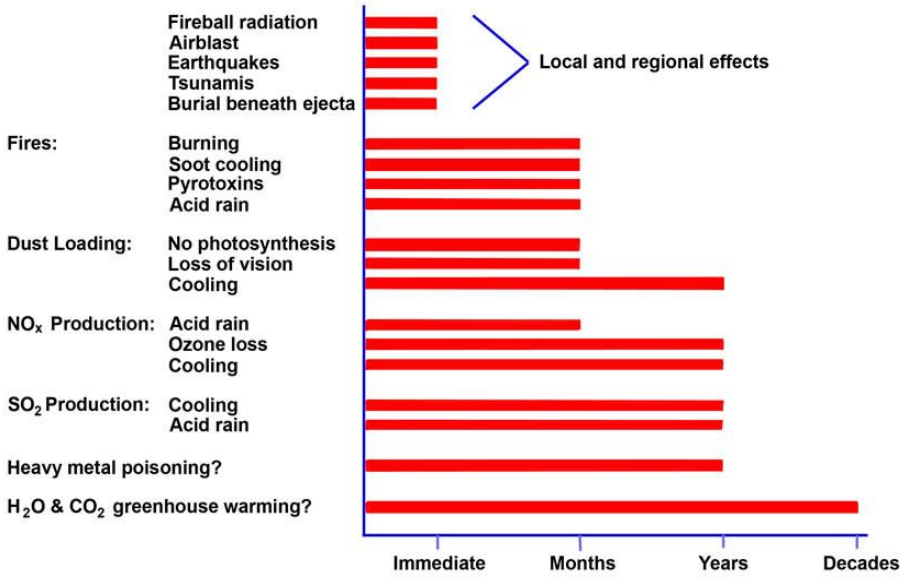

Figure 5. Environmental consequences of the Chicxulub impact with respect to time periods. The local and regional effects occurred immediately after the impact, whereas global effects continued for a long period of time (Kring 2000).

To calibrate time-relation between the Chicxulub impact and the K-Pg boundary, Renne et al. (2013) examined samples of tektites formed by the Chicxulub impact and bentonites (altered volcanic ashes) associated with the K-Pg boundary. Their $^{40}Ar/^{39}Ar$ age dating revealed that there is synchrony between the Chicxulub impact and the K-Pg boundary (and associated mass extinctions) both happened within 32,000 years. They found out that the Chicxulub impact corresponds to the K-Pg boundary.

The K-Pg boundary event deposits are categorized into four groups (Fig. 6) (Schulte et al. 2010 and references therein):

a) Very proximal settings: comprises locations up to 500 km from the Chicxulub impact such as Central American regions surrounding the crater. These deposits are quite thick. Cores close to the rim of the impact crater show more than 100 m-thick impact breccia and 1 m to more than 80 m-thick ejecta rich deposits.

b) Proximal settings: These locations are 500 to 1000 km away from the Chicxulub impact situated around NW Gulf of Mexico. The deposits include cm to m-thick spherule rich ejecta and ‘’event’’ deposits, such as tsunamis and gravity flows.

c) Intermediate settings: They are about 1000 to 5000 km away from the crater. The boundary deposits consist of 2 to 10 cm thick spherule layer covered by 2 to 5 mm thick layer abundant in Platinum Group Elements (PGE), shocked minerals, granitic clasts and Ni-rich spinels.

d) Distal settings: These locations are more than 5000 km away from the impact site. Its deposits are characterized by reddish 2 to 5 mm-thick clay layer usually rich in impact ejecta material.

The Cretaceous/Paleogene (K-Pg) boundary working group voted to define Global Stratotype Section Point (GSSP) of the Danian Stage is at mm-thick reddish layer base of the boundary clay near El Kef, Tunisia. That is, all sediments generated by the impact belong to the Danian. This mm-thick reddish ferruginous layer (both marks and overlies the K-Pg boundary) composed of reddish hematitic and goethitic laminae and coincides with sudden catastrophic mass extinction event. It contains Ir anomaly, a peak of Ni-rich spinels, less than 1% $CaCO_3$, a maximum in Total Organic Carbon

(TOC), and clear ^{18}O and ^{13}C excursions. Besides, the K-Pg boundary is exactly delineated by the horizon corresponding the moment of the meteorite impact (Molina et al. 2006).

Apart from primary boundary marker of mm-thick reddish layer and boundary clay, International Commission of Stratigraphy (ICS) designates: first appearance of Paleogene planktonic foraminifera at the base or within a few cm of the boundary clay, and negative ^{13}C shift found in marine calcareous plankton through low to middle latitudes as ‘’secondary markers’’. The commission also suggested Ir anomaly associated with a major extinction horizon in dinosaurs, ammonites and foraminifers as ‘’correlation events’’.

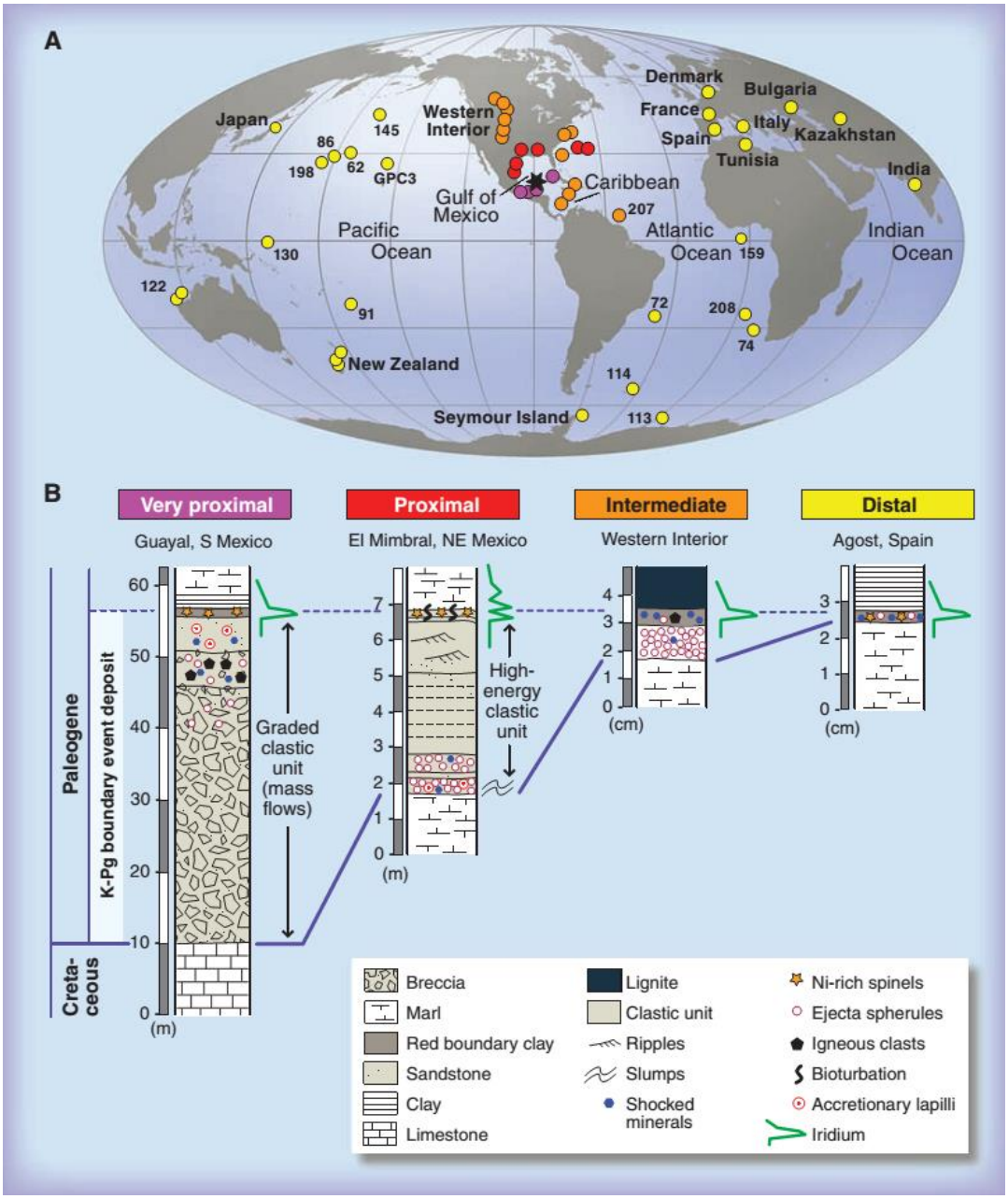

Figure 6. A) Global locations of various K-Pg boundary locations. Black star represents the Chicxulub impact location. Numbers indicates Deep Sea Drilling Project (DSDP) and ODP drill sites leg numbers. B) Four distinct K-Pg boundary event deposits exists with respect to their distance from the Chicxulub crater. Magenta: Very proximal areas (up to 500 km from the crater), Red: Proximal areas (up to 1000 km), Orange: Intermediate areas (1000 to 5000 km), Yellow: Distal areas (>5000 km) (Schulte et al. 2010).

On the contrary, another theory claims that the Chicxulub impact played no role in the K-Pg boundary mass extinction such that the impact predates the boundary by 80-100 k.y., according to data from NE Mexico, the Chicxulub crater, and Brazos River (Texas) (Keller 2014, Keller et al. 2016 and references therein).

The Chicxulub impact coincided with the major late Maastrichtian rapid warming period of 8°C on the land and 4°C in the oceans caused by Deccan volcanism. The impact might have contributed the warming, intensified volcanic eruptions and exacerbated catastrophic conditions. The main Deccan Phase 2 eruption accounts for 80% of total Deccan volume begins at 66.250 Ma and corresponds to base of C29r magnetochron and CF2-1 planktonic foraminiferal biozones. This eruption phase created rapid warming and high environmental stress eventually led to the K-Pg mass extinction. On the other hand, the final phase 3 eruption delayed ecosystem recovery for at least 500 k.y. (Keller 2014, Keller et al. 2016) (Fig. 7).

Total SO_2 and CO_2 output from the Deccan Traps may have been order of 20-200 times larger than that of the Chicxulub impact (Courtillot and Fluteau 2014). This large-scale volcanism has deleterious effect on seawater carbonate chemistry. Moreover, stepwise injection of CO_2 in the oceans results in ocean acidification which leads calcification crisis for the carbonate secreting planktons and therefore food chain collapse (Keller 2014 and references therein).

Keller (2014 and references therein) claimed that: bio-events of: near total and relatively abrupt mass extinction of planktonic foraminifera and almost immediately evolution of new species from long term K-Pg boundary survivor *Guembelitria cretacea* are the most reliable worldwide K-Pg boundary defining criteria. All other boundary markers, such as Ir anomaly, red layer, clay layer, ^{13}C excursion, and impact glass spherules, are useful but not unique signals because of reworking and redeposition. In the absence of unique biomarkers, these impact signals would not describe the K-Pg boundary. She followed standard K-Pg boundary defining criteria as: ‘’mass extinction and evolution of first Danian species’’ while identifying K-Pg boundary in the Deccan Traps in central and southeastern India.

Additionally, Keller (2014) asserted that impact ejecta can be easily eroded, transported, and redeposited after the primary deposition. It may be found stratigraphically below, at or above the K-Pg boundary. Iridium anomalies, on other hand, can be remobilized and concentrated at redox layers. Ir concentrations smaller than 1-1.5 ppb are undependable impact markers. Out of 345 worldwide K-Pg boundary locations, only 85 have Ir enrichments and only Denmark, Tunisia (El Kef and Elles), Meghalaya (India), and New Zealand sections have large Ir anomalies. These larger Ir anomalies concentrated at redox boundaries (red clay layers) and reveal substantial Ir influx from nearby marine and continental sites. Moreover, she claimed that no Ir anomaly has ever been observed in Chicxulub impact ejecta.

Recently, Renne et al. (2015) suggested that strong seismic activities of the Chicxulub impact may have triggered the eruptional phase of Deccan volcanism within ~50 ky years which would have contributed extinctions. This close coincidence of the impact and accelerated volcanism complicates to decipher environmental perturbations related to each mechanism. The K-Pg boundary extinctions might have occurred superimposed effects of both phenomena. Ongoing eruptions for ~500 ky after the impact would have suppressed post-extinction ecological recovery in marine ecosystems.

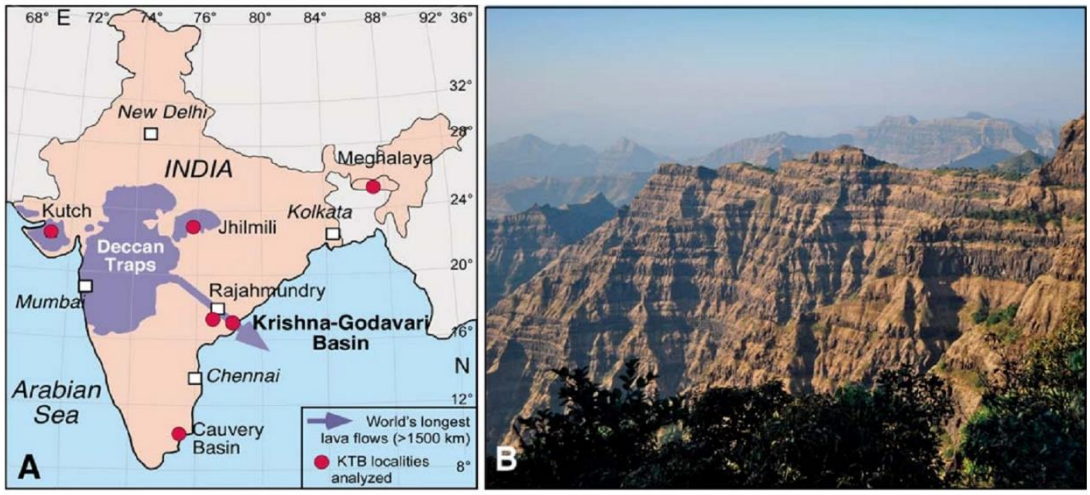

Figure 7. A) Location and distribution of the Deccan Traps and K-Pg boundary localities. B) Field appearance of the Deccan Traps in Mahabaleshwar mountains (Keller 2014).

1.4.2 Previous works on K-Pg boundary in Turkey

In Turkey, until now only a few studies have been carried out directly on the K-Pg boundary deposits, its lithological and paleontological aspects and correlation with other well-known K-Pg boundary localities. Previous studies generally demonstrate overall planktonic foraminiferal and/or calcareous nanoplankton biozonation of Maastrichtian to Danian sequences by identifying index fossils (e.g. Toker 1977, Dizer and Meriç 1981, Özkan and Altıner 1987, Özkan Altıner and Özcan 1999, Özer et al. 2001, Kaya Özer and Toker 2012, Sarı 2013, Açıkalın et al. 2015, Esmeray-Senlet et al. 2015).

Regarding to quantitative micropaleontology, only two studies have been carried out thus far by Güray (2006) and Kaya-Özer (2017). This is possibly because of very high labor intensity of quantitative work. This present study is one of the first studies in Turkey which shows clear representation of the boundary deposits (distal location >5000 km) and represents the first detailed quantitative analyses of planktonic foraminifera for both 63-150 μm and >150 μm size fractions across the Cretaceous-Paleogene boundary in the Haymana Basin.

Previous works crossing K-Pg boundary deposits were summarized in Table 1 and the boundary localities were demonstrated in Figure 8.

Table 1. Previous works crossing the K-Pg boundary deposits, the study areas and scope of the

Purpose of the Study	Region	Method/Focus of Study
Toker (1977, 1980)	Haymana basin, Ankara	Nannoplankton and planktonic foraminifera biostratigraphy
Dizer and Meriç (1981)	(Eğerce) Bursa, (Medetli, Osmaneli) Bilecik, (Düzce, Akçakoca, Göynük) Bolu, (Alaplı, Tefen, Devrek, Bartın, Kozcağız, Kokaksu, Eflani) Zonguldak, (Taşköprü, Devrekani) Kastamonu, (Gebze) Kocaeli	Planktonic, benthic foraminifera
Özkan (1985)	Gercüş, Batman	Planktonic foraminifera
Sirel et al (1986)	Haymana basin, Ankara	Larger benthic foraminifera
Meriç and Şengüler (1986)	Göynük, Bolu	Planktonic foraminifera, nannoplankton
Meriç et al. (1987)	Adıyaman	Sedimentation and biostratigraphy, foraminifera, ostracoda, nannofossil
Özkan and Altıner (1987)	Gercüş, Batman	Planktonic foraminifera
Tansel (1989)	Ağva, İstanbul	Planktonic foraminifera
Erdoğan (1990a)	Karaburun, Balıklıova, İzmir	Stratigraphy, paleontology
Bozkaya and Yalçın (1991a,b; 1992)	Hekimhan region, Malatya	Mineralogy and geochemistry
İnan and Temiz (1992)	Erencik Section, Niksar, Tokat	Larger benthic foraminifera
Yalçın and İnan (1992a, b)	Tecer Section, Tecer, Sivas	Benthic foraminifera, mineralogy and geochemistry
Görmüş and Kahraman (1992)	Çünür region, Isparta	Planktonic and larger benthic foraminifera
Toker et al. (1993)	Northern part of Akseki region, Antalya	Stratigraphy, paleontology, microfacies analysis
İnan (1995)	Kuzulu Section, Koyulhisar, Sivas	Benthic foraminifera
Yıldız and Toker (1995)	Gürün region, Sivas	Planktonic foraminifera and nannoplankton
Yalçın and Bozkaya (1996)	Hekimhan Basin, Malatya	Mineralogy and geochemistry
Özcan and Özkan-Altıner (1997)	Haymana Basin, Ankara	Planktonic foraminifera, Larger benthic and orbitoidal foraminifera
Kaya (1997)	Niksar, Tokat	Planktonic and larger benthic foraminifera
Sirel (1998)	Haymana basin, Ankara	Larger benthic foraminifera
Meriç and İnan (1998)	Gölköy Section, Gölköy, Ordu	Benthic foraminifera
Özkan-Altıner and Özcan (1999)	Cide, Çaycuma, Hanönü, Yenikonak, and Haymana regions	Planktonic foraminifera biostratigraphy calibration with benthic foraminifera
İnan et al. (1999)	Eastern Pontides, SE Black Sea	Larger benthic foraminifera
Özer et al. (2001)	Menderes Massif	Planktonic foraminifera, nannoplankton, rudists
Arawaka et al. (2003)	Medetli, Gölpazarı, Bilecik	Element profiles and Ir concentration
Yıldız and Gürel (2005)	Ordu, Yavuzlu and Uzunisa areas, NE Turkey	Paleontology, diagenetic and facies characteristics
Inan et al. (2005)	Eastern Pontides, NE Turkey	Microfacies, benthic foraminifera
Güray (2006)	Kokaksu region, Bartın	Planktonic foraminifera
Bayhan (2007)	Kalecik region, Ankara	Clay mineralogy
Kaya-Özer and Toker (2009)	Bartın	Planktonic foraminifera biostratigraphy
Özcan et al. (2012)	Black Sea-Bursa transect NW Turkey	Stratigraphy, Larger benthic foraminifera, planktonic foraminifera
Kaya-Özer and Toker (2012)	Bartın province	Nannofossil biostratigraphy
Sarı (2013)	Bornova Flysch Zone, İzmir	Planktonic foraminifera
Esmeray-Senlet et al. (2015)	Haymana Basin, Ankara	Planktonic foraminifera, Microfacies, Sequence Stratigraphy
Açıkalın et al. (2015)	Okçular and Göynük sections, Mudurnu-Göynük basin, Bolu	Ir and PGE's, bulk carbon isotopes, nannofossils, planktonic foraminifera, dinocysts
Solak et al. (2015)	Spil Mountain, Manisa	Micropaleontology and microfacies
Kaya-Özer and Cakir (2015)	İzmit Province, Kocaeli Peninsula	Planktonic foraminifera
Ayyıldız et al. (2015)	Hekimhan Basin, Malatya	Petrography, mineralogy and sedimentology of K-T boundary evaporites. Sr isotopes.
Robertson et al. (2015)	Adıyaman Region	Calcareous microfossil
Sarıgül et al. (2017)	Southern Kocaeli Peninsula (NW Turkey)	Planktonic foraminifera biostratigraphy

Figure 8. Some K- Pg boundary localities in Turkey compiled from the literature. Image from Google Earth.

1.4.3 Previous Works on the Haymana Basin

The Haymana Basin has been intensely studied from beginning of the 20th century because of its industrial and academic value. In 1930's, Chaput (1932, 1935a, b, 1936) initiated the first studies in the region. He identified existence of Cretaceous and Eocene rocks in the basin. After that Erentöz (1942) found Paleocene fauna around Kusçu village while Lokman and Lahn (1946) examined stratigraphy and tectonic evolution of the region. As stated in Lokman and Lahn (1946) the basin is represented by flyschoidal deposits from Late Cretaceous to Middle Eocene with some radiolarites. The oldest rocks in the area were considered as ophiolite and radiolarite series. However, they could not identify ages of the series due to faults and thrusts. Additionally, they found a variety of fossils with different ages, such as *Turritella sexcincta, Hippurites loftusi, Ostrea lateralis* and *Gryphaea vesiculosa* of Senonian; *Cyclolites krumbecki* of Maastrichtian; and *Assilina, Nummulites* along with *Cerithium giganteum, Cardita* sp., *Limas* sp. of Eocene age. They put forward that algal limestones might be a proxy for Cretaceous-Tertiary transition at which they came across with around Yeşilyurt village (Kadıköy village in old usage). They also maintained that marine deposition ended in Middle Eocene and continental deposits and basalts covered the Eocene succession. They inferred tectonics of the Haymana basin as an ''arriere-fosse'' type of geologic terrane and its movements occurred from Late Mesozoic to Eocene.

In order to characterize petroleum potential and tectonic evolution of the region, more elaborative lithostratigraphic and paleogeographic works were carried out in 1960's and 1970's. Studies of Rigo de Righi and Cortesini (1959), Reckamp and Özbey (1960), Schmidt (1960), and Akarsu (1971) constructed the base comprehensive researches.

Later, Arıkan (1975) investigated petroleum potential of the Tuz Gölü and the Haymana basins. He suggested that the Tuz Gölü and the Haymana basins comprised a uniform and continuous depression from late Senonian to Early-Middle Eocene. After the deposition of Middle Eocene nummulitic limestones, the Tuz Gölü Basin would have been pulled apart from the Haymana Basin. He pointed out that the

Cretaceous-Paleogene transition could be delineated in a great extent by occurrence of algal limestones, yet this transition is more gradual when they are absent.

Ünalan et al. (1976) carried out stratigraphic and paleogeographic studies in the Haymana-Polatlı region. They examined Upper Cretaceous to Lower Tertiary rocks, measured stratigraphic sections (up to 4000 meters), and created 1:25000 scale geological and facies maps to reveal paleogeography of the region. They classified lithostratigraphic units from Maastrichtian to mid-Eocene. At the bottom-most part, flyschoidal deposits of Haymana Formation rest about 1850 m thickness. It passes laterally and vertically to sandstones, conglomerates and limestones of Maastrichtian Beyobası Formation. After the K-Pg boundary from beginning of the Paleocene, three different lithologic units cover these two formations. From shallower to deeper: red-colored conglomerates, sandstones and marls of Kartal Formation; algal limestones of Çaldağ Formation; and marls and shales of Yeşilyurt Formation. Then, all these three formations are in turn overlain by: algal limestones and grey marls of Kırkkavak Formation; grey conglomerates and sandstones of Ilgınlıkdere Formation; and grey sandstones and marls of Paleocene to Eocene aged Eskipolatlı Formation. Through Eocene, Eskipolatlı Formation is covered by three intertounging units: grey conglomerates, sandstones and marls of Yamak Formation; yellow-beige nummulitic limestones and marls of Çayraz Formation; and red conglomerates, sandstones and marls of Beldede Formation. Then, whole system is unconformably covered by Neogene conglomerates, lacustrine limestones and volcanics and finally Quaternary alluvium.

According to their paleogeographic study, Ünalan et al. (1976) demonstrated a crescentic-shaped shelf in the region which deepens towards south and east directions. They suggested that the Çaldağ and the Çayraz formations were deposited on the inner shelf area while the Haymana and the Yeşilyurt formations were located towards outer shelf to basin. Similar with Arıkan (1975), they also claimed that Haymana Basin was once connected with the Tuz Gölü Basin during Late Cretaceous to Early Tertiary.

Apart from Ünalan et al. (1976), Gökçen (1976) carried out a series of sedimentological researches in southern part of the Haymana region by focusing on regional-structural geology and stratigraphy of the area. He measured stratigraphic

sections, identified eight lithostratigraphic units and correlated them with previous studies. He concluded that clastic units were deposited in an area which deepens during Maastrichtian to Eocene and shallows in Middle Eocene. In tectonic aspect, positions and locations of folds, faults and discordances in the investigation site indicate that deformation existed on north-south directional forces. Additionally, he researched on textural features and paleocurrent patterns of sedimentary deposits in the basin. His statistical work on paleocurrent directions shows that the basin was fed by four major directions during Late Cretaceous to Early Tertiary.

Moreover, Batman (1978) studied geologic evolution of northern part of the Haymana region and structural and tectonic features of mélange units in the area. He organized 1:25000 scale geological map and identified formations from Triassic to Pliocene and correlated these lithostratigraphic units with other previous studies. He used following formation names: Hisarlıkaya (Triassic), Lalelik (Upper Jurassic/Lower Cretaceous), Dereköy (Lower Cretaceous-Campanian), Dikilitaş (Upper Campanian-Maastrichtian), Karaömerli (Paleocene), Derindere (Paleocene/Eocene), Kartaltepe (Eocene), Ankara volcanics (Miocene), and Deveci (Pliocene). He also discovered two different mélange units in the area. One is mélange with limestone blocks and the other is ophiolitic mélange. First mélange resides on upper level of the Hisarlıkaya Formation and the latter represents the Dereköy Formation. He concluded that these two mélanges were formed by different geologic processes and emplaced the area in different geologic times.

Paleontology-oriented studies initiated in 1960s and accelerated throughout 1970s. Dizer (1964, 1968) carried out researches on Eocene *Alveolina* and *Nummulites* populations.

Sirel (1975 and 1976 a, b, c) investigated general stratigraphy of the Çaldağ, Kartal, Kırkkavak and Eskipolatlı formations in southern part of the Polatlı region, identified benthic foraminifera taxonomy, such as *Nummulites*, *Assilina*, and *Alveolina*, delineated the Cretaceous-Paleogene boundary, and designated Paleocene-Eocene biozones. Subsequently, Sirel et al. (1986) studied lithostratigraphic and biostratigraphic features of the Cretaceous-Paleogene boundary in the Haymana-Polatlı region. They measured four sections from the Beyobası Formation and

recorded fundamental change in the larger benthic foraminifera populations across the boundary. They identified disappearances of many benthic foraminifera at the end of Maastrichtian and appearances of new assemblages at the beginning of the Danian. They delineated the boundary via paleontological and lithological parameters and concluded that the Danian stage must be attributed biostratigraphically to the Tertiary (i.e. Paleogene).

On the other hand, first planktonic foraminifera studies were initiated by Vedia Toker in 1970s (e.g. Toker 1975, 1977, 1979). Toker (1979, 1980) established *Globotruncana elevata*, *Globotruncana havanensis*, *Globotruncana gansseri* and *Globotruncana mayaroensis* biozones for deposits of Haymana and Beyobası formations.

From the 1990s onward, Özkan-Altıner and Özcan conducted a series of paleontological studies in the Haymana region primarily focused on planktonic and larger benthic foraminifera. In 1997, Özcan and Özkan-Altıner worked on initial chamber arrangement and phylogenic development stages of *Lepidorbitoides* and *Orbitoides* specimens from the Haymana and the Kavak (Beyobası) formations and established a map representing K-Pg boundary locations in Haymana region. In 1999, they studied Upper Cretaceous-Lower Tertiary sections in NW Turkey (around Bartın). They established planktonic and larger benthic foraminifera biozones on Upper Cretaceous-Lower Tertiary strata and correlated them with the Haymana area. They established from older to younger: *Dicarinella concavata*, *Dicarinella asymetrica*, *Globotruncanita elevata*, *Globotruncana ventricosa*, *Radotruncana calcarata*, *Globotruncanella havanensis*, *Globotruncana aegyptiaca*, *Gansserina gansseri*, *Abathomphalus mayaroensis* and *Morozovella pseudobulloides* planktonic foraminifera biozones.

Most recent studies on Haymana area were done by concerning sequence stratigraphy, sediment cyclicity, planktonic foraminifera taxonomy or regional tectonic history of the basin (e.g. Huseynov 2007, Amirov 2008, Rojay 2013, Esmeray-Senlet et al. 2015 and Okay and Altıner 2016).

1.5.4 Regional Geology

The Haymana Basin is situated on southern margin of the Pontides. It is located approximately 60 km southwest of Ankara and 45 km northeast of the İzmir-Ankara suture (Okay and Altıner 2016) (Fig. 9). Starting from the Cretaceous, the northern branch of Neo-Tethys begins its subduction underneath the Eurasian Plate (Şengör and Yılmaz 1981, Görür et al. 1984, Torsvik et al. 2012). At that time, the Pontides were an active margin and grew southward by addition of accretionary complexes (Okay and Altıner 2016). Although subduction initiated as early as Albian, the arc volcanism started in Turonian and became widespread in Santonian (Okay and Altıner 2016). This volcanism was considered as submarine character because of its volcanoclastic deposits intercalated with deep marine limestones (Okay and Altıner 2016) (Fig. 10). At the end of Campanian, volcanism faded out and carbonate deposition prevailed in northern, and siliciclastic turbidites were deposited in southern part of the Pontides through Maastrichtian. As a result of this on-going convergence of the Anatolide-Tauride Platform (to the south) and the Pontides (to the north), the Haymana Basin was opened as a fore-arc basin (Dickinson and Seely 1979, Görür et al. 1984, Koçyiğit et al. 1988, Koçyiğit 1991, Nairn et al. 2013) (Fig. 10).

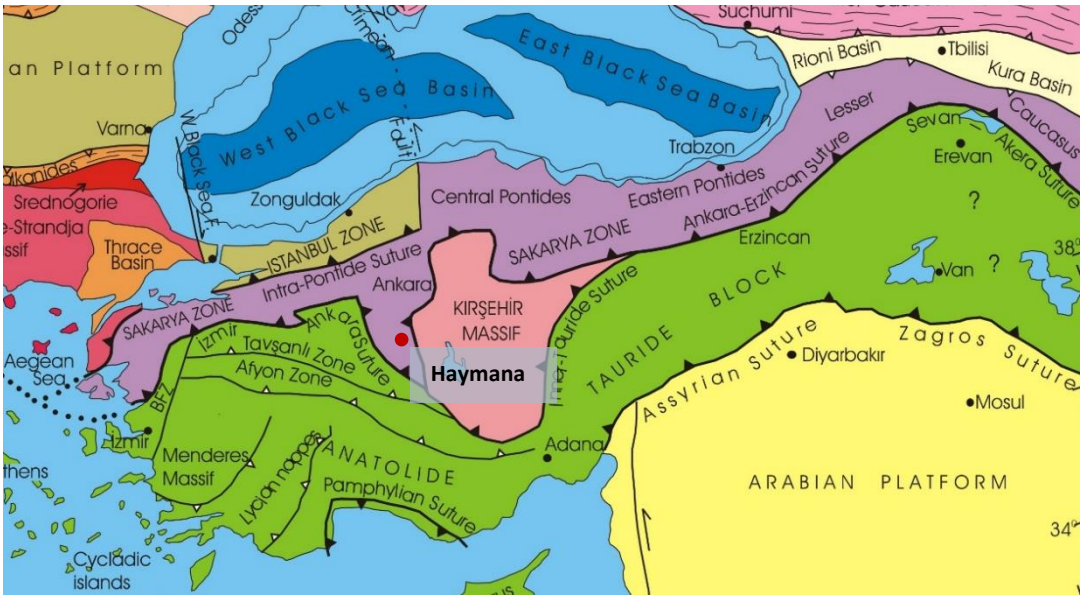

Figure 9. Main tectonic units of Turkey and position of the Haymana Basin (red dot). The Haymana Basin is located on southern part of the Pontides 45 km NE of the Izmir-Ankara Erzincan Suture. Image modified after Okay and Tüysüz (1999).

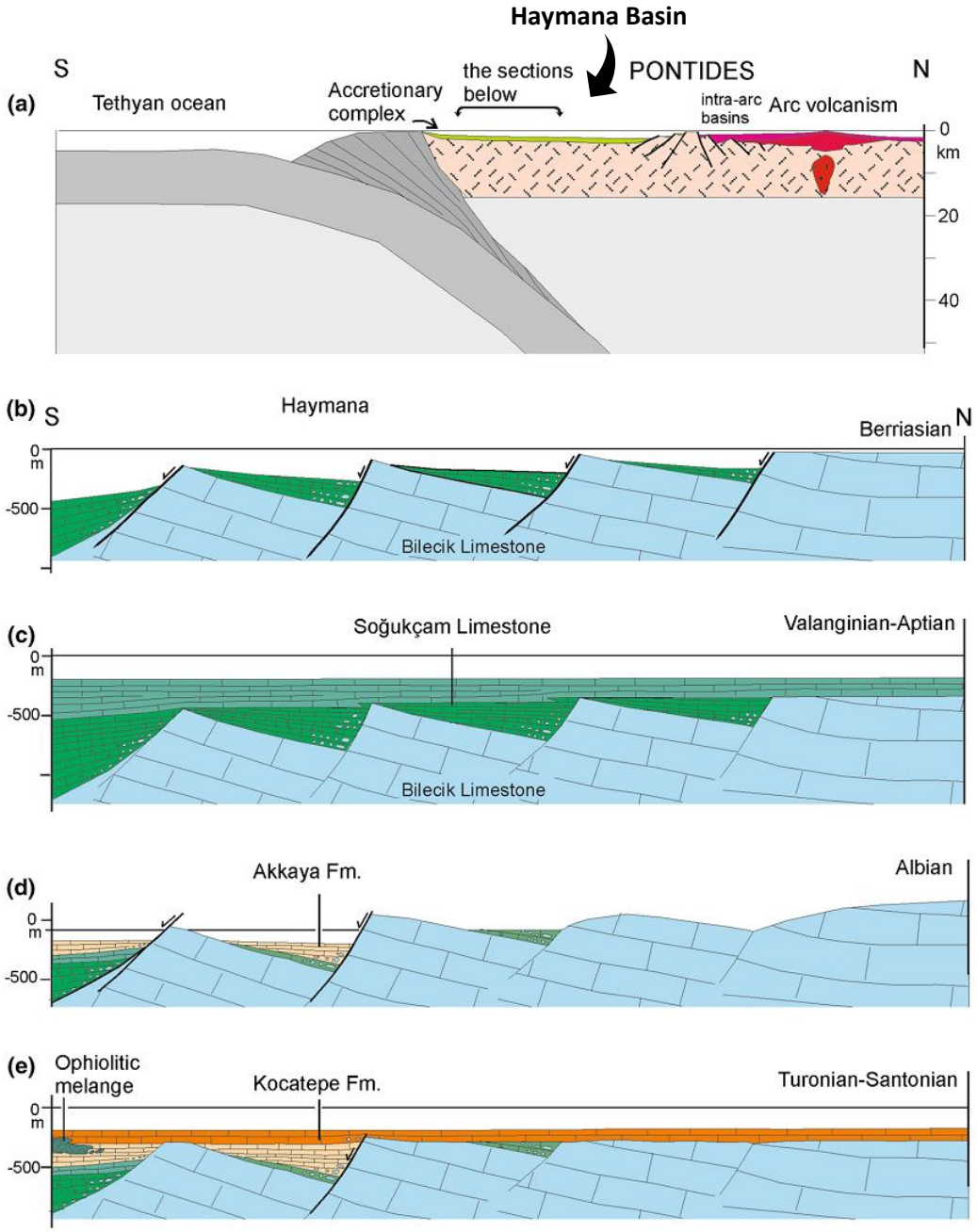

Figure 10. A) Development of the Haymana Basin as a fore-arc position due to subduction of the Northern Branch of Neo-Tethys beneath the Pontides. B-E) Cretaceous sedimentation and tectonism in the basin. After the deposition of the Kocatepe Formation, flyschoidal Haymana Formation prevails starting from the Campanian. Image retrieved and modified after Okay and Altıner (2016).

The basement of the Haymana region is made up of deformed Triassic Karakaya Complex which is in turn overlain by Middle Jurassic-Lower Cretaceous carbonates (Bilecik and Soğukçam limestones) and Upper Cretaceous flysch (i.e. Haymana Formation) (Okay 1989, Okay and Altıner 2016) (Fig. 11). Especially, this sequence is highly characteristic through the Sakarya Zone (combination of Sakarya Continent of Şengör and Yılmaz 1981 and Eastern Pontides) (Okay 1989). On the other hand, shallow marine Upper Jurassic-Lower Cretaceous carbonates (Bilecik Limestone) are a marker horizon such that it can be traced all along the Pontides (Okay and Altıner 2016). The Bilecik Limestone is covered by pelagic deposits of Soğukçam Limestone corresponding a sea level transgression. The Soğukçam Limestone deposits can reach up to ~900 m thickness in eastern Pontides, yet in Haymana Basin they reach only 100 m thickness with Berriasian age (Okay and Altıner 2016) which represents huge erosional phase occurred after the deposition of the Soğukçam Limestone (Aral Okay & Demir Altıner pers. commun.). From Albian to Cenomanian, both Bilecik and Soğukçam limestones are unconformably overlain by breccias and glauconite and radiolaria-bearing limestones of 500 m thick Akkaya Formation. Then, these deposits are unconformably covered by pelagic limestones and shales of 100 m thick Kocatepe Formation of Turonian-Santonian age. Subsequently, flyschoidal deposits of 1800 m-thick Haymana Formation covers the whole basin starting from the Campanian (Okay and Altıner 2016) (Fig. 11).

As mentioned earlier, Ünalan et al. (1976) indicated that the Haymana Formation consists of grey shales, sandstones and conglomerate lenses. It shows flute-load coasts and Bouma sequences. During Maastrichtian, these conglomerates were fed through channels from accretionary prism (North Anatolian Ophiolitic Mélange) towards to depocenter of hemipelagic marls and sandstone turbidites (Nairn et al. 2013). The Haymana Formation accumulated on and outer shelf setting where turbiditic currents prevail (Fig. 12).

Around the basin margins, the Haymana Formation passes both laterally and vertically into *Hippurites* sp., *Cyclolites* sp., *Orbitoides* sp. bearing yellowish sandstones, pebbly limestones and sandy marls of shallow-marine Beyobası Formation (Asmaboğazı Formation of Görür et al. 1984) (Figs. 11, 12)

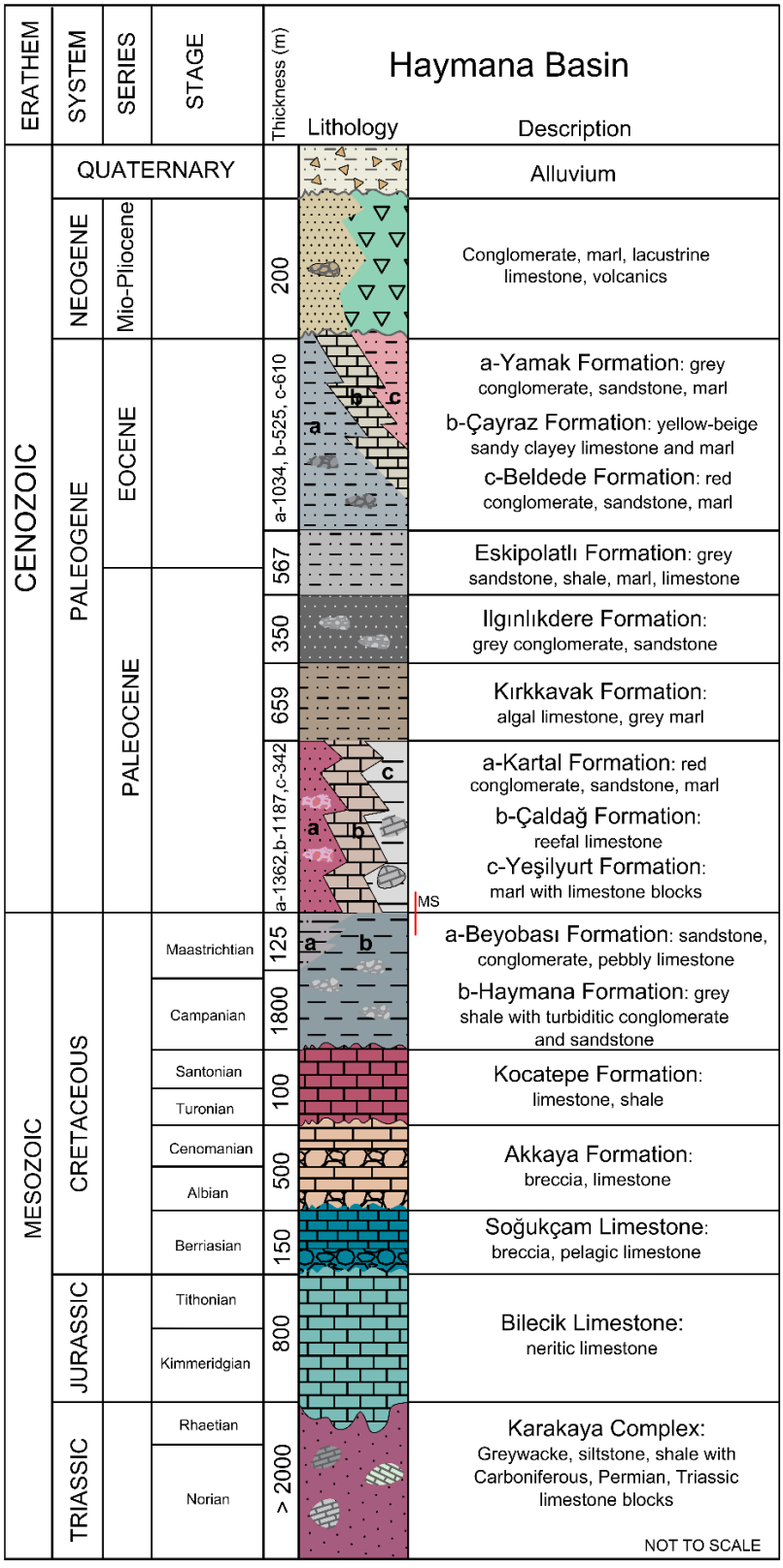

Figure 11. Generalized columnar section of the Haymana Basin modified after Ünalan et al. (1976) and Okay and Altıner (2016). MS: Measured section in this study covering the Haymana and Yeşilyurt formations.

At the end of Maastrichtian, the Beyobası Formation was deposited on shallow areas of northern, western and southern part of the basin, while flyschoidal Haymana Formation were deposited on deeper southeastern part. Depositional characteristics of the Beyobası and Haymana formations indicate that Haymana region had a shelf setting to the north, west and south, and deep-marine environment to the southeast (Figs. 12, 13).

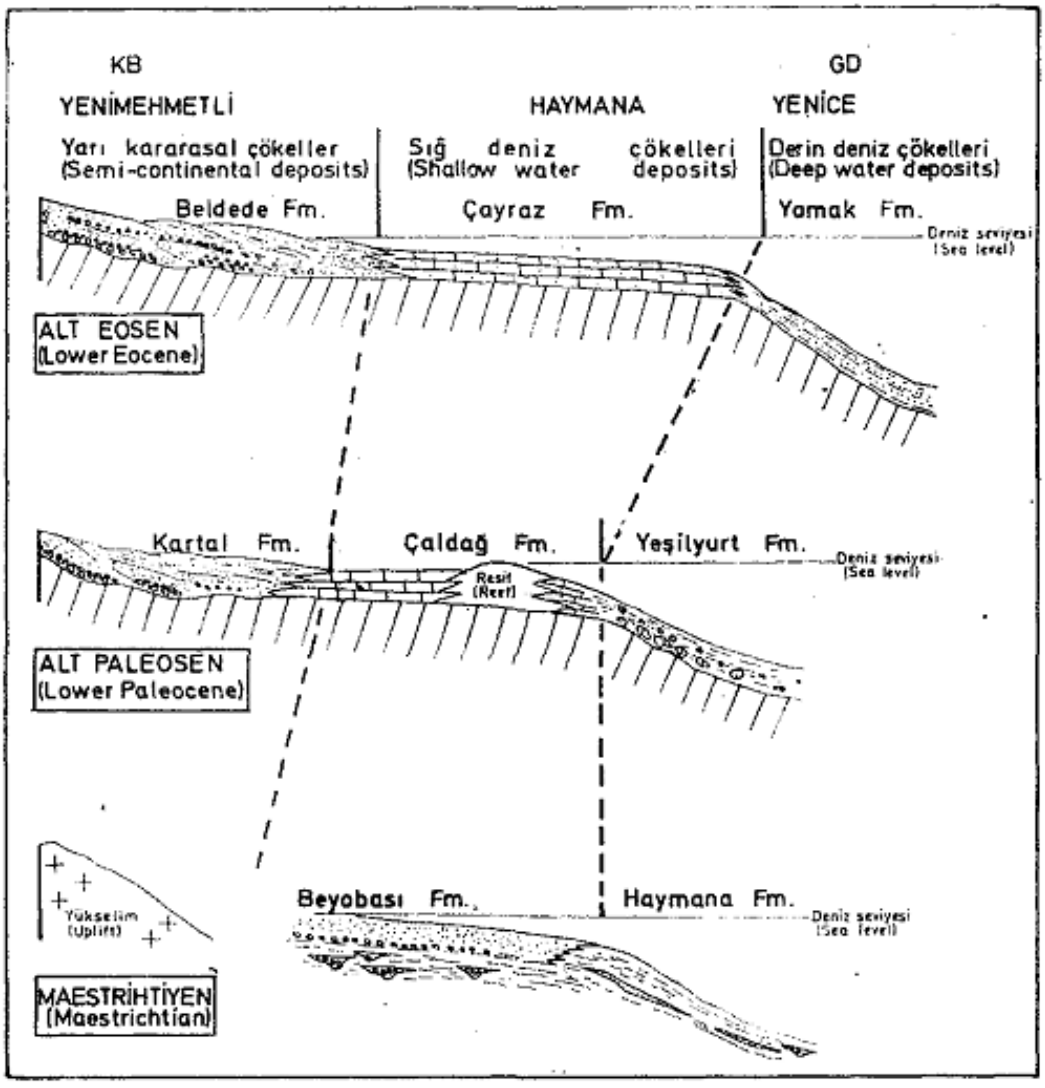

Figure 12. NW-SE transects of the Haymana Basin representing relations of formations during Maastrichtian, Early Paleocene, and Early Eocene time periods (Ünalan et al. 1976). Our study area covers deposits of Haymana Formation below and Yeşilyurt Formation above the K-Pg boundary.

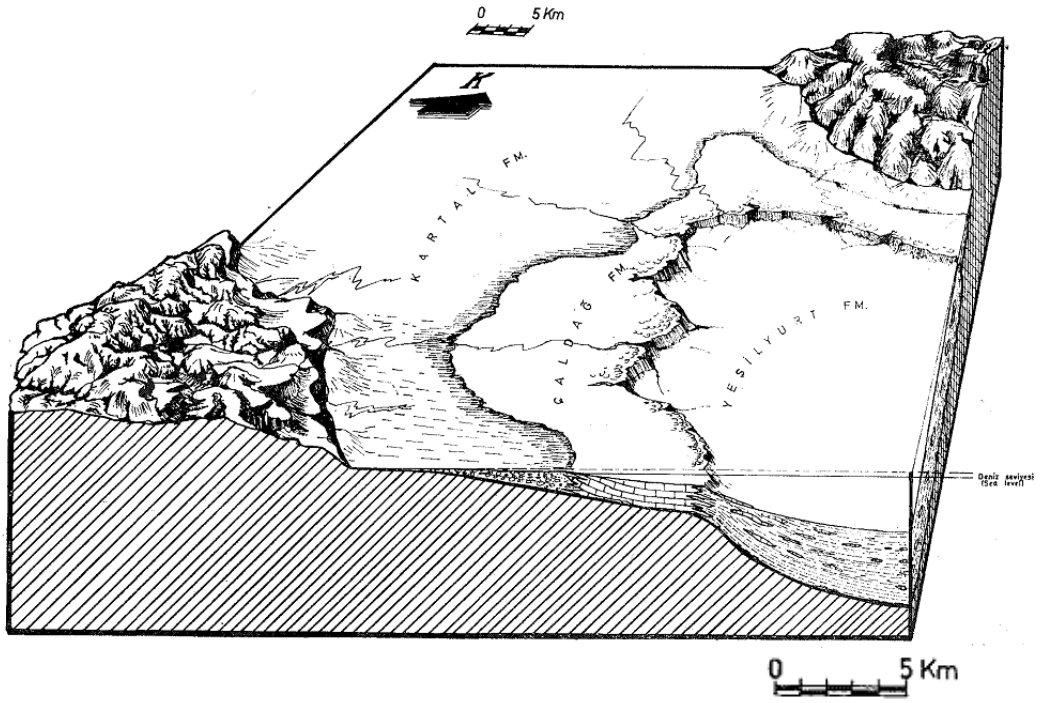

Figure 13. Paleoenvironment of the Haymana Basin for Early Paleocene (Ünalan et al. 1976).

In the beginning of the Paleocene, the Haymana Basin has three different depositional facies intertounging with each other and both overlie the below-lying Beyobası and Haymana formations (Fig. 11). On shallowest part, semi-continental red conglomerates, sandstones and marls of Kartal Formation were deposited (Fig. 11). Fluvial environment majorly controlled the deposition of the Kartal Formation while marine sedimentation occurred sporadically.

The Kartal Formation passes laterally up to algal and coral-bearing limestones of the Çaldağ Formation (Figs. 11, 12, 13). The limestones are rich in algae, echinoderm, coral, and bryozoan particles. Main lithology is grainstone with high abundance of algal fragments. Çaldağ Formation represents shelf of the Haymana Basin in early Paleocene while the Kartal and Yeşilyurt formations indicate inner shelf and outer shelf environments, respectively (Figs. 12, 13). Limestones of the Çaldağ Formation intertounging with black shales and marls of the Yeşilyurt Formation to deeper parts (Figs. 12, 13). To the eastern and south-eastern part of the Haymana region, limestone content decrease and shale deposition prevails. Turbidity currents transported

limestone blocks of the Çaldağ Formation into deep-marine black shale deposits of the Yeşilyurt Formation.

Late Paleocene (Thanetian) is represented by algal limestones and grey marls of the Kırkkavak Formation. Its lower and upper boundaries are conformable with below-lying Kartal, Çaldağ and Yeşilyurt formations, and above-lying Ilgınlıkdere Formation (Fig. 11). Algal and reefal communities indicate shallow marine deposition for the Kırkkavak Formation which pass deep marine deposits towards to the southeast of the basin.

The Kırkkavak Formation is also identified by work of Görür et al. (1984). However, their definition corresponds to a combination of: black shales and limestones blocks of the Yeşilyurt Formation, algal limestones and grey marls of the Kırkkavak Formation (*sensu* Ünalan et al.., 1976), and grey conglomerates and sandstones of the Ilgınlıkdere Formation. They consider that the Kırkkavak Formation has turbiditic character and deposited throughout Paleocene.

Additionally, Nairn et al. (2013) claim that through Late Paleocene-Early Eocene interval shallowing sequences and sediment instability in central Anatolian basins reflect progressive and diachronic collision between the Pontides and the Anatolide-Taurides.

Paleocene-Eocene transition in the basin was recorded in the Eskipolatlı Formation which conformably overlies flyschoidal sandstone-shale intercalations of Ilgınlıkdere Formation (Fig. 11). Depositional characteristic of this formation indicates a change in depositional environment from flysch (bottom) to shallow-marine (top).

At the end of Middle Eocene, sedimentation was ceased due to emplacement of thrusts and regional uplift. By Late Eocene, the collision was complete and non-marine terrestrial sedimentation and post-collisional magmatism started (Görür et al. 1984, Şengör and Yılmaz 1981). Finally, Neogene terrestrial clastics and volcanics unconformably cover the whole region (Yüksel 1970, Ünalan et al. 1976, Görür et al. 1984).

Our study area crosses deposits of the Haymana and Yeşilyurt formations (Fig. 12). Figure 13 demonstrates map of the Haymana basin and the studied section.

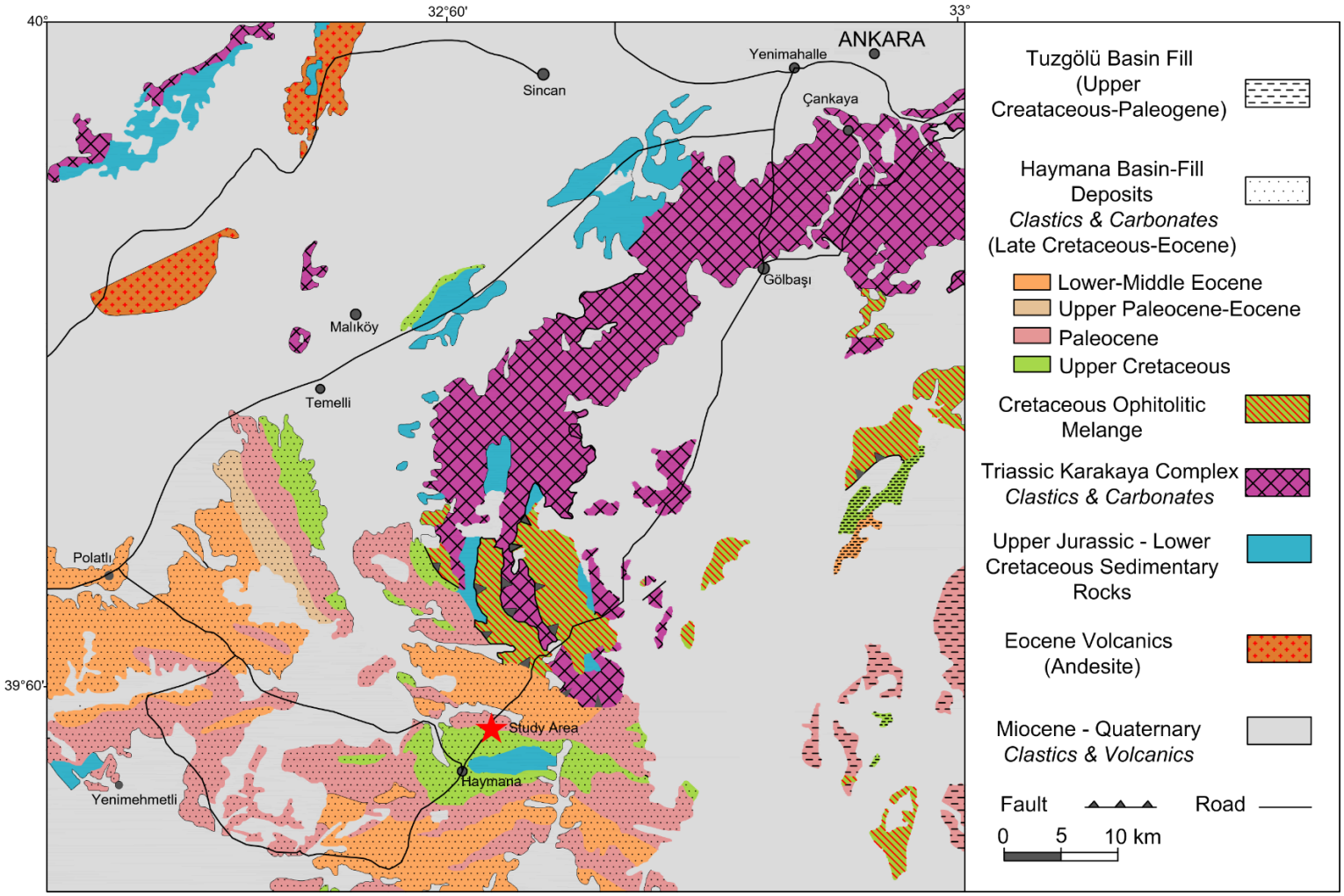

Figure 14. Geological map of the Haymana Region and location of the study area (Modified after 1/500.000 Map of MTA and Rojay 2013).

CHAPTER 2

STRATIGRAPHY

2.1 LITHOSTRATIGRAPHY

As mentioned earlier, two sections were measured in the study area: UH section and UKHB section (Figs. 15, 16, 20). UH section is characterized by monotonous mudstone deposits of the Haymana Formation. Right after the K-Pg boundary a conspicuous change in the sedimentation regime was observed from mudstones of the Haymana Formation to marls and calcareous mudstones of Yeşilyurt Formation (Figs. 15, 16, 17). These marls and calcareous mudstones alternate with each other through the Paleocene (Fig. 16).

The UH section starts with Upper Cretaceous dull-gray shales of Haymana Formation passes the K-Pg boundary and ends in first centimeters of cream-colored marls of Yeşilyurt Formation. It is 9.70 m in total corresponding uppermost 9.55 m of the Maastrichtian, the K-Pg boundary, and first 15 cm of the Danian. Sampling interval is 20 cm (Fig. 18) in stratigraphically lower parts and it narrows into 10 cm and 5 cm as getting closer to the K-Pg boundary. Additional samples, such as 2 cm before and after the K-Pg boundary, sampling of the K-Pg boundary itself and samples from important points were collected during the auxiliary field campaign. In total 51 samples, labeled from UH-1 to UH-51, were gathered from the main field campaign; and 10 samples, labeled from E-2 to E+50, collected from the auxiliary field campaign through the UH section.

On the other hand, the UKHB section is 5.14 m in total. It starts from 5 cm below the K-Pg boundary, and ranges 5.09 m through the Danian. Sampling interval is 5 cm above and below the K-Pg boundary and widens (10 to 20 cm) through the up-section in Danian. In total 38 samples, labeled from UKHB-1 to UKHB-38, were gathered from the UKHB section. These two measured sections were calibrated via laterally continuous K-Pg boundary and paleontological associations of key stratigraphic levels.

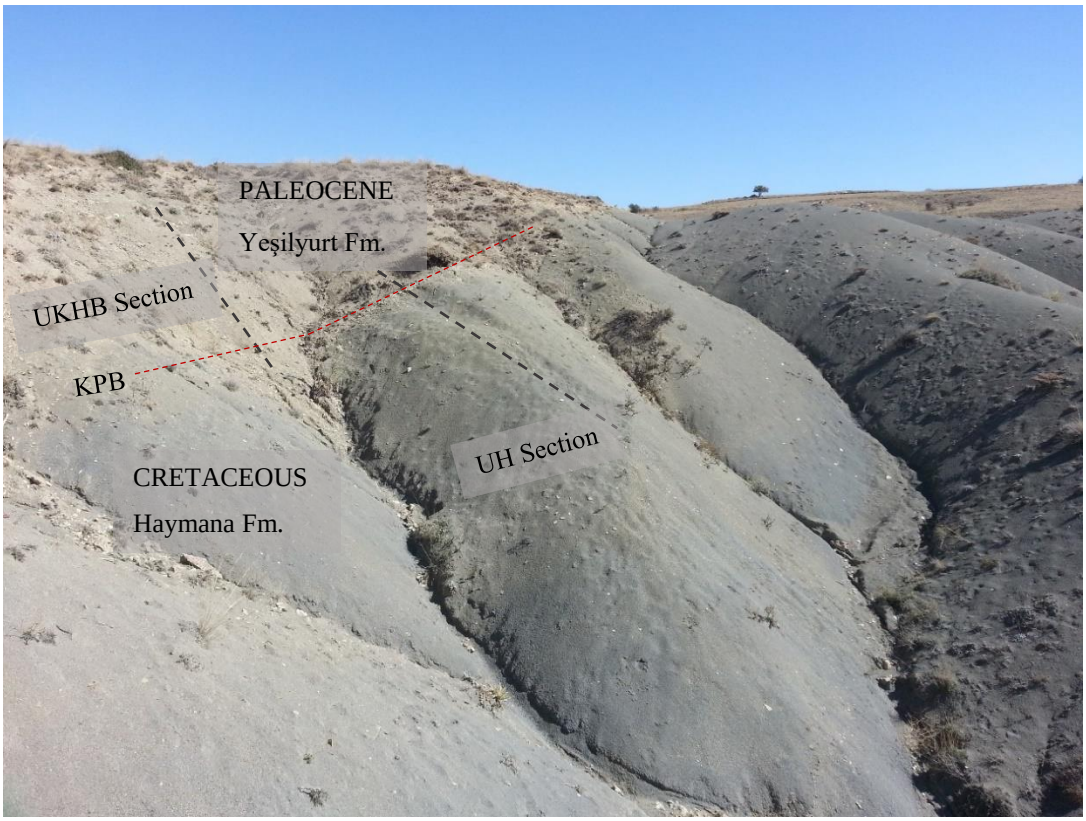

Figure 15. Field view of the study area and the measured sections. Cretaceous successions (dark grey) are characterized by mudstone deposits (Haymana Formation). Right after the K-Pg boundary, these mudstones rapidly change to marl and calcareous mudstone alternations (cream color) (Yeşilyurt Formation).

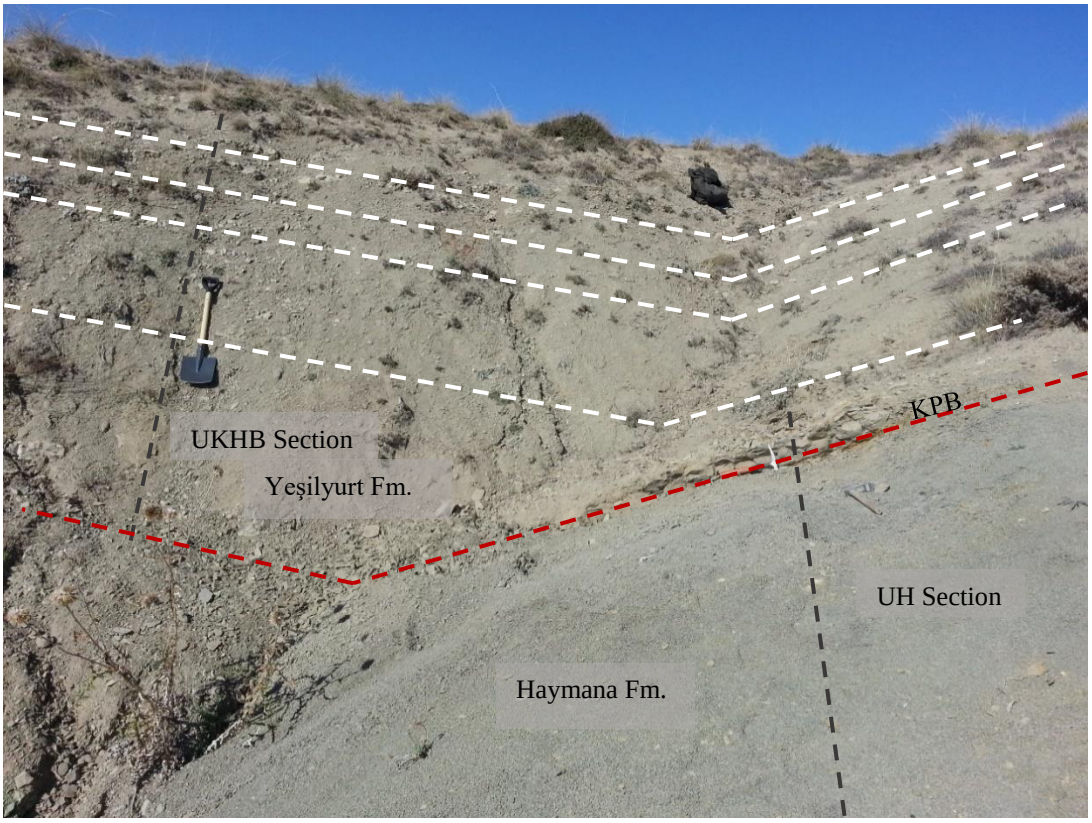

Figure 16. Closer look to the measured sections. Black dashed line: Positions of the measured sections. Red dashed line: Position of the K-Pg boundary (KPB). White dashed lines: marl-calcareous mudstone alternations through Danian.

The K-Pg boundary is characterized by 2-3 mm thick reddish oxidized layer (Fig. 17, 19A) found between UH-49 and E+2. No prominent boundary clay was found above of this layer. However, occasionally this 2-3 mm thick reddish layer are divided into two consecutive mm-thick horizons and a ~2 cm-thick clay layer in between (Fig. 19B). But, through the lateral continuity of the outcrop this clay layer fades out and these two reddish horizons unite a single prominent 2-3 mm thick boundary layer (i.e. the K-Pg boundary). Similarly, Açıkalın et al. (2015) was also identified a second mm-thick reddish horizon on top of 17 cm-thick dark clay layer in Okçular section (Mudurnu-Göynük Basin). Differently from our observation in Haymana Basin, their clay layer (which separates the two reddish horizons) is laterally continuous.

Figure 17. Sedimentation rapidly changes right after the K-Pg boundary (KPB) from mudstones of the Haymana Formation to marls and calcareous mudstones of the Yeşilyurt Formation. Please note the reddish oxidized mm-thick layer corresponding the K-Pg boundary and change in the character of the deposits afterwards.

Moreover, their paleontological and geochemical analyses revealed that the first reddish layer corresponds to the principal K-Pg boundary which shows abrupt increase in Ir content to ~7.4 ppb, high siderophile elemens and negative ^{13}C shift. They claimed that the second mm-thick horizon would have been formed due to remobilization and re-deposition. Similar to Mudurnu-Göynük basin, in our section, although the separating 2 cm thick clay layer diminishes in the lateral continuity and mm-thick layers form a single 2-3 mm thick reddish layer, one of these two horizons might have been formed due to the remobilization. On the other hand, given the deposition similarity of the Haymana and Mudurnu-Göynük basins, although geochemical analysis is yet to be done, the 2-3 mm thick reddish layer in our study highly possible to rich in Ir and siderophile elements.

Previous studies on southern part of the Haymana region (e.g. Amirov 2008 unpub., Esmeray-Senlet et al. 2015) have failed to find 2-3 mm thick reddish layer corresponding the K-Pg boundary. This may be because of differential preservation, remobilization or complete sweeping of this mm-thick layer with bottom currents. In fact, Amirov (2008, unpub.) and Esmeray-Senlet et al. (2015) delineated the K-Pg boundary between Beyobası-Çaldağ and Beyobası-Yeşilyurt formations, respectively. Through Maastrichtian, the Haymana Formation turns to Beyobası Formation in shallower parts of the basin then the Yeşilyurt Formation covers the Haymana Formation and relatively deeper part of the Beyobası Formation starting from beginning of the Danian (Ünalan et al. 1976, see fig. 12). In this regard, wave action may have swept away the 2-3 mm thick reddish layer in shallower parts of the basin. On the other hand, both studies could observe marl/limestone-mudstone alternations after the K-Pg boundary.

Figure 18. Sample spacing is about 20 cm in lower levels of the Maastrichtian and upper levels of the Danian. Spacing decreased 10 cm, 5 cm and 2 cm close to the K-Pg boundary.

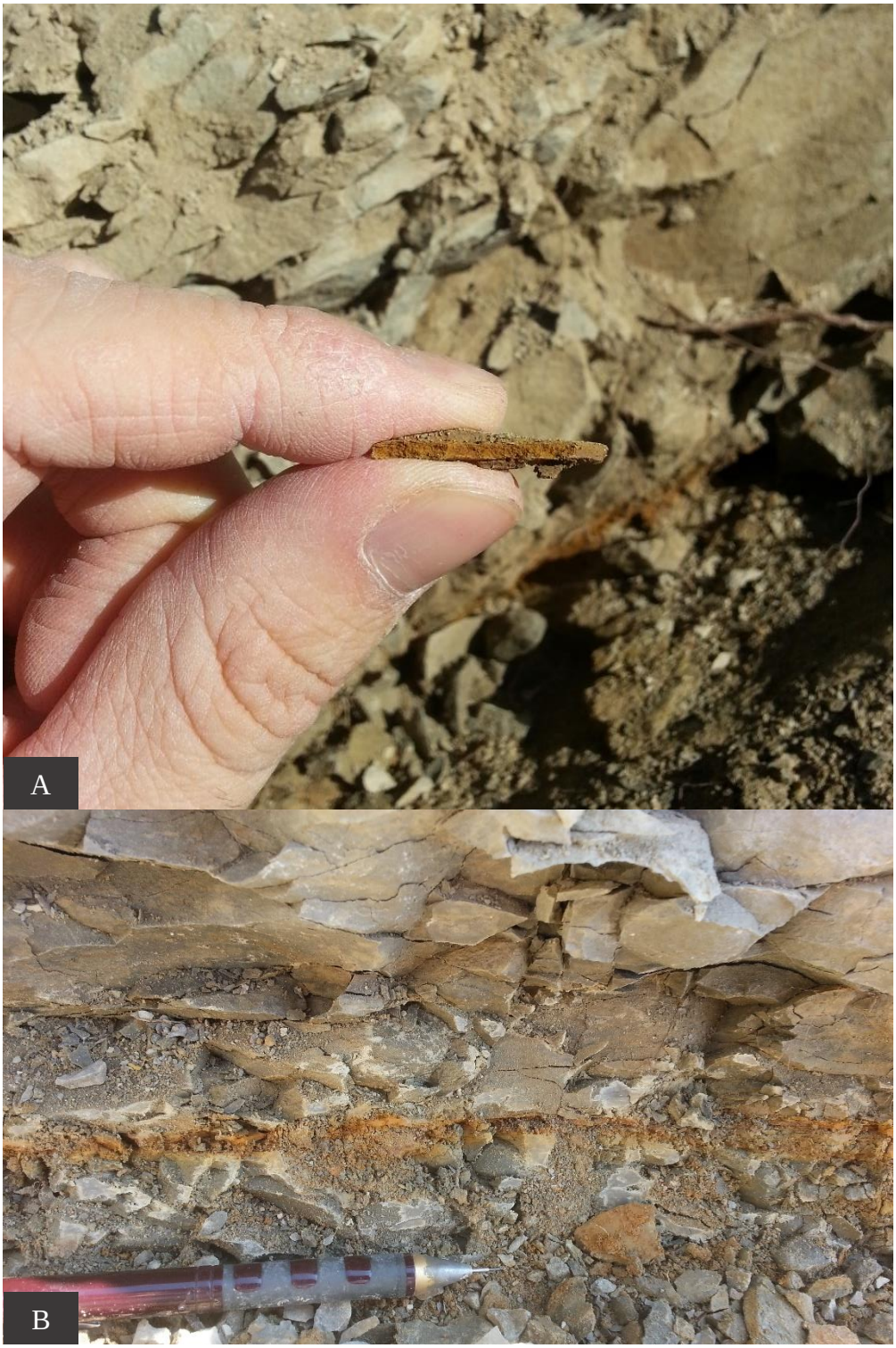

Figure 19. A) The Cretaceous-Paleogene (K-Pg) boundary. It corresponds to 2-3 mm thick reddish layer. A huge majority of the planktonic foraminifera sharply extinct at the boundary. Two reddish horizons are separated by ~2 cm thick clay layer. B) Two reddish horizons and interjacent 2 cm-thick clay are not continuous and laterally unite into a single prominent 2-3 mm thick boundary layer.

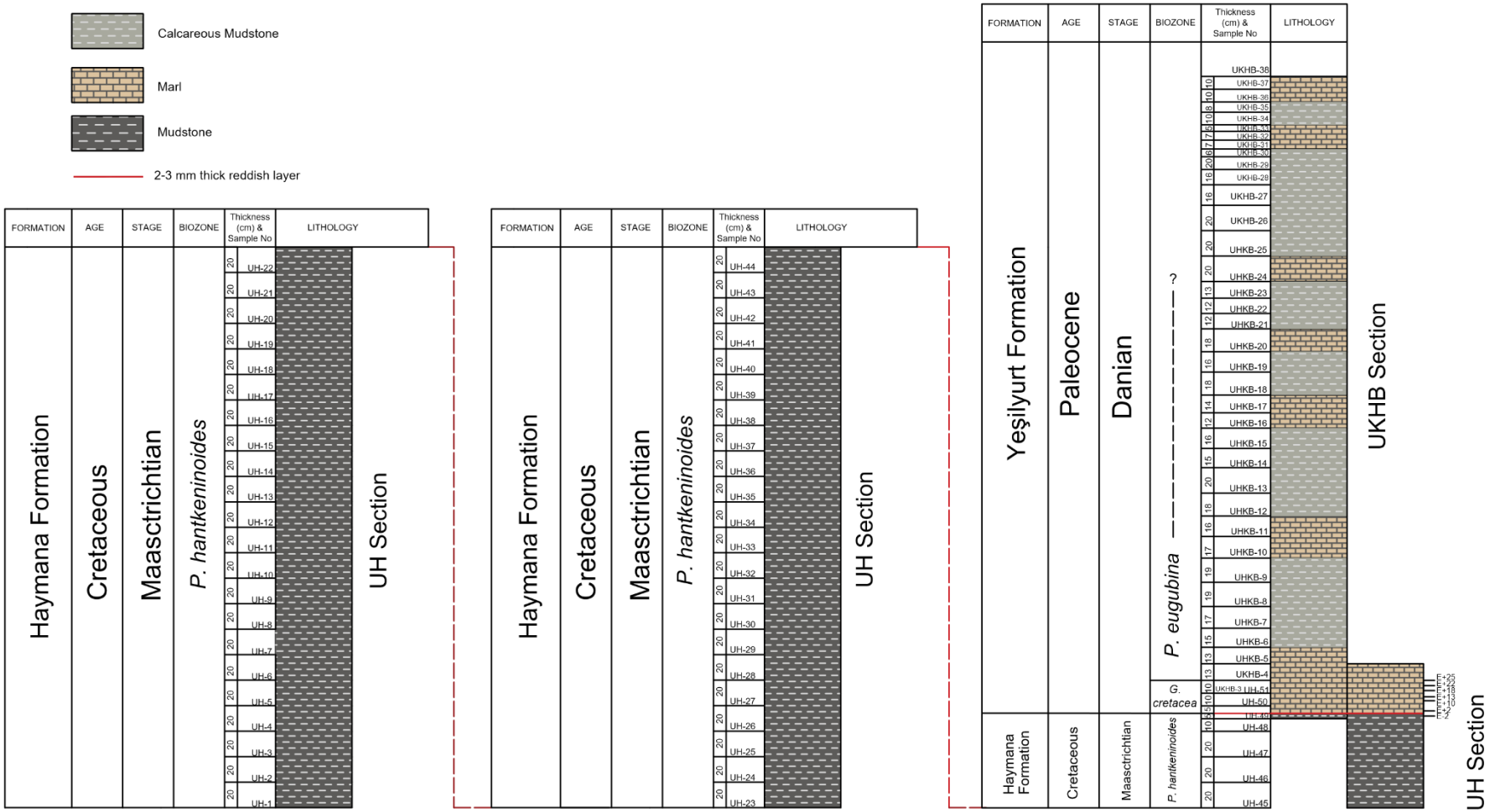

Figure 20. Lithostratigraphy and biostratigraphy of the measured sections. Please note marl-calcareous mudstone alternations after the K- Pg boundary.

Açıkalın et al. (2015) demonstrated a similar depositional pattern in the Mudurnu-Göynük Basin with our study in the Haymana Basin through Maastrichtian and Danian. They revealed that Upper Maastrichtian dark gray colored monotonous mudstones were interrupted by 2-3 mm-thick red oxidized layer corresponding the K-Pg boundary which subsequently covered by Lower Danian light colored rhythmic mudstone-limestone alternations. They determined outer neritic-upper bathyal paleodepth for their study area in the Mudurnu-Göynük Basin which we proposed same paleobathymetry for our study area in the Haymana Basin (see Paleobathymetry Chapter). They also claimed that for outer neritic-upper bathyal settings, such as Caravaca (Spain), Agost (Spain) and Bjala (Bulgaria) and Mudurnu-Göynük Basin, a prominent limestone bed overlies the boundary clay and marks the base of the Pα Zone. Likewise, we determined ~30 cm-thick marl bed directly overlies the K-Pg boundary (see figs 17, 21). Its base corresponds to the base of earliest Danian P0 Zone. Previously in southern part of the Haymana Basin, this bed was also identified by Amirov (2008, unpub.) and Esmeray-Senlet et al. (2015) which marks the base of Pα or middle part of the P0 Zone, respectively. Deposition of this limestone/marl bed right after the boundary might be a function of decreased surface productivity following the K-Pg mass extinction (see Discussion and Conclusion Chapter).

Finally, given the lithologies and the depositional patterns of the Haymana and Mudurnu-Göynük basins, these two basins may have connected with each other at least for Maastrichtian to Danian time interval.

Figure 21. Thick marl bed directly overlies the K-Pg boundary (reddish horizon). Note the change in the sedimentation from mudstones to marls after the boundary.

2.1.1 Microfacies Types

The aim of the microfacies analysis was to investigate depositional regime of the basin by means of paleontological and sedimentological proxies. Apart from the field observations, more than 90 thin section slides were examined covering each level of the UH (from UH-1 to UH-51) and UKHB (from UKHB-1 to UKHB-38) sections. Consequently, two main rock types were identified: mudstones and marls (Fig. 22). These Upper Cretaceous mudstones are interrupted by 2-3 mm thick reddish layer and overlying 2 cm-thick boundary clay. As mentioned earlier, a sharp change in sedimentation happens right after the K-Pg boundary which yields marl deposition in Early Danian. In fact, a 30-cm-thick marl bed abruptly overlies the boundary clay. Through the up-section, these marl deposits alternate with calcareous mudstones (Fig. 22).

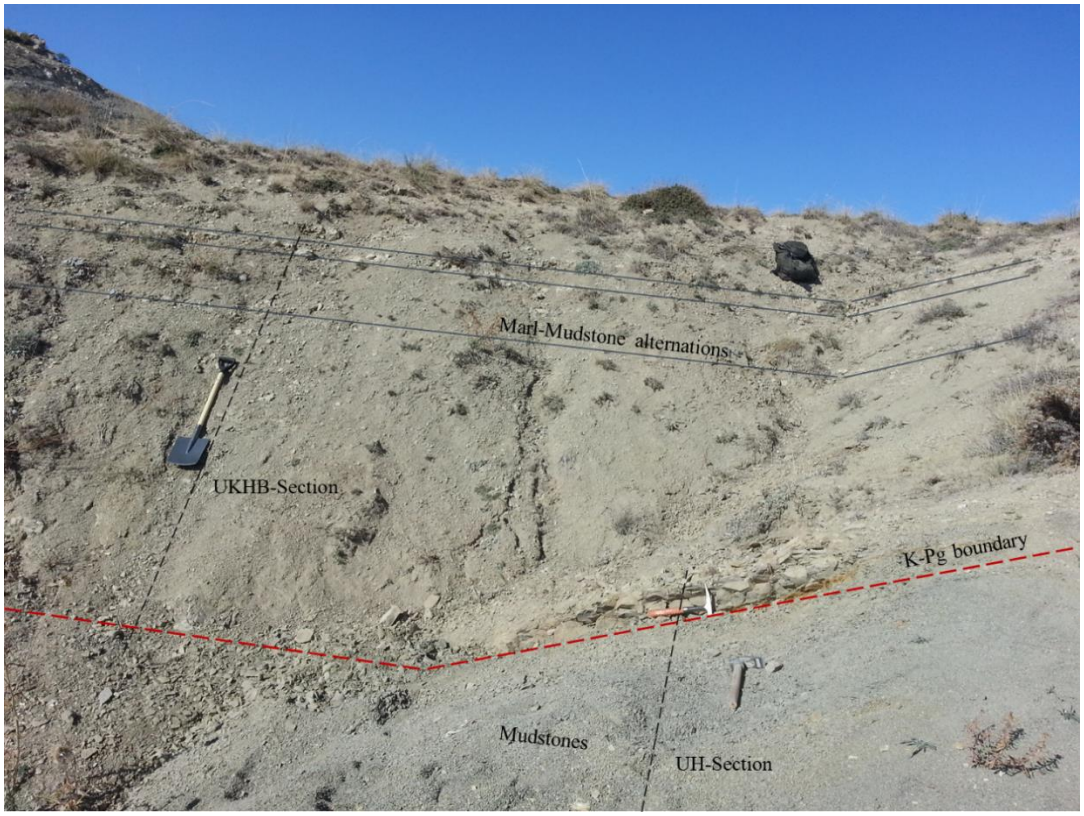

Figure 22. Two basic rock types were revealed in the study area: Mudstones and Marls. Mudstones have dull gray color in the field while marls have thick bedding and cream color.

Mudstone

Mudstone is the most abundant rock type in the studied section as it corresponds to the all Cretaceous deposits (i.e. whole UH section until the K-Pg boundary). It is dull-gray color in the field and lack of fissility (Figs. 15, 16, 17, 18, 21). Mudstones are rich in planktonic and benthic foraminifera. Silt sized quartz and feldspar grains are common with minor amount of micas. Occasionally iron oxide stained the infillings (Fig. 23). Mudstones correspond to the samples from UH-1 to UH-49 until the K-Pg boundary. During times of relatively high carbonate influx these mudstones turn into calcareous mudstones during Danian. Yet, mudstones and calcareous mudstones do not show distinct change in the thin section views.

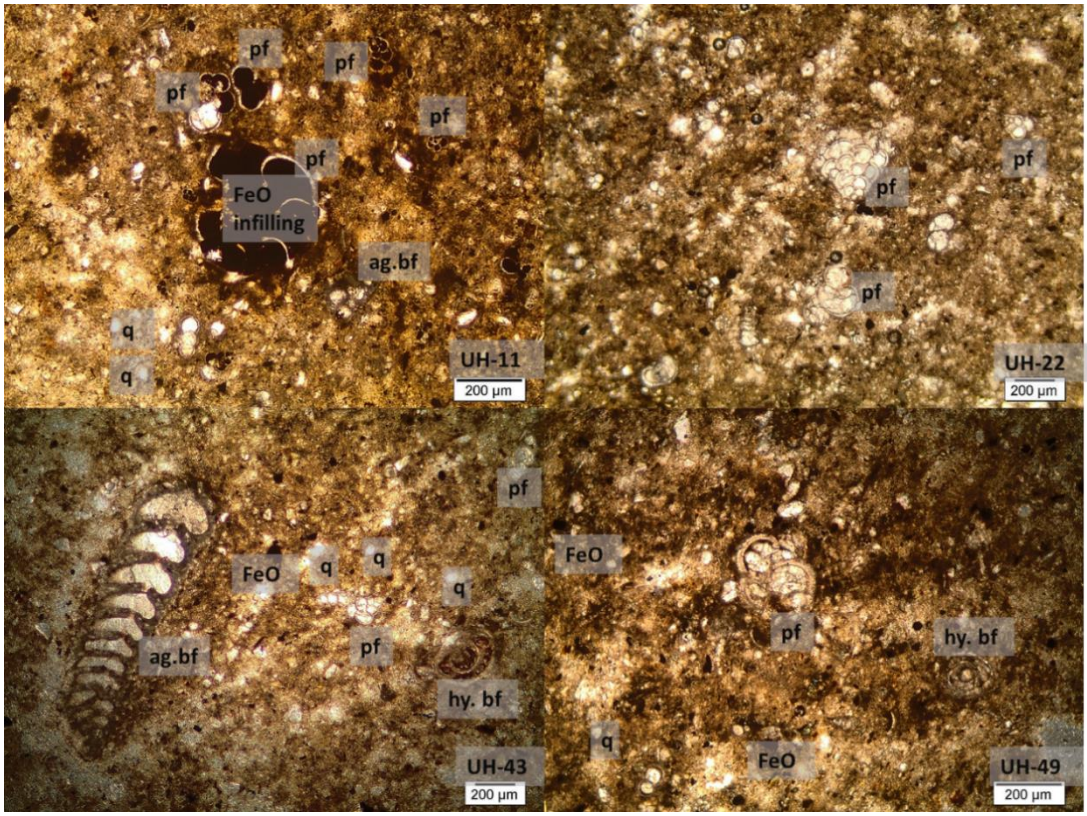

Figure 23. Mudstones in thin section view. pf: Planktonic foraminifera, hy bf: Hyaline benthic foraminifera, ag. bf: Agglutinated benthic foraminifera, q: Quartz, m: muscovite, FeO: Iron Oxide infilling. All samples are from the Cretaceous deposits.

Marl

Hubbard et al. (1990) suggest that marl deposits are soft, loose and earthy rocks with changeable amounts of clay, silt, and carbonate particles. In the study area, marl facies were deposited right after the K-Pg boundary. They are cream color in the field, yet in thin section, they appear dark to light gray. In some intervals, alteration and/or FeO stain the sediments and change their appearance to orange-yellowish green color in thin sections. As siliciclastic influx increases (or carbonate influx ceases vice versa) marl deposits turn into calcareous mudstones.

The abrupt change in the sedimentation and mass extinction of large, complex planktonic foraminifera were detected also in thin sections. Right after the K-Pg boundary, starting from the very first samples of Danian P0 zone (e.g. UH-50, UH-51), hardly ever planktonic foraminifera was detected in the marl deposits (Note the

difference in sediment type/color and fossil assemblage between Fig. 23 and Fig. 24). However, high amounts of quartz, feldspar grains and clay minerals were found with extremely high amount of tiny calcareous spheres in the background (Fig. 24). Through up-section, number of planktonic foraminifera increases as these spheres decreases in accordance with ecological recovery. Origin of these calcareous spheres was discussed in ‘’*Thoracospharea* blooms’’ chapter.

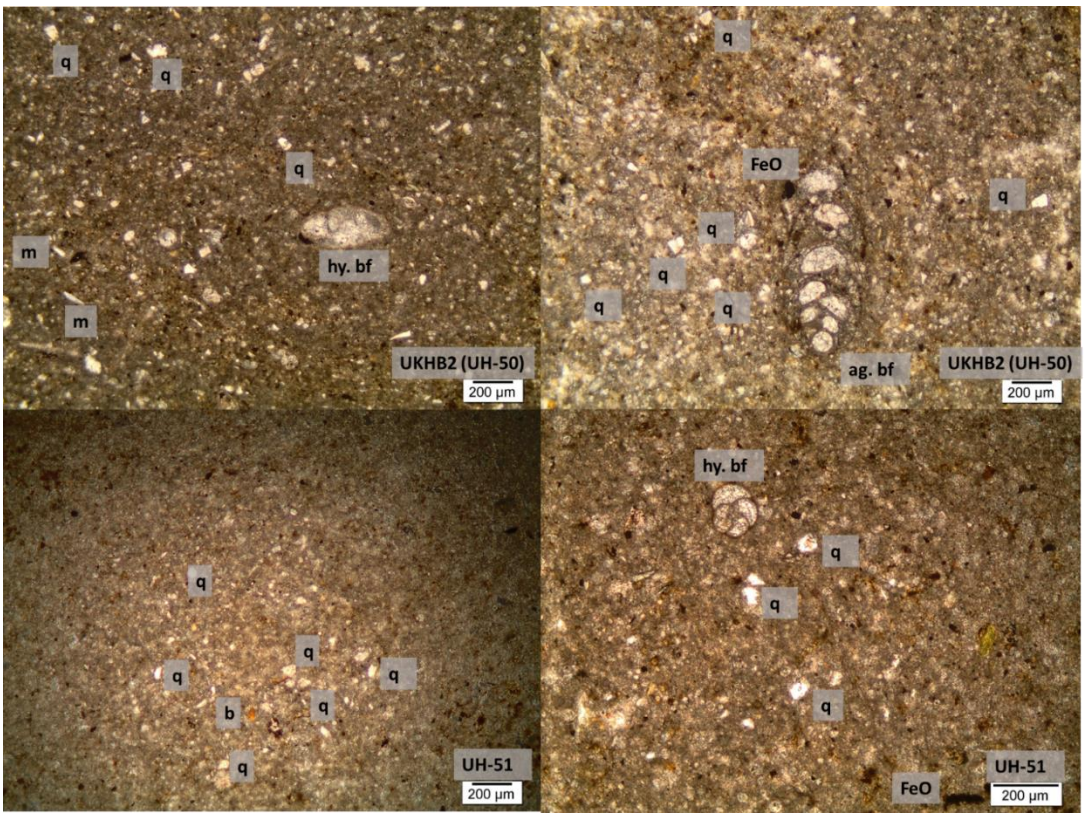

Figure 24. Marls were deposited after the K- Pg boundary. Note the tiny spherulids covering the background area (clearly seen at right- top figure). See Fig.23 for letter abbreviations.

2.2 BIOSTRATIGRAPHY

Biozones were established based on major bio-events corresponding First Appearance and Last Appearance datums (FAD and LADs).

Biostratigraphic scheme of Caron (1985) have been used for decades for low and mid latitudes. It divides the Maastrichtian Stage into four biozones which are from older to younger: *Globotruncanella havanensis*, *Globotruncana aegyptiaca*, *Gansserina gansseri*, and *Abathomphalus mayaroensis* biozones. *Abathomphalus mayaroensis* biozone has been widely used for the latest subdivision of the Maastrichtian (Smit 1982, Robaszynski et al. 1984, Caron 1985, Sliter 1989, Premoli-Silva and Sliter 1995, Berggren et al. 1995). However, *Abathomphalus mayaroensis* taxon has diachronic last appearance, long stratigraphic range (~1.2 m.y.), and thrives in thermocline or deeper waters therefore it is generally absent in shallow neritic environments, such as Brazos River, Stevns Klint and Nye Kløv (Pardo et al. 1996). Because of these reasons, *A. mayaroensis* is a poor-stratigraphic marker. It hampers high-resolution biostratigraphy and thus completeness of the sedimentary record would not trustworthy (Pardo et al. 1996). In fact, in El Kef section (GSSP of the Danian Stage) *Abathomphalus mayaroensis* is extremely rare and disappears 4 m below the K-Pg boundary (Keller 1988a).

In the Haymana Basin, *Abathomphalus mayaroensis* was identified by various authors, such as Toker (1979, 1980) and Özkan-Altıner and Özcan (1999), whereas Amirov (2008, unpubl.) and Esmeray-Senlet et al. (2015) failed to find any in their samples. In our study, *Abathomphalus mayaroensis* was found but sporadically.

On the other hand, Robaszynski and Caron (1995) calibrated conventional globotruncanid biozonation with heterohelicids. In their correlation, *Gansserina gansseri* and *Abathomphalus mayaroensis* biozones corresponds to *Planoglobulina acervulinoides*, *Racemiguembelina fructicosa*, and *Pseudoguembelina hariaensis* zones, respectively.

Subsequently, Li and Keller (1998b) subdivided the Maastrichtian stage into nine CF zones. In their subdivision, the latest Maastrichtian *Abathomphalus mayaroensis* biozone correspond to four CF zones, which are: *Racemiguembelina fructicosa* (CF4),

Pseudoguembelina hariaensis (CF3), *Pseudoguembelina palpebra* (CF2), and *P. hantkeninoides* (CF1).

Plummerita hantkeninoides Zone was first proposed by Masters (1984) and subsequently by Pardo et al. (1996) as the latest subdivision of the Maastrichtian which marks last 170-200 ka prior to the K-Pg boundary. Currently, it is being highly used (e.g. Keller et al. 2002a, Arenillas et al. 2004, Abramovich et al. 2010, Coccioni and Premoli-Silva 2015). It is important to note that, *P. hantkeninoides* is a tropical species and absent in the middle and high latitudes (Li and Keller 1998b), and preferred to live in paleodepth corresponds to eutrophic shelf to upper-slope continental margins with no report from open-ocean carbonates (Huber et al. 2008 and references therein). In Haymana Basin, we were able to detect the *P. hantkeninoides* in our samples (see Table 5). Similar to the literature, our section corresponds to upper bathyal zone (see Paleobathymetry Chapter).

In total 3 biozones were established from upper Maastrichtian to lower Danian, which are: *Plummerita hantkeninoides* Zone, P0 Zone (*Guembelitria cretacea* zone), and Pα Zone (*Parvularugoglobigerina eugubina* zone).

For Cretaceous part CF zonation of Li and Keller (1998b) was used while biozonations of Berggren et al. (1995) and Berggren and Pearson (2005) were used for Paleocene. Biozonal correlation of this work with other K-Pg boundary studies was shown in Table 2.

2.2.1 *Plummerita hantkeninoides* Total Range Zone

Author: Masters 1984

Definition: This zone represents an interval from the first appearance datum (FAD) of the nominate taxon to the extinction horizon of large, complex, ornate tropical-subtropical Cretaceous taxa at or across the K-Pg boundary. It spans last 170-200 ka before the boundary (Pardo et al. 1996).

Estimated age: 66.170/66.200 to 66.0 (Age of the K-Pg boundary was taken from Ogg et al. 2016)

Remarks: Similar with Coccioni and Premoli Silva (2015), *Plummerita hantkeninoides* was rare and sporadic throughout our samples found only in two samples (UH-1 and UH-41). But, First Occurrence Datum (FOD) of the *P. hantkeninoides* corresponds to the first Cretaceous sample (UH-1), thus whole Maastrichtian interval (from UH-1 to UH-49) was characterized by *P. hantkeninoides* Zone. This zone has the same thickness for the Cretaceous part of the UH section which is 9.55 m. For planktonic foraminifera assemblage see Table 3 and 5.

In literature, the *P. hantkeninoides* Zone ranges 1.5 m, 3.45 m, 6 m, 8 m, 10 m of the uppermost Maastrichtian from Sinai (Egypt), Agost (Spain), El Kef (Tunisia), Negev (Israel), and Elles (Tunisia) sections, respectively (Farouk 2014, Pardo et al. 1996, Li and Keller 1998a, Abramovich and Keller 2002 and references therein). Additionally, Keller et al. (2002) claim that the presence of *P. hantkeninoides* more than uppermost 6 m suggests good estimates of the completeness of the latest Maastrichtian interval. Moreover, Abramovich and Keller (2002) calculated sedimentation rate of Elles section as 3.2 cm/1000 yr for 9.6 m *P. hantkeninoides* (CF1) Zone.

9.55-m-thick *P. hantkeninoides* Zone in the Haymana Basin may indicate approximately 3 cm/ 1000 yr sedimentation rate for our study area. If we take fore-arc setting of the Haymana Basin and the flysch deposits into account, a fairly high sedimentation rate of ~3 cm/1000 yr for our study area sound reliable.

2.2.2 P0 (*Guembelitria cretacea*) Partial Range Zone

Author: Keller 1988, emendation of Smit 1982

Estimated age: 65.0-64.97 Ma- earliest Paleocene (Danian), ~30 ka (Berggren and Pearson 2005).

Definition: This is a Partial Range Zone which represents an interval between mass extinction of the large, complex Cretaceous taxa (*Globotruncana*, *Planoglobulina*, *Rugoglobigerina* etc.), and first appearance datum (FAD) of *Parvularugoglobigerina eugubina*.

Remarks: This zone represents the first Danian biozone from K-Pg boundary (2-3 mm thick reddish layer) to the FOD of *Parvularugoglobigerina eugubina* (UKHB-4).

K-Pg boundary survivor and disaster opportunistic *Guembelitria cretacea* dominate this interval. In total, this biozone extends 25 cm. For planktonic foraminifera assemblage see Table 3 and 5.

2.2.3 Pα (*Parvularugoglobigerina eugubina*) Total Range Zone

Author: Liu (1993) emendation of Pα Zone of Blow (1979) and *Globigerina eugubina* Zone of Luterbacher and Premoli Silva (1964).

Estimated age: 64.97-64.8 Ma- early Paleocene (Danian), ~170 ka (Berggren and Pearson 2005).

Definition: This is total range zone which represents an interval between FAD and LAD of the nominate taxon.

Remarks: This zone starts 25 cm above the K-Pg boundary with FOD of nominate taxon (UKHB-4). Only the lowermost part of this zone was identified for now because our scope was primarily on Cretaceous-Paleogene transition.

Table 2. Correlation of Campanian-Maastrichtian and Danian Biozones and our biozonation for the Haymana Basin.

Age	Datum events	This Study	Huber *et al.* (2008)	Coccioni and Premoli-Silva 2015	Keller *et al.* 1995 Pardo *et al.* 1996 Li and Keller 1998b	Berggren *et al.* 1995 Berggren & Pearson 2005	Robaszynski & Caron 1995 Globotruncanids	Robaszynski & Caron 1995 Heterohelicids	Robaszynski *et al.* 1984-1984	Caron 1985	Olsson *et al.* 1999	Nederbragt 1991	Molina *et al.* 1996 Arz & Molina 2002	Arenillas *et al.* 2002 Stages	Arenillas *et al.* 2002 Benthic Foraminifera	Arenillas *et al.* 2004	
Danian	*Gl. compressa* *S. triloculinoides* *P.pseudobulloides* *P. eugubina* *P. eugubina*	UNZONED Pα *P. eugubina* P0 *G.cretacea*			P1c: P1c(2), P1c(1) P1b P1a: P1a(2), P1a(1) P0	P1: P1c *Gl. compressa/Pr.inconstans*; P1b *S. triloculinoides*; P1a *P. pseudobulloides* Pα *P. eugubina* P0 *G.cretacea*					P1c P1b P1a Pα P0		*Gl.compressa* *P.pseudobulloides* *P.eugubina* *G.cretacea*	Predominance of *Parasubbotina, Eoglobigerina, Globanomalina* Predominance of *Chiloguembelina, Woodringina* Predominance of *Parvularugoglobigerina, Globoconusa* Predominance of *Guembelitria*	Gradual increase of infaunal species Predominance of epifaunal species "Lazarus" effect in infaunal species	*P. pseudobulloides* *P. eugubina* *G.cretacea*	*S. triloculinoides* *E. trivalis* *E. simplicissima* *P. sabina* *P. longiapertura* *H. holmdelensis*
66.0																	
Maastrichtian	*P. hantkeninoides*	*P. hantkeninoides*	*Ps. hariaensis* *A.mayaroensis* *R. fructicosa* *Ps. palpebra*	*P. hantkeninoides* *P. elegans* *Ps. hariaensis* *A .mayaroensis* *C.contusa* *G. gansseri*	*P. hantkeninoides* CF1 *Ps. palpebra* CF2 *Ps. hariaensis* CF3 *R. fructicosa* CF4 *P. intermedia* CF5 *C. contusa* CF6 *G. gansseri* CF7	*A.mayaroensis*	*A.mayaroensis* *G. gansseri*	*Ps.hariaensis* *R.fructicosa* *P. acervulinoides*	*A.mayaroensis* *G. gansseri*	*A.mayaroensis* *G. gansseri*	*A.mayaroensis*	*Ps. hariaensis* *R. fructicosa* *P. acervulinoides*	*P. hantkeninoides* *Ps.hariaensis* *A. mayaroensis* *R. fructicosa* *P. acervulinoides* *R. scotti* *R. rotundata* *C. plicata* *R.hexacamerata/ G'na. aegyptiaca* *G'la. havanensis*	Terminal Maastrichtian assemblages -Predominance of *Heterohelix* -*Globotruncanids* abundant	Infaunal-epifaunal mixed assemblages		
72.1																	
Campanian			*G'la. havanensis*	*G'na. aegyptiaca* *G'la. havanensis*	*G'na. aegyptiaca* CF8 *G.subcarinatus* CF9		*G'na. aegyptiaca* *G'la havanensis*	*Ps. excolata* *P. elegans*	*G'na falsostuarti*	*G'na. aegyptiaca* *G'la. havanensis*		*Ps. excolata*					

CHAPTER 3

ABUNDANCE AND DIVERSITY TRENDS IN PLANKTONIC FORAMINIFERA ACROSS THE K-PG BOUNDARY BEDS

3.1 PLANKTONIC FORAMINIFERAL LIFE STRATEGY

There are two major types of life strategy within late Cretaceous planktonic foraminiferal community which are K-strategy and r-strategy. K-strategists are diverse ‘’ecological specialists’’ which have large, complex morphologies (e.g. trochospiral, multiserial) with robust and heavily-calcified tests with large number of chambers, and large apertures. They may possess highly ornamented tests with keels, spines and ridges. They have narrow tolerance for temperature, salinity, oxygen, and nutrient fluctuations. This group of taxa specialized in certain ecological niches therefore they occupy limited ecological niches and have restricted paleogeographic ranges (generally restricted to lower latitude environments). Also, they have long life spans and produce small number of offspring. Their sizes are generally above 100 μm. Globotruncanids, racemiguembelinids, planoglobulinids, rugoglobigerinids, and pseudotextularids are examples of this life strategy (Hallock 1985, Abramovich and Keller 2002, Keller et al. 2002, Punekar et al. 2014 and references therein).

On the other hand, r-strategists, which are considered as ‘’ecological generalists’’, are of small and simple morphologies with little surface ornamentation and shorter life spans. They have short prenatal period and produce large number of offspring, tolerate a variety of environments, and thus they have almost global paleogeographic distribution (Hallock 1985, Abramovich and Keller 2002, Keller et al. 2002). Biserial heterohelicids, low-trochospiral hedbergellids, planispiral globigerinelloids, triserial guembelitrids, and trochospiral globotruncanellids are examples for these taxa.

The K-Pg mass extinction resulted in total demise of these ecological specialists without any survivor left from these group. On the other hand, ecological generalists have 16 species survived in the Danian (Molina et al. 1996, Keller et al. 2002). This phenomenon demonstrates selective extinction among Cretaceous planktonic foraminiferal community (for more see Species Survivorship Chapter).

Within the group of generalists, *Guembelitria* species represent opportunistic life strategy after the K-Pg boundary. During absence of competitors, this group take advantage of disturbed and stressed environment and amplify its population exponentially (Pardo and Keller 2008). They retreat when nutrient levels insufficient to maintain their population growth which eventually open niches for recovery of other ecological generalists, first that of low oxygen tolerant biserials and subsequently small planispirals and trochospirals (Pardo and Keller 2008).

3.2 QUANTITATIVE ANALYSIS

In order to assess relative abundances of planktonic foraminifera before and after the K-Pg boundary, detailed quantitative work was carried out in two size fractions from 63-150 μm and >150 μm. Approximately an average of 380 and 394 individuals per sample were counted from representative splits of 63-150 μm and >150 μm fractions, respectively (see Table 3 and 5). All specimens were analyzed under Nikon SMZ-645 stereo-microscope, identified, picked, and mounted on slide holders.

3.2.1 63-150 μm SIZE FRACTION

Census and relative abundance data of the planktonic foraminiferal counts were shown in Table 3 and 4. This size fraction is dominated by ecological generalists (90% average relative abundance) with small, simple morphologies and fragile tests. Hardly ever large, complex and heavily ornamented ecological specialists were found in this size fraction. Three species correspond to an average 86% of the total population which are: *Heterohelix* (~54%), *Guembelitria* (~20%), and *Globigerinelloides* (~12%). Remaining assemblage is shared by *Hartella*, *Hedbergella*, and *Globotruncanella* species (see Table 4).

Table 3. Census data and species richness for population between 63-150 μm.

System	CRETACEOUS																			PALEOGENE			
Biozone	*P. hantkeninoides*																			P0			*P. eugubina*
Sample No	UH-30	UH-31	UH-32	UH-33	UH-34	UH-35	UH-36	UH-37	UH-38	UH-39	UH-40	UH-41	UH-42	UH-43	UH-44	UH-45	UH-46	UH-47	UH-48	UH-49	E+2cm	UH-50	UH-51	UH-52 (UHKB-4)
Split No	10 split	10 split	10 split	10 split	11 split	11 split	10 split	11 split	10 split	10 split	9 split	10 split	10 split	11 split	11 split	11 split	11 split	12 split	11 split	12 split	9 split	no split	no split	
Guembelitria cretacea	100	98	87	96	49	41	91	68	135	98	127	46	38	35	46	27	35	33	156	71	83			
Globotruncana hilli																		1						
Globotruncanita pettersi	1						2									1				1				
Globotruncanella citae	1	1		1				1	1															
G. havanensis	2	2									1						1							
G. petaloidea																2								
G. minuta		5	5	1	2	1	1	1	6		3		2				1	1		2				
Globotruncanella sp.	1								1				1	1		2	4							
Rugoglobigerina hexacamerata		1																						
R. macrocephala		1																						
Archaeoglobigerina blowi																1								
A. cretacea																	1							
Plummerita hantkeninoides	1																							
Hedbergella holmdelensis	6	5	11	4				2		1						11	3				1			
H. monmouthensis	6	2	1	2					1	1						2	4				2			
Hedbergella sp.	12	8	2	3	1					2	2	1				5								
Globigerinelloides subcarinatus	8	7	5	7	4	4	3	2	4	2	3	4	4	3	4	3	5	4	2					
G. prairiehillensis			1	1			1																	
G. asper	4	9	7	8	2	5	2	1	4	8	4	9	5	7	4	1		4	6	4		No Data.		
G. alvarezi	2	4	2	3	1	1	6	4	3	3	6	8	3	9	7	15	14	7	9	9	2	Recrystallization		
G. ultramicrus													1			3	6		2	3		and Poor		
G. rosebudensis	1	1																	3			Preservation		
G. mendezensis	1	1															1		1					
Globigerinelloides sp.	38	39	28	26	18	14	54	26	29	20	39	29	24	22	31	36	51	6	27	9	1			
Heterohelix globulosa	71	86	87	67	64	40	97	78	99	98	133	88	56	42	106	134	189	63	335	124	27			
H. labellosa							1																	
H. navarroensis	15	5	16	9	6	8	6	9	5	4	12	8	2	2	7	5	14	9	40	15	1			
H.planata	27	16	28	10	16	10	12	14	18	5	8	24	14	15	19	17	15	14	23	13	1			
H. punctulata			2	7	2	2	4		6	3	5	2	5	6	3	3	3	3	1					
Heterohelix sp.	41	39	29	44	56	40	75	39	80	54	83	60	45	33	80	97	167	32	115	42	23			
Laeviheterohelix dentata	13	8	13	5	4	4	6	2	3	6	18	20	4	14	18	4	6	10	20	18	2			
L. glabrans	7	16	6	3	6	2	3	5	12	13	10	11	1		2	2	2		3	4	1			
Pseudotextularia nuttalli		1		1	1																			
Pseudoguembelina costulata		2																1						
P. kempensis																	1							
Hartella harti	11	10	4	2	5	7	9	5	8	2	7	9	8	3	13	1	21	12	26	16				
Unidentified planktonic foraminifer	22	29	35	55	33	21	40	40	38	25	54	46	15	23	34	49	63	15	38	19	26			
Total Count	**391**	**396**	**369**	**355**	**270**	**200**	**413**	**297**	**453**	**345**	**515**	**365**	**228**	**215**	**374**	**421**	**607**	**215**	**807**	**350**	**170**			
Species Richness	18	21	15	17	13	12	15	13	14	13	13	11	13	10	11	17	18	13	14	12	9			
Average richness	**14**																							

Table 4. Relative abundances of population between 63-150 μm.

System	CRETACEOUS																				PALEOGENE			
Biozone	*P. hantkeninoides*																				P0			*P. eugubina*
Sample No	UH-30	UH-31	UH-32	UH-33	UH-34	UH-35	UH-36	UH-37	UH-38	UH-39	UH-40	UH-41	UH-42	UH-43	UH-44	UH-45	UH-46	UH-47	UH-48	UH-49	E+2cm	UH-50	UH-51	UH-52 (UHKB-4)
Split No	10 split	10 split	10 split	10 split	11 split	11 split	10 split	11 split	10 split	10 split	9 split	10 split	10 split	11 split	11 split	11 split	11 split	12 split	11 split	12 split	9 split	no split	no split	
Guembelitria cretacea	25,6	24,7	23,6	27,0	18,1	20,5	22,0	22,9	29,8	28,4	24,7	12,6	16,7	16,3	12,3	6,4	5,8	15,3	19,3	20,3	48,8			
Globotruncana hilli																		0,5						
Globotruncanita pettersi	0,3						0,5									0,2				0,3				
Globotruncanella citae	0,3	0,3		0,3				0,3	0,2															
G. havanensis	0,5	0,5									0,2						0,2							
G. petaloidea																0,5								
G. minuta		1,3	1,4	0,3	0,7	0,5	0,2	0,3	1,3		0,6		0,9				0,2	0,5		0,6				
Globotruncanella sp.	0,3								0,2				0,4	0,5		0,5	0,7							
Rugoglobigerina hexacamerata		0,3																						
R. macrocephala		0,3																						
Archaeoglobigerina blowi																0,2								
A. cretacea																	0,2							
Plummerita hantkeninoides	0,3																							
Hedbergella holmdelensis	1,5	1,3	3,0	1,1				0,7		0,3						2,6	0,5				0,6			
H. monmouthensis	1,5	0,5	0,3	0,6					0,2	0,3						0,5	0,7				1,2			
Hedbergella sp.	3,1	2,0	0,5	0,8	0,4					0,6	0,4	0,3				1,2								
Globigerinelloides subcarinatus	2,0	1,8	1,4	2,0	1,5	2,0	0,7	0,7	0,9	0,6	0,6	1,1	1,8	1,4	1,1	0,7	0,8	1,9	0,2					
G. prairiehillensis			0,3	0,3			0,2															No Data.		
G. asper	1,0	2,3	1,9	2,3	0,7	2,5	0,5	0,3	0,9	2,3	0,8	2,5	2,2	3,3	1,1	0,2		1,9	0,7	1,1		Recrystallization		
G. alvarezi	0,5	1,0	0,5	0,8	0,4	0,5	1,5	1,3	0,7	0,9	1,2	2,2	1,3	4,2	1,9	3,6	2,3	3,3	1,1	2,6	1,2	and Poor		
G. ultramicrus													0,4			0,7	1,0		0,2	0,9		Preservation		
G. rosebudensis	0,3	0,3																	0,4					
G. mendezensis	0,3	0,3															0,2		0,1					
Globigerinelloides sp.	9,7	9,8	7,6	7,3	6,7	7,0	13,1	8,8	6,4	5,8	7,6	7,9	10,5	10,2	8,3	8,6	8,4	2,8	3,3	2,6	0,6			
Heterohelix globulosa	18,2	21,7	23,6	18,9	23,7	20,0	23,5	26,3	21,9	28,4	25,8	24,1	24,6	19,5	28,3	31,8	31,1	29,3	41,5	35,4	15,9			
H. labellosa							0,2																	
H. navarroensis	3,8	1,3	4,3	2,5	2,2	4,0	1,5	3,0	1,1	1,2	2,3	2,2	0,9	0,9	1,9	1,2	2,3	4,2	5,0	4,3	0,6			
H.planata	6,9	4,0	7,6	2,8	5,9	5,0	2,9	4,7	4,0	1,4	1,6	6,6	6,1	7,0	5,1	4,0	2,5	6,5	2,9	3,7	0,6			
H. punctulata			0,5	2,0	0,7	1,0	1,0		1,3	0,9	1,0	0,5	2,2	2,8	0,8	0,7	0,5	1,4	0,1					
Heterohelix sp.	10,5	9,8	7,9	12,4	20,7	20,0	18,2	13,1	17,7	15,7	16,1	16,4	19,7	15,3	21,4	23,0	27,5	14,9	14,3	12,0	13,5			
Laeviheterohelix dentata	3,3	2,0	3,5	1,4	1,5	2,0	1,5	0,7	0,7	1,7	3,5	5,5	1,8	6,5	4,8	1,0	1,0	4,7	2,5	5,1	1,2			
L. glabrans	1,8	4,0	1,6	0,8	2,2	1,0	0,7	1,7	2,6	3,8	1,9	3,0	0,4		0,5	0,5	0,3		0,4	1,1	0,6			
Pseudotextularia nuttalli		0,3		0,3	0,4																			
Pseudoguembelina costulata		0,5																0,5						
P. kempensis																	0,2							
Hartella harti	2,8	2,5	1,1	0,6	1,9	3,5	2,2	1,7	1,8	0,6	1,4	2,5	3,5	1,4	3,5	0,2	3,5	5,6	3,2	4,6				
Unidentified planktonic foraminifer	5,6	7,3	9,5	15,5	12,2	10,5	9,7	13,5	8,4	7,2	10,5	12,6	6,6	10,7	9,1	11,6	10,4	7,0	4,7	5,4	15,3			
Total Count	**391**	**396**	**369**	**355**	**270**	**200**	**413**	**297**	**453**	**345**	**515**	**365**	**228**	**215**	**374**	**421**	**607**	**215**	**807**	**350**	**170**			

Heterohelix and *Guembelitria* Blooms

This study for the first time in Turkey demonstrates *Heterohelix* and *Guembelitria* dominance before, and *Guembelitria* bloom immediately after the K-Pg boundary.

It is important to note that *Laeviheterohelix* species, because of being a heterohelicid, were considered within the domain of *Heterohelix* genus. Addition of *Laeviheterohelix* spp. created an average of 4% increase in the total percentage of *Heterohelix* spp. *Heterohelix* species together with *Guembelitria cretacea* occupy more than 70% of the assemblage in 63-150 μm size fraction. Figure 25 represents relative abundance changes of *Heterohelix* and *Guembelitria* species.

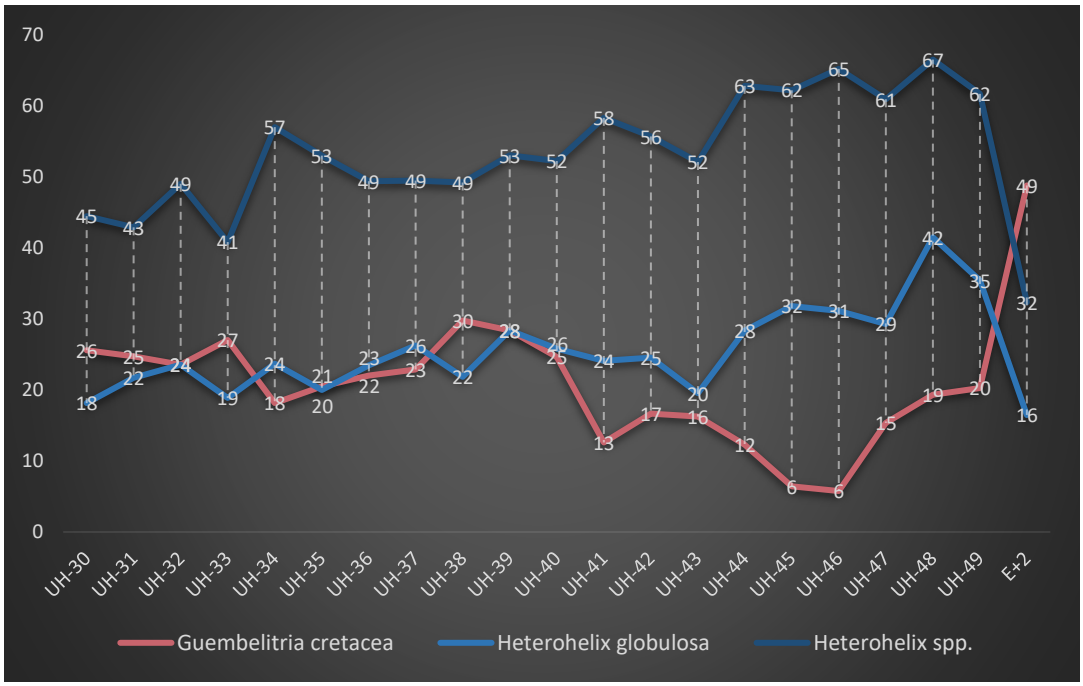

Figure 25. Relative abundance patterns of *Guembelitria cretacea*, *Heterohelix globulosa*, and *Heterohelix* spp. The K-Pg boundary is located between UH-49 and E+2. Before the boundary, *Guembelitria cretacea* has declining trend on the contrary to increasing trend in *Heterohelix globulosa* and total amount of heterohelicids (*Heterohelix* spp.). After the boundary, relative abundance of *Guembelitria cretacea* rapidly increases.

Throughout the Maastrichtian, total amount of low-oxygen tolerant heterohelicids (*Heterohelix* spp.) is more dominant than the disaster opportunistic *Guembelitria cretacea*. At UH-30, there is a 13% difference between total abundance of *Heterohelix* spp. and *Guembelitria cretacea*. As a result of different abundance trends in *Guembelitria cretacea* and *Heterohelix* spp., this gap grows through up-section to 42% by the 5 cm before the K-Pg boundary at UH-49.

Inverse correlation between *Guembelitria cretacea* and *Heterohelix* species can be clearly seen in Figure 25. Starting from UH-30, the relative abundance of low-oxygen tolerant heterohelicids gradually increase over time with intermittent drops (Fig. 25). Whereas *Guembelitria cretacea*, gradually decrease through time, until UH-46. These alternating blooms may depend on nutrient influx and/or sea level fluctuations (Keller and Pardo 2004b, Pardo and Keller 2008).

There are three major turning points exist in the relative abundance patterns of these species (Fig. 25). From UH-30 to UH-34 *Guembelitria cretacea* undergoes a decline trend whereas that of *Heterohelix* spp. increase. Conversely, between UH-34 and UH-38, total abundance of *Heterohelix* spp. decrease, while *Guembelitria cretacea* shows increasing values and reaches at its peak abundance (30%) in the Maastrichtian at UH-38. Starting from UH-38, *Heterohelix* spp. gradually increase and reach their highest value at 15 cm below the K-Pg boundary (at UH-48). On the contrary, from UH-38 to UH-46, *Guembelitria cretacea* gradually declines such that at UH-46 it corresponds to only 6% of the total assemblage. After that point, its relative abundance surges rapidly until the UH-49.

The K-Pg boundary is located in between UH-49 (5 cm below the boundary) and E+2 (corresponds 2 cm above the boundary). At UH-49 *Heterohelix* spp. dominate the population by 62% of relative abundance while *Guembelitria cretacea* corresponds to 20% of the total population. However, immediately after the K-Pg boundary, from UH-49 to at E+2, *Guembelitria cretacea* abruptly increases and corresponds to 49% of the total Danian assemblage. This sudden increase characterizes the ‘’bloom’’ of the disaster opportunistic *Guembelitria cretacea* in earliest Danian P0 Zone. It takes advantage of the environmental perturbation and during the absence of competitors it rapidly reproduces itself and dominates the environment (Keller and Pardo 2004b).

On the contrary, relative abundance of heterohelicids sharply drops after the boundary. Although a number of heterohelicids are present in sample E+2, they are not as dominant as *Guembelitria cretacea*.

Dominance of low oxygen tolerant *Heterohelix* species throughout the Maastrichtian samples and their increasing trend indicate expansion of oxygen minimum zone (OMZ) and might have associated with high sea level (Keller and Pardo 2004b). Whereas heterohelicid drops signal reduced OMZ, well-oxygenated water column and increased water mass stratification while high *Guembelitria* abundance is a proxy for nutrient-rich surface water (Keller and Pardo 2004b).

Keller and Pardo (2004b) reported varying amounts of *Heterohelix* and *Guembelitria* dominance before, and *Guembelitria* blooms right after the K-Pg boundary. Those blooms are found all across the world, such as Negev (Israel), Seldja (Tunisia), Agost (Spain), and Bjala (Bulgaria), Brazos (USA), Nye Kløv (Denmark), and Beloc (Haiti). They propose that *Guembelitria* blooms vary between 40-80% of relative abundance in low to middle latitudes in Danian P0 to P1a zones. In our study, *Guembelitria cretacea* reaches at 49% relative abundance at 2 cm above the boundary in Danian P0 Zone. Our findings agree with their scenario and reveal crucial information for worldwide correlation of these blooms both before and after the K-Pg boundary.

Relative abundance patterns of the remaining generalists are shown in Figure 26. *Globigerinelloides* species correspond to the third largest group within the 63-150 μm assemblage. They are common in our samples with an average of 12% relative abundance through the Maastrichtian. They have two major peaks at UH-36 and UH-43 which correspond to times of high water depth. Additionally, increasing trend in the paleobathymetric depth from UH-41 to UH-43 is also correlated with a flourish in the *Globigerinelloide*s species (Figs. 26, 30).

Hartella harti nov. gen., nov. sp. was first described by Georgescu and Abramovich (2009) from Maastrichtian samples of the Atlantic Ocean. Our study is one of the earliest studies which demonstrates its relative abundance within the Maastrichtian population (Table 4, Fig. 26). *Hartella harti* is consistently present in the 63-150 μm size fraction (see Table 3 and 4) and even sporadically occurs in some samples above

150 µm screen size (Table 5). Its relative abundance throughout the Maastrichtian within 63-150 µm fraction ranges only between 0,6 to 5,6% with an average of 2,4%. Yet, it shows increasing values starting from UH-45 and at 5 cm below the K-Pg boundary (UH-49), it reaches 4,6% relative abundance of the total population. No *Hartella harti* individual was encountered after the K-Pg boundary, thus this taxon might have undergone extinction at the boundary.

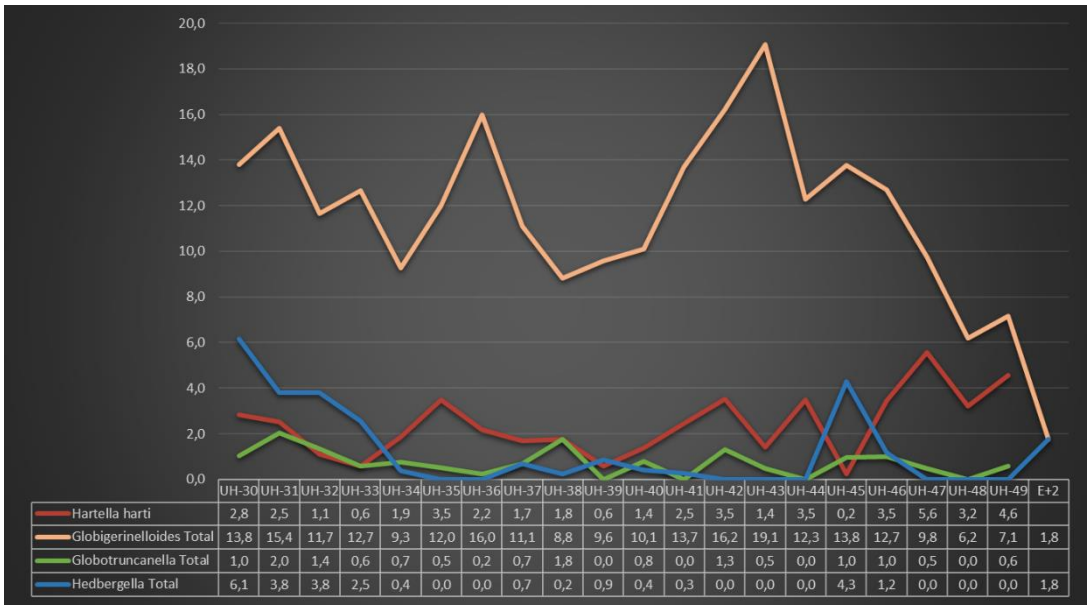

	UH-30	UH-31	UH-32	UH-33	UH-34	UH-35	UH-36	UH-37	UH-38	UH-39	UH-40	UH-41	UH-42	UH-43	UH-44	UH-45	UH-46	UH-47	UH-48	UH-49	E+2
Hartella harti	2,8	2,5	1,1	0,6	1,9	3,5	2,2	1,7	1,8	0,6	1,4	2,5	3,5	1,4	3,5	0,2	3,5	5,6	3,2	4,6	
Globigerinelloides Total	13,8	15,4	11,7	12,7	9,3	12,0	16,0	11,1	8,8	9,6	10,1	13,7	16,2	19,1	12,3	13,8	12,7	9,8	6,2	7,1	1,8
Globotruncanella Total	1,0	2,0	1,4	0,6	0,7	0,5	0,2	0,7	1,8	0,0	0,8	0,0	1,3	0,5	0,0	1,0	1,0	0,5	0,0	0,6	
Hedbergella Total	6,1	3,8	3,8	2,5	0,4	0,0	0,0	0,7	0,2	0,9	0,4	0,3	0,0	0,0	0,0	4,3	1,2	0,0	0,0	0,0	1,8

Figure 26. Relative abundances *Hartella harti*, *Globigerinelloides* spp., *Globotruncanella* spp., and *Hedbergella* spp., through Maastrichtian and earliest Danian.

In consequence of having less diverse generalists, species diversity in this size fraction is only average of 14 species (ranges between 21 and 10) (Fig. 28). The diversity gently declines as approaching to the K-Pg boundary, although it remains stable most of the studied interval. For survivors of the K-Pg boundary, see ‘’Species Survivorship’’ Chapter.

3.2.2 >150 μm SIZE FRACTION

Census data and relative abundances of >150 μm size fraction is shown Table 5 and Table 6. This size fraction is composed of a combination between highly diverse, large, ornamented ecological specialists (K-strategy species), such as *Globotruncana*, *Pseudotextularia*, *Rugoglobigerina*, *Planoglobulina*, *Racemiguembelina*, and smaller ecological generalists (r-strategists), such as *Heterohelix*, *Globigerinelloides*, and *Globotruncanella*.

Similar to 63-150 μm fraction, heterohelicids are again the most dominant group within >150 μm population with an average of 40% relative abundance (Table 5, 6). On the other hand, total abundance of large, ornamented, and diverse ecological specialists (K-strategy species) reach only 33% average richness before the boundary (between 39% and 19%, Fig. 27).

The specialist population are composed of: *Pseudotextularia* (9.4%), *Globotruncana* (7.3%), and *Planoglobulina* (6%) species with smaller amounts of *Globotruncanita* (4.1%), *Archaeoglobigerina* (1.9%), and *Rugoglobigerina* (1.8%) (Table 7). On the other hand, *Contusotruncana*, *Gansserina*, *Trinitella*, *Kuglerina*, *Plummerita*, *Gublerina*, *Racemiguembelina*, and *Abathomphalus* have minor abundances, thus their contributions are insignificant (Table 7).

Table 5. Census data, species diversities, and benthic counts of samples from >150 μm size fraction. Paleobathymetric calculations were done via two different formula (see Paleobathymetry Chapter) * Reworking exists in early Danian so only abundant and consistent ecological generalists were considered as survivors.

System	CRETACEOUS																			PALEOGENE			
Biozone	*P. hantkeninoides*																			P0			*P. eugubina*
Sample No	UH-30	UH-31	UH-32	UH-33	UH-34	UH-35	UH-36	UH-37	UH-38	UH-39	UH-40	UH-41	UH-42	UH-43	UH-44	UH-45	UH-46	UH-47	UH-48	UH-49	E+2cm	UH-50	UH-51	UH-52 (UHKB-4)
Split No	5 split	5 split	5 split	5 split	5 split	5 split	5 split	6 split	5 split	5 split	5 split	5 split	5 split	6 split	5 split	6 split	5 split	6 split	6 split	6 split	2 split	no split	no split	
Guembelitria cretacea		1	1	7	1	5	2	4	2	12										1				
Globotruncana aegyptiaca	4	4	3	6	7	4	1		1			1			2	5		2			3			
G. arca	3	5	6	8	2	3		1				3	7	1	4	7	7	4	2		1			
G. bulloides										1										1				
G. dupeublei			1	2		1	1			1	1		2		1									
G. esnehensis	13	2	4	12	4	4	4		1	9	11	2	2	5	11	4	6	9	2		1			
G. falsostuarti	1	3	3		4		3	1	4	1	3		2	2	1		3	1	1		1			
G. lapparenti				1																				
G. linneiana									3															
G. hilli	1	1		1					1	1	2	9	1											
G. mariei	8	6	14	6	6	4	1	3		7	1		1	1	2	12	10	1	6		2			
G. orientalis	5	1	3	5	8	4	2	4			3	1	1	1	1	8	1	2	2				1	
G. rosetta			2	1			2	2	3	2	1		1	1	3	1			4	1	2		2	
G. ventricosa							2	1				2	1		1									
Globotruncana sp.	7	5	12	7	3	7	5	3	5	7	9	7	6	5	13	10	9	8	4	3	3			
Globotruncanita angulata	3	1		1	5	1	1	1	5	2						2								
G. conica			1			1		1	1							1								
G. insignis	4			1			3	4	4	9	2	9	6	1	8	1		1	1		3			
G. pettersi	7	9	7	11	10	15	6	6	5	8	3	3	2	5	4	4	15	5	5	2	6			
G. stuarti		1		1		1		1			4		1				3		1		1			
G. stuartiformis	4	1	2	1	2			1	3	3	1	3	1	3	1	2	1	3	2					
Globotruncanita sp.	1			4	5	7	4	6	4	5	1	3	2	3		1	2		1		2			
Contusotruncana contusa																								
C. patelliformis	1	3		1	1												3				1			
C. plummerae																			1					
C. fornicata																								
C. plicata																2								
C. walfischensis																								
Contusotruncana sp.									2															
Globotruncanella pschadae	2	2	2	2	2	6			2	2			2	2		2			5		1			
G. havanensis	15	7	7	6	18	9	1	5	4	5	4	3	1	1	2	2	2	4	5	1	1		1	
G. petaloidea	3	9	6	7	4	1	2	1	1	5	1	2	2		3	1	2	1	2	2	3		1	
G. minuta	1	3	1		2	1		1	1	2	3				1									
Globotruncanella sp.	2		2	1	4	1	3	1	1	4	3	1	1				1	1						
Gansserina gansseri		1		1																				
G. wiedenmayeri		2		1										1				2						
Rugoglobigerina rugosa	11	5	6	3	7	11	2	1	9	3	4	10	3		1	1	1		4	3	1			
R. hexacamerata			2						3		1	4												
R. macrocephala				1				1	3	1		1							1					
R. milamensis	3	1	1	1	1	2		1																
R. pennyi	2	1	1	3	2	3			2				1					1	1					
Rugoglobigerina sp.	1		3	2		1	1	2	1	1	1	1									2			
Trinitella scotti	4	1	1	1			3	1	2	4	5	2						1			1			
Kuglerina rotundata	1																							
Archeoglobigerina blowi	6		1	2	5	3	6	10	7	2	11	1	4	1	2	13	16	8	4	1				
A. cretacea									1							1								
A. australis	1									3	2	1	2			2	2	5						
Archeoglobigerina sp.					2	1										3	4	2						
Plummerita reichelli	3		1		1				1			1			1									
Plummerita hantkeninoides	1											1												
Plummerita sp.					1	3			2	1		3		1										
Hedbergella holmdelensis	2	1		3	3	1			3				2	1		1					2			
H. monmouthensis	4	1	3	5	2	2	2	1	1	2	2		2				2	1	2	2	6			
H. sliteri				1							1													
Hedbergella sp.	1		1			1		1	1															
Globigerinelloides multispinus	4	18	23	21	7	5	1	2	1	4		4	5		4	1		3	4					
G. subcarinatus	10	14	7	6	3	12	1		4	3		3	6	2	5	3	2	4	2	4	2	1		
G. prairiehillensis								1	3	4		5	1		1			2	3		1	1		
G. asper	9	9	5	4	2	6			1	6		5	4	5	4	5		3	1	3	5	1	3	
G. ultramicrus																								
G. alvarezi			1			2	2	1	1	1	1	1	2	1	3	1		1	1					
G. bolli																								
G. rosebudensis	3	3	1		1								2	1		1								
G. mendezensis									1															
Globigerinelloides sp.	19	30	12	28	19	24	23	10	16	12	7	10	16	10	16		4		4		1		1	
Heterohelix globulosa	111	120	92	113	62	77	37	28	50	85	67	93	126	58	95	65	95	54	75	77	4	11	2	
H. labellosa	16	11	10	7	20	4	1	2	9	12	12	20	5	5	1	4	6	6	4				1	
H. navarroensis	1	1	2	1		3		1		4			9	1	2		1	4	3	2	1		2	
H.planata	12	12	15	22	6	31	21	18	10	11	8	15	9	9	16	10	8	10	8	5	2		1	
H. punctulata	31	24	26	16	16	25	10	10	16	6	2	12	13	8	12	12	7	3	4	10	1	1	1	
Heterohelix sp.	39	49	44	34	45	53	20	23	31	68	23	51	41	34	38	37	35	36	27	28	34	8		
Laeviheterohelix dentata	1	5	4	2	7	6	5	3	1	2	1		2	3	2	2	1	4	1	3	1			
L. glabrans	6	10	1	3	4	17	5	2	1	2		1				1	1		1	3	1			
Pseudotextularia elegans	12	12	21	9	4	8	10	4	6	11	7	15	6	1	1	13	3	3	6	3	1	4		
P. nuttalli	41	69	31	20	14	19	11	4	14	11	17	38	24	24	29	17	37	14	23	13	2	8	2	
P. intermedia	10	4	5	8	3	3	3		2	7	5	6	3	1	3	7	7	1	4	1	1	2		
Pseudotextularia sp.	6	6	5	8		7	3	3	7	3	3	1		1	2	8		4					1	
Planoglobulina acervulinodes	11	8	11	1	6	1	1	2	3	3	3	1	2	3	6	3	5	5	5			2		
P. brazoensis	2	3	3	2		1	2	3	5	4	1	5	5	6	5	3	3	3	3	5	3	1		
P. carseyae	28	24	20	12	6	6	8	6	3	11	10	12	11	5	16	13	12	3	11	6	2		1	
P. multicamerata															1									
Planoglobulina sp.	2	14	9	4	2	3	3	3	5	4	4	5	5	3	12	8	9	6	7	4	9			
Pseudoguembelina costulata				2		1			1	1	1		1	1	2									
P. excolata																								
P. hariaensis	2	1	3	5	8		2	1	3	4	1	1	4		2	1	2	1	6	2				
P. kempensis																								
P. palpebra	1		1	3		2		5	4				1	2	4	1		2	2	1	1			
Gublerina acuta																								
G. cuvilleri		3										1			1								1	
Racemiguembelina powelli	3	2	2			1	1					3	1				1							
R. fructicosa	2			2	1					1	2	1	2	1										
Abathomphalus intermedius													1						2					
A. mayaroensis		2			1	6				2						5					1			
Hartella hartl						1	1			2														
Unidentified planktonic	69	81	54	55	27	51	37	29	26	59	72	71	63	74	74	86	91	42	56	60	58	34		
Total Count	**576**	**612**	**505**	**504**	**376**	**478**	**266**	**226**	**313**	**446**	**327**	**454**	**426**	**294**	**419**	**393**	**420**	**276**	**319**	**247**	**174**	**74**	**21**	
BENTHIC COUNT	**297**	**227**	**231**	**253**	**247**	**181**	**197**	**133**	**256**	**328**	**228**	**284**	**162**	**79**	**194**	**148**	**223**	**152**	**139**	**117**				
Estimated Depth (m) by formula of Van der Zwaan et al. (1990)	372	476	408	380	305	469	275	334	252	277	290	318	468	586	405	471	363	353	424	398				
Average Depth (m)	**381**																							
Estimated Depth (m) by formula of De Rijk et al. (1999)	474	634	529	486	375	623	332	418	300	335	353	394	621	810	524	626	461	446	553	513				
Average Depth (m)	**490**																							
Species Richness	48	46	45	50	40	43	37	39	47	45	36	39	46	33	40	40	31	36	40	24	11*	5*	6*	
Average richness before K-Pg	40																							

Table 6. Relative abundance of the population from >150 μm size fraction.

System	CRETACEOUS																			PALEOGENE			
Biozone	*P. hantkeninoides*																			*P0*			*P. eugubina*
Sample No	UH-30	UH-31	UH-32	UH-33	UH-34	UH-35	UH-36	UH-37	UH-38	UH-39	UH-40	UH-41	UH-42	UH-43	UH-44	UH-45	UH-46	UH-47	UH-48	UH-49	E+2cm	UH-50	UH-51	UH-52 (UHKB-4)
Split No	5 split	5 split	5 split	5 split	5 split	5 split	5 split	6 split	5 split	5 split	5 split	5 split	5 split	6 split	5 split	6 split	5 split	6 split	6 split	6 split	2 split	no split	no split	
Guembelitria cretacea		0,2	0,2	1,4	0,3	1,0	0,8	1,8	0,6	2,7										0,4				
Globotruncana aegyptiaca	0,7	0,7	0,6	1,2	1,9	0,8	0,4		0,3			0,2			0,5	1,3		0,7			1,7			
G. arca	0,5	0,8	1,2	1,6	0,5	0,6		0,4				0,7	1,6	0,3	1,0	1,8	1,7	1,4	0,6		0,6			
G. bulloides										0,2										0,4				
G. dupeublei			0,2	0,4		0,2	0,4			0,2	0,3		0,5		0,2									
G. esnehensis	2,3	0,3	0,8	2,4	1,1	0,8	1,5		0,3	2,0	3,4	0,4	0,5	1,7	2,6	1,0	1,4	3,3	0,6		0,6			
G. falsostuarti	0,2	0,5	0,6		1,1		1,1	0,4	1,3	0,2	0,9		0,5	0,7	0,2		0,7	0,4	0,3		0,6			
G. lapparenti				0,2																				
G. linneiana									1,0															
G. hilli	0,2	0,2		0,2					0,3	0,2	0,6	2,0	0,2											
G. mariei	1,4	1,0	2,8	1,2	1,6	0,8	0,4	1,3		1,6	0,3		0,2	0,3	0,5	3,1	2,4	0,4	1,9		1,1			
G. orientalis	0,9	0,2	0,6	1,0	2,1	0,8	0,8	1,8			0,9	0,2	0,2	0,3	0,2	2,0	0,2	0,7	0,6				4,8	
G. rosetta			0,4	0,2			0,8	0,9	1,0	0,4	0,3		0,2	0,3	0,7	0,3			1,3	0,4	1,1		9,5	
G. ventricosa							0,8	0,4				0,4	0,2		0,2									
Globotruncana sp.	1,2	0,8	2,4	1,4	0,8	1,5	1,9	1,3	1,6	1,6	2,8	1,5	1,4	1,7	3,1	2,5	2,1	2,9	1,3	1,2	1,7			
Globotruncanita angulata	0,5	0,2		0,2	1,3	0,2	0,4	0,4	1,6	0,4						0,5								
G. conica			0,2			0,2		0,4	0,3							0,3								
G. insignis	0,7			0,2			1,1	1,8	1,3	2,0	0,6	2,0	1,4	0,3	1,9	0,3		0,4	0,3		1,7			
G. pettersi	1,2	1,5	1,4	2,2	2,7	3,1	2,3	2,7	1,6	1,8	0,9	0,7	0,5	1,7	1,0	1,0	3,6	1,8	1,6	0,8	3,4			
G. stuarti		0,2		0,2		0,2		0,4			1,2		0,2				0,7		0,3		0,6			
G. stuartiformis	0,7	0,2	0,4	0,2	0,5		0,4	0,4	1,0	0,7	0,3	0,7	0,2	1,0	0,2	0,5	0,2	1,1	0,6					
Globotruncanita sp.	0,2			0,8	1,3	1,5	1,5	2,7	1,3	1,1	0,3	0,7	0,5	1,0		0,3	0,5		0,3		1,1			
Contusotruncana contusa																								
C. patelliformis	0,2	0,5		0,2	0,3												0,7				0,6			
C. plummerae																			0,3					
C. fornicata																								
C. plicata																0,5								
C. walfischensis																								
Contusotruncana sp.									0,6															
Globotruncanella pschadae	0,3	0,3	0,4	0,4	0,5	1,3			0,6	0,4			0,5	0,7		0,5			1,6		0,6			
G. havanensis	2,6	1,1	1,4	1,2	4,8	1,9	0,4	2,2	1,3	1,1	1,2	0,7	0,2	0,3	0,5	0,5	0,5	1,4	1,6	0,4	0,6		4,8	
G. petaloidea	0,5	1,5	1,2	1,4	1,1	0,2	0,8	0,4	0,3	1,1	0,3	0,4	0,5		0,7	0,3	0,5	0,4	0,6	0,8	1,7		4,8	
G. minuta	0,2	0,5	0,2		0,5	0,2		0,4	0,3	0,4	0,9				0,2									
Globotruncanella sp.	0,3		0,4	0,2	1,1	0,2	1,1	0,4	0,3	0,9	0,9	0,2	0,2				0,2	0,4						
Gansserina gansseri		0,2		0,2																				
G. wiedenmayeri		0,3		0,2										0,3				0,7						
Rugoglobigerina rugosa	1,9	0,8	1,2	0,6	1,9	2,3	0,8	0,4	2,9	0,7	1,2	2,2	0,7		0,2	0,3	0,2		1,3	1,2	0,6			
R. hexacamerata			0,4						1,0		0,3	0,9												
R. macrocephala				0,2				0,4	1,0	0,2		0,2							0,3					
R. milamensis	0,5	0,2	0,2	0,2	0,3	0,4		0,4																
R. pennyi	0,3	0,2	0,2	0,6	0,5	0,6			0,6				0,2					0,4	0,3					
Rugoglobigerina sp.	0,2		0,6	0,4		0,2	0,4	0,9	0,3	0,2	0,3	0,2									1,1			
Trinitella scotti	0,7	0,2	0,2	0,2			1,1	0,4	0,6	0,9	1,5	0,4						0,4			0,6			
Kuglerina rotundata	0,2																							
Archaeoglobigerina blowi	1,0		0,2	0,4	1,3	0,6	2,3	4,4	2,2	0,4	3,4	0,2	0,9	0,3	0,5	3,3	3,8	2,9	1,3	0,4				
A. cretacea									0,3							0,3								
A. australis	0,2									0,7	0,6	0,2	0,5			0,5	0,5	1,8						
Archeoglobigerina sp.					0,5	0,2										0,8	1,0	0,7						
Plummerita reichelli	0,5		0,2		0,3				0,3			0,2			0,2									
Plummerita hantkeninoides	0,2											0,2												
Plummerita sp.					0,3	0,6			0,6	0,2		0,7		0,3										
Hedbergella holmdelensis	0,3	0,2		0,6	0,8	0,2			1,0				0,5	0,3		0,3					1,1			
H. monmouthensis	0,7	0,2	0,6	1,0	0,5	0,4	0,8	0,4	0,3	0,4	0,6		0,5				0,5	0,4	0,6	0,8	3,4			
H. sliteri				0,2							0,3													
Hedbergella sp.	0,2		0,2			0,2		0,4	0,3															
Globigerinelloides multispinus	0,7	2,9	4,6	4,2	1,9	1,0	0,4	0,9	0,3	0,9		0,9	1,2		1,0	0,3		1,1	1,3					
G. subcarinatus	1,7	2,3	1,4	1,2	0,8	2,5	0,4		1,3	0,7		0,7	1,4	0,7	1,2	0,8	0,5	1,4	0,6	1,6	1,1	1,4		
G. prairiehillensis								0,4	1,0	0,9		1,1	0,2		0,2			0,7	0,9		0,6	1,4		
G. alvarezi			0,2			0,4	0,8	0,4	0,3	0,2	0,3	0,2	0,4	0,3	0,7	0,3		0,4	0,3					
G. bolli																								
G. rosebudensis	0,5	0,5	0,2		0,3								0,5	0,3		0,3								
G. mendezensis									0,3															
Globigerinelloides sp.	3,3	4,9	2,4	5,6	5,1	5,0	8,6	4,4	5,1	2,7	2,1	2,2	3,8	3,4	3,8		1,0		1,3		0,6		4,8	
Heterohelix globulosa	19,3	19,6	18,2	22,4	16,5	16,1	13,9	12,4	16,0	19,1	20,5	20,5	29,6	19,7	22,7	16,5	22,6	19,6	23,5	31,2	2,3	14,9	9,5	
H. labellosa	2,8	1,8	2,0	1,4	5,3	0,8	0,4	0,9	2,9	2,7	3,7	4,4	1,2	1,7	0,2	1,0	1,4	2,2	1,3				4,8	
H. navarroensis	0,2	0,2	0,4	0,2		0,6		0,4		0,9			2,1	0,3	0,5		0,2	1,4	0,9	0,8	0,6		9,5	
H.planata	2,1	2,0	3,0	4,4	1,6	6,5	7,9	8,0	3,2	2,5	2,4	3,3	2,1	3,1	3,8	2,5	1,9	3,6	2,5	2,0	1,1		4,8	
H. punctulata	5,4	3,9	5,1	3,2	4,3	5,2	3,8	4,4	5,1	1,3	0,6	2,6	3,1	2,7	2,9	3,1	1,7	1,1	1,3	4,0	0,6	1,4	4,8	
Heterohelix sp.	6,8	8,0	8,7	6,7	12,0	11,1	7,5	10,2	9,9	15,2	7,0	11,2	9,6	11,6	9,1	9,4	8,3	13,0	8,5	11,3	19,5	10,8		
Laeviheterohelix dentata	0,2	0,8	0,8	0,4	1,9	1,3	1,9	1,3	0,3	0,4	0,3		0,5	1,0	0,5	0,5	0,2	1,4	0,3	1,2	0,6			
L. globrans	1,0	1,6	0,2	0,6	1,1	3,6	1,9	0,9	0,3	0,4		0,2				0,3	0,2		0,3	1,2	0,6			
Pseudotextularia elegans	2,1	2,0	4,2	1,8	1,1	1,7	3,8	1,8	1,9	2,5	2,1	3,3	1,4	0,3	0,2	3,3	0,7	1,1	1,9	1,2	0,6	5,4		
P. nuttalli	7,1	11,3	6,1	4,0	3,7	4,0	4,1	1,8	4,5	2,5	5,2	8,4	5,6	8,2	6,9	4,3	8,8	5,1	7,2	5,3	1,1	10,8	9,5	
P. intermedia	1,7	0,7	1,0	1,6	0,8	0,6	1,1		0,6	1,6	1,5	1,3	0,7	0,3	0,7	1,8	1,7	0,4	1,3	0,4	0,6	2,7		
Pseudotextularia sp.	1,0	1,0	1,0	1,6		1,5	1,1	1,3	2,2	0,7	0,9	0,2		0,3	0,5	2,0		1,4					4,8	
Planoglobulina acervulinodes	1,9	1,3	2,2	0,2	1,6	0,2	0,4	0,9	1,0	0,7	0,9	0,2	0,5	1,0	1,4	0,8	1,2	1,8	1,6			2,7		
P. brazoensis	0,3	0,5	0,6	0,4		0,2	0,8	1,3	1,6	0,9	0,3	1,1	1,2	2,0	1,2	0,8	0,7	1,1	0,9	2,0	1,7	1,4		
P. carseyae	4,9	3,9	4,0	2,4	1,6	1,3	3,0	2,7	1,0	2,5	3,1	2,6	2,6	1,7	3,8	3,3	2,9	1,1	3,4	2,4	1,1		4,8	
P. multicamerata															0,2									
Planoglobulina sp.	0,3	2,3	1,8	0,8	0,5	0,6	1,1	1,3	1,6	0,9	1,2	1,1	1,2	1,0	2,9	2,0	2,1	2,2	2,2	1,6	5,2			
Pseudoguembelina costulata				0,4		0,2			0,3	0,2	0,3		0,2	0,3	0,5									
P. excolata																								
P. hariaensis	0,3	0,2	0,6	1,0	2,1		0,8	0,4	1,0	0,9	0,3	0,2	0,9		0,5	0,3	0,5	0,4	1,9	0,8				
P. kempensis																								
P. palpebra	0,2		0,2	0,6		0,4		2,2	1,3				0,2	0,7	1,0	0,3		0,7	0,6	0,4	0,6			
Gublerina acuta																								
G. cuvilleri		0,5										0,2			0,2								4,8	
Racemiguembelina powelli	0,5	0,3	0,4			0,2	0,4					0,7	0,2				0,2							
R. fructicosa	0,3			0,4	0,3					0,2	0,6	0,2	0,5	0,3										
Abathomphalus intermedius													0,2						0,6					
A. mayaroensis		0,3			0,3	1,3				0,4						1,3					0,6			
Hartella hartí						0,2	0,4			0,4														
Unidentified planktonic foraminifer	12,0	13,2	10,7	10,9	7,2	10,7	13,9	12,8	8,3	13,2	22,0	15,6	14,8	25,2	17,7	21,9	21,7	15,2	17,6	24,3	33,3	45,9		
Total Count	576	612	505	504	376	478	266	226	313	446	327	454	426	294	419	393	420	276	319	247	174	74	21	

Table 7. Close view to relative abundances of ‘’ecological specialists’’ in >150 μm fraction.

System	CRETACEOUS																				PALEOGENE		*Ave% Before K-Pg*
Sample No	UH-30	UH-31	UH-32	UH-33	UH-34	UH-35	UH-36	UH-37	UH-38	UH-39	UH-40	UH-41	UH-42	UH-43	UH-44	UH-45	UH-46	UH-47	UH-48	UH-49	UH-50	UH-51	
***Globotruncana* TOTAL**	7,3	4,4	9,5	9,7	9,0	5,6	7,9	6,6	5,8	6,5	9,5	5,5	5,6	5,4	9,3	12,0	8,6	9,8	6,6	2,0			**7,3**
***Globotruncanita* TOTAL**	3,3	2,0	2,0	3,8	5,9	5,2	5,6	8,8	7,0	6,1	3,4	4,0	2,8	4,1	3,1	2,8	5,0	3,3	3,1	0,8			**4,1**
***Contusotruncana* TOTAL**	0,2	0,5	0,0	0,2	0,3	0,0	0,0	0,0	0,6	0,0	0,0	0,0	0,0	0,0	0,0	0,5	0,7	0,0	0,3	0,0			**0,2**
***Gansserina* TOTAL**	0,0	0,5	0,0	0,4	0,0	0,0	0,0	0,0	0,0	0,0	0,0	0,0	0,0	0,3	0,0	0,0	0,0	0,7	0,0	0,0			**0,1**
***Rugoglobigerina* TOTAL**	3,0	1,1	2,6	2,0	2,7	3,6	1,1	2,2	5,8	1,1	1,8	3,5	0,9	0,0	0,2	0,3	0,2	0,4	1,9	1,2			**1,8**
***Trinitella + Kuglerina* TOTAL**	0,9	0,2	0,2	0,2	0,0	0,0	1,1	0,4	0,6	0,9	1,5	0,4	0,0	0,0	0,0	0,0	0,0	0,4	0,0	0,0			**0,3**
Arheoglobigerina TOTAL	1,2	0,0	0,2	0,4	1,9	0,8	2,3	4,4	2,6	1,1	4,0	0,4	1,4	0,3	0,5	4,8	5,2	5,4	1,3	0,4			**1,9**
***Plummerita* TOTAL**	0,7	0,0	0,2	0,0	0,5	0,6	0,0	0,0	1,0	0,2	0,0	1,1	0,0	0,3	0,2	0,0	0,0	0,0	0,0	0,0			**0,2**
***Pseudotextularia* TOTAL**	12,0	14,9	12,3	8,9	5,6	7,7	10,2	4,9	9,3	7,2	9,8	13,2	7,7	9,2	8,4	11,5	11,2	8,0	10,3	6,9			**9,4**
***Planoglobulina* TOTAL**	7,5	8,0	8,5	3,8	3,7	2,3	5,3	6,2	5,1	4,9	5,5	5,1	5,4	5,8	9,5	6,9	6,9	6,2	8,2	6,1			**6,0**
***Pseudoguembelina* TOTAL**	0,5	0,2	0,8	1,6	2,1	0,4	0,8	2,7	2,2	0,9	0,3	0,2	1,2	0,7	1,4	0,5	0,5	1,1	2,5	1,2			**1,1**
***Gublerina* TOTAL**	0,0	0,5	0,0	0,0	0,0	0,0	0,0	0,0	0,0	0,0	0,0	0,2	0,0	0,0	0,2	0,0	0,0	0,0	0,0	0,0			**0,0**
***Racemiguembelina* TOTAL**	0,9	0,3	0,4	0,4	0,3	0,2	0,4	0,0	0,0	0,2	0,6	0,9	0,7	0,3	0,0	0,0	0,2	0,0	0,0	0,0			**0,3**
***Abathomphalus* TOTAL**	0,0	0,3	0,0	0,0	0,3	1,3	0,0	0,0	0,0	0,4	0,0	0,0	0,2	0,0	0,0	1,3	0,0	0,0	0,6	0,0			**0,2**
Specialists Combined	**37**	**33**	**37**	**31**	**32**	**28**	**35**	**36**	**40**	**30**	**36**	**35**	**26**	**27**	**33**	**40**	**39**	**35**	**35**	**19**			**33**

Figure 27 represents relative abundance variations of ecological specialists and generalists in >150 μm size fraction. A conspicuous pattern can be seen that once generalists increase the specialists decrease (or the opposite pattern). This converse relation between these two life forms may suggest niche competition. When environment becomes more suitable for one group to proliferate, their population increases whereas that of the other group drops.

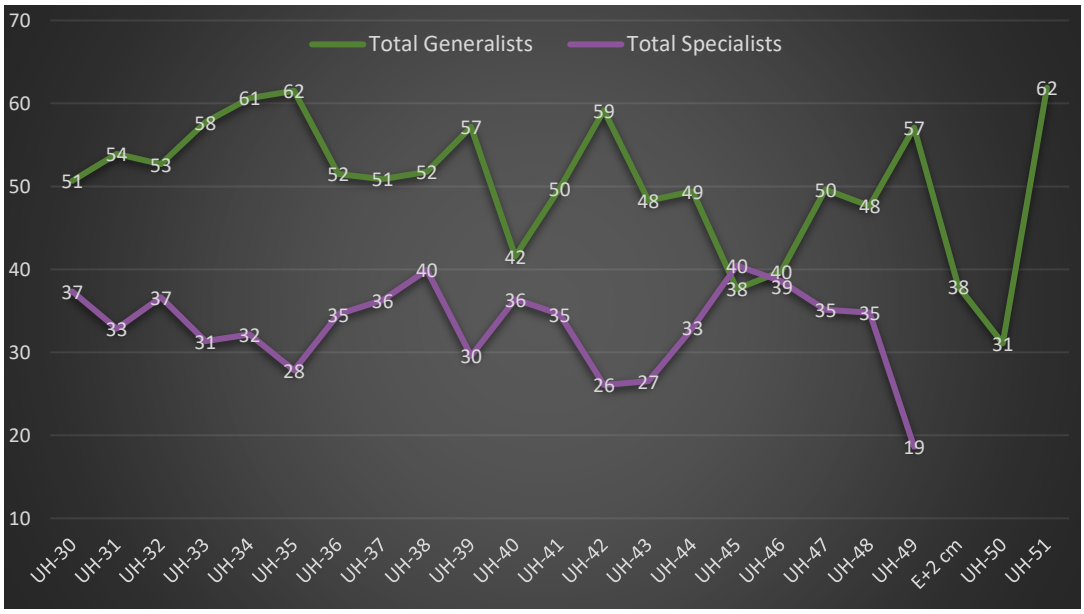

Figure 27. Relative abundance variations of generalists and specialists in >150 size fraction. Please note the increase in abundance of ecological generalists after the K-Pg boundary. There is no survivor amongst ecological specialists from the K-Pg boundary. Relative abundance values after the K-Pg boundary may not truly represent the planktonic foraminifera assemblage due to reworking and ill-preserved taxa (see Table 5).

Late Maastrichtian optimum environment is characterized by high diversity of large, complex and specialized K-strategists (ecological specialists) and background of small, low diversity r-strategists. These environments have high species richness (~55-60 species >63 µm), and under dominance of *Heterohelix* species within oligotrophic open marine settings (Pardo and Keller 2008).

Figure 28 represents species diversities of two size fraction (i.e. 63-150 µm, >150 µm), and the total diversity (i.e. >63 µm).

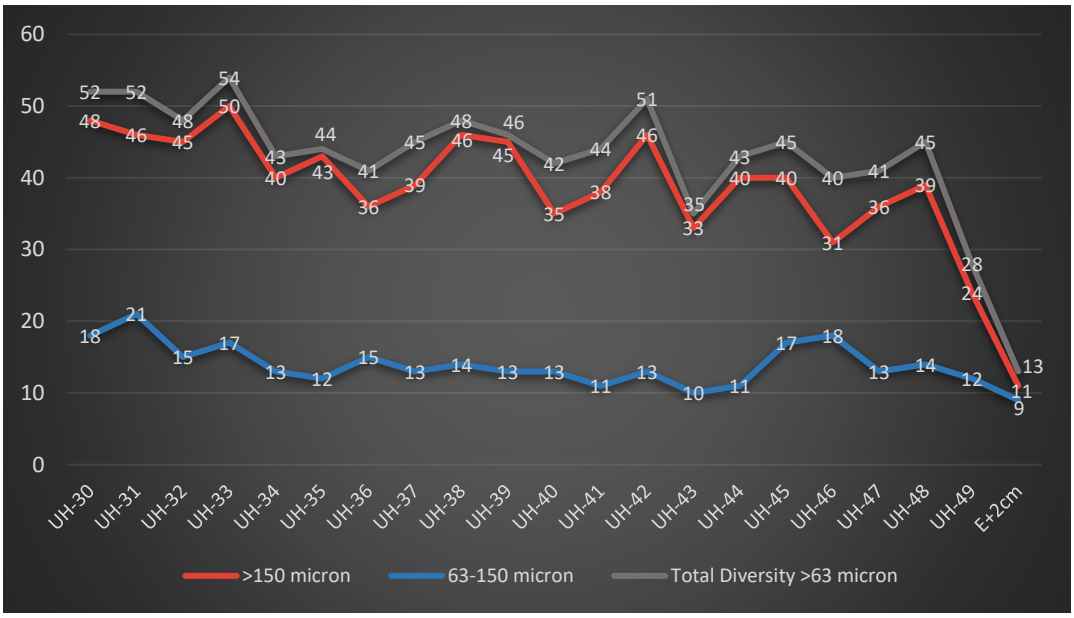

Figure 28. Species diversities of populations from 63-150 µm, >150 µm, and the total (>63 µm). Please note the diversity difference between 63-150 µm and >150 µm fractions and the contribution of the population from >150 µm fraction to the total diversity.

As demonstrated in Figure 28, it is clear that large, ornamented K-strategists within >150 µm fraction are the major contributor of the late Maastrichtian total diversity. There is only a slight difference between total diversity and the diversity in >150 µm fraction. This slight deviation may be resulted from presence of small species only in smaller (63-150 µm) fraction.

It is noteworthy that diversity of >150 μm fraction vary largely which results in similar response in the total diversity (Fig. 28). However, diversity of the 63-150 μm fraction reveals only slight changes. It may be due to the fact that this fraction chiefly composed of small-sized ecological generalists which are generally less diverse. In fact, they are highly capable to tolerate wide range of environmental variabilities, so any change in the environment may not be well-responded by this group.

On the other hand, highly specialized large species (ecological specialists) are common in >150 μm fraction. They occupy restricted habitats and thus vulnerable to temperature, nutrient and oxygen variations so any change in the environment may create huge variations in the richness of the large fraction.

Moreover, although there are some increases (especially in >150 μm fraction and in the total), species diversities of both fractions decline through Maastrichtian (Fig. 28). This decline is more prominent especially in >150 μm fraction. These drops eventually result in 45% (from 54 to 28) decrease in the total species diversity from UH-30 to UH-49 (5 cm before the K-Pg boundary).

This drop occurred by three major intervals which are: from UH-33 to 34, UH-42 to 43, and UH-48 to 49. First drop between UH-33 to 34 eliminated 20% of the total population. Subsequent drop between UH-42 to UH-43 ruled out 31% of the total diversity. The final and the most severe drop happened in between UH-48 to UH-49 which corresponds to 15 cm and 5 cm below the K-Pg boundary. This interval removed 38% of the late Cretaceous taxa just before the K-Pg boundary.

Overall, 45% of the planktonic foraminifera were eliminated in function of the step by step drops from UH-30 to UH-49 within 3.75 m. This phenomenon demonstrates environmental stress before the K-Pg boundary. It may be caused by Deccan volcanism or fore-arc setting of the Haymana Basin during late Maastrichtian.

The K-Pg mass extinction is selective on the planktonic foraminiferal community. All survivors are small, cosmopolitan, low-diversity r-strategists (ecological generalists) found in both size fractions. However, large, complex, specialized tropical and subtropical K-strategists (ecological specialists), found only in >150 μm fraction, completely annihilated.

The K-Pg boundary mass extinction eliminated 25% (from 12 to 9 species) of the population from 63-150 μm fraction. However, in consequence of total extinction of larger species, the diversity of >150 μm fraction dropped by 54% (from 24 to 11). Similarly, the total diversity (>63 μm) also decreased by 54% (from 28 to 13) (Fig. 28).

3.3 SPECIES SURVIVORSHIP

After the K-Pg boundary, species diversity of 63-150 μm fraction was investigated only in one sample at 2 cm above the boundary (E+2) since this sample was the only one which permitted fossil identification. Almost all fragments in samples UH-50 and UH-51 are recrystallized. On the other hand, three samples were examined in >150 μm fraction, albeit reworking exists. Therefore, ‘’survivors’’ were selected from those which revealed continuous and relatively abundant. Yet, some individuals which are not consistent in our samples but marked as survivor in the literature were also considered as survivor in this study.

In this regard, *Guembelitria cretacea*, *Heterohelix globulosa* and *Globigerinelloides asperum* are present and abundant in each fraction, therefore they considered as survivor. Additionally, in sample E+2, *Heterohelix planata*, *Heterohelix navarroensis*, *Heterohelix punctulata*, *Laeviheterohelix dentata*, *Laeviheterohelix glabrans*, *Hedbergella holmdelensis*, *Hedbergella monmouthensis*, *Globigerinelloides alvarezi*, *Globigerinelloides prairiehillensis* and *Globigerinelloides subcarinatus* were found both size fractions (Fig. 29). Although there are some differences in 2 or 3 species, these species are also considered as survivor in the literature (Keller et al. 1995, Molina et al. 1996, 1998, Keller et al. 2002b, Keller et al. 2013). Therefore, they were put in the survivor category.

In total, 13 out of 28 species above >63 μm fraction were considered as survivors with approximately 46% survival rate (54% extinction rate). Our survival rate in this study is more that findings of Keller et al. (1993, 2002b) in which they found near one third of the Cretaceous planktonic foraminifera survived into the Danian.

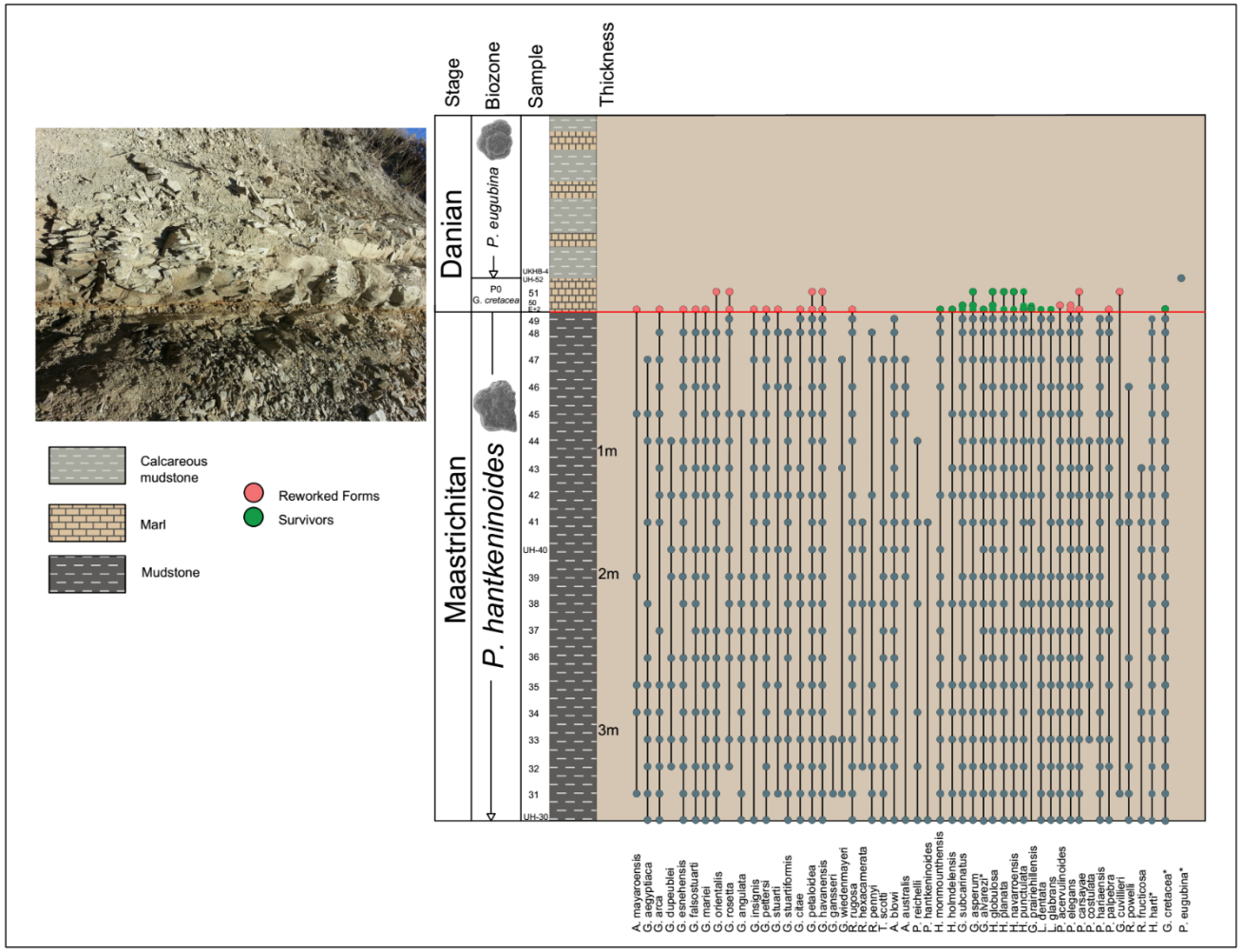

Figure 29. In total 13 species were considered as survivor. * represents presence between 63- 150 µm fraction.

3.4 PALEOBATHYMETRY OF THE STUDIED SECTION

Depositional depth of the study area was calculated via planktonic-benthic ratios of the >150 μm size fraction (Table 5). In order to do that, firstly remaining benthic foraminifera of the representative splits were counted from each sample (Table 5). Then, planktonic foraminiferal fraction (%P) within total abundance of foraminiferal community was calculated. The following formula represents %P fraction at which P and B denotes total numbers of planktonic and benthic foraminifera:

$$\%P = \left(\frac{P}{P+B}\right) \times 100$$

Two different paleodepth calculations were done for our study area in Haymana Basin by following formulas of Van der Zwaan et al. (1990) and De Rijk (1999).

Van der Zwaan et al. (1990) and subsequently Van Hinsbergen et al. (2005) posit that deep infaunal species (%S) should be excluded from the %P calculation, as they live below the sediment-water interface and they are not depended on organic matter flow to the sea floor. Moreover, Van Hinsbergen et al. (2005) claim that the best paleobathymetric estimation would be obtained from: a) samples with very low %S levels, and b) well-ventilated intervals because %P value is highly sensitive to oxygen depletion in poorly-ventilated basins.

Paleobathymetric estimation formula of Van der Zwaan et al. (1990) is:

$$Depth\ (D) = e^{3.58718+(0.03534*\%P)}$$

Apart from Van der Zwaan et al (1990), De Rijk et al (1999) studied 15 recent Mediterranean transects and established following regression these sections:

$$Depth\ (D) = e^{(\%P+81.9)/24}$$

Their %P calculation differs from that of Van der Zwaan et al. (1990) and Van Hinsbergen et al. (2005) as they do not deduct deep infaunal species (S) from the %P equation. In our study, no infaunal benthic foraminifera (S) was also subtracted from the %P calculation.

Figure 30 represents estimated paleodepths in our study area by following two different formula. By regression of Van der Zwaan et al. (1990), an average of 380 m paleodepth was found, whereas calculation from formula of De Rijk et al. (1999) revealed about 490 m water depth. Both graphs have almost identical responses to paleobathymetric changes and they have an average of 110 m difference between their depth estimations. It is noteworthy that difference between these two calculations becomes smaller during shallower water depths (Fig. 30). For example, at UH-38, there is only 48 m difference, whereas at UH-43 there is 224 m disparity.

Calculations from Van der Zwaan et al. (1990) and De Rijk et al (1999) have 83 m and 126 m standard deviations, respectively. Moreover, standard error for Van der Zwaan et al. (1990) is 11 m, and for De Rijk et al. (1999) is 20 m.

Overall, formula of De Rijk et al. (1999) represented an average of 490 m paleodepth which corresponds to upper bathyal level (according to palebathymeric subdivision of Berggren and Miller 1989). Likewise, calculation from Van der Zwaan et al. (1990) yielded an average of 381 m water depth which also fall into upper bathyal zone.

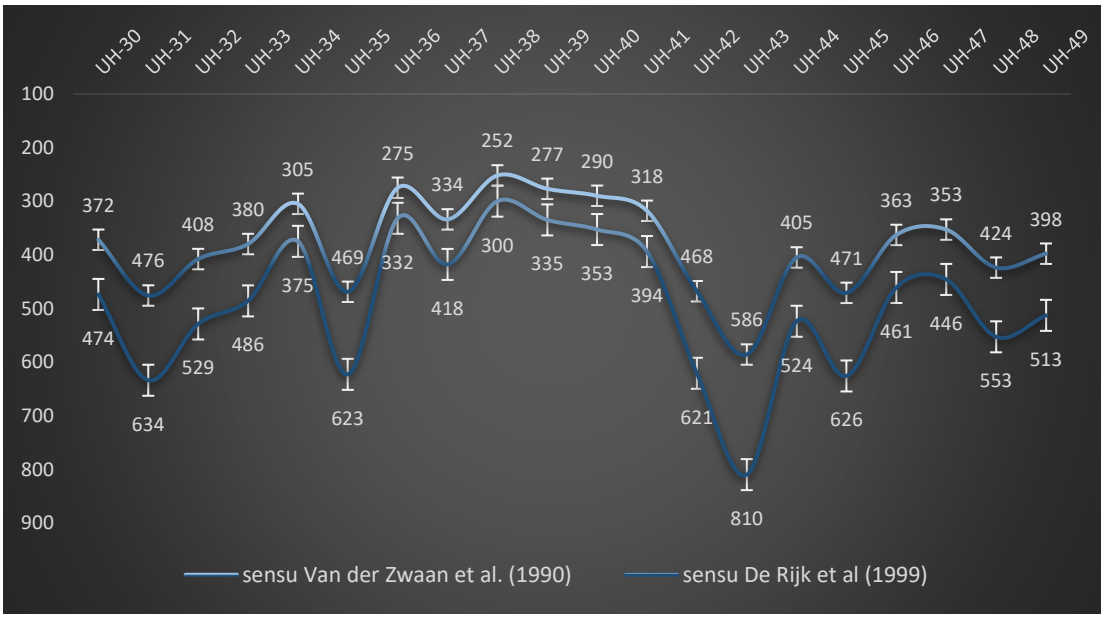

Figure 30. Paleobathymetric variations through Maastrichtian from formula of Van der Zwaan et al. (1990): upper graph, and De Rijk et al. (1999): lower graph. White bars represent standard errors.

Although Van Hinsbergen et al. (2005) claim that some corrections are necessary in order to obtain reliable paleobathymetric estimations, such as correction for eustatic sea level changes and for flexural effects, this study, without doing them, was able to represent more or less sound portrayal of the depositional area.

Additionally, Abramovich et al. (2003) revealed *Planoglobulina multicamerata*, *Heterohelix rajagopalani*, *Abathomphalus mayaroensis*, *Globotruncanella havanensis*, *Gublerina cuvillieri* and *Laeviheterohelix glabrans* occupy sub-thermocline (deep) habitats. Presence of these forms in our study may corroborate our paleodepth estimation since they dwell at relatively deeper waters.

Ultimately, these two depth formulas yielded an average of approximately 400 m paleobathymetry for our study area corresponding upper bathyal zone. Comparison of our section (i.e. Haymana Basin) with other K-Pg boundary localities are shown in Figure 31.

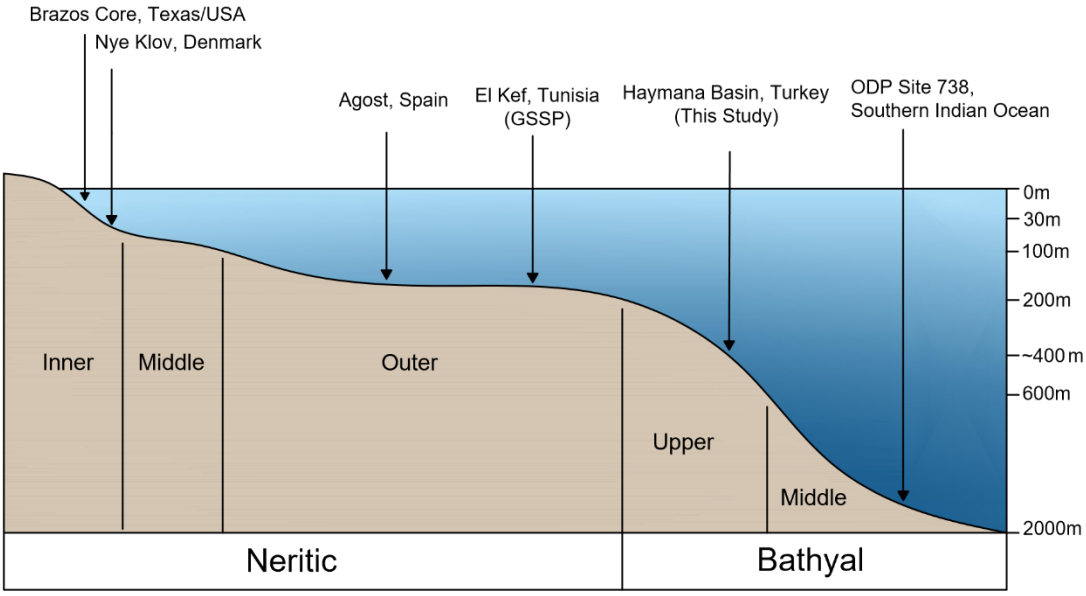

Figure 31. Paleodepth of the study area in the Haymana Basin and its comparison with worldwide K-Pg boundary sections. Image modified after MacLeod and Keller 1994 and Molina et al. 2006 and references therein.

3.5 PLANKTONIC FORAMINIFERAL DEPTH HABITATS

Very few studies had been done on depth habitats of Cretaceous planktonic foraminifera before the pioneering works of Saito and Van Donk (1974) and Douglas and Savin (1978). It was Saito and Van Donk (1974) who for the first time differentiated planktonic foraminifera from their benthic counterparts by demonstrating oxygen and carbon isotope values. Before them, paleontologists empirically identify a planktonic foraminifer if: it has a wide geographic distribution, its abundance increase in deep-sea basins, and its test morphology resemble to modern planktonic foraminifera. Earlier, Sliter (1972) mentioned depth distribution of planktonic foraminifera of shelf to slope environments. He claimed that towards shallow-water habitats heterohelicids and globigerinellids increase coupled with a surge of hedbergellids, whereas deep-water settings are dominated by globotruncanids and less common in heterohelicids, hedbergellids and globigerinellids. Accordingly, Saito and Van Donk (1974) represented that single-keeled globotruncanids show heavier oxygen isotope values (i.e. colder water) than double-keeled ones while pseudotextularids show the heaviest value. They also discovered depth-stratification of planktonic foraminifera of various geologic time.

Subsequently, Douglas and Savin (1978) analyzed oxygen isotopes of Cretaceous to Cenozoic planktonic foraminifera and found out they were depth-stratified over the last 100 million years. Changes in temperature and salinity with depth governs the habitat preference of planktonic foraminifera. They classified depth habitats of a well-stratified tropical ocean into three categories: shallow (20-50 m), intermediate (100-200 m), and deep (200-400 m) habitats. In waters shallower than 100 m, planktonic foraminiferal density is at its highest and sharply decreases as it gets deeper. Likewise, within range of 100-400 m, planktonic foraminifera assemblage is almost 10% of the population density of the uppermost 100 m. They suggested that owing to the dependence of planktonic foraminifera to phytoplankton as a food source, there must be a depth limit below which is unfavorable for them the thrive. They predicted that the lowermost depth limit of planktonic foraminifera would not far from the lower limit of the phytoplankton productivity, which delineates the top of the aphotic zone. Consequently, although some individuals may thrive below this level (Be and

Tolderlund, 1971), Douglas and Savin (1978) suggested 400 m as the lower habitat limit of the planktonic foraminifera.

Similar to Saito and Van Donk (1978), Douglas and Savin (1978) also observed progressive change in planktonic foraminiferal assemblage and density within a traverse of outer shelf to slope setting. They revealed that outer shelf and slope deposits contain abundant and diversified *Globotruncana* species with fewer numbers of *Rugoglobigerina*, *Globigerinelloides*, and *Archaeoglobigerina*. Whereas, near-shore deposits contain abundant *Heterohelix*, *Pseudoguembelina*, *Globigerinelloides* and *Rugoglobigerina* assemblages. They calibrated these findings with oxygen isotope measurements which revealed that near-shore settings contain shallow dwellers, while both shallow and deep dwellers thrive in the outer shelf and slope settings. Additionally, they suggested that tests of shallower dwelling species are more vulnerable to dissolution than those of deeper dwellers. Their oxygen isotope signals demonstrated that *Globigerinelloides*, *Rugoglobigerina* and *Pseudoguembelina* species yield warmest temperatures whereas that of *Globotruncana* and *Planoglobulina* point cooler temperatures.

More recently, Abramovich et al. (2003) analyzed habitat patterns and ecological traits of 56 late Campanian-Maastrichtian planktonic foraminifera via oxygen and carbon isotopes. Given the isotope signals they established 3 different depth stratification levels which are from shallower to deeper: mixed layer (both surface and subsurface waters), thermocline, and deep (sub-thermocline) habitats.

They demonstrated that *Pseudoguembelina* species occupy the surface waters while *Planoglobulina multicamerata*, *Heterohelix rajagopalani*, *Abathomphalus mayaroensis*, *Globotruncanella havanensis*, *Gublerina cuvillieri*, and *Laeviheterohelix glabrans* thrive in deep-water habitats. Moreover, they claimed that most species thrive within subsurface depths between subsurface mixed and thermocline layers. Planktonic foraminifera assemblages vary during cool and warm intervals such that during cool climates keeled globotruncanids dominate the thermocline layer while *Pseudotextularia*, *Planoglobulina* and heterohelicids advance in the subsurface mixed layer, whereas during warm climates globotruncanids dwell in the subsurface mixed layer.

In this thesis, we attempted to check whether any change is present within the depth groups through late Maastrichtian. Table 8 represents species which take part in the depth groupings. It is noteworthy that we especially selected individuals which represent consistent presence in the work of Abramovich et al. (2003), for this reason some genera and species were excluded from our depth groupings. In total, relative abundances of four different habitat groups were analyzed which are: mixed layer (both surface and subsurface), thermocline, and deep-water dwellers.

Table 8. Relative abundance values of different depth groups throughout Maastrichtian

Sample No	UH-30	UH-31	UH-32	UH-33	UH-34	UH-35	UH-36	UH-37	UH-38	UH-39	UH-40	UH-41	UH-42	UH-43	UH-44	UH-45	UH-46	UH-47	UH-48	UH-49
Mixed Layer Dwellers (a+b)																				
a-Surface Dwellers																				
Pseudoguembelina costulata				0,4		0,2			0,3	0,2	0,3		0,2	0,3	0,5					
P. excolata																				
P. hariaensis	0,3	0,2	0,6	1,0	2,1		0,8	0,4	1,0	0,9	0,3	0,2	0,9		0,5	0,3	0,5	0,4	1,9	0,8
P. kempensis																				
P. palpebra	0,2		0,2	0,6		0,4		2,2	1,3				0,2	0,7	1,0	0,3		0,7	0,6	0,4
Total	**0,5**	**0,2**	**0,8**	**2,0**	**2,1**	**0,6**	**0,8**	**2,7**	**2,6**	**1,1**	**0,6**	**0,2**	**1,4**	**1,0**	**1,9**	**0,5**	**0,5**	**1,1**	**2,5**	**1,2**
b-Subsurface Dwellers																				
Rugoglobigerina rugosa	1,9	0,8	1,2	0,6	1,9	2,3	0,8	0,4	2,9	0,7	1,2	2,2	0,7		0,2	0,3	0,2		1,3	1,2
R. milamensis	0,5	0,2	0,2	0,2	0,3	0,4		0,4												
Rugoglobigerina sp.	0,2		0,6	0,4		0,2	0,4	0,9	0,3	0,2	0,3	0,2								
Heterohelix globulosa	19,3	19,6	18,2	22,4	16,5	16,1	13,9	12,4	16,0	19,1	20,5	20,5	29,6	19,7	22,7	16,5	22,6	19,6	23,5	31,2
H. labellosa	2,8	1,8	2,0	1,4	5,3	0,8	0,4	0,9	2,9	2,7	3,7	4,4	1,2	1,7	0,2	1,0	1,4	2,2	1,3	
H.planata	2,1	2,0	3,0	4,4	1,6	6,5	7,9	8,0	3,2	2,5	2,4	3,3	2,1	3,1	3,8	2,5	1,9	3,6	2,5	2,0
H. punctulata	5,4	3,9	5,1	3,2	4,3	5,2	3,8	4,4	5,1	1,3	0,6	2,6	3,1	2,7	2,9	3,1	1,7	1,1	1,3	4,0
Heterohelix sp.	6,8	8,0	8,7	6,7	12,0	11,1	7,5	10,2	9,9	15,2	7,0	11,2	9,6	11,6	9,1	9,4	8,3	13,0	8,5	11,3
P. carseyae	4,9	3,9	4,0	2,4	1,6	1,3	3,0	2,7	1,0	2,5	3,1	2,6	2,6	1,7	3,8	3,3	2,9	1,1	3,4	2,4
P. brazoensis	0,3	0,5	0,6	0,4		0,2	0,8	1,3	1,6	0,9	0,3	1,1	1,2	2,0	1,2	0,8	0,7	1,1	0,9	2,0
Pseudotextularia elegans	2,1	2,0	4,2	1,8	1,1	1,7	3,8	1,8	1,9	2,5	2,1	3,3	1,4	0,3	0,2	3,3	0,7	1,1	1,9	1,2
Total	**46,2**	**42,6**	**47,7**	**43,8**	**44,4**	**45,8**	**42,1**	**43,4**	**44,7**	**47,5**	**41,3**	**51,5**	**51,4**	**42,9**	**44,2**	**40,2**	**40,5**	**42,8**	**44,5**	**55,5**
Thermocline Dwellers																				
G. arca	0,5	0,8	1,2	1,6	0,5	0,6		0,4				0,7	1,6	0,3	1,0	1,8	1,7	1,4	0,6	
G. dupeublei			0,2	0,4		0,2	0,4			0,2	0,3		0,5		0,2					
G. esnehensis	2,3	0,3	0,8	2,4	1,1	0,8	1,5		0,3	2,0	3,4	0,4	0,5	1,7	2,6	1,0	1,4	3,3	0,6	
G. falsostuarti	0,2	0,5	0,6		1,1		1,1	0,4	1,3	0,2	0,9		0,5	0,7	0,2		0,7	0,4	0,3	
G. hilli	0,2	0,2		0,2					0,3	0,2	0,6	2,0	0,2							
G. orientalis	0,9	0,2	0,6	1,0	2,1	0,8	0,8	1,8			0,9	0,2	0,2	0,3	0,2	2,0	0,2	0,7	0,6	
G. ventricosa							0,8	0,4				0,4	0,2		0,2					
Globotruncana sp.	1,2	0,8	2,4	1,4	0,8	1,5	1,9	1,3	1,6	1,6	2,8	1,5	1,4	1,7	3,1	2,5	2,1	2,9	1,3	1,2
Globotruncanita angulata	0,5	0,2		0,2	1,3	0,2	0,4	0,4	1,6	0,4						0,5				
G. insignis	0,7			0,2			1,1	1,8	1,3	2,0	0,6	2,0	1,4	0,3	1,9	0,3		0,4	0,3	
G. pettersi	1,2	1,5	1,4	2,2	2,7	3,1	2,3	2,7	1,6	1,8	0,9	0,7	0,5	1,7	1,0	1,0	3,6	1,8	1,6	0,8
G. stuarti		0,2		0,2		0,2		0,4			1,2		0,2				0,7		0,3	
G. stuartiformis	0,7	0,2	0,4	0,2	0,5		0,4	0,4	1,0	0,7	0,3	0,7	0,2	1,0	0,2	0,5	0,2	1,1	0,6	
Globotruncanita sp.	0,2			0,8	1,3	1,5	1,5	2,7	1,3	1,1	0,3	0,7	0,5	1,0		0,3	0,5		0,3	
Total	**8,5**	**4,7**	**7,5**	**10,7**	**11,4**	**9,0**	**12,0**	**12,8**	**10,2**	**10,3**	**12,2**	**9,3**	**8,0**	**8,8**	**10,7**	**9,9**	**11,2**	**12,0**	**6,6**	**2,0**
Deep Dwellers																				
P. multicamerata															0,2					
A. mayaroensis		0,3			0,3	1,3				0,4						1,3				
G. havanensis	2,6	1,1	1,4	1,2	4,8	1,9	0,4	2,2	1,3	1,1	1,2	0,7	0,2	0,3	0,5	0,5	0,5	1,4	1,6	0,4
G. cuvilleri		0,5										0,2			0,2					
L. glabrans	1,0	1,6	0,2	0,6	1,1	3,6	1,9	0,9	0,3	0,4		0,2				0,3	0,2		0,3	1,2
Total	**3,6**	**3,6**	**1,6**	**1,8**	**6,1**	**6,7**	**2,3**	**3,1**	**1,6**	**2,0**	**1,2**	**1,1**	**0,2**	**0,3**	**1,0**	**2,0**	**0,7**	**1,4**	**1,9**	**1,6**

Figure 32 shows changes in the relative abundance patterns of depth groups with respect to sea level fluctuations. Surface dwellers, characterized by *Pseudoguembelina* species slightly increased during decreasing trends of sea level. Subsurface dwellers are composed of heterohelicids, rugoglobigerinids, pseudotextularids, and planoglobulinids. As a result of *Heterohelix* domination in the basin, total abundance of mixed subsurface water dwellers is high. This group vaguely mimics the sea level fluctuations. On the other hand, relative abundance of thermocline dwellers, which are characterized by globotruncanids, slightly increased

during decreasing water depths. Deep-water dwellers consist of *Planoglobulina multicamerata*, *Gublerina cuvillieri*, *Abathomphalus mayaroensis*, *Globotruncanella havanensis* and *Laeviheterohelix glabrans* species. In accordance with increasing water column depth from UH-34 to UH-35 (Fig. 30), deep water dwellers markedly increased. However, same increment in this group was not detected during similar water depth increase from UH-42 to UH-43 (Fig. 30). Therefore, response of this group to paleobathymetric fluctuations remain enigmatic.

Overall, the relative abundance of subsurface water dwellers is proportional to water level variations, whereas that of surface water and thermocline dwellers are inversely correlated. Additionally, behavior of the deep-water dwellers to sea level fluctuations is unstable.

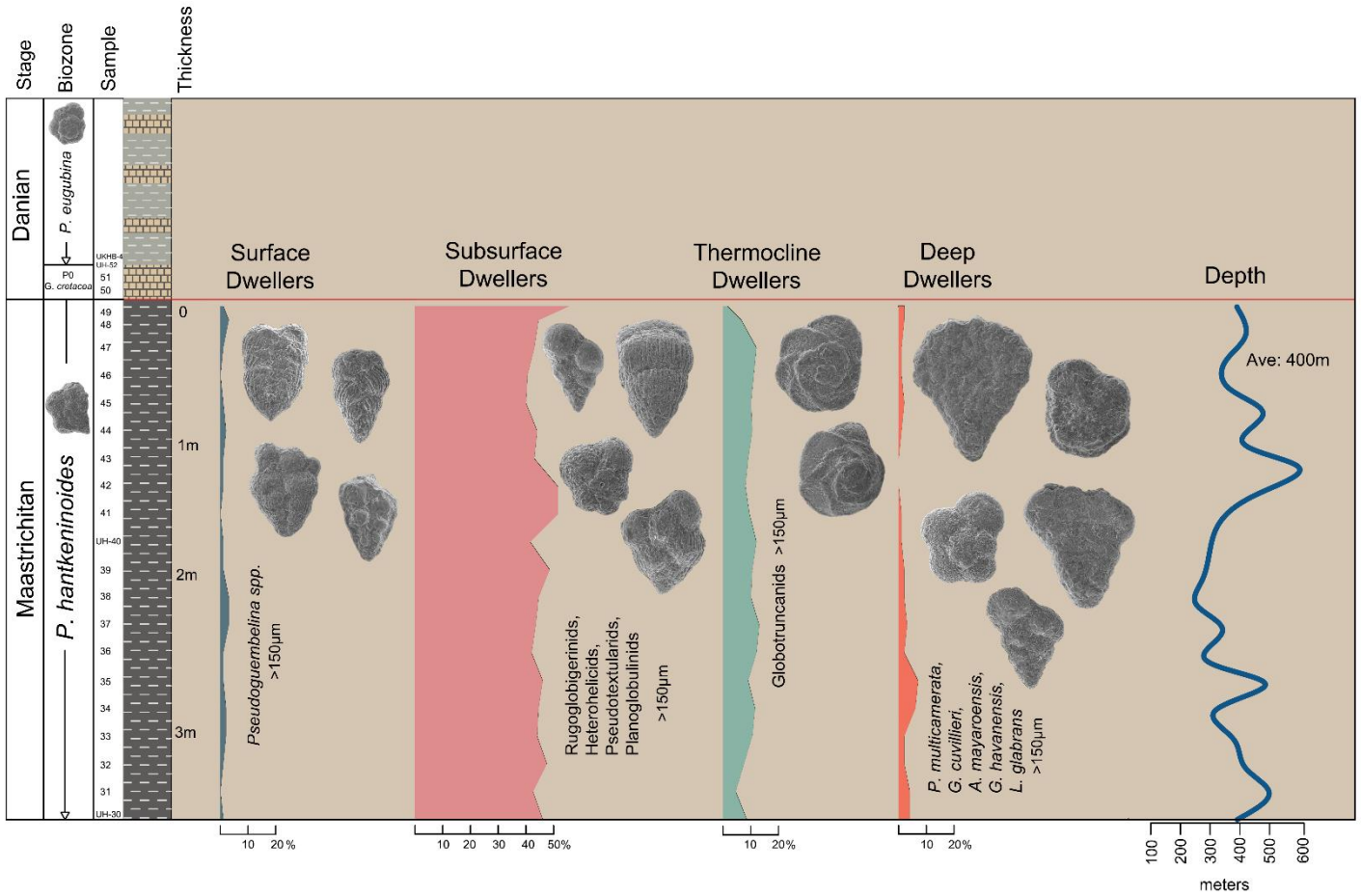

Figure 32. Responses of various depth groups with respect to changes in the water column. Note: Only depth variations calculated by formula of Van der Zwaan et al. (1990) was shown here. Average water depth represents average of two depth formula used in Paleobathymetry Chapter.

CHAPTER 4

EVENTS ACROSS THE K-PG BOUNDARY

4.1 *THORACOSPHAERA* BLOOM AFTER THE K-PG BOUNDARY

Right after the K-Pg boundary, there is a huge amount of increase in the number of calcareous spherical forms in our samples (Figs. 33, 34, 35, 36). They have almost perfectly spherical and hollow tests, and their sizes range between 10-20 microns (Figs. 33, 34, 35). These spheres cover almost all background area of thin sections in samples following the K-Pg boundary (e.g. E+2, UH-50, UH-51) from Danian P0 zone (Fig. 33, 34, 35). Number of these spheres reaches at their highest during the P0 zone and decrease through up-section as the planktonic foraminiferal community recovers.

These spherical forms are originated from relicts of cyst-producing calcareous dinoflagellate individuals which are grouped under: ‘’*Thoracosphaera*’’. Although Açıkalın et al. (2015) announced *Thoracosphaera* bloom at 1.38 m above the base of the boundary clay, this thesis is the first study in Turkey representing the earliest detection of *Thoracosphaera* bloom immediately after the K-Pg boundary (2 cm above the boundary).

World-wide *Thoracosphaera* blooms right after the K-Pg boundary have been proposed by a variety of studies (Romein 1979, Pospsichal and Wise 1990, Eshet et al. 1992, Gardin and Monechi 1998, Hildebrant-Habel et al. 1999, Keller et al. 2001, Smit 2004, Lamolda et al. 2005, 2015). In fact, Hildebrant-Habel et al. (1999) claim that these blooms were caused by marked increase in relative abundance of single species: *Operculodinella* (*Thoracosphaera*) *operculata* (Bramlette et Martini 1964) (Fig. 37).

Perch-Nielsen et al. (1982) claimed that sharp increase in *Thoracosphaera* can be used as K-Pg boundary marker. Subsequently, Tantawy (2003) demonstrated that the K-Pg boundary is characterized by *Thoracosphaera* acme (back then *Thoracosphaera* was categorized under nanoplankton group).

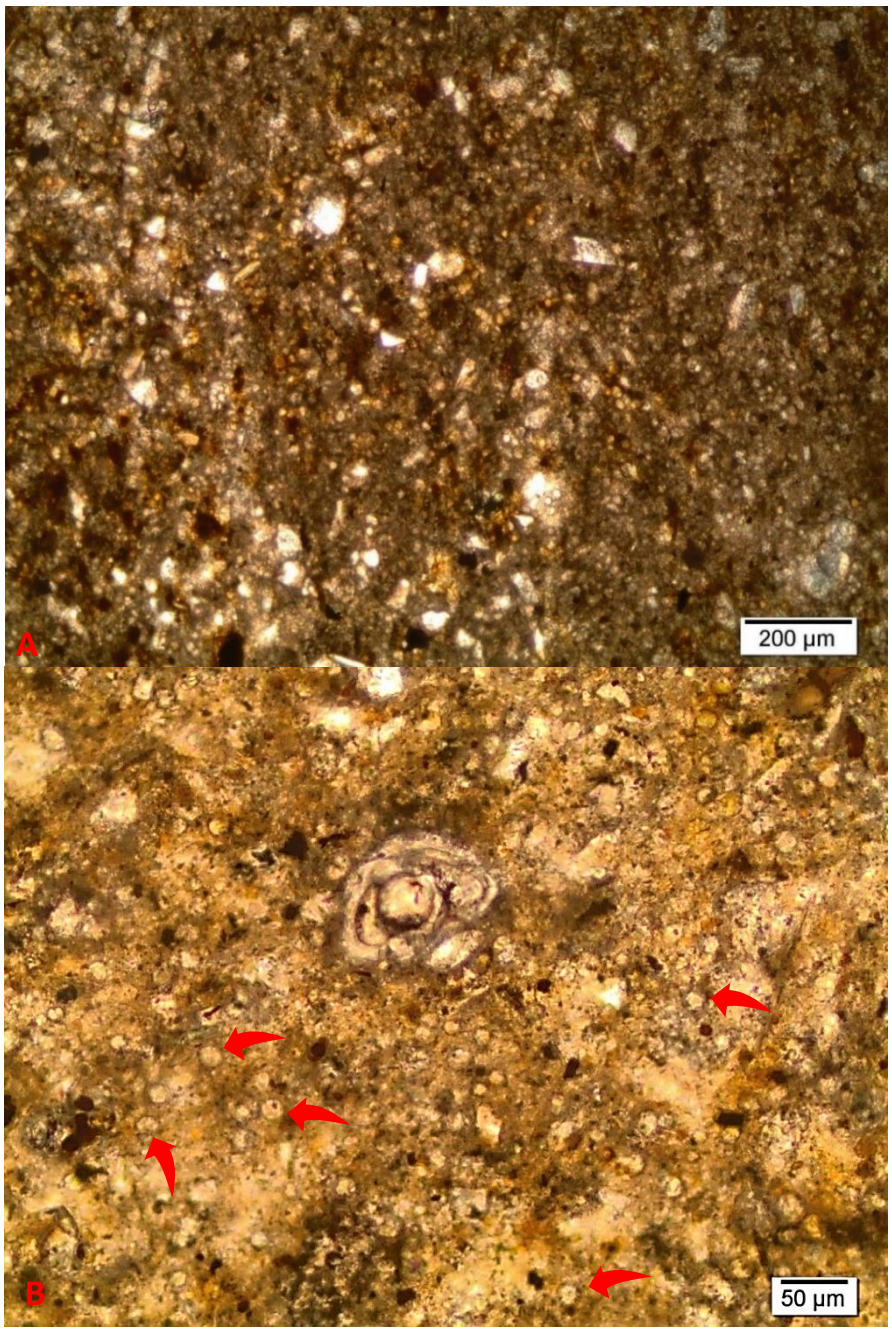

Figure 33. Whole background area is covered by *Thoracospharea* individuals (Note the tiny spherules). A) sample UH-50, 5 cm above the boundary, P0 Zone. B) sample UKHB-4, 25 cm above the boundary, Pα Zone (point of arrows indicating some *Thoracosphaera* specimens).

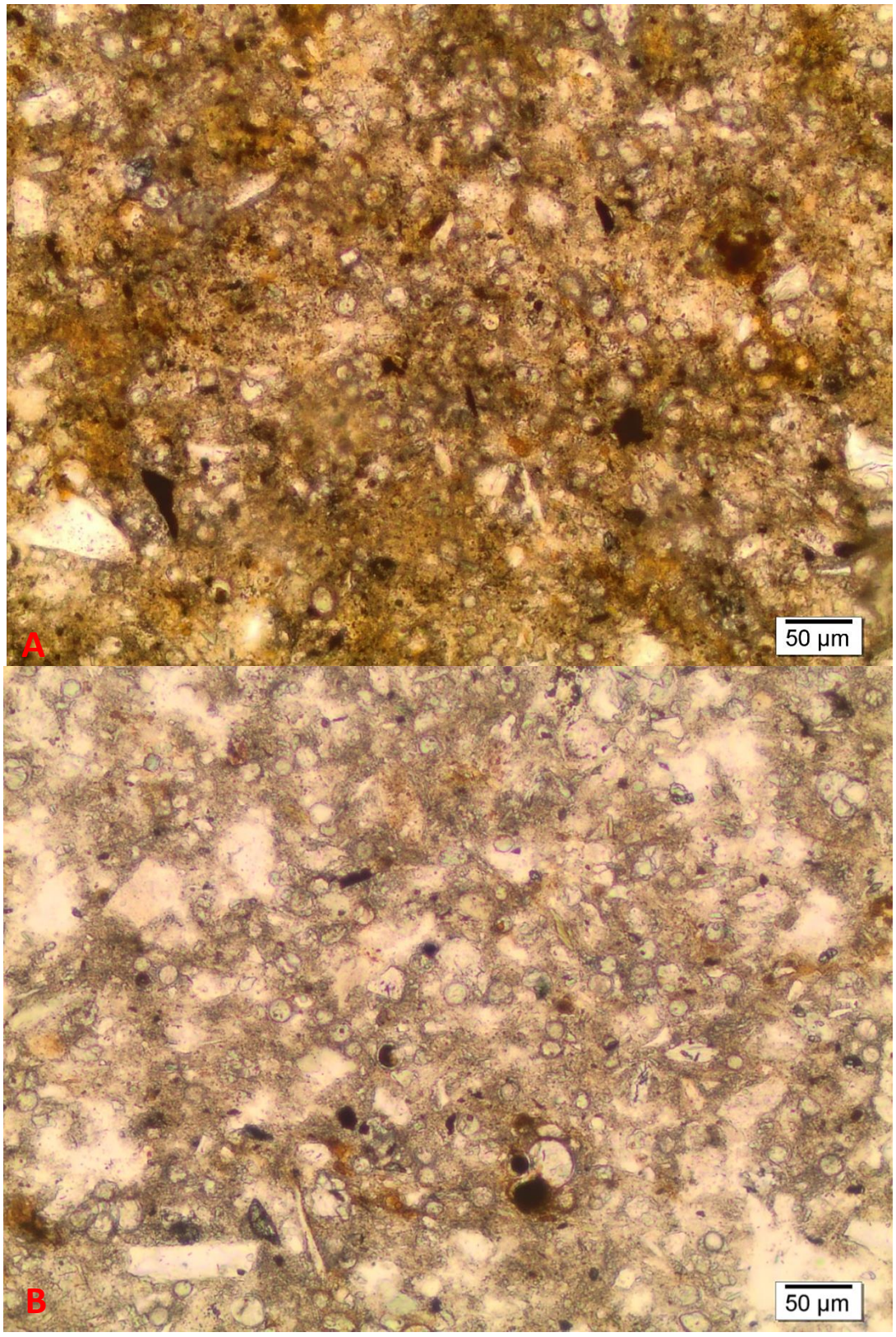

Figure 34. *Thoracospharea* blooms. A) sample E+2, 2 cm above the boundary, P0 Zone B) sample UH-50, 5 cm above the boundary, P0 Zone

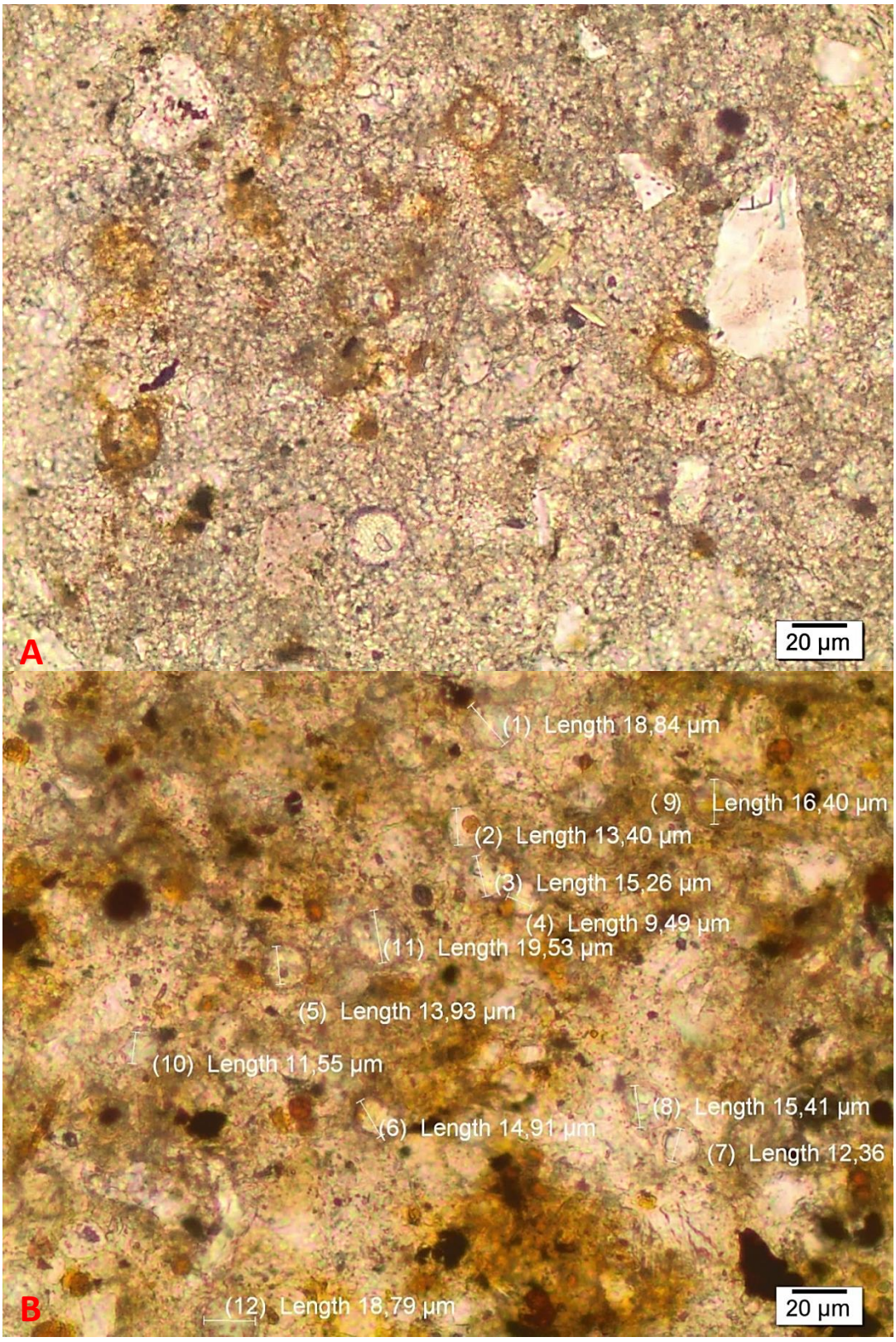

Figure 35. Close-up views and dimensions of *Thoracosphaera* individuals. A) sample UH-51, 15 cm above the boundary, P0 Zone B) sample UKHB-4, 25 cm above the boundary, Pα Zone.

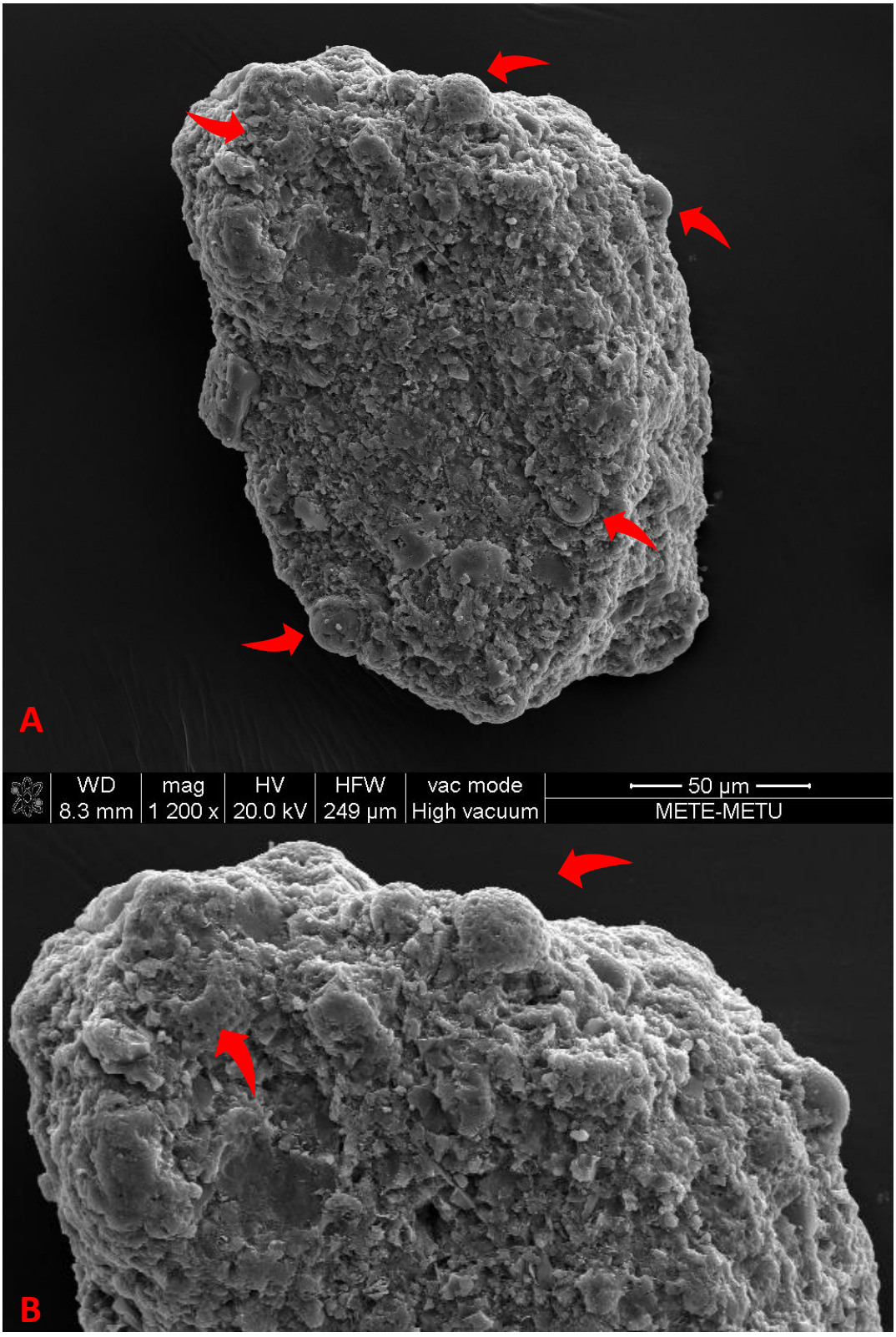

Figure 36. A) Scanning Electron Microscope (SEM) Image of *Thoracosphaera* individuals (tip of red arrow) embedded in a clast. Sample from E+25 >63 µm, 25 cm above the K-Pg boundary, Pα Zone. B) Close-up view of *Thoracosphaera* specimens in A.

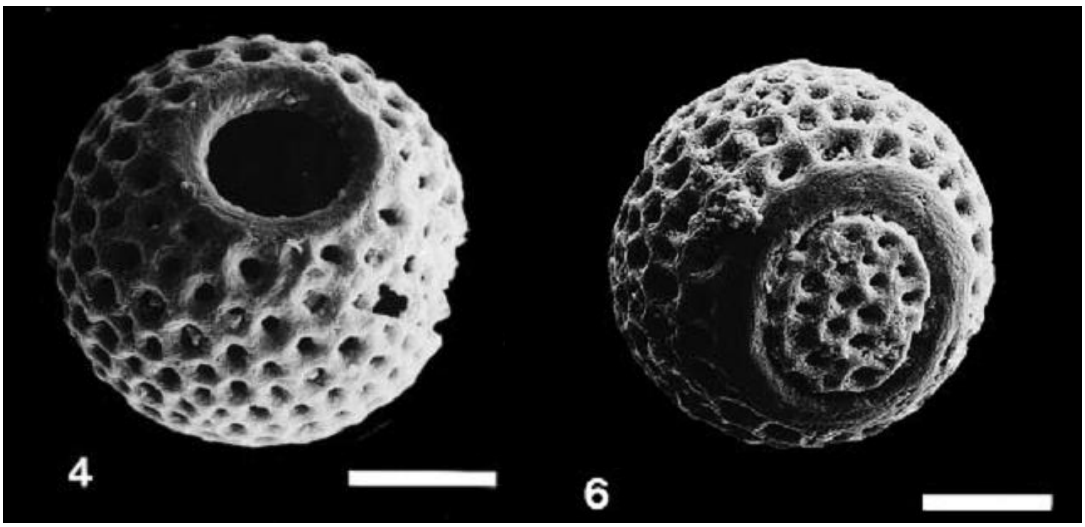

Figure 37. *Thoracosphaera* specimens from work of Hildebrand-Habel et al. (1999). Scale bar 10 μm.

Opportunistic *Thoracosphaera* blooms reflect harsh conditions after the K-Pg boundary in early Danian, such as high amount of CO_2, fluctuations in salinity and pH or large variations in surface-water temperature during low sunlight would have occurred (Eshet et al. 1992, Tantawy 2003, Lamolda et al. 2005, 2015). Moreover, Smit (2004) postulated that *Thoracosphaera* acme indicate unstable adaptive radiation and corroborate the idea of sudden, catastrophic extinction event at the K-Pg boundary as it radiates only in a vacant, chiefly empty ecospace. In our study, the bloom of the disaster opportunistic *Guembelitria cretacea* corresponds to same level with *Thoracosphaera* bloom.

As mentioned earlier, in our section the K-Pg boundary corresponds to 2-3 mm thick reddish oxidized layer. To investigate nature of the boundary itself 50 gr sample corresponding 2-3 mm thick layer was washed and screened with the same technique that we used for planktonic foraminifera identification.

According to washed residues, there are almost no planktonic/benthic foraminifera present in the boundary layer. We encountered some benthic foraminifera in >150 μm fraction, and a spot of *Guembelitria, Heterohelix* and *Globigerinelloides* species in 63-150 μm fraction. Similarly, Smit (2004) reported that ejecta layer is free of planktonic foraminifera and claimed that most species disappear at this level. His findings fit with our observation from washed specimens of the K-Pg boundary.

On the other hand, there are certain materials which we came across with at or very close to the boundary.

4.2 SPHERULES FOUND RIGHT AT THE K-PG BOUNDARY

The most enigmatic features are spherules found right at the K-Pg boundary layer. These were collected from washed residues of 63-150 μm fraction and none was found in >150 μm. They are black, amber, yellowish-brown to transparent color and are in spherical to disk shapes (Fig. 38). Many of them are hollow and some transparent colored ones are even pliable. No spherule was recovered in any level above or below the boundary. The spherules were categorized under two categories by their colors. Spherule group 1 yields brown/amber to yellow colors while spherule group 2 are made up to black-colored specimens (Fig. 38). Scanning Electron Microscope (SEM) analysis showed that the brown to yellow colored ones have characteristic texture on their surface while black colored ones have smooth surface (Figs. 39, 40). Energy Dispersive X-ray (EDX) analysis was carried out in order to identify chemical compositions of these spherules. Table 9 represents major oxides found their structure.

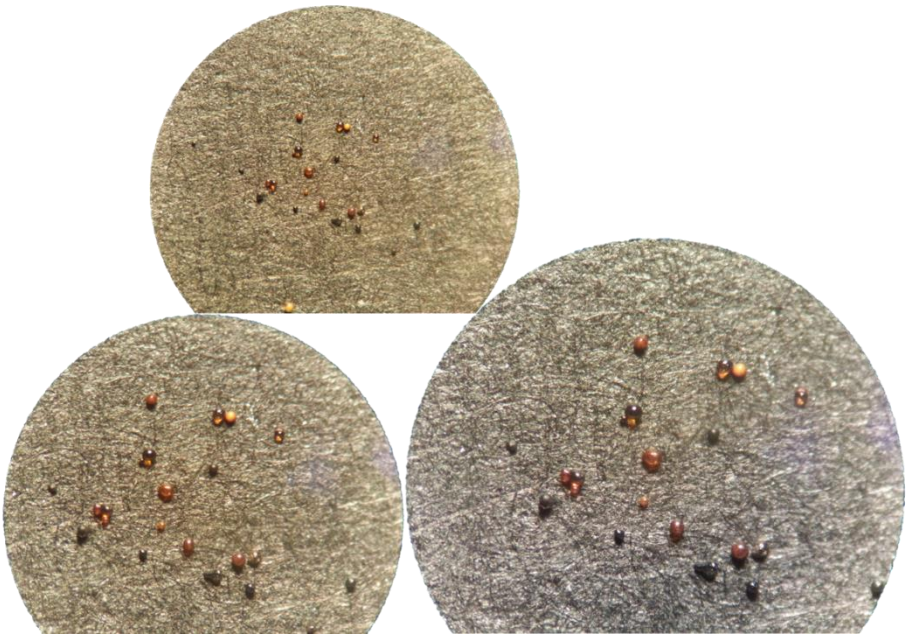

Figure 38. Spherules were recovered right at the K-Pg boundary above 63 μm fraction. No spherule was found at any level above or below the boundary. Spherules were separated into two groups by their colors: Amber color to transparent ones, and black ones. Top view X40, bottom left X60, bottom right X80 magnification.

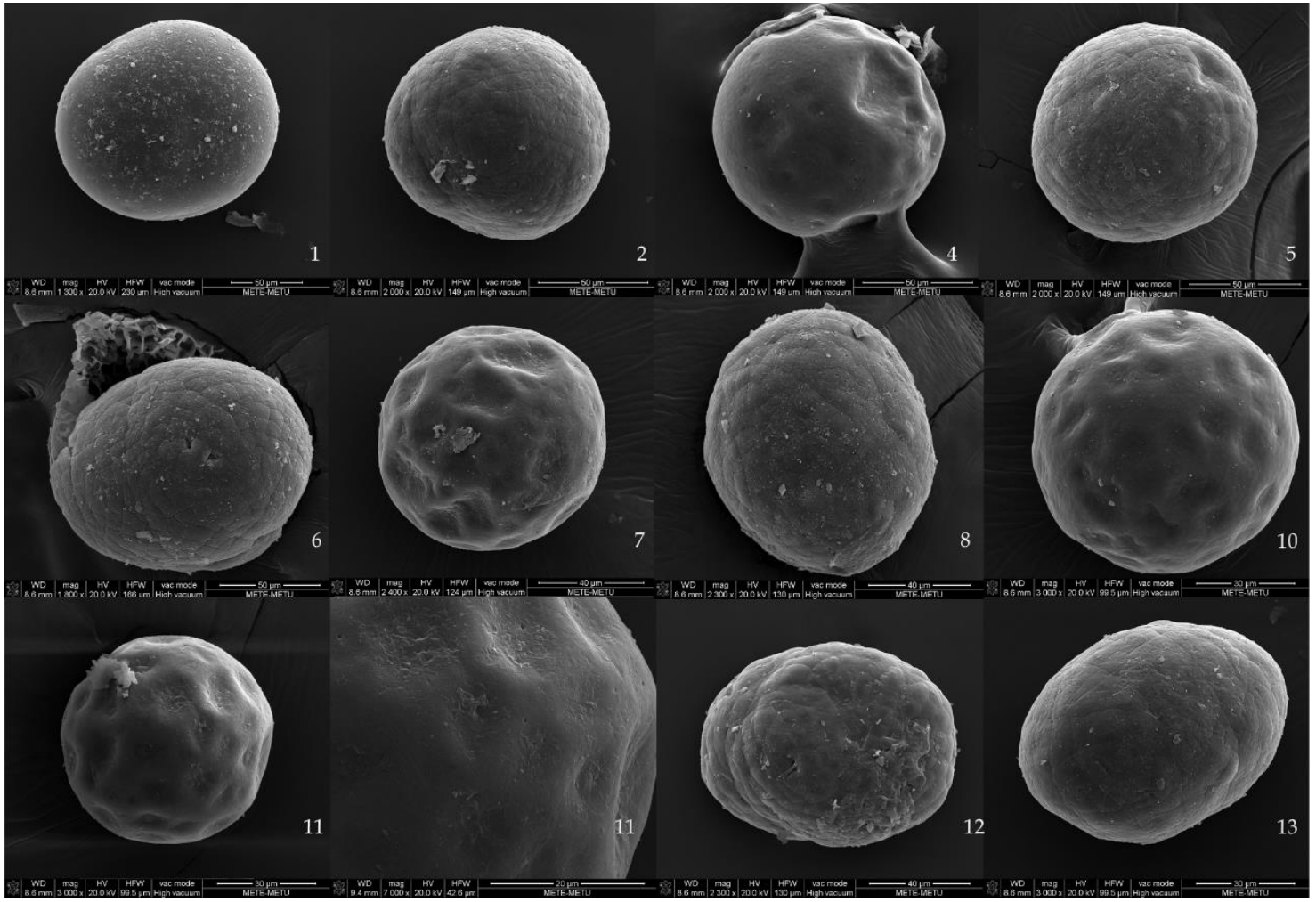

Figure 39. SEM images of the brown to yellow and transparent spherules. Some spherules are pliable.

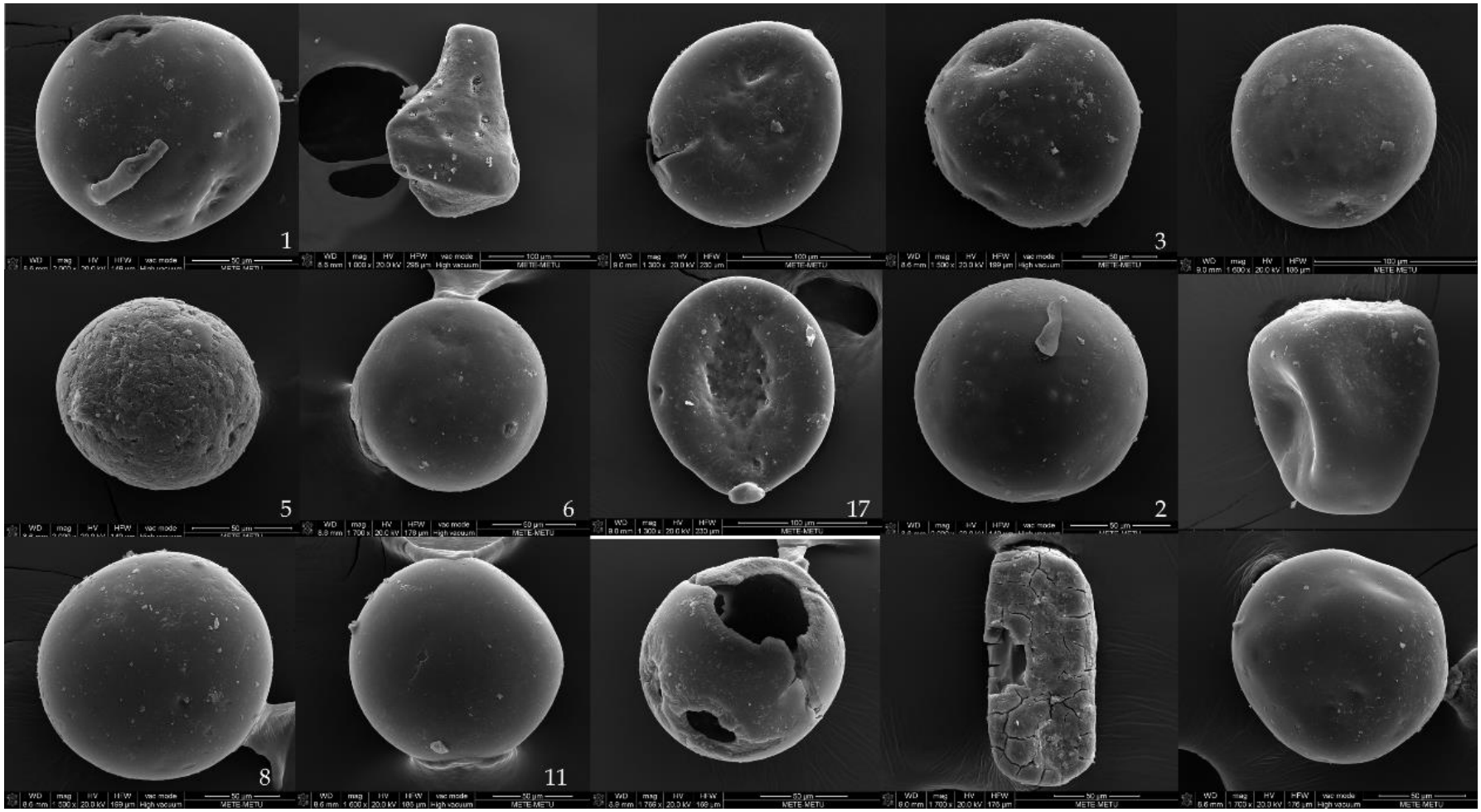

Figure 40. SEM images of the black spherules which show a variety of shapes.

Table 9. EDX results of the brown-yellow and black spherules. They are highly rich in CaO but low in SiO_2.

Brown-Yellow								
Sample No:	Series 1-1	Series 1-2	Series 1-5	Series 1-6	Series 1-7	Series 1-10	Series 1-11	
Wt %								Average
SiO_2	15,37	12,55	9,55	16,63	3,38	3,86	3,46	**9,3**
CaO	56,08	57,03	38,72	47,97	80,49	80	74,42	**62,1**
Na_2O	n.d.	3,13	10,91	4,42	n.d.	n.d.	2,44	**5,2**
MgO	12,94	13,53	15,92	16	9,88	8,9	15,47	**13,2**
Al_2O_3	6,2	6,9	4,76	4,91	1,88	3	1,85	**4,2**
Fe_2O_3	9,4	6,86	6,14	10,07	4,38	4,24	2,37	**6,2**
Cl_2O	n.d.	n.d.	13,99	n.d.	n.d.	n.d.	n.d.	
Black								
Sample No:	Series 2-1	Series 2-2	Series 2-5	Series 2-6	Series 2-8	Series 2-11	Series 2-17	
Wt %								Average
SiO_2	9,31	n.d.	20,1	n.d.	6,58	n.d.	11,11	**11,8**
CaO	73,01	91,01	46,98	73,01	76,78	81,92	66,39	**72,7**
Na_2O	4,65	n.d.	n.d.	2,82	n.d.	n.d.	n.d.	**3,7**
MgO	8,43	7,1	10,87	8,93	12,75	10,99	6,6	**9,4**
Al_2O_3	4,59	1,89	9,4	4,14	3,89	3,98	4,61	**4,6**
Fe_2O_3	n.d.	n.d.	12,44	7,79	n.d.	n.d.	11,29	**10,5**
Cl_2O	n.d.	n.d.	n.d.	3,31	n.d.	3,11	n.d.	**3,2**

Belza et al. (2015) compiled compositional data of black, green and yellow glasses from: Beloc (Haiti), Arroyo El Mimbral (NE Mexico), DSDP 540 and DSDP 536 sites. All sites yield high amount of SiO_2 (47.9-68.49 wt%), and low amount of CaO (0.26-24.7 wt%). Our EDX analysis revealed that our spherules are extremely high in Ca (ave. 72.7 wt% in black spherules, 62.1 wt% in brown to yellow spherules), but very low in SiO_2 (ave. 11.78 wt% in black spherules, 9.3 wt% in brown to yellow spherules) with respect to compositions of world-wide impact spherules. Given the EDX results, our spherules may not have impact origin or if so, they might have undergone exceptional alteration at which large amounts of SiO_2 would have turned into CaO.

On the other hand, brown to yellow pliable spherules (2, 4, 5, 6, 7, 8, 10, 11, 12, 13 in Fig. 39) may be relicts of inner wall of extremely large *Thoracosphaera* individuals.

4.3 AMORPHOUS GRAINS FROM THE K-PG BOUNDARY

In addition to Ca-rich spherules, there are some grains collected only from the K-Pg boundary layer (Figs. 41, 42). They have shiny light-brown color in reflected light, and elongated in their long axis. They are dominantly found at 150 μm fraction but also less common in 63-150 μm. EDX results show that they are rich in Si and Fe with moderate amount of Al and Mg (Table 10).

Figure 41. Light brown grains were found right at the washed residues of 2-3 mm thick reddish layer corresponding the K-Pg boundary. Displayed grains were recovered from >150 μm screen. Top view X40 magnification, bottom left and right views X60 magnification.

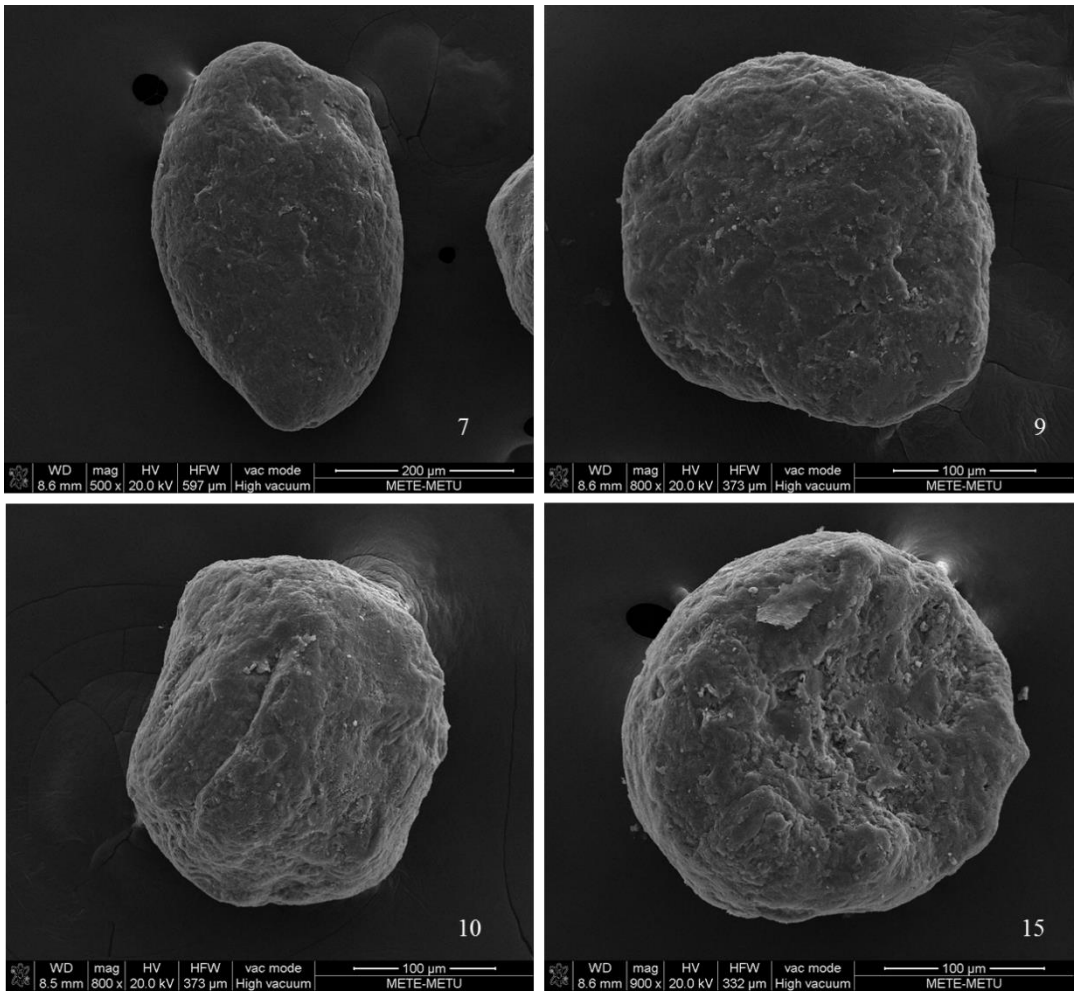

Figure 42. SEM images of the light brown grains which were found only within the K-Pg boundary layer.

Table 10. EDX results of the light brown grains show that they are rich in SiO_2 and Fe_2O_3 and moderate in Al_2O_3.

Sample No:	7	9	10	15	
Wt %					Average
SiO_2	44,65	42,91	36,35	44,92	**42,2**
CaO	1,87	2,13	1,92	1,92	**2,0**
K_2O	1,76	0,77	0,29	1,17	**1,0**
MgO	8,19	8,95	9,21	8,53	**8,7**
Al_2O_3	15,32	16,19	14,29	17,27	**15,8**
Fe_2O_3	28,21	29,05	37,95	26,19	**30,4**

Professor Jan Smit (pers. commun.) claimed that although these grains are low in K, they might be altered microkrystites between smectite and sanidine alteration. However, there is not any quench crystal identified on their broken surface as microkrystites usually have (Smit, pers. commun.) (Fig. 42). Unlike microkrystites, when they are broken into half, its internal part represents a thin crust and homogenous inner part without dendritic or fibroradial texture. For now, no solid interpretation will be pronounced at this stage about the genesis of these grains. Yet, being present only in the 2-3 mm thick layer corresponding the K-Pg boundary may infer impact origin.

4.4 EUHEDRAL GRAINS

There are euhedral grains collected from couple of cm below and right at the K-Pg boundary layer (Fig. 43). Their shape and inner zonal structure are quite similar zircon. We checked the composition of these grains to understand whether they are zircon or not. If so, then these grains might have induced by the Chicxulub impact. However, EDX analyses revealed that they are rich in Ba and moderate in S (Table 11). Namely, they have different chemical formula than zircon mineral. Professor Aral Okay (pers. commun.) remarked that these grains might have authigenic origin which would have deposited at or close to the K-Pg boundary layer (2-3 mm thick reddish horizon) as a result of redox conditions.

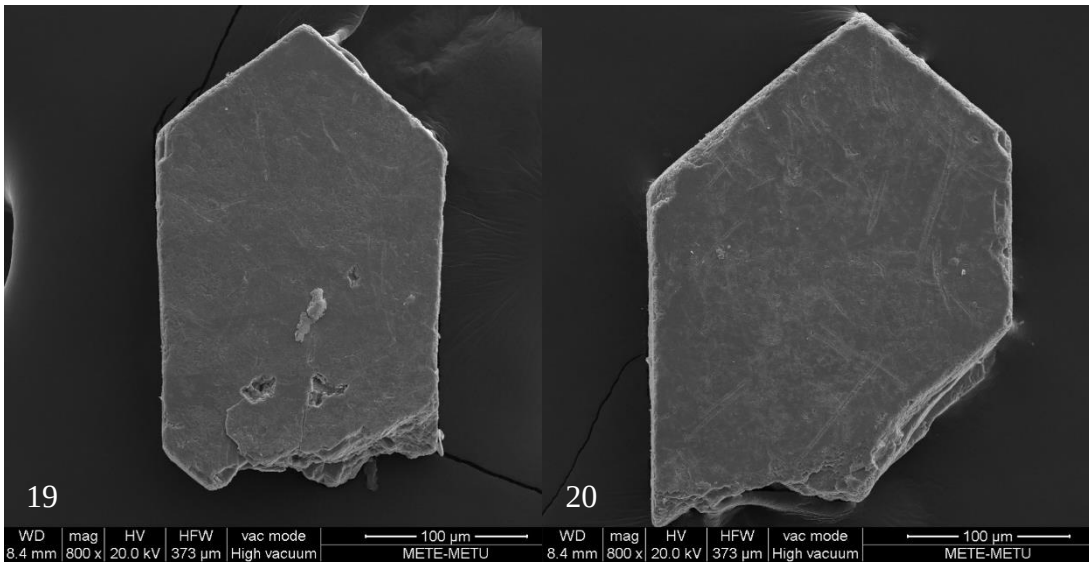

Figure 43. SEM images of the euhedral grains.

Table 11. EDX results of the euhedral grains show that they are rich in Ba.

Sample No: Wt %	19	20	Average
Ba	74,5	61,03	**67,8**
S	19,85	34	**26,9**
Sr	5,65	4,97	**5,3**

4.5 ECHINOID FECAL PELLETS

Apart from spherules and grains there is an abrupt increase in echinoid fecal pellets (Fig. 44) peak at 2 cm above the K-Pg boundary (Figs. 45, 46). These grains are pale brown color in reflected light and EDX results have shown that they are high in Ca & P and minor in Si (Table 12).

Previously, Esmeray-Senlet et al. (2015) announced same increment from their work in the southern part of the Haymana Basin. As discussed earlier, they delineated the K-Pg boundary between the Beyobası and Çaldağ formations, which are shallower than the Haymana and Yeşilyurt formations corresponding our studied sections. According to their observations, there are remarkably high amount of echinoid pellet accumulation in first sample just after the boundary (12 pellets per gram) in earliest Danian P0 Zone with respect to zero background value in latest Maastrichtian *P. hariaensis* Zone.

In our study on northern part of the Haymana Basin, echinoid pellets start increasing at the K-Pg boundary, reach peak abundance at 2 cm after the boundary and then rapidly turns back zero value throughout the P0 (*G. cretacea*) Zone. The second but smaller increase was encountered at UKHB-6 (51 cm above the K-Pg boundary) in early Pα Zone which was also detected by Esmeray-Senlet et al. (2015). However, the fecal pellet horizon after the K-Pg boundary is absent in Campo Pit and Buck Pit (New Jersey) sections where represent shoreface settings. This may have caused by facies control on the deposition of this horizon via nondeposition or post-depositional alteration (Esmeray-Senlet et al. 2015) in shallower water areas. On the contrary, it may have favored the pellet deposition in deeper water settings, such as in the

Haymana Basin, deep New Jersey and Swedish sections (Esmeray-Senlet et al. 2015 and references therein).

Miller et al. (2010) suggested and later supported by Esmeray-Senlet et al. (2015) that the surge in the number of echinoid pellets can be used as a stratigraphic marker horizon for correlation of the K-Pg boundary. Our results corroborate this idea since the increase right after the boundary is highly conspicuous from the background pellet values.

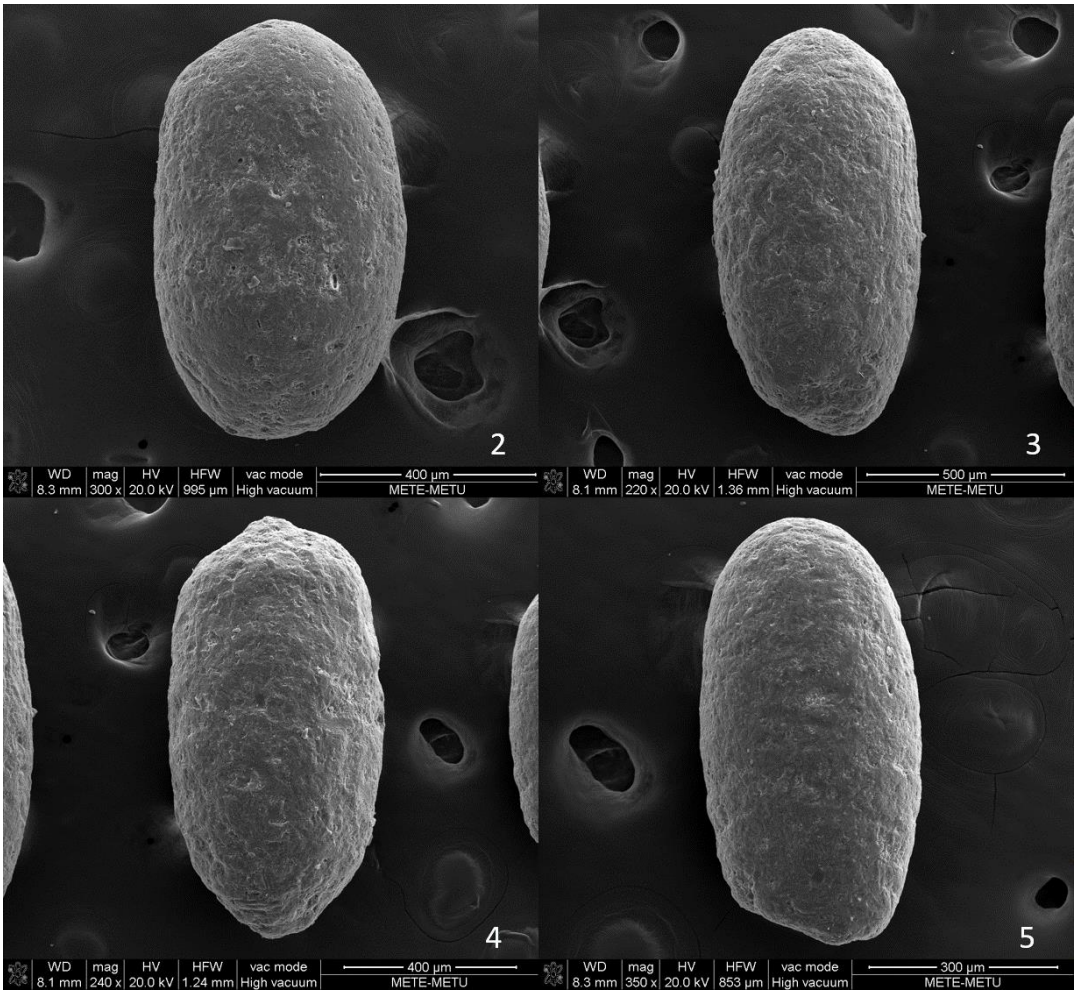

Figure 44. SEM images of echinoid pellets peak at 2 cm above the K-Pg boundary. 2 and 3 are from sample E+2 cm; 4 from Ejecta layer, 5 from sample E-2 cm.

Sample No	Pellet Count per gram
UKHB-9	4
UKHB-8	2
UKHB-6	19
UKHB-5	0
E+25 UKHB-4	0
E+22	0
E+13	0
E+10	3
UH-50	5
E+2	35
K-Pg boundary	5
E-2	2
UH-49	0
UH-48	3
UH-47	1
UH-46	0
UH-45	0
UH-44	0
UH-43	1

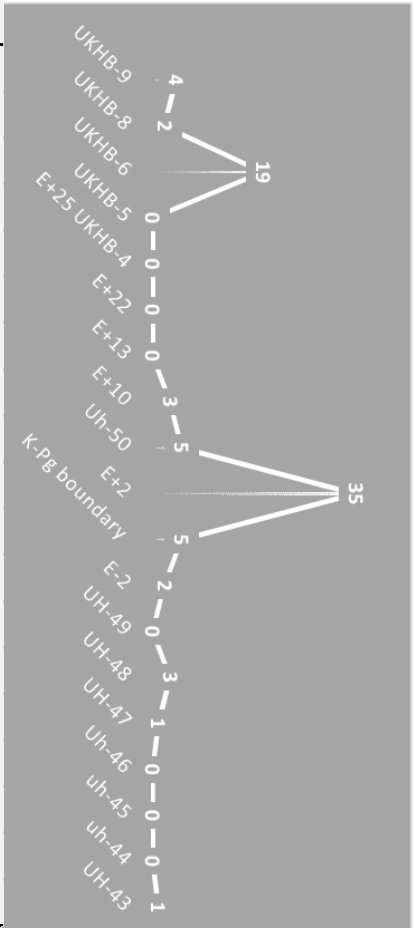

Figure 45. Echinoid pellet counts. Note the abrupt increase right after the K-Pg boundary.

Table 12. EDX analysis of pellets revealed that they are rich in CaO and P_2O. Note: numbers in parenthesis show pellets in Fig. 44.

Sample No: Wt %	E-2 (5)	Boundary = E (4)	E+2 (3)	E+10 (2)	Average
SiO_2	2,1	10,28	11,5	5,26	**7,3**
CaO	53,41	43,18	42,2	50,82	**47,4**
Na_2O	0,65	0,75	0,8	0,86	**0,8**
MgO	0,52	2,62	3,74	1,02	**2,0**
Al_2O_3	0,7	4,25	4,19	1,74	**2,7**
Fe_2O_3	0,69	4,31	4	2,32	**2,8**
K_2O	0,26	0,67	0,3	0,38	**0,4**
P_2O	41,66	33,93	33,29	37,6	**36,6**

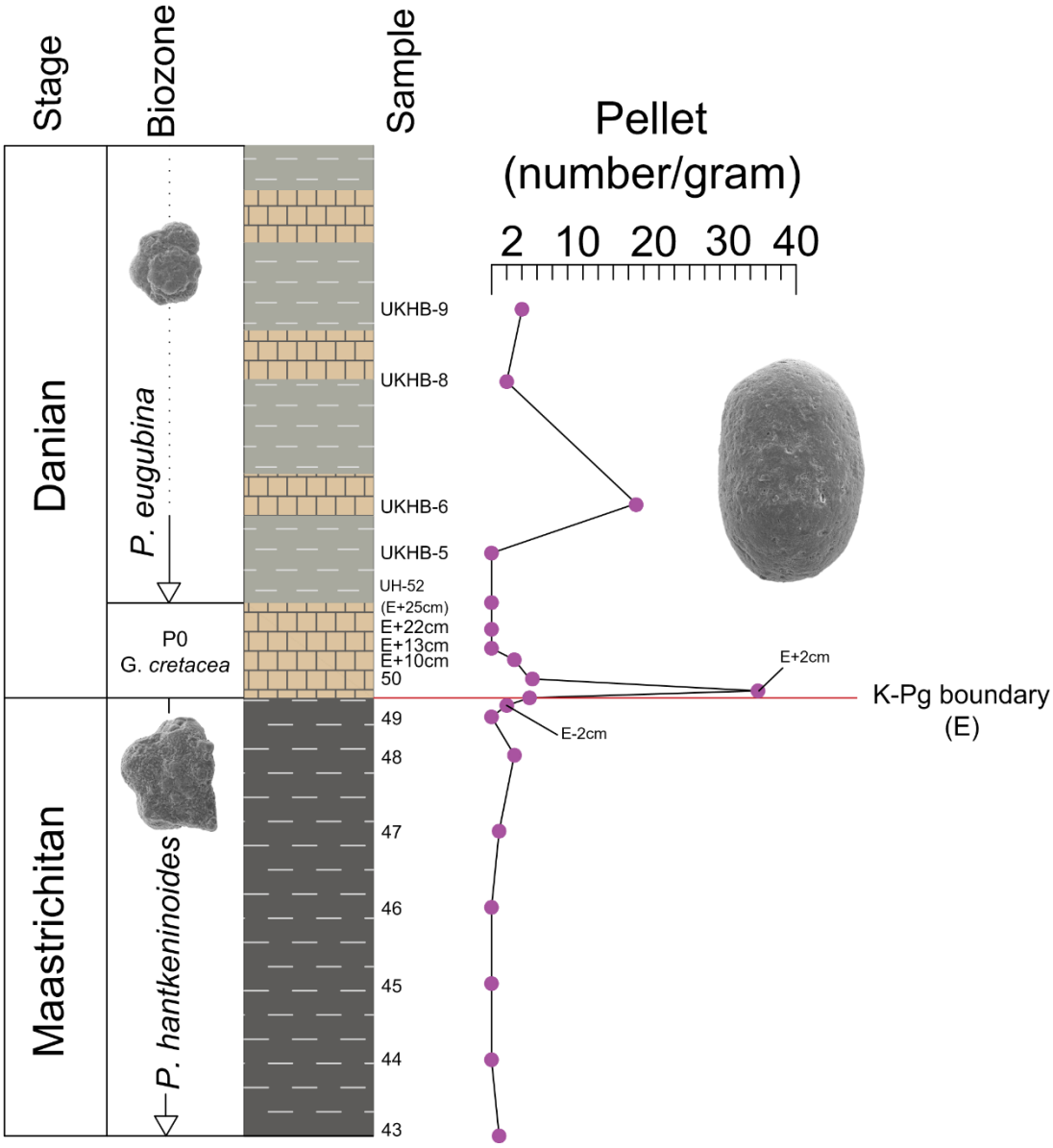

Figure 46. Echinoid pellets peak right after the K-Pg boundary in Danian P0 Zone. Another but much lesser increase was observed in Pα Zone.

CHAPTER 5

SYSTEMATIC TAXONOMY

This chapter attempts to explain: general description of the Cretaceous-Paleogene planktonic foraminifera, characteristic morphologic features in our samples, and relatively updated synonym list.

The systematic taxonomy of the planktonic foraminifera was done by identifying species from both washed samples and thin section views. The classification was majorly based on the following features: wall structure, test morphology (coiling/uncoiling mode), angle of spire (e.g. high/ low throcospiral), presence/absence and number of keels, behavior of sutures (radial-depressed/ raised-beaded etc.), shape and arrangement of chambers, umbilical structure (e.g. tegilla, portici) and primary-secondary apertures. Yet, some features were obscured and filled with sediment, such as umbilical structure (tegilla, portici), therefore test morphology, angle of spire and behavior of sutures were the chief recognition criteria.

Foraminifera identification was mainly based on descriptions of: Chronos Portal website (http://portal.chronos.org/gridsphere/gridsphere), Robaszynski et al. (1984), Nederbragt (1991), and Premoli-Silva and Verga (2004). Stratigraphic ranges of each foraminifera were discussed at the end of each species descriptions.

Superfamily UNCERTAIN

Family GUEMBELITRIIDAE MONTANARO GALLITELLI, 1957

Genus *Guembelitria* CUSHMAN, 1933

Type species: *Guembelitria cretacea* CUSHMAN, 1933

Guembelitria cretacea CUSHMAN, 1933

Plate 1, Figs. 1-9; Plate 34, Figs. 10-13.

1933 *Guembelitria cretacea* CUSHMAN, pl. 4, fig. 12 a, b.

1990 *Guembelitria cretacea* CUSHMAN- Kroon & Nederbragt, pl. 2, figs. 4-6, 7, 11.

2002 *Guembelitria cretacea* CUSHMAN- Keller *et al*., pl. 4, figs. 1-5.

2002 *Guembelitria cretacea* CUSHMAN- Keller, pl. 4, figs. 1-6.

2004 *Guembelitria cretacea* CUSHMAN- Arenillas *et al*., fig. 4f.

2004 *Guembelitria cretacea* CUSHMAN- Pardo & Keller, pl. 1, figs. 1, 2.

2011 *Guembelitria cretacea* CUSHMAN- Georgescu *et al*., pl. 7, figs. 1-6.

2015 *Guembelitria cretacea* CUSHMAN- Esmeray-Senlet *et al*. fig. 5 (16).

2016 *Guembelitria cretacea* CUSHMAN- Arenillas & Arz, fig. 6d.

Description & Remarks:

This species is characterized by small triserial test, globular chambers and highly arched aperture.

Starting from the very first sample of the *P. hantkeninoides* Zone, *Guembelitria cretacea* coupled with *Heterohelix* spp. dominate the 63-150 μm size fraction throughout the Maastrichtian. Unusual large individuals of this species were also found in >150 μm. It makes opportunistic bloom right after the K-Pg boundary in Danian P0 Zone. *Guembelitria cretacea* was found entire interval of the quantitative study (i.e. UH-30 to E+2).

Stratigraphic distribution in the literature: Santonian to Danian P1b zone (Georgescu et al. 2011, Olsson et al. 1999).

Genus *Parvularugoglobigerina* HOFKER, 1978

Type species: *Globigerina eugubina* Luterbacher and Premoli-Silva, 1964

Parvularugoglobigerina eugubina LUTERBACHER and PREMOLI-SILVA, 1964

Plate 2, Figs. 1-9; Plate 34, Fig. 24.

1964 *Globigerina eugubina* LUTERBACHER and PREMOLI-SILVA, pl. 2, figs. 8a-c.

2011 *Parvularugoglobigerina eugubina* LUTERBACHER and PREMOLI-SILVA-Keller *et al*., pl. 3, figs. 9-11.

2013 *Parvularugoglobigerina eugubina* LUTERBACHER and PREMOLI-SILVA-Arenillas and Arz, figs. 3 (L-O).

2016 *Parvularugoglobigerina eugubina* LUTERBACHER and PREMOLI-SILVA-Arenillas and Arz, figs. 5 (e-f).

Description & Remarks:

Parvularugoglobigerina eugubina is characterized by having low to moderate trochospiral test with gradually increasing 6 chambers in the last whorl with larger last chamber. It has wide range of morphotypes.

In our study, it was found between 63-150 μm fraction starting from 25 cm above the K-Pg boundary. Its first appearance datum (FAD) marks the beginning of the Pα Zone. Its last appearance datum (LAD) was not identified due to out of scope of this study.

Stratigraphic distribution in the literature: Danian Pα Zone (Olsson et al. 1999).

Superfamily HETEROHELICACEA CUSHMAN, 1927

Family HETEROHELICIDAE CUSHMAN, 1927

Subfamily HETEROHELICINAE CUSHMAN, 1927

Genus *Heterohelix* EHRENBERG, 1843

Type species: *Textularia globulosa* EHRENBERG, 1843

***Heterohelix globulosa* EHRENBERG, 1840**

Plate 3, Figs. 1-5; Plate 34, Figs. 1-4.

1840 *Heterohelix globulosa* EHRENGERG, pl. 4, figs. 2b, 4b, 5b, 7b, 8b.

1938 *Guembelina reussi* CUSHMAN- pl.2, figs. 6-9.

1991 *Heterohelix globulosa* EHRENBERG- Nederbragt, pl. 2, fig. 1, 2.

2011 *Heterohelix globulosa* EHRENBERG- Keller *et al*., pl. 1, fig. 7.

2015 *Planoheterohelix globulosa* EHRENBERG- Haynes *et al*., figs. 11.1-11.14.

Description & Remarks:

Heterohelix globulosa is distinguished by its biserial test where globular chambers increasing gradually during its ontogeny. Two terminal chambers are much larger than earlier ones. There may be a complete bi-seriality or an initial coil.

In our samples, *Heterohelix globulosa* represents significant variation in chamber size, chamber number and ornamentation strength. Some specimens represent an offset in their last chamber onto previous two. This criterion has been used to distinguish between *Heterohelix globulosa* and *Heterohelix reussi* (Haynes et al. 2015). However, these specimens were considered as *H. globulosa* rather than *H. reussi* since *H. reussi* ranges only up to Coniacian *Dicarinella concavata* Zone, while *H. globulosa* ranges through the Maastrichtian.

Recently, this species has been identified by different genus and species names, such as *Planoheterohelix globulosa* (Haynes et al. 2015) or *Planoheterohelix paraglobulousa* (Georgescu and Huber 2009). Yet, we follow the traditional usage as ‘’*Heterohelix globulosa*’’ of Nederbragt (1991) to be consistent with the literature.

In our samples, *Heterohelix globulosa* has been identified throughout the *P. hantkeninoides* Zone (UH-30 to K-Pg boundary) and it survives after the K-Pg boundary in Danian P0 Zone.

Stratigraphic distribution in the literature: Turonian to K-Pg boundary (Nederbragt 1991) or uppermost Cenomanian to K-Pg boundary (Haynes et al. 2015).

Heterohelix labellosa NEDERBRAGT, 1991

Plate 3, Fig. 6.

1991 *Heterohelix labellosa* NEDERBRAGT, pl. 2, fig. 3-5.
2003 *Heterohelix labellosa* NEDERBRAGT- Abramovich *et al*., pl. 2, fig. 3.
2004 *Heterohelix labellosa* NEDERBRAGT- Premoli-Silva & Verga, pl. 71, fig. 1-3

Description & Remarks:

Heterohelix labellosa is easily distinguished from other *Heterohelix* species by its larger test, distinct costae and most importantly its subparallel adult chambers and apertural flange relicts on its median suture. In our samples, this form looks like *Pseudoguembelina palpebra* since *Psg. palpebra* has rapidly flaring juvenile and subparallel adult stage as well as its surface covered by continuous to discontinuous costae. However, *Psg. palpebra* can be differentiated from *H. labellosa* by its inflated adult and strongly laterally compressed ultimate chambers, large semilunar apertures bordered by lip-like rim.

Nederbragt (1991) mentioned that *Psg. palpebra* is phylogenetically unrelated form and might be descended from *Heterohelix* species. By judging from aforementioned similarity of *Heterohelix labellosa* with *Pseudoguembelina palpebra* in our samples. It could be concluded that *Heterohelix labellosa* might be ancestor of *Pseudoguembelina palpebra*.

In accordance with its larger size, *H. labellosa* has been found only above >150 μm fraction with consistent occurrence throughout *P. hantkeninoides* Zone in samples from UH-30 to UH-48. Due to its lack of unsteady and poor abundance after the K-Pg boundary, *H. labellosa* might have undergone extinction.

Stratigraphic distribution in the literature: Throughout the Maastrichtian (Nederbragt 1991).

Heterohelix navarroensis LOEBLICH, 1951

Plate 3, Figs. 7-8, Plate 34, Fig. 7.

1844 *Spiroplecta americana* EHRENBERG, 1844, p. 75.

1854 *Spiroplecta americana* EHRENBERG- pl. 32, fig. II-25.

1951 *Heterohelix navarroensis* LOEBLICH- pl. 12, fig. 1-3- text fig. 2.

1991 *Heterohelix navarroensis* LOEBLICH- Nederbragt, pl. 3, fig. 5.

2002 *Heterohelix navarroensis* LOEBLICH- Keller, pl. 3, fig. 3.

2002 *Heterohelix navarroensis* LOEBLICH- Abramovich *et al*., pl. 1, fig. 2.

2009 *Spiroplecta americana* EHRENBERG- Georgescu & Abramovich, figs. 4 (5-11), 5 (1-2, 5-8).

2011 *Heterohelix navarroensis* LOEBLICH- Keller *et al*., pl. 1, fig. 12.

Description & Remarks:

Heterohelix navarroensis is characterized by its distinct planispirally coiled 3-5 early chambers, then biserial test throughout the adult stage.

Taxonomy of this species has been highly disputed. It was considered either as: a junior synonym of *Spiroplecta americana* or junior synonym of *Heterohelix americana* or a valid species (Georgescu and Abramovich 2009 and references therein). Georgescu and Abramovich (2008a) considered *Spiroplecta* as a descendant of *Heterohelix globulosa*. However, we followed the criteria of Nederbragt (1991) and called this species ‘’*Heterohelix navarroensis*’’.

Similar with Nederbragt (1991), *H navarroensis* is rare and sporadic in >150 μm fraction, whereas it is common and highly abundant between 63-150 μm throughout the *P. hantkeninoides* Zone. This species in our study was considered as K-Pg boundary survivor.

Stratigraphic distribution in the literature: Campanian-Maastrichtian (Nederbragt 1991).

Heterohelix planata CUSHMAN, 1938

Plate 4, Figs. 1-3; Plate 34, Fig. 6.

1938 *Guembelina planata* CUSHMAN, pl. 2, fig. 13, 14

1938 *Guembelina pseudotessera* CUSHMAN, pl. 2, figs. 19-21.

1991 *Heterohelix planata* CUSHMAN- Nederbragt, pl. 3, fig. 3.

2008 *Heterohelix planata* CUSHMAN- Georgescu *et al*., pl. 1, fig. A(1); pl. 3, figs. 1-5.

Description & Remarks:

Heterohelix planata has a wide range of morphological variability. It may or may not initial early planispiral coiling in juvenile stage. Its biserial test has globular to subrectangular chambers in adult stage. Sometimes this subrectangular chambers may become reniform shape in last stage of its ontogeny. In our samples, these rectangular shape chambers correspond to 2/3 of the test (~early to medium stage of its ontogeny) and resemble ‘’sweetcorn’’ shape. Its medium to high arched aperture is bordered by apertural flanges and rarely rimmed. Most importantly, *Heterohelix planata* is characterized by having last two chambers slightly elongate onto each other.

This species may be confused with *Praegublerina pseudotessera*. However, Georgescu et al. (2008) claimed that *Praegublerina pseudotessera* differs from *Heterohelix planata* by having: divergent rows of biserial chambers creating a central non-septate area in the adult part; reniform chambers in the adult stage; larger apertural flanges and coarser costae.

Heterohelix planata has been encountered consistently throughout the *P. hantkeninoides* Zone (UH-30 to UH-49) in both fractions. It also survives into Danian P0 Zone.

Stratigraphic distribution in the literature: Upper Santonian to Maastrichtian (from *Dicarinella asymetrica* Zone to top of the *Pseudoguembelina hariaensis* Zone (Nederbragt 1991, Georgescu et al. 2008).

***Heterohelix punctulata* CUSHMAN, 1938**

Plate 4, Figs. 4-6.

1938 *Guembelina punctulata* CUSHMAN, p. 13, pl. 2, fig. 15, 16.

1989 *Heterohelix punctulata* CUSHMAN- Nederbragt, pl. 3, figs. 5-7.

1991 *Heterohelix punctulata* CUSHMAN- Nederbragt, pl. 3, figs. 6a-b.

Description & Remarks:

Heterohelix punctulata is described by its relatively large biserial test widely flares in juvenile and become subparallel in its adult stage. The initial portion rapidly tapers while later portion has nearly uniform width. Due to its accessory apertures, this species often included in *Pseudoguembelina* genus (Nederbragt 1991 and references therein). However, its apertures are rare and when present they lack distinct lip which is characteristic in *Pseudoguembelina* (Nederbragt 1989b).

Heterohelix punctulata currently is considered as *Braunella punctulata* after emendation of Georgescu (2007). Yet, we follow the classification of Nederbragt (1991).

Because of having larger test, this species consistently found in larger size fraction, whereas it is sporadic between 63-150 μm through *P. hantkeninoides* Zone. It shows relatively common occurrence after the K-Pg boundary. Thus, it was considered as survivor in our study.

Stratigraphic distribution in the literature: Upper part of the *D. asymetrica* Zone to the top of the Maastrichtian (Nederbragt 1991).

Heterohelix rajagopalani GOVINDAN, 1972

Plate 4, Fig. 7.

1972 *Gublerina rajagopalani* GOVINDAN, pl. 2, figs. 1-5.

1976 *Gublerina cuvillieri* WRIGHT and APTHORPE- non Kikoine, pl. 1, fig. 1.

1983 *Heterohelix semicostata* WEISS- non Cushman, pl. 3, figs. 3,4.

1991 *Heterohelix rajagopalani* GOVINDAN- Nederbragt, pl. 4, figs. 1a-b, 3a-b.

2001 *Heterohelix rajagopalani* GOVINDAN- Petrizzo, fig. 10 (9a, b; 10a, b).

2004 Heterohelix rajagopalani GOVINDAN- Premoli-Silva and Verga, pl. 73, figs. 6-9

2008 *Gublerina rajagopalani* GOVINDAN- Georgescu *et al*., pl. 5, figs. 1-5.

Description & Remarks:

Wedge-shaped test is biserial throughout, early part of test rapidly flares than the later part. Shape of the adult chambers are earlier subglobular then reniform or subrectangular. The most characteristic feature of this species is having one or two almost continuous strong costae which result in keeled appearance along the periphery. Unlike *Pseudoguembelina palpebra*, which has laterally compressed ultimate chambers may look like reniform chambers of *H. rajagopalani*, low to medium arch shape aperture at the base of the last formed chamber is bordered by well-developed flanges.

Heterohelix rajagopalani differs from *Gublerina cuvillieri* by its large, relict apertural flanges do not connect to chambers which happens in *Gublerina*, and two rows of chambers meet along the median suture (Nederbragt, 1991).

We encountered with *Heterohelix rajagopalani* only in one sample throughout the *P. hantkeninoides* Zone at UH-5.

Stratigraphic distribution in the literature: Upper part of the *G. calcarata* Zone to the top of the Maastrichtian (Nederbragt 1991). Lower part of the *Radotruncana calcarata* to the top of the *Abathomphalus mayaroensis* Zone (Georgescu et al. 2008).

Genus *Laeviheterohelix* NEDERBRAGT, 1991

Type species: *Guembelina pulchra* BROTZEN, 1936

Laeviheterohelix dentata STENESTAD, 1968

Plate 5, Figs. 3-5; Plate 34, Fig. 8.

1968 *Heterohelix dentata* STENESTAD, pl. 1, fig. 3-6, 8, 9; pl. 2, fig. 1-3.

1991 *Laeviheterohelix dentata* STENESTAD- Nederbragt, pl. 5, fig. 1-2.

2004 *Laeviheterohelix dentata* STENESTAD- Premoli-Silva and Verga, pl. 77, fig. 1-5

2009 *Fleisherites glabrans* CUSHMAN- Georgescu, figs. 12.1-12.6, 13.1-13.6.

Description & Remarks:

Nederbragt (1991) proposed *Laeviheterohelix* species as ‘’smooth’’ heterohelicids that their wall structure is non-costate and microperforate. *Laeviheterohelix dentata* has biserial test and most importantly reniform chambers. In our samples, this species has been continuously found in both size fractions throughout the Maastrichtian (UH-30 to UH-49) in *P. hantkeninoides* Zone. Also, it was considered as K-Pg boundary survivor.

Stratigraphic distribution in the literature: Late Campanian to the end of Maastrichtian (Nederbragt 1991).

Laeviheterohelix glabrans CUSHMAN, 1938

Plate 5, Figs. 6-8.

1938 *Guembelina glabrans* CUSHMAN, pl. 3, fig. 1, 2.

1991 *Laeviheterohelix glabrans* CUSHMAN- Nederbragt, pl. 5, fig. 6.

2003 *Laeviheterohelix glabrans* CUSHMAN- Abramovich *et al*., pl. 2, fig. 6.

2009 *Fleisherites glabrans* CUSHMAN- Georgescu, figs. 12.1-12.6, 13.1-13.6.

Description & Remarks: This species is distinguished by its biserial test, smooth surface and characteristic ‘’lentil’’-shape chambers with slightly inflated middle part. In studied samples, *L. glabrans* do not represent early initial coil. Throughout the

Maastrichtian in *P. hantkeninoides* Zone, it has been encountered majorly between 63-150 μm, although it is present sporadically in larger fraction. Similar with *L. dentata*, this species was considered as K-Pg boundary survivor, therefore it's last occurrence datum is in Danian P0 Zone (E+2).

Stratigraphic distribution in the literature: Late Campanian to the end of Maastrichtian (Nederbragt 1991).

Genus *Hartella* GEORGESCU & ABRAMOVICH, 2009

Type species: *Hartella harti* GEORGESCU & ABRAMOVICH, 2009

Hartella harti GEORGESCU & ABRAMOVICH, 2009

Plate 6, Figs. 1-9. Plate 7, Figs. 1-4.

2009 *Hartella harti* GEORGESCU & ABRAMOVICH, figs. 4 (1–4), 5 (3, 4, 9–12), 6 (1–12) and 7 (1–12).

2016 *Hartella harti* GEORGESCU & ABRAMOVICH- Punekar *et al*., pl.1, fig. J.

Description & Remarks:

The genus *Hartella* is monospecific. *Hartella harti* is characterized by its compressed test, most importantly well-developed early planispiral coiled part composed of 3 to 4 chambers. Subsequent adult biserial stage has nine to eleven chambers. The chamber surfaces are ornamented with pustules and sutures are straight and depressed. *Hartella harti* has highly characteristic ‘’bottle-neck’’ structure which happens during transition from early planispirally coiled part to biserial stage. It can be differentiated from *Laeviheterohelix glabrans* by its well-developed early planispiral coil, bottle-neck structure from planispiral to biserial test and conspicuous costate ornamentation.

Although work of Punekar et al. (2016) was one of the earliest study representing *Hartella harti* in their samples, they incorrectly demonstrated the *Hartella harti* in their Plate 1 as K, however it should be the form at J.

This species has been consistently found throughout the Maastrichtian in *P. hantkeninoides* Zone within 63-150 µm fraction (UH-30 to UH-49). It might have undergone extinction because we have failed to any *Hartella harti* in Danian samples.

Stratigraphic distribution in the literature: Upper Maastrichtian-from middle part of the *Abathomphalus mayaroensis* Zone to the end of Maastrichtian (Georgescu and Abramovich 2009).

Genus *Planoglobulina* CUSHMAN, 1927

Type species: *Guembelina acervulinoides* EGGER, 1899

Planoglobulina acervulinoides EGGER, 1899

Plate 8, Figs. 1-3; Plate 33, Figs. 7-9.

1899 *Guembelina acervulinoides* EGGER, pl. 14, fig. 20.
1972 *Planoglobulina acervulinoides* EGGER- Martin, pl. 3, figs. 3-4.
1991 *Planoglobulina acervulinoides* EGGER- Nederbragt, pl. 6, fig.5-6.
2003 *Planoglobulina acervulinoides* EGGER- Abramovich *et al*., pl. 4, fig. 11.
2014 *Planoglobulina acervulinoides* EGGER- Georgescu, figs. 6 (4-9); 7 (1-3, 7-9).

Description & Remarks:

This species is distinguished by its early biserial then multiserial test. Chamber surfaces are covered by continuous/discontinuous costae. *Planoglobulina acervulinoides* differs from *Planoglobulina brazoensis* by its shallower test and more multiserial chamberlets.

Recently, Georgescu (2014) classified *Planoglobulina* into two main morpho-groups: *Planoglobulina sphaeralis* (Georgescu) and *Planoglobulina acervulinoides* (Egger). *Planoglobulina sphaeralis* (Georgescu) corresponds to traditional morphotypes of *Heterohelix striata* (Ehrenberg). On the other hand, he lumped all the *Planoglobulina* species which represent multiserial growth in their adult stage, such as *Pl. acervulinoides* (Egger), *Pl. brazoensis* (Martin) and *Pl. carseyae* (Plummer), into *Planoglobulina acervulinoides* (Egger). He basically defined *P. acervulinoides* as a

‘’*Planoglobulina* with chamber proliferation in adult stage’’. On the contrary, in our study we did not lump all the species with multiserial chamber growth in to *Pl. acervulinoides*, we kept the traditional categorization.

In our samples, *Planoglobulina acervulinoides* was consistently encountered throughout the Maastrichtian section in *P. hantkeninoides* Zone until the K-Pg boundary (UH-30 to UH-49).

Stratigraphic distribution in the literature: Maastrichtian, middle part of the *Gansserina gansseri* Zone to top of the *Abathomphalus mayaroensis* Zone (Nederbragt 1991).

***Planoglobulina brazoensis* MARTIN, 1972**

Plate 8, Figs. 4-6.

1972 *Planoglobulina brazoensis* MARTIN, pl. 3, fig. 7; pl.4, fig. 1-2.
2003 *Planoglobulina brazoensis* MARTIN- Abramovich *et al*., pl. 4, fig. 10.
2011 *Planoglobulina brazoensis* MARTIN- Korchagin, pl.1, fig. 7a-7c.

Description & Remarks:

Planoglobulina brazoensis highly looks like *P. acervulinoides*, whereas it differs by its more robust-deeper test and fewer multiserial chamberlets (Nederbragt, 1991).
In our samples, this difference has been observed. Individuals correspond to *P. brazoensis* generally have more robust test, smaller juvenile biserial stage, larger chambers, one or two multiserial chamber sets and thick costae.

P. brazoensis was found consistently through the Maastrichtian samples in *P. hantkeninoides* Zone. Although it was encountered in some Danian samples, this species underwent extinction across the K-P boundary.

Stratigraphic distribution in the literature: Uppermost *G. gansseri* Zone to the K-Pg boundary (Martin, 1972).

***Planoglobulina carseyae* PLUMMER, 1931**

Plate 8, Figs. 7-8; Plate 9, Figs. 1-2; Plate 33, Figs. 1-3.

1931 *Ventilabrella carseyae* PLUMMER, 179, pl. 9, fig. 7-10.

1972 *Planoglobulina*(?) *carseyae* PLUMMER- Martin, pl. 4, figs. 4-7

1991 *Planoglobulina carseyae* PLUMMER- Nederbragt, pl. 7, figs. 2, 3.

2004 *Planoglobulina carseyae* PLUMMER- Premoli-Silva and Verga, pl. 102, fig. 5; pl. 103, fig. 1-5; pl. 31, fig. 12, 13.

2014 *Planoglobulina acervulinoides* EGGER- Georgescu, fig. 5 (7-10).

Description & Remarks:

Planoglobulina carseyae is distinguished by having multiserial chamberlets, generally composed of three ultimate multiserial chambers which bend in a certain direction. Its biserial stage rapidly increases followed by one or two sets of multiserial chamberlets, its surface is covered by fine costae and thin flanges border its aperture. Practically, if it has only one set of multiserial chambers (i.e. composed of three chamberlets), it would commonly have inclined ‘’Y’’ shape where the top of ‘’Y’’ gently tilted towards one side.

In our samples, this curved ‘Y’ shape has been commonly observed. Furthermore, this morphotype comprised majority of the *Planoglobulina carseyae* species. *P. carseyae* was consistently found throughout the Maastrichtian in *P. hantkeninoides* Zone (UH-30 to UH-49).

Stratigraphic distribution in the literature: Throughout the Maastrichtian (Nederbragt 1991).

***Planoglobulina multicamerata* DE KLASZ, 1953**

Plate 9, Figs. 3-4.

1953 *Ventilabrella multicamerata* DE KLASZ, pl. 5, fig. la, b.

1972 *Ventilabrella multicamerata* DE KLASZ- Martin, pl. 3, figs. 1, 2.

1991 *Planoglobulina multicamerata* DE KLASZ- Nederbragt, pl. 7, figs. 4, 5.

2002 *Planoglobulina multicamerata* PLUMMER- Keller *et al*., pl. 3, fig. 4.

2004 *Ventilabrella multicamerata* DE KLASZ- Premoli-Silva and Verga, pl. 143, fig. 8; pl. 144, figs. 1-4.

2012 *Planoglobulina multicamerata* DE KLASZ- Perez-Rodriguez *et al*., pl. 7, fig. E1-2

Description & Remarks:

Planoglobulina multicamerata is highly characteristic with its rapidly increasing numerous, extremely compressed chambers with poorly defined sutures, vermicular ornamentation covering the early small biserial part and elongate-subtriangular test (Martin 1972). Its sides rapidly flaring throughout or becoming subparallel in the adult stage (Nederbragt 1991). Its maximum text length can be as large as 800 μm.

Practically, this species can be recognized with its ‘’V-shaped’’ test on which vermicular ornamentation is denser in areas where two lines converge and comprise the ‘‘V’’ shape, while numerous compressed chambers occupy the space between these two lines diverge.

Planoglobulina manuelensis (Martin) highly looks like *Planoglobulina multicamerata.* Yet, *P. manuelensis* differs from *P. multicamerata* by having rapidly flaring subcircular test, and fewer chambers in the multiserial portion.

In this present study, *Planoglobulina multicamerata* was found in samples UH-14 and UH-41, and an intermediate form between *Pl. manuelensis* and *Pl. multicamerata* was identified in UH-48. This study is the first work in Turkey demonstrating complete features of the *Planoglobulina multicamerata*.

Stratigraphic distribution in the literature: From *Gansserina gansseri* Zone to top of *Abathomphalus mayaroensis* Zone (Nederbragt 1991).

Genus *Pseudotextularia* RZEHAK, 1891

Type species: *Cuneolina elegans* RZEHAK, 1891

Pseudotextularia elegans RZEHAK, 1891

Plate 10, Figs. 1-2; Plate 33, Figs. 13-14.

1891 *Cuneolina elegans* RZEHAK, p. 4.

1991 *Pseudotextularia elegans* RZEHAK- Nederbragt, pl. 10, fig. 1,2.

2015 *Pseudotextularia elegans* RZEHAK- Coccioni and Premoli-Silva, pl. 2, figs. 1, 2.

2016 *Pseudotextularia elegans* RZEHAK- Punekar *et al*., pl.1, fig. F.

Description & Remarks:

Pseudotextularia elegans is distinguished by its large biserial test, adult chambers strongly reniform in edge view, chamber surface covered by thick continuous costae. It has bi-convex appearance in lateral view.

This species is consistently present in >150 μm fraction throughout the Maastrichtian in *P. hantkeninoides* Zone. Although some individuals were recovered in Danian samples (see Table 5), *Pst. elegans* underwent extinction.

Stratigraphic distribution in the literature: Throughout the Maastrichtian (Nederbragt 1991).

Pseudotextularia nuttalli VOORWIJK, 1937

Plate 10, Figs. 3-4; Plate 33, Figs. 15-16.

1937 *Guembelina nuttalli* VOORWIJK, pl. 2, fig. 1-9.

1991 *Pseudotextularia nuttalli* VOORWIJK- Nederbragt, pl. 10, fig. 4, 6.

2014 *Bronnimannella nuttalli* VOORWIJK- Georgescu, fig. 2:1-10.

2015 *Planoheterohelix praenuttalli* HAYNES, HUBER & MACLEOD, fig. 19.11,.12,.13.

2015 *Pseudotextularia nuttalli* VOORWIJK- Haynes, Huber & MacLeod, fig. 19 (14,15).

2017 *Pseudotextularia nuttalli* VOORWIJK- Petrizzo et al., fig. 9 (11a, b).

Description & Remarks:

Pseudotextularia nuttalli is one of the easiest form to identify. Its biserial test bi-convex in edge view, it has characteristic strongly reniform chambers in side view and finer costae than *Pseudotextularia elegans*.

In our samples, some individuals exhibit less tapering edge view and less strong reniform chambers and their last chamber slightly offset onto previous penultimate chambers. Although, we lumped these specimens into *Pst. nuttalli* morphotype, these forms were categorized under new genera as: *Planoheterohelix praenuttalli* by Haynes et al. (2015).

On the other hand, as mentioned above, some *Heterohelix* specimens have last chambers slightly or largely offset onto previous two. This offset has been pronounced a discrimination criteria of *H. reussi* from *H. globulosa* (Haynes et al. and references therein). However, as mentioned before, we have 'lumped' these forms under *H. globulosa* morphotype due to indefinite upper stratigraphic range of *H. reussi*. In our study, a certain ancestor-descendant evolutionary pattern has been observed amongst: *Heterohelix globulosa- Heterohelix reussi- Planoheterohelix praenuttalli- Pseudotextularia nuttalli* species.

Similarly, Haynes et al. (2015) observed that *Heterohelix reussi* (Cushman) is likely descendant from *Heterohelix globulosa* (Ehrenberg) and ancestor of *Planoheterohelix praenuttalli* (Haynes, Huber & MacLeod), and *Pl. praenuttalli* is direct ancestor of *Pseudotextularia nuttalli* (Voorwijk).

Haynes et al. (2015) claimed that ''*Planoheterohelix praenuttalli* differs from *Planoheterohelix (Heterohelix) globulosa* by having: larger and broader test which more strongly tapers in both side and edge view''. On the other hand, *Pseudotextularia nuttalli* has larger reniform chambers and strongly tapers in edge view than *Planoheterohelix praenuttalli*. Yet, they are tapering similarly in side view.

Pseudotextularia nuttalli is abundant and continuous throughout the Maastrichtian samples above 150 μm fraction in *P. hantkeninoides* Zone (see Table 5). Although some specimens were encountered after the boundary, this form was interpreted as undergone extinction.

Stratigraphic distribution in the literature: First occurrence is in *Dicarinella concavata* Zone near the Coniacian-Santonian boundary and ranges into upper Maastrichtian (Haynes et al. 2015). Coniacian to the end of the Maastrichtian (Nederbragt 1991).

Pseudotextularia intermedia **DE KLASZ, 1953**

Plate 10, Figs. 5-6; Plate 33, Figs. 4, 5, 10.

1953 *Pseudotextularia intermedia* DE KLASZ, pl. 5, figs. 2a-c.
1991 *Pseudotextularia intermedia* DE KLASZ- Nederbragt, pl. 10, figs. 3a-b.
2014 *Racemiguembelina intermedia* DE KLASZ- Georgescu, fig. 5
2015 *Pseudotextularia intermedia* DE KLASZ- Coccioni and Premoli-Silva, pl. 2, figs. 3, 4.

Description & Remarks:

Pseudotextularia intermedia, as its name implies, is intermediate form between its ancestor *Pseudotextularia nuttalli* and its descendant *Racemiguembelina powelli*.

This species has strongly reniform chambers, small multiserial chamberlets at its terminal stage, and have a ornamented wall with thin to coarse costae. Nederbragt (1991) described that these chamberlets are arranged in racemiguembelinid pattern, but not connected by a bridge. The most characteristic features are these small, unbridged terminal chamberlets different from connecting chamberlets of *Racemiguembelina*. Individuals with larger chamberlets comprise transitional forms to *Racemiguembelina powelli*.

In our samples, *Pseudotextularia intermedia* was found consistently throughout the Maastrichtian above 150 μm fraction in *P. hantkeninoides* Zone. It went extinction at the K-Pg boundary, although some reworked specimens were found in Danian.

Stratigraphic distribution in the literature: Maastrichtian, middle part of the *Gansserina gansseri* Zone to end of the *Abathomphalus mayaroensis* Zone (Nederbragt, 1991).

Genus Racemiguembelina MONTANARO GALLITELLI, 1957

Type species: Guembelina fructicosa EGGER, 1899

Racemiguembelina fructicosa EGGER, 1899

Plate 11, Figs. 1-2.

1899 *Guembelina fructicosa* EGGER, pl. 14, fig. 8, 9, 24

1972 *Racemiguembelina fructicosa* EGGER- Martin, pl. 4, fig. 3.

1991 *Racemiguembelina fructicosa* EGGER- Nederbragt, pl. 10, fig. 5.

2002 *Racemiguembelina fructicosa* EGGER- Keller *et al*., pl. 3, fig. 2.

2003 *Racemiguembelina fructicosa* EGGER- Abramovich *et al*., pl. 4, figs. 7, 8.

2015 *Racemiguembelina fructicosa* EGGER- Coccioni and Premoli-Silva, pl. 2, figs. 11-13.

Description & Remarks:

Racemiguembelina fructicosa is characteristic with its perfect conical shape and large number of multiserial chamber sets (usually 4 to 5). Its surface is covered by continuous costae. At top of the test, the bridges are microperforate, without ornamentation and bordered by imperforate rims. The wall structure of the bridges of *R. fructicosa* differs from that of *R. powelli*. It has more but smaller chambers in the multiserial stage than *R. powelli*.

In this present study, *R. fructicosa* was sporadically encountered and none was found in any sample close to the K-Pg boundary (see Table 5). This may reflect earlier extinction or diminished abundance of this species due to ongoing environmental stress.

Stratigraphic distribution in the literature: Throughout the *Abathomphalus mayaroensis* Zone (Nederbragt 1991).

***Racemiguembelina powelli* SMITH and PESSAGNO, 1973**

Plate 11, Figs. 3-5; Plate 33, Fig. 6.

1973 *Racemiguembelina powelli* SMITH and PESSAGNO, pl. 11, fig. 4-12.

1991 *Racemiguembelina powelli* SMITH and PESSAGNO- Nederbragt, pl. 11, fig. 1.

2002 *Racemiguembelina powelli* SMITH and PESSAGNO- Keller *et al*., pl. 3, fig. 3.

2012 Racemiguembelina powelli SMITH and PESSAGNO- Perez-Rodriguez *et al*., pl. 7, fig. H1-2.

2015 *Racemiguembelina powelli* SMITH and PESSAGNO- Coccioni and Premoli-Silva, pl. 2, figs. 7-10.

Description & Remarks:

This species is characterized by its biserial initial test and 1 or 2 sets of 3-dimensionally arranged multiserial chambers. It has ellipsoid top view and its connecting final pair of chamberlets create a short bridge. The wall structure of the bridges is same as that of the entire test. It differs from *Racemiguembelina fructicosa* by its smaller size, fewer but larger multiserial chambers, incomplete multiserial growth and imperfect conical shape. Practically, *R. powelli* demonstrates more flaring morphology due to addition of multiserial chamberlets, whereas *R. fructicosa* has more bullet shape. Also, *R. powelli* can be distinguished by its high resemblance to *Pseudotextularia intermedia*.

In our study, *Racemiguembelina powelli* sporadically present in our samples throughout the Maastrichtian in *P. hantkeninoides* Zone.

Stratigraphic distribution in the literature: Throughout the *Abathomphalus mayaroensis* Zone (Nederbragt 1991).

Subfamily PSEUDOGUEMBELININAE ALIYULLA, 1977

Genus *Pseudoguembelina* BRONNIMANN and BROWN, 1953

Type species: *Guembelina excolata* CUSHMAN, 1926

***Pseudoguembelina costulata* CUSHMAN, 1938**

Plate 12, Figs. 1-2.

1938 *Guembelina costulata* CUSHMAN, pl. 3, fig. 7-9.
1991 *Pseudoguembelina costulata* CUSHMAN- Nederbragt, pl. 8, fig. 3, 4.
2003 *Pseudoguembelina costulata* CUSHMAN- Abramovich *et al*., pl. 2, fig. 12.
2007 *Pseudoguembelina costulata* CUSHMAN- Georgescu, pl. 1, fig. 2.
2014 *Pseudoguembelina praecostulata* GEORGESCU, p. 61, fig. 11.1-13.
2014 *Pseudoguembelina costulata* CUSHMAN- Meilijson et al., fig. 10.1.

Description & Remarks:

Pseudoguembelina costulata is characterized by its biserial test with continuous coarse costae following the curve of the chambers. Adult chambers are slightly reniform. Last 3 to 4 chambers may have accessory apertures covered by lid-like extensions directed towards to median suture. Practically, the outline of the ultimate chambers resembles oblique crescent or ‘’C’’ shape and its bimodal ornamentation made up of coarser costae somehow create a ‘’comb’’ like trace on the surface of the chambers.

In our study, *Pseudoguembelina costulata* was found sparse and sporadically in >150 μm and 63-150 μm fraction in *P. hantkeninoides* Zone.

Stratigraphic distribution in the literature: Upper part of the *G. elevata* Zone (Campanian) to top of the Maastrichtian (Nederbragt 1991).

Pseudoguembelina hariaensis NEDERBRAGT, 1991

Plate 12, Figs. 3-8.

1983 *Pseudoguembelina* sp. WEISS- pl.7, figs. 8, 9.

1991 *Pseudoguembelina hariaensis* NEDERBRAGT, pl. 8, fig. 6, 7; pl. 9, fig. 1, 2.

2002 *Pseudoguembelina hariaensis* NEDERBRAGT- Keller *et al*., pl. 2, fig. 12.

2014 *Nederbragtina hariaensis* GEORGESCU, pg. 63, text fig. 12.

2014 *Nederbragtina prima* GEORGESCU, pg. 63, text fig. 12, fig. 13 (4-12).

2015 *Pseudoguembelina hariaensis* NEDERBRAGT- Coccioni and Premoli-Silva, pl. 3, fig. 8-11.

Description & Remarks:

Pseudoguembelina hariaensis is distinguished with its biserial to multiserial test. Biserial part flaring throughout or rapidly flaring in juvenile stage. Surface is covered by discontinuous costae and aperture has small, distinct flanges. It differs from *Pseudoguembelina palpebra* by having no accessory apertures, less inflated chambers, more sets of multiserial chamberlets and thinner costae.

Practically, *Pseudoguembelina hariaensis* can be easily recognized by having an imaginary line on which multiserial chamberlet(s) located which bend towards to one side.

Pseudoguembelina hariaensis in our study was consistently found throughout the Maastrichtian in *P. hantkeninoides* Zone. It disappears after the K-Pg boundary.

Stratigraphic distribution in the literature: Uppermost *A. mayaroensis* Zone, Maastrichtian (Nederbragt 1991).

***Pseudoguembelina palpebra* BRONNIMANN and BROWN, 1953**

Plate 12, Fig. 9.

1953 *Pseudoguembelina palpebra* BRONNIMANN and BROWN, text figs. 9, 10.

1976 *Pseudoguembelina polypleura* MASTERS, pl. 1, fig. 9.

1991 *Pseudoguembelina palpebra* BRONNIMANN and BROWN- Nederbragt, pl. 9, figs. 5-7b.

2003 *Pseudoguembelina palpebra* BRONNIMANN and BROWN- Abramovich *et al*., pl. 2, figs. 16-18.

2012 *Pseudoguembelina palpebra* BRONNIMANN and BROWN- Perez Rodriguez *et al*., fig. 7 (L1-2).

2015 *Pseudoguembelina palpebra* BRONNIMANN and BROWN- Coccioni and Premoli-Silva, pl. 3, figs. 1-3.

Description & Remarks:

Biserial test of *Pseudoguembelina palpebra* rapidly flares in juvenile stage and becomes subparallel with inflated chambers through the adult stage. It is characteristic with its accessory apertures bordered by lip-like rim and covered by an eye-shaped lid directed away from the median suture. Practically, these apertural borders seem like small notches concentrated across the median suture and generally point opposite directions. Generally, the supplementary apertures are located on last 2 to 4 (Nederbragt 1991) or 2 to 5 (Georgescu 2014) chambers. Last two chambers are generally compressed.

Pseudoguembelina palpebra is common but sporadic within samples above 150 μm fraction throughout the Maastrichtian in *P. hantkeninoides* Zone

Stratigraphic distribution in the literature: Throughout the *G. gansseri* Zone and the *A. mayaroensis* Zone (Nederbragt 1991).

Pseudoguembelina kempensis ESKER, 1968

Plate 13, Figs. 1-4.

1968 *Pseudoguembelina kempensis* ESKER, p. 168, text figs. 1-5.

1991 *Pseudoguembelina kempensis* ESKER- Nederbragt, pl. 9, figs. 3a-4.

2003 *Pseudoguembelina kempensis* ESKER- Abramovich *et al*., pl. 2, fig. 14.

2012 *Pseudoguembelina kempensis* ESKER- Perez Rodriguez *et al*., fig. 7 (K1-2).

2014 *Pseudoguembelina kempensis* ESKER- Georgescu, text fig. 8.

Description & Remarks:

Pseudoguembelina kempensis is highly characteristic with its pinched chambers along the edges giving an acute to keeled periphery. Due to its pinched edges, chambers somehow create nod-like features concentrated along the median suture. Accessory apertures are situated on the last-formed 1 to 4 (Georgescu 2014) or 2 to 4 (Nederbragt 1991) chambers with a lid-like extension directed to median suture. Practically, this species looks like a ‘’dagger’’ shape.

In our specimens *Pseudoguembelina kempensis* was found only in one sample between 63-150 μm size fraction in *P. hantkeninoides* Zone.

Stratigraphic distribution in the literature: Throughout the *G. gansseri* Zone and the *A. mayaroensis* Zone (Nederbragt 1991).

Genus *Gublerina* KIKOINE, 1948

Type species: *Gublerina cuvillieri* KIKOINE, 1948

Gublerina acuta DE KLASZ, 1953

Plate 14, Figs. 1-2.

1953 *Gublerina acuta* DE KLASZ, pl. 8, figs. 3a, b.
1953 *Gublerina acuta robusta* DE KLASZ, pl. 8, figs. 4, 5.
1953 *Gublerina hedbergi* BRÖNNIMANN and BROWN, text figs. 11, 12.
1991 *Gublerina acuta* DE KLASZ- Nederbragt, pl. 1, figs. 1-4.
2003 *Gublerina acuta* DE KLASZ- Abramovich *et al*., pl. 2, fig. 9.
2009 *Praegublerina robusta* DE KLASZ- Georgescu *et al*., pl. 4, figs. 5-11.
2009 *Praegublerina acuta* DE KLASZ- Georgescu *et al*., pl. 1, fig. 3; pl.4, figs. 1-4.

Description & Remarks:

Gublerina acuta is characteristic with a test made up of two divergent rows creates a central nonseptate area. Its early part is covered by distinctive vermicular/reticulate ornamentation. Test is biserial in early stage and multiserial in adult. Early chambers globular then become reniform in adult chambers and they gradually tilt with respect to the test growth axis. The multiserial stage poorly developed which composed of a single set of two chambers.

Gublerina acuta robusta characterized by bearing heavy vermicular ornamentation was considered by Nederbragt (1991) as extreme morphologic variant of *Gublerina acuta*. Here we followed her suggestion and lumped this morpho-group within the range of *Gublerina acuta*.

In our samples *Gublerina acuta* has been rarely encountered in *P. hantkeninoides* Zone. Moreover, none was found through the scope of quantitative study. Georgescu et al. (2009) claimed that *Praegublerina robusta* (de Klasz) and *Praegublerina acuta* (de Klasz), named here as *Gublerina acuta*, are cosmopolitan species.

Stratigraphic distribution in the literature: Upper Campanian-Maastrichtian. From upper part of the *Radotruncana calcarata* Zone throughout the top of the *Pseudoguembelina hariaensis* Zone (Georgescu et al. 2009).

Gublerina cuvillieri KIKOINE, 1948

Plate 14, Figs. 3-7.

1948 *Gublerina cuvillieri* KIKOINE, pl. 2, figs. 10a-c.

1953 *Gublerina cuvillieri* DE KLASZ, pl. 8, fig. 1.

1991 *Gublerina cuvillieri* KIKONE- Nederbragt, pl.1, figs. 3-4b.

2009 *Gublerina cuvillieri* KIKONE- Georgescu *et al*., pl. 1, figs. A (5-6); pl. 5, figs. 6-11; pl. 6, figs. 7-9.

2014 *Gublerina cuvillieri* KIKONE- Meilijson *et al*., fig. 10 (5).

Description & Remarks:

Gublerina cuvillieri has been described by early biserial then multiserial adult test. It has wide nonseptate central area. Multiserial chambers are variable in shape rather than elongate as in *G. acuta*. Its test ornamentation consists of strongly ornamented parts concentrated over the chambers while the rest of the test is rather smooth or finely costate.

In our samples *Gublerina cuvillieri* was found sporadically throughout Maastrichtian section in *P. hantkeninoides* Zone.

Stratigraphic distribution in the literature: Upper Maastrichtian. From the upper part of the *Gansserina gansseri* Zone to the uppermost part of the *Abathomphalus mayaroensis* Zone (Georgescu et al. 2009).

Superfamily PLANOMALINACEA BOLLI, LOEBLICH and TAPPAN, 1957

Family GLOBIGERINELLOIDIDAE LONGORIA, 1974

Subfamily GLOBIGERINELLOIDINAE LONGORIA, 1974

Genus *Globigerinelloides* CUSHMAN & ten DAM, 1948

Type species: *Globigerinelloides algeriana* CUSHMAN and ten DAM,1948

***Globigerinelloides alvarezi* ETERNOD OLVERA, 1959**

Plate 15, Figs. 1-4, Plate 34, Fig. 22.

1841 *Allotheca megathyra* EHRENBERG, pl. 3, fig. 49.
1959 *Planomalina alvarezi* ETERNOD OLVERA, pl. 4, figs. 5-7.
1960 *Planomalina yaucoensis* PESSAGNO, pl. 2, figs. 14-15; pl. 5, fig. 4.
1962 *Planomalina yaucoensis* PESSAGNO, pl. 1, figs. 1-2.
1968 *Globigerinelloides alvarezi* ETERNOD OLVERA- Sliter, pl. 15, figs 1, 2.
1980 *Globigerinelloides yaucoensis* PESSAGNO- Peryt, pl. 7, fig. 7.
1988 *Globigerinelloides alvarezi* ETERNOD OLVERA- El-Nakhal, pl. 1, fig. 12.
2013 *Allotheca megathyra* EHRENBERG- Georgescu, pl. 10, figs. 1, 3-6.
2017 *Globigerinelloides yaucoensis* PESSAGNO, Petrizzo *et al*., fig. 12 (11a-b).

Description & Remarks:

Recently, Georgescu (2013) considered *Globigerinelloides yaucoensis* (Pessagno) as junior synonym of *Globigerinelloides alvarezi* (Eternod Olvera). This relation was also mentioned by Sliter (1968) as cited in CHRONOS Portal. Hence, here in this study we followed same taxonomic categorization and considered *Globigerinelloides yaucoensis* (Pessagno) as junior synonym of *Globigerinelloides alvarezi* (Eternod Olvera).

Globigerinelloides alvarezi is distinguished by its evolute-involute test slowly arranged in 2.5 to 3 whorls and 7-8.5 chambers in the last tour. Test is symmetrical and slightly compressed in the edge view. Biaperturate last chambers occasionally

occurs in gerontic specimens. Relict periapertural structures of the last-formed 3 to 4 chambers may exist in the umbilical area.

In our specimens through *P. hantkeninoides* Zone, *Globigerinelloides alvarezi* was sparse until the sample UH-39, thereafter it was abundant and consistent throughout the Maastrichtian samples in 63-150 μm. However, this increase after the sample UH-39 was not observed in >150 μm fraction. It was found a few throughout the Maastrichtian samples in >150 μm. None was found after the K-Pg boundary.

Stratigraphic distribution in the literature: Campanian-Maastrichtian (Georgescu 2013).

***Globigerinelloides asperum* EHRENBERG, 1854**

Plate 15, Figs. 5-6; Plate 34, Figs. 14-19.

1854 *Phanerostomum asperum* EHRENBERG, pl. 30, figs. 26a, 26b, non pl. 32, group 1, fig. 24, non pl. 32, group II, fig. 42.

1929 *Globigerinella aspera* EHRENBERG- non Carman, pl. 34, fig. 6.

1958 *Globigerina aspera* EHRENBERG- Hofker, pl. 5, fig. 27.

1961 *Planomalina aspera* EHRENBERG- Barr, pl. 69, fig. 4.

1966 *Globigerinelloides aspera* EHRENBERG- Barr, pl. 37, figs. 3, 6.

1968 *Globigerinelloides messinae* BRONNIMANN- Sliter, pl. 15, figs. 3, 5.

1969 *Globigerinelloides multispina* LALICKER- Douglas, pl. 9, fig. 6.

1973 *Globigerinelloides multispina* LALICKER- Smith and Pessagno, figs. 1-2.

1980 *Globigerinelloides prairiehillensis* PESSAGNO- Peryt, pl. 8, figs. 1-4.

1983 *Globigerinelloides asper* EHRENBERG- Masters, pl. 1, figs. 1-5.

1982 *Globigerinelloides* aff. *multispina* LALICKER- Bergstresser and Frerichs, pl. 1, figs. 11-12.

2003 *Globigerinelloides aspera* EHRENBERG- Abramovich *et al*., pl. 3, figs. 1-2.

2012 *Globigerinelloides asperum* EHRENBERG- Georgescu, pl. 2, figs. 1-13, pl. 3, figs. 1-15, text-fig. 2: 1-7.

2013 *Allotheca asperum* EHRENBERG- Georgescu, pl. 9, figs. 1-5.

Description & Remarks:

According to emended description by Georgescu (2012). *Globigerinelloides asperum* is characterized by an involute planispiral test with 5.5-6 globular chambers in the final whorl, and ornamented with dome-like pustules equally developed on the test surface. Its aperture is covered by a thin lip, gerontic specimens generally possess biaperturate final chamber and no relict apertures present in the umbilical area.

Globigerinelloides asperum differs from:

Globigerinelloides prairiehillensis by having a test with fewer whorls (1.25 to 1.5 in *G. asperum* rather than 2 to 2.5 in *G. prairiehillensis*), fewer chambers in the last whorl (5.5 to 6 in *G. asperum* rather than 6 to 7 in *G. prairiehillensis*), and its chamber size increases more rapidly; from *Globigerinelloides alvarezi* by having less number of chambers in the final whorl which increase in a higher rate;

Globigerinelloides subcarinatus with absent subacute periphery and imperforate peripheral band on the earlier chambers of the final whorl;

Globigerinelloides messinae by having higher rate of increase in chamber thickness since the opposite feature results in compressed appearance in edge view in *G. messinae*.

In our study, *Globigerinelloides asperum* was commonly found in both 63-150 μm and >150 μm size fractions throughout the Maastrichtian samples in *P. hantkeninoides* Zone. Additionally, it was encountered in both three samples (E+2, UH-50, UH-51) representing Danian P0 Zone. Because of this consistent and abundant presence, *Globigerinelloides asperum* was considered as K-Pg boundary survivor.

Stratigraphic distribution in the literature: Santonian-Maastrichtian; it is most commonly observed in the Santonian-lower Campanian and lower-middle Maastrichtian sediments (Georgescu 2012). Rare in Santonian, more frequent in the upper Campanian-Maastrichtian (Georgescu 2013).

Globigerinelloides multispinus LALICKER, 1948

Plate 15, Figs. 7-9.

1943 *Globigerinelloides multispina* LALICKER, pl. 92, figs 1a-c.

1973 *Globigerinelloides multispina* LALICKER- Smith & Pessagno, pl. 13, figs 1–4.

2001 *Globigerinelloides multispinus* LALICKER- Petrizzo, figs. 10.4a, b, 6a, b.

2004 *Macroglobigerinelloides multispinus* LALICKER; Premoli-Silva and Verga, pl. 86, fig. 3a-b.

2011 *Globigerinelloides multispinus* LALICKER- Keller et al., pl. 1, fig. 16.

Description & Remarks:

Globigerinelloides multispinus is one of the most characteristic morpho-group within the *Globigerinelloides* genus. It is distinguished by its very large last chamber mostly divided into two sub-chamberlets. It has 5-7 chambers in the last whorl of the test. This species is generally confused with *Globigerinelloides prairiehillensis*. However, it differs from *G. prairiehillensis* by having biapartite apertural apparatus, smaller umbilici and more involute test.

Petrizzo (2001) claimed that a taxonomic revision is needed between these two species since they show strong similarity and even they may be morphotypes of the same species.

In our samples, *Globigerinelloides multispinus* specimens generally have 5 chambers in their last whorl and well divided last chamber into two chamberlets.

It has been commonly found throughout the Maastrichtian samples above >150 μm fraction although it was sparse between 63 and 150 μm screen size. None was encountered after the K-Pg boundary.

Stratigraphic distribution in the literature: Campanian-Maastrichtian. From the *Radotruncana calcarata* Zone through the *Abathomphalus mayaroensis* Zone (CHRONOS Portal).

Globigerinelloides mendezensis ETERNOD OLVERA, 1959

Plate 16, Figs. 1-3.

1959 *Planomalina mendezensis* ETERNOD OLVERA, p. ?, fig. ?.

Description & Remarks:

This species is highly characteristic with its radially elongated penultimate chambers. It has 5 to 6 chambers on the last whorl. First three chambers of the last tour are subspherical to globular. Test is compressed, biumbilicate, and the chambers in the last whorl progressively increase in size. Aperture is arched, large and interiomarginal. No accessory aperture was attained with this species.

In our study, we have found some *Globigerinelloides* specimens with abovementioned morphologic features. Apart from Eternod Olvera (1959), who described this species for the first time, yet we have failed to find any publication announcing *Globigerinelloides mendezensis* form in their samples or its morphologically similar species. Therefore, although there has not been enough study in the literature, I took my samples resembling *G. mendezensis* as affinity of this species.

In our samples, such forms resembling *G. mendezensis* have: elongated last chambers, different from the holotype of Eternod Olvera (1959), 5 to 7 chambers in the last whorl, semi-involute and compressed test, an apertural lip, and the chambers increase moderate to rapidly in size.

It has been rarely encountered in our Maastrichtian samples between 63-150 μm, and 150 μm in *P. hantkeninoides* Zone.

Stratigraphic distribution in the literature: Campanian-Maastrichtian, From the *G. gansseri* Zone to the *A. mayaroensis* Zone (CHRONOS Portal).

***Globigerinelloides prairiehillensis* PESSAGNO, 1967**

Plate 16, Figs. 4-6.

1967 *Globigerinelloides prairiehillensis* PESSAGNO, pl. 60, fig. 2, 3; pl. 80, fig. 1; pl. 90, fig. 1, 2-4; pl. 97, fig. 3, 4.

2000 *Globigerinelloides prairiehillensis* PESSAGNO- Petrizzo, text fig. 10, fig. 7.

2004 *Macroglobigerinelloides prairiehillensis* PESSAGNO- Premoli Silva and Verga, pl. 86, fig. 4-6; pl. 26, fig. 4-9.

2017 *Globigerinelloides prairiehillensis* PESSAGNO- Petrizzo et al., fig. 12 (10a to 10b).

Description & Remarks:

Globigerinelloides prairiehillensis is characterized by: 2 to 2.5 whorls in the test, 5 to 7 chambers in the last whorl, and slow increase in chamber size. This species highly looks like *G. multispinus* due to its compressed/largely compressed last chamber. However, it differs by lacking wide and highly arched aperture on each size of the last chamber and lacking the last chamber divided into two chamberlets. It generally has 5 chambers in the last whorl in our samples.

Petrizzo (2001) claimed that a taxonomic revision is required because these species have strong similarity even may be morphotypes of the same species.

In our study, *Globigerinelloides prairiehillensis* is sporadic and commonly found within >150 μm fraction throughout the Maastrichtian in *P. hantkeninoides* Zone. It is found after the K-Pg boundary and considered as survivor species. In our samples, *G. prairiehillensis* generally has 5 chambers in its last whorl.

Stratigraphic distribution in the literature: Campanian to Maastrichtian. From the *Radotruncana calcarata* Zone to the *Abathomphalus mayaroensis* Zone (CHRONOS Portal).

Globigerinelloides rosebudensis SMITH and PESSAGNO, 1973

Plate 16, Figs. 7-9.

1973 *Globigerinelloides rosebudensis* SMITH and PESSAGNO, fig. ?

Description & Remarks:

Globigerinelloides rosebudensis is highly characteristic with is elongated, ellipsoidal last chamber lean backwards. It has 6-7 chambers in its last whorl, chambers gradually increase in size, evolute test in one side showing early chambers of previous whorl while the opposite side is involute, and liplike relict apertural borders of final 2-3 chambers preserved in umbilical region.

In our samples, I have encountered some specimens quite similar to holotype of this species. They have well established retro-inclined, compressed final chambers and relict apertural features in their umbilicus (Plate 16, figs. 7-9).

They have been found rarely and sporadically in both size fraction throughout the Maastrichtian samples and none was encountered after the K-Pg boundary.

Stratigraphic distribution in the literature: Campanian-Maastrichtian. From *Gansserina gansseri* Zone to *Abathomphalus mayaroensis* Zone (CHRONOS Portal).

Globigerinelloides subcarinatus BRONNIMANN, 1952

Plate 17, Figs. 1-3; Plate 34, Figs. 20, 21.

1952 *Globigerinella messinae subcarinata* BRONNIMANN, pl. 1, fig. 10, 11; text fig. 21a-m.

1988 *Globigerinelloides subcarinatus* BRONNIMANN- Keller, pl. 2, fig. 2.

2001 *Globigerinelloides subcarinatus* BRONNIMANN- Petrizzo, text fig. 10, fig 5.

2004 *Macroglobigerinelloides subcarinatus* BRONNIMANN- Premoli Silva and Verga, pl. 87, fig. 1-3; pl. 26, fig. 10-13.

2016 *Globigerinelloides subcarinatus* BRONNIMANN- Mateo *et al*., pl. 2, fig. 6.

Description & Remarks:

Globigerinelloides subcarinatus is characterized by its highly-compressed chambers. Generally, there are 4-5 final chambers in the last whorl. Although, *Globigerinelloides messinae* (Brönnimann) resembles *G. subcarinatus* with its compressed test and rapid increase in chambers size, it was attained junior synonym of *Globigerinelloides asper* (Ehrenberg) (CHRONOS Portal).

In this present study, *Globigerinelloides subcarinatus* was abundant and commonly found in both size fractions throughout the Maastrichtian samples. It was found after the K-Pg boundary and considered as survivor species.

Stratigraphic distribution in the literature: Maastrichtian (CHRONOS Portal).

***Globigerinelloides ultramicrus* SUBBOTINA, 1949**

Plate 17, Figs. 4-6.

1949 *Globigerinelloides ultramicrus* SUBBOTINA, fig. ?

1998 *Globigerinelloides ultramicrus* SUBBOTINA- Nederbragt, pl. 1, figs. 4a-5.

2004 *Macroglobigerinelloides ultramicrus* SUBBOTINA- Premoli Silva and Verga, pl. 87, figs. 4-6.

2015 *Globigerinelloides ultramicra* SUBBOTINA- Mateo *et al*., pl. 2, fig. 4.

Description & Remarks:

Globigerinelloides ultramicrus is the smallest form amongst the *Globigerinelloides* genus. It is distinguished with its flat, rounded, smaller test and high number of chambers in the last whorl. In total, it has two whorls and the first whorl is disproportionally smaller than the final whorl. Chambers of the first whorl are visible in the depressed median portion. There are 6 to 8 slowly increasing chambers on the last whorl. In some specimens, first couple of chambers of the last whorl almost have similar size.

In our study, because of its smaller test size, none was found in >150 μm fraction. On the other hand, some individuals were recovered between 63-150 μm screen size close

to the K-Pg boundary. No *Globigerinelloides ultramicru*s was encountered after the K-Pg boundary.

Stratigraphic distribution in the literature: Albian to Maastrichtian. From the *R. subticinensis* Zone to the *G. gansseri* Zone (CHRONOS Portal).

Superfamily ROTALIPORACEA SIGAL, 1958

Family HEDBERGELLIDAE LOEBLICH and TAPPAN, 1961

Subfamily HEDBERGELLINAE LOEBLICH and TAPPAN, 1961

Genus *HEDBERGELLA* BRONNIMANN and BROWN, 1958

Type species: *Anomalina lorneiana* d'ORBIGNY var. trochoidea GANDOLFI, 1942

Hedbergella holmdelensis OLSSON, 1964

Plate 18, Figs. 1-3.

1964 *Hedbergella holmdelensis* OLSSON, pl. 1, fig. 2a-c.

2001 *Hedbergella holmdelensis* OLSSON- Luciani, pl. 1, figs. 22-23.

2004 *Muricohedbergella holmdelensis* OLSSON- Premoli-Silva and Verga, pl. 96, fig. 3-5; pl. 30, fig. 6-8.

2013 *Hedbergella holmdelensis* OLSSON- Arenillas and Arz, fig. 3C-I.

2016 *Hedbergella holmdelensis* OLSSON- Arenillas and Arz, fig. 6a-c.

Description & Remarks:

Hedbergella holmdelensis is distinguished by its larger size (up to 300 μm), very low (almost flat) trochospiral test, 5 to 6/6.5 compressed and rapidly increasing chambers in the last whorl. Chambers are somehow elongate in the direction of the coiling. Sutures are curved on the spiral and radial on the umbilical side. It also has umbilical-extraumbilical aperture bordered by a lip and angular axial periphery (asymmetrical globular final chamber).

Hedbergella holmdelensis was sporadic and uncommon in both size fractions throughout the Maastrichtian. It, however, was found after the K-Pg boundary and in accordance with the literature it was considered as survivor species.

Stratigraphic distribution in the literature: From the *Radotruncana calcarata* Zone to the P0 Zone (CHRONOS Portal, Olsson et al. 1999).

***Hedbergella monmouthensis* OLSSON, 1960**

Plate 18, Figs. 4-7; Plate 35, Figs. 1, 2.

1960 *Globorotalia monmouthensis* OLSSON, pl. 9, fig. 22-24.

2002 *Hedbergella monmouthensis* OLSSON- Keller *et al*., pl. 1, figs. 5, 6.

2004 *Muricohedbergella monmouthensis* OLSSON; Premoli-Silva and Verga, pl. 97, fig. 1-4; pl. 30, fig. 9, 10.

2013 *Hedbergella monmouthensis* OLSSON- Arenillas and Arz, fig. 3a-b.

Description & Remarks:

Hedbergella monmouthensis is characterized by its small size (less than 200 μm diameter), low trochospiral test, with 4-5 subglobular chambers in the last whorl different from *H. holmdelensis* which has 5-6.5 moderately compressed hemispherical chambers in its last whorl. *H. monmouthensis* also has moderate increasing chambers, umbilical-extraumbilical aperture bordered by lip, pustulose surface, and rounded axial periphery (symmetrical globular final chamber). This species has frequently been confused with similar juvenile forms of other species (Huber 1990).

Practically, *H. monmouthensis* differs from *H. holmdelensis* by its denser pustulose surface, more globular, rapidly increasing and fewer chambers in the last whorl.

In our samples *Hedbergella monmouthensis* was sporadic and uncommon between 63-150 μm fraction but it was common and more or less consistent in >150 μm fraction. In accordance with literature, it was found after the K-Pg boundary.

Stratigraphic distribution in the literature: Maastrichtian. From *Abathomphalus mayaroensis* Zone to P0 Zone (CHRONOS Portal, Olsson et al. 1999).

Hedbergella sliteri HUBER, 1990

Plate 18, Figs. 8-9.

1990 *Hedbergella sliteri* HUBER, pl. 2, figs. 5, 9-10; pl. 2, figs. 4-5.

2000 *Hedbergella sliteri* HUBER- Strong, fig. 7a, b.

2001 *Hedbergella sliteri* HUBER- Petrizzo, fig. 9 (5a-c).

Description & Remarks:

Hedbergella sliteri is distinguished by its nearly planispiral to low trochospiral test, gradually increasing chamber size, 5 to 6 chambers in the final whorl, broad and shallow umbilicus, extra-umbilical aperture bordered by narrow porticus and smooth to finely pustulose surface. Maximum diameter of the holotype is 370 μm (Huber 1990).

It differs from *H. monmouthensis* by having larger size, more gradually increasing chambers and, larger umbilical area.

In our study only two *Hedbergella sliteri* was identified throughout the Maastrichtian samples (UH-33 & UH-40) above 150 μm fraction. None was found after the K-Pg boundary.

Stratigraphic distribution in the literature: From the *Globotruncanella havanensis* Zone through the *Abathomphalus mayaroensis* Zone (Huber 1990).

ORDER FORAMINIFERIDA EICHWALD, 1830

Suborder GLOBIGERININA DELAGE and HEROURAD, 1896

Superfamily GLOBOTRUNCANACEA BROTZEN, 1942

Family RUGOGLOBIGERINIDAE SUBBOTINA, 1959

Subfamily ARCHAEOGLOBIGERININAE emend. GEORGESCU, 2005

Genus *Archaeoglobigerina* PESSAGNO, 1967

Type species: *Archaeoglobigerina blowi* PESSAGNO, 1967

***Archaeoglobigerina australis* HUBER, 1990**

Plate 19, Figs. 1-5.

1977 *Hedbergella monmouthensis* OLSSON- Sliter, pl. 3, figs. 1-3.

1983 *Rugoglobigerina pilula* BELFORD- Krasheninnikov and Basov, pl. 11, figs. 3-6.

1988 *Rugoglobigerina rotundata* BRONNIMANN- Huber, figs. 28 (12-14).

1990 *Archaeoglobigerina australis* HUBER, pl. 2, figs. 11-13; pl. 3, figs. 1-7; pl. 6, figs. 7-9.

1991 *Archaeoglobigerina australis* HUBER- van Eijden and Smit, pl. 1, figs 1-3.

2001 *Archaeoglobigerina australis* HUBER- Petrizzo, fig. 9 (1-3, 9).

2011 *Archaeoglobigerina australis* HUBER- Korchagin, pl. 2, fig. 7a-7c.

Description & Remarks:

Archaeoglobigerina australis is distinguished by its biconvex moderate to high trochospiral test, more convex spiral size, 4 to 6 globular chambers in the last whorl, final chambers usually kummerform, and umbilical to slightly extra-umbilical apertures bordered by broad flap. Test surface is covered by fine to coarse random pustules and final chamber has finer pustules than previous ones. Average diameter of the adult specimen is about 280 μm (Huber 1990). According to van Eijden and Smit (1991) intermediate forms can be seen between *Rugoglobigerina* species and *Archaeoglobigerina australis*.

In our present study, *Archaeoglobigerina australis* was uncommon and infrequent throughout the Maastrichtian samples above 150 μm screen fraction in *P. hantkeninoides* Zone.

Stratigraphic distribution in the literature: Campanian-Maastrichtian. From the *Globotruncana falsostuarti* Zone through the *Abathomphalus mayaroensis* Zone (CHRONOS Portal).

Archaeoglobigerina blowi PESSAGNO, 1967

Plate 19, Figs. 6-7.

1967 *Archaeoglobigerina blowi* PESSAGNO, pl. 59, figs. 5-7.

2004 *Archaeoglobigerina blowi* PESSAGNO, Premoli Silva and Verga, pl. 1, figs. 9-12.

2005 *Archaeoglobigerina blowi* PESSAGNO, Georgescu, fig. 2 (1-3).

2006 *Archaeoglobigerina blowi* PESSAGNO, Georgescu, fig. 8.8-8.10.

Description & Remarks:

Archaeoglobigerina blowi is characterized by having nearly flat to low trochospiral test, 4 to 5 globular chambers rapidly increasing in the last whorl, broadly rounded periphery with imperforate peripheral band either bordered or not by two weak keels. Van Eijken and Smit (1991) claimed that this form commonly occurs between 125 to 250 μm fraction due to the lumping of small archaeoglobigerinids into this species.

In our study, *Archaeoglobigerina blowi* was frequent throughout the Maastrichtian samples in >150 μm fraction. Whereas, only one specimen was identified between 63-150 μm size.

Stratigraphic distribution in the literature: Santonian to Maastrichtian (CHRONOS Portal).

***Archaeoglobigerina cretacea* PESSAGNO, 1967**

Plate 19, Fig. 9.

1840 *Globigerina cretacea* d'ORBIGNY, pl. 3, figs. 12-14.

1991 *Archaeoglobigerina cretacea* d'ORBIGNY- van Eijken and Smit, pl. 1, figs, 4, 5.

2004 *Archaeoglobigerina cretacea* d'ORBIGNY- Premoli Silva and Verga, pl. 2, figs. 1-3.

2005 *Archaeoglobigerina cretacea* d'ORBIGNY- Georgescu, fig. 2 (4-6).

2006 *Archaeoglobigerina cretacea* d'ORBIGNY- Georgescu, fig. 8.14-8.16.

Description & Remarks:

Archaeoglobigerina cretacea has a very low trochospiral test covered by fine pustules (not meridionally arranged), 5 to 6 chambers in the last whorl, and an aperture in umbilical position covered by delicate tegilla. Its periphery either have broadly rounded with imperforate peripheral band or one faint keel or two slightly developed keels or without any sort of peripheral structure.

It differs form:
A. blowi in having more chambers in the last whorl, and slowly increasing chambers;
R. pennyi in not having meridionally arranged costellae.

Intermediate forms with *R. hexacamerata* and *A. australis* may exist (van Eijken and Smit 1991).

In our study *Archaeoglobigerina cretacea* was very uncommon in both size fractions throughout the Maastrichtian in *P. hantkeninoides* Zone.

The specimen shown in Plate 19 was considered as ''affinity'' because of lacking imperforate peripheral band.

Stratigraphic distribution in the literature: Turonian to Maastrichtian. From the *M. schneegansi* Zone through the *G. gansseri* Zone (CHRONOS Portal).

Genus *Kuglerina* BRONNIMANN and BROWN, 1956

Type species: *Rugoglobigerina* (*Rugoglobigerina*) *rugosa rotundata* BRONNIMANN, 1952

Kuglerina rotundata BRONNIMANN, 1952

Plate 20, Fig. 1.

1952 *Rugoglobigerina* (*Rugoglobigerina*) *rugosa rotundata* BRONNIMANN, pl. 4, figs. 7-9.

1984 *Rugoglobigerina rotundata* BRONNIMANN- Robaszynski *et al*., pl. 50, fig. 2.

2005 *Kuglerina rotundata* BRONNIMANN- Georgescu, fig. 2 (7-8).

Description & Remarks:

Kuglerina rotundata is characterized by its high to very high trochospiral and larger test, 4.5 to 6 big globular chambers covered by strong rugosities but not meridionally arranged costellae. Chambers in the last whorl are slightly elongated and final chamber offset towards to umbilicus.

In our study, only one specimen was found in >150 μm fraction throughout the Maastrichtian in *P. hantkeninoides* Zone.

Stratigraphic distribution in the literature: Campanian-Maastrichtian. From the *Gansserina gansseri* Zone through the *Pseudoguembelina hariaensis* Zone (CHRONOS Portal). From beginning of the *Globotruncanella havanensis* Zone through the end of *Abathomphalus mayaroensis* Zone (Georgescu 2005).

Subfamily RUGOGLOBIGERININAE SUBBOTINA, 1959

Genus *Rugoglobigerina* BRONNIMANN, 1952

Type species: *Globigerina rugosa* PLUMMER, 1927

***Rugoglobigerina rugosa* PLUMMER, 1926**

Plate 20, Figs. 2-3; Plate 35, Figs. 3-5.

1926 *Globigerina rugosa* PLUMMER, pl. 2, fig. 10a.

1984 *Rugoglobigerina rugosa* PLUMMER- Robaszynski *et al*., pl. 49, figs. 4, 6.

1991 *Rugoglobigerina rugosa* PLUMMER- van Eijden and Smit, pl. 1, figs. 10, 11.

2004 *Rugoglobigerina rugosa* PLUMMER- Premoli Silva and Verga, pl. 132, fig. 1-3; pl. 39, fig. 8-11.

2005 *Rugoglobigerina rugosa* PLUMMER- Georgescu, fig. 3.3.

2011 *Rugoglobigerina rugosa* PLUMMER- Keller *et al*., pl. 1, fig. 5, 6.

2014 *Rugoglobigerina rugosa* PLUMMER- Meilijson *et al*., fig. 9.1.

2014 Rugoglobigerina rugosa PLUMMER- Falzoni *et al*., text figs. 2, 7; figs. 3 (1-4); 4 (1-4); 5 (1).

Description & Remarks:

Rugoglobigerina rugosa is characterized by its low to almost flat trochospiral test, rapidly increasing 4 to 5 globular chambers in the last whorl, thick meridionally arranged rugosities on the test surface.

In our samples, *Rugoglobigerina rugosa* was consistently found throughout the Maastrichtian samples above the 150 μm fraction in *P. hantkeninoides* Zone. It underwent extinction at the K-Pg boundary.

Stratigraphic distribution in the literature: Campanian-Maastrichtian. From the *G. ventricosa* Zone throughout the *P. hariaensis* Zone (CHRONOS Portal).

Rugoglobigerina hexacamerata BRONNIMANN, 1952

Plate 20, Figs. 4-5.

1952 *Rugoglobigerina* (*Rugoglobigerina*) *reicheli hexacamerata* BRONNIMANN, pl. 2, fig. 10-12.

1998 *Rugoglobigerina hexacamerata* BRONNIMANN- Nederbragt, pl. 4, fig. 1-4.

2004 *Rugoglobigerina hexacamerata* BRONNIMANN- Premoli Silva and Verga, pl. 129, fig. 1, 2; pl. 39, fig. 1, 2.

2014 *Rugoglobigerina hexacamerata* BRONNIMANN- Falzoni *et al*., text figs. 2, 7; figs. 3 (5, 6); 4 (5, 6); 5 (2).

Description & Remarks:

Rugoglobigerina hexacamerata is characterized by its low to flat trochospiral test, 6 chambers in the final whorl, slowly increasing chamber size and coarsely rugose surface.

It differs from:
R. rugosa by its more and slowly increasing chambers;
R. pennyi by its flat trochospiral test and frequently 6 chambers in the last whorl.

In our study, *Rugoglobigerina hexacamerata* was sparse and uncommon throughout the Maastrichtian samples in both size fraction.

Stratigraphic distribution in the literature: From within the *G. falsostuarti* Zone throughout the *A. mayaroensis* Zone (Robaszynski et al. 1984).

***Rugoglobigerina macrocephala* BRONNIMANN, 1952**

Plate 20, Figs. 6-8; Plate 35, Figs. 6-9.

1952 *Rugoglobigerina* (*Rugoglobigerina*) *macrocephala macrocephala* BRONNIMANN, pl. 2, fig. 1-3.

1984 *Rugoglobigerina macrocephala* BRONNIMANN- Robaszynski *et al*., pl. 49, fig.7.

2004 *Rugoglobigerina macrocephala* BRONNIMANN- Premoli Silva and Verga, pl. 130, fig. 1-4; pl. 39, fig. 3, 4.

2009 *Rugoglobigerina macrocephala* BRONNIMANN- Keller *et al*., fig. 5 (4).

2016 *Rugoglobigerina macrocephala* BRONNIMANN- Punekar *et al*., pl. 1, fig. N.

Description & Remarks:

Rugoglobigerina macrocephala is distinguished by its low to flat trochospiral test, 3 to 3.5 (exceptionally 4) chambers in the last whorl, rapidly increasing chambers with highly large last chamber, and meridionally arranged thick rugosities. The final chamber can be so prominent that it may sometimes comprise the half of the test volume.

In our study, *Rugoglobigerina macrocephala* was very rare and uncommon in both size fractions throughout the Maastrichtian in *P. hantkeninoides* Zone.

Stratigraphic distribution in the literature: From the *G. gansseri* Zone throughout the *A. mayaroensis* Zone (CHRONOS Portal).

***Rugoglobigerina milamensis* SMITH and PESSAGNO, 1973**

Plate 20, Fig. 8, Plate 35, Figs. 10-12.

1973 *Rugoglobigerina milamensis* SMITH and PESSAGNO, pl. 24, fig. 4-7.

1984 *Rugoglobigerina milamensis* SMITH and PESSAGNO- Robaszynski *et al*., pl. 50, fig. 3.

2004 *Rugoglobigerina milamensis* SMITH and PESSAGNO- Premoli Silva and Verga, pl. 39, fig. 5, 6.

2014 *Rugoglobigerina milamensis* SMITH and PESSAGNO- Falzoni *et al*., figs. 3 (9, 10), 4 (9, 10); text fig. 8.

Description & Remarks:

Rugoglobigerina milamensis is distinguished by its large very high trochospiral test, conspicuously more convex spiral side, early whorls offset higher than ultimate whorls, 5 to 6 chambers in the last whorl, rapidly increasing chambers in the first whorls and then slowly in the last whorl, and closely spaced meridionally arranged thick rugosities.

In our samples, *Rugoglobigerina milamensis* was frequent in early samples of the quantitative study (see Table 5) but rare and uncommon through up-section.

The specimen shown in Plate 20 was considered as ‘’affinity’’ because of lacking: prominent offset of initial chambers in a higher plane and larger final chamber. On the contrary, although the specimen shown in Plate 35, Fig. 10 lacks a variety of characteristic morphologic features, it was considered as ‘’affinity’’ because of having initial chambers offset in a higher plane and larger last chamber.

Stratigraphic distribution in the literature: From the *R. fructicosa* through the *A. mayaroensis* (CHRONOS Portal).

Rugoglobigerina pennyi BRONNIMANN, 1952

Plate 20, Fig. 9.

1952 *Rugoglobigerina* (*Rugoglobigerina*) *rugosa pennyi* BRONNIMANN, pl. 4, fig. 1-3.

1984 *Rugoglobigerina pennyi* BRONNIMANN- Robaszynski et al., pl. 50, fig. 1.

2004 *Rugoglobigerina pennyi* BRONNIMANN- Premoli Silva and Verga, pl. 131, fig. 2-4; pl. 39, fig. 7.

2014 *Rugoglobigerina pennyi* BRONNIMANN- Falzoni *et al*., figs. 3 (7, 8); 4 (7, 8); 5 (3, 4); tex fig. 8.

Description & Remarks:

Rugoglobigerina pennyi is intermediate form between *R. rugosa* and *R. milamensis* (Robaszynski et al. 1984). It is characterized by moderate to high trochospiral test, 5 to 6 globular slowly increasing chambers in the last whorl, more convex spiral side, and surface covered by rugosities arranged in meridionally pattern.

It differs from:

a) *Rugoglobigerina rugosa* by having much larger test, more convex spiral side, more developed rugosities, slower increase in chamber size in the last whorl, and more chambers in the last whorl.

b) *Rugoglobigerina milamensis* by having smaller trochospiral test, thinner and fewer rugosities, slower increase in chamber size.

c) *Rugoglobigerina hexacamerata* by having more convex trochospiral test instead of almost flat trochospire as in *R. hexacamerata*, and changeable number of chambers in the last whorl,

In our samples, *Rugoglobigerina pennyi* was common in first samples of the quantitative study, yet it was rare and infrequent throughout the up-section.

Stratigraphic distribution in the literature: From the *G. gansseri* Zone throughout the *A. mayaroensis* Zone (CHRONOS Portal).

Genus *Trinitella* BRONNIMANN, 1952

Type species: *Trinitella scotti* BRONNIMANN, 1952

Trinitella scotti BRONNIMANN, 1952

Plate 21, Figs. 1-3.

1952 *Trinitella scotti* BRONNIMANN, pl. 4, figs. 4-6.
1984 *Rugoglobigerina scotti* BRONNIMANN- Robaszynski et al., pl. 50, fig. 4.
2002 *Rugoglobigerina scotti* BRONNIMANN- Keller et al., pl. 2, figs. 3, 4.
2012 *Rugoglobigerina scotti* BRONNIMANN- Perez Rodriguez *et al*., fig. 8. (L).

Description & Remarks:

Trinitella scotti is distinguished by its pinched last chamber, almost flat trochospiral test, 4 to 6 chambers in the last whorl covered by costellae weaker or absent on the last chambers, flattened spiral and convex umbilical side.

In our study *Trinitella scotti* was frequent in early parts of the quantitative analysis then became rare to almost absent through up-section in > 150 μm fraction.

Stratigraphic distribution in the literature: Campanian-Maastrichtian. From the *G. gansseri* Zone throughout the *P. hariaensis* Zone (CHRONOS Portal).

Genus *Plummerita* BRONNIMANN, 1952

Type species: *Rugoglobigerina* (*Plummerella) hantkeninoides* BRONNIMANN, 1952

Plummerita hantkeninoides BRONNIMANN, 1952

Plate 21, Figs. 4-8.

1952 *Rugoglobigerina* (*Plummerella) hantkeninoides* BRONNIMANN, pl. 3, fig. 1-3.
1984 *Plummerita hantkeninoides* BRONNIMANN- Robaszynski *et al*., pl. 50, figs. 6-8.
2000 *Plummerita hantkeninoides* BRONNIMANN- Arenillas *et al*., pl. 1, figs. 11, 12.

2002 *Plummerita hantkeninoides* BRONNIMANN- Keller, pl. 2, figs. 7-10.

2002 *Plummerita hantkeninoides* BRONNIMANN- Keller *el al*., pl. 2, fig. 14.

2004 *Plummerita hantkeninoides* BRONNIMANN- Premoli Silva and Verga, pl. 32, fig. 6-7.

2009 *Plummerita hantkeninoides* BRONNIMANN- Keller et al., fig. 5 (1-2).

2015 *Plummerita hantkeninoides* BRONNIMANN- Coccioni and Premoli Silva, pl. 3, figs. 12-14.

Description & Remarks:

Plummerita hantkeninoides has highly characteristic by having radially elongated chambers possessing axially situated spines in the final whorl. These spines may exist in some or all chambers of the last whorl. The chambers that lack spines are triangular and inflated. It also distinguished by having very low to almost flat trochospiral test, 5 to 6 chambers in the final tour, umbilical aperture covered by tegilla, and meridionally arranged costellae on the surface of the chambers.

In our study, *Plummerita hantkeninoides* was found only a few samples in both fractions throughout the Maastrichtian.

It was encountered in the very first sample of the measured section (UH-1), then in samples UH-30 and UH-41 above 150 μm fraction (see Table 5). Whereas, it was found only in UH-30 between 63-150 μm fraction (see Table 3).

Keller et al. (2002) claimed that stratigraphic range of *P. hantkeninoides* Zone larger than 6 m may provide a good estimate of the completeness the section. In our study, *P. hantkeninoides* Zone ranges the last 9.55 m of the Maastrichtian. Therefore, it is highly possible that our section is complete.

The specimen in Plate 21, Fig 8. was considered as ‘’affinity’’ since its rudimentary spine bearing chambers.

Stratigraphic distribution in the literature: FAD of *Plummerita hantkeninoides* marks the latest subdivision of the Maastrichtian. *Plummerita hantkeninoides* Zone spans across ~160 k.y. before the K-Pg boundary (Mateo et al. 2016).

Plummerita reicheli BRONNIMANN, 1952

Plate 21, Fig. 9.

1952 *Rugoglobigerina* (Rugoglobigerina) *reicheli reicheli* BRONNIMANN, pl. 3, fig. 10-12.

1984 *Rugoglobigerina reicheli* BRONNIMANN- Robaszynski *et al*., pl. 50, fig. 5.

2011 *Plummerita reicheli* BRONNIMANN- Keller et al., pl. 1, fig. 3.

Description & Remarks:

Plummerita reicheli is characterized by strong spines on the peripheral margin developed on the first chambers of the last whorl, low to flat trochospire, 4 to 6 chambers on the final whorl, chambers covered by thick coarse rugosities and costellae arranged in meridionally pattern.

In our study, *Plummerita reicheli* has rarely been encountered throughout the Maastrichtian above >150 μm fraction.

The specimen in Plate 21, Fig. 9 was considered as ‘’affinity’’ since it lacks coarsely rugose chamber surface.

Stratigraphic distribution in the literature: Throughout the *A. mayaroensis* Zone (CHORNOS Portal).

Subfamily ABATHOMPHALINAE PESSAGNO, 1967

Genus *Abathomphalus* BOLLI, LOEBLICH and TAPPAN, 1957

Type Species: *Globotruncana mayaroensis* BOLLI, 1951

Abathomphalus intermedius BOLLI, 1951

Plate 22, Figs. 7-9.

1951 *Globotruncana intermedia* BOLLI, pl. 35, figs. 7-9.

1984 *Abathomphalus intermedius* BOLLI- Robaszynski et al., pl. 45, figs. 1, 2, 3, 7; pl. 46, fig. 1-2.

2001 *Abathomphalus intermedius* BOLLI- Petrizzo, fig. 9 (10a-c); fig. 10 (1a-c).

2004 *Abathomphalus intermedius* BOLLI- Premoli Silva and Verga, p. 1, figs. 1-3.

Description & Remarks:

Abathomphalus intermedius is intermediate form between *Globotruncanella citae* (*pschadae*) and *Abathomphalus mayaroensis* (Robaszynski et al. 1984). It is distinguished by its low to moderate trochospiral test, 4 to 6 chambers on the last whorl, umbilical area ornamented by meridionally arranged rugosities, spiral side covered by elongated rugosities arranged in direction of coiling, two keels or one keel, and spiral sutures joining at right angles.

It differs from:

a) *Globotruncanella havanensis* by having second keel, less convex spiral side, and meridionally arranged pustules on umbilical side;

b) *Abathomphalus mayaroensis* by having narrower keel band, more convex spiral side, more prominent one equatorial keel, and two keels diminish into one.

Throughout the Maastrichtian, *Abathomphalus intermedius* was found only in two samples (UH-42 and UH-48) above 150 μm fraction in *P. hantkeninoides* Zone.

Specimen in Plate 22, Fig. 7 was considered as ‘’affinity’’ because of lacking striations on the spiral side which follow the coiling direction.

Specimen in Plate 22, Fig. 9 was considered as ‘’affinity’’ since it has less developed radial sutures on the umbilical side.

Stratigraphic distribution in the literature: From middle of the *G. gansseri* Zone throughout the *A. mayaroensis* Zone (Robaszynski et al. 1984).

***Abathomphalus mayaroensis* BOLLI, 1951**

Plate 22, Figs. 1-6.

1951 *Globotruncana mayaroensis* BOLLI, pl. 35, figs. 10-12.

1984 *Abathomphalus mayaroensis* BOLLI- Robaszynski *et al.*, pl. 45, figs. 5, 6, 8, 9; pl. 46, fig. 5.

2001 *Abathomphalus mayaroensis* BOLLI- Petrizzo, fig. 10 (2a-c).

2004 *Abathomphalus mayaroensis* BOLLI- Premoli Silva and Verga, pl. 1, figs. 3-8.

2014 *Abathomphalus mayaroensis* BOLLI- Orabi and Zahran, pl. 2, figs. 8, 9.

2015 *Abathomphalus mayaroensis* BOLLI- Coccioni and Premoli Silva, pl. 3, figs. 6, 7.

Description & Remarks:

Abathomphalus mayaroensis is characterized by having low trochospiral test, 4.5 to 6 commonly 5 slowly increasing chambers in the last whorl, flat umbilical chambers with meridionally arranged rugosities, commonly ‘’butterfly’’ shape in lateral view due to concavity of spiral and umbilical side, and two keels composed of radially arranged rugosities equally developed on all chambers and separated by imperforate peripheral band.

In our study, *Abathomphalus mayaroensis* was uncommon and sporadic throughout the Maastrichtian *P. hantkeninoides* Zone.

Stratigraphic distribution in the literature: *Abathomphalus mayaroensis* spans ~3 m.a. (69.18 to 66) before the K-Pg boundary (CHRONOS Portal).

Genus *Globotruncanella* REISS, 1957

Type species: *Globorotalia pschadae* KELLER, 1946

Globotruncanella petaloidea GANDOLFI, 1955

Plate 23, Figs. 1-3.

1955 *Globotruncana* (*Rugoglobigerina*) *petaloidea* GANDOLFI subsp. *petaloidea* GANDOLFI, pl. 3, fig. 13.

1984 *Globotruncanella petaloidea* GANDOLFI- Robaszynski *et al*., pl. 44, fig. 1-2.

2004 *Globotruncanella havanensis* GANDOLFI- Premoli Silva and Verga, p. 16, fig. 12.

2006 *Globotruncanella petaloidea* GANDOLFI- Güray, pl. 6, fig. 2 (a-c).

Description & Remarks:

Globotruncanella petaloidea is distinguished by its high to very high trochospiral test, 4 rapidly increasing chambers in the last whorl. Practically, it seems like an eagle claw which has a high-arch outline.

It differs from *G. havanensis* by having only 4 chambers in the last whorl and high arch claw shape outline. In *G. havanensis*, on the other hand, this high arch decreases, becomes moderate trochospire, and chamber size increase. Then in *G. pschadae,* this claw shape diminishes prominently and become low trochospire with peripheral keel on the chambers. *G. minuta*, however, highly differs from these species as it has small test and minute spines on its chamber surface.

In our samples, *Globotruncanella petaloidea* was found only one sample in the 63-150 μm fraction (UH-45), whereas it was frequent and consistently found throughout the Maastrichtian in >150 μm size fraction. Although it was found two samples after the boundary (E+2, UH-51), these specimens might have reworked into Danian.

Stratigraphic distribution in the literature: Campanian-Maastrichtian. From the *G. gansseri* Zone to the *A. mayaroensis* Zone (CHRONOS Portal).

***Globotruncanella havanensis* VOORWIJK, 1937**

Plate 23, Figs. 4-8, Plate 34, Fig. 23.

1937 *Globotruncana havanensis* VOORWIJK, pl. 1, figs. 25, 26.
1984 *Globotruncanella havanensis* VOORWIJK- Robaszynski *et al*., pl. 44, fig. 4-6.
2004 *Globotruncanella havanensis* VOORWIJK- Premoli Silva and Verga, p. 16, figs. 1-9.

Description & Remarks:

Globotruncanella havanensis is characterized by having moderately trochospiral test composed of generally 5 (sometimes 4.5) rapidly increasing chambers in the last whorl. Its surface may bear pustules or rugosities denser on the first chambers.

It differs from:

G. petaloidea by having more than 4 chambers in the final whorl and less trochospiral test;

G. citae by having unkeeled periphery.

In our study throughout the Maastrichtian, *Globotruncanella havanensis* was rare and uncommon in 63-150 μm fraction but quite frequent and abundant in >150 μm screen. Although some specimens were found after the K-Pg boundary, these specimens might have reworked into Danian.

Stratigraphic distribution in the literature: Uppermost Campanian-Maastrichtian. From middle of the *Radotruncana calcarata* Zone throughout the *Abathomphalus mayaroensis* Zone (Robaszynski et al. 1984).

***Globotruncanella pschadae* KELLER, 1946**

Plate 24, Figs. 1-5.

1946 *Globorotalia pschadae* KELLER, pl. 2, figs. 4, 5, 6.

1984 *Globotruncanella pschadae* KELLER- Robaszynski et al., pl. 44, fig. 7.

2004 *Globotruncanella pschadae* KELLER- Premoli Silva and Verga, p. 16, figs. 13-15.

Description & Remarks:

Globotruncanella pschadae differs from other *Globotruncanella* species by having peripheral keel in its periphery.

In our samples throughout the Maastrichtian, *G. pschadae* was sporadic and uncommon in 63-150 μm fraction, whereas it was more abundant but again sporadic in >150 μm fraction.

Stratigraphic distribution in the literature: Middle and upper parts of the Maastrichtian. From the *G. gansseri* Zone throughout the *A. mayaroensis* Zone (Robaszynski et al. 1984).

Globotruncanella minuta CARON and GONZALEZ DONOSO, 1984

Plate 24, Figs. 6-7.

1984 *Globotruncanella minuta* CARON and GONZALEZ DONOSO, pl. 43, fig. 5.

1984 *Globotruncanella minuta* CARON and GONZALEZ DONOSO- Robaszynski *et al*., pl. 43, figs. 5-8.

2004 *Globotruncanella minuta* CARON and GONZALEZ DONOSO- Premoli-Silva and Verga, pl. 16, fig. 10, 11.

Description & Remarks:

Globotruncanella minuta has 4 to 4.5 rapidly chambers in its last whorl, very low trochospiral to planispiral test, chamber surface bearing pustules more developed on the first chambers of the final whorl, and umbilical system composed of portici.

It highly resembles *Hedbergella monmouthensis* by bearing small fine spines on first chambers of the final whorl, almost flat trochospiral test and globular chambers, whereas it differs by having umbilical system bearing portici not bordered by a distinct lip.

In our study throughout the Maastrichtian, it was common but sporadic in both size fractions.

Specimens in Plate 24, Figs. 6 and 7 were considered as ‘’affinity’’ since they lack well-developed globular chambers with minute spines on the surface.

Stratigraphic distribution in the literature: Campanian to Maastrichtian. From the G. *gansseri* Zone to the *A. mayaroensis* Zone (CHRONOS Portal).

Subfamily GLOBOTRUNCANINAE BROTZEN, 1942

Genus *Gansserina* CARON et al., 1984

Type Species: *Globotruncana gansseri* BOLLI, 1951

Gansserina gansseri BOLLI, 1951

Plate 25, Figs. 1-2; Plate 36, Fig. 1.

1951 *Globotruncana gansseri* BOLLI, pl. 35, figs. 1-3.

1984 *Gansserina gansseri* BOLLI- Robaszynski *et al.*, pl. 51, figs. 1-7, 10, 11; pl. 52, figs. 1-5.

2004 *Gansserina gansseri* BOLLI- Premoli-Silva and Verga, pl. 8, figs. 1-11.

2014 *Gansserina gansseri* BOLLI- Meilijson *et al*., fig. 9 (9a-b).

2015 *Gansserina gansseri* BOLLI- Coccioni and Premoli Silva, pl. 1, fig. 9a-c.

Description & Remarks:

Gansserina gansseri is characterized by almost flat trochospiral test, 4 to 7 chambers in the last whorl, chambers in the umbilical side lack adumbilical ridges and bear pustules, petaloid to crescentic shape chambers with flat surface and central bulge in the middle of the spiral side. Also, chambers on the spiral side may create a staircase pattern as they grow. Practically, *G. gansseri* looks like a half sphere in the lateral view.

It differs from *Globotruncanita angulata* by chambers lacking adumbilical ridges but bearing pustules on the umbilical side.

In our study, *Gansserina gansseri* was found only in two samples (UH-31 and UH-33) throughout the Maastrichtian. These specimens may be reworked.

The specimen in Plate 25, Fig. 1 was considered as ‘’affinity’’ due to less rugose and less inflated final chambers in the last whorl.

The specimen in Plate 25, Fig. 2 was considered as ‘’affinity’’ due to narrower umbilicus.

Stratigraphic distribution in the literature: Campanian to Maastrichtian. From the *G. gansseri* Zone to within the *A. mayaroensis* Zone (CHRONOS Portal). Late

Maastrichtian. From bottom of the CF-7 Zone to top of the CF-3 Zone (Li and Keller 1998).

Gansserina wiedenmayeri GANDOLFI, 1955

Plate 25, Figs. 3-4.

1955 *Globotruncana wiedenmayeri* GANDOLFI, pl. 7, fig. 4.

1984 *Gansserina wiedenmayeri* GANDOLFI- Robaszynski *et al*., pl. 51, figs. 8-9; pl. 54, figs. 1-6.

2004 *Gansserina wiedenmayeri* GANDOLFI- Premoli-Silva and Verga, pl. 8, figs. 12-13.

Description & Remarks:

Gansserina wiedenmayeri share almost all characteristic features of *G. gansseri* but it has two keels at least on first chambers of the last whorl and generally has more chambers in the final whorl.

It also differs from:

Globotruncana ventricosa in having less well-developed and closer keels, an umbilical side with pustulose surface and generally lacking adumbilical ridges.

Globotruncana aegyptiaca in having flatter chamber surface on the spiral side rather than inflated chambers, an umbilical side with pustulose surface and generally lacks adumbilical ridges.

In our study throughout the Maastrichtian *P. hantkeninoides* Zone, *Gansserina wiedenmayeri* was found only in 4 samples with low abundances (UH-31, UH-33, UH-43 and UH-47).

The specimen in Plate 25, Fig. 3 was considered as ‘’affinity’’ due to less developed second keel.

The specimen in Plate 25, Fig. 4 was considered as ‘’affinity’’ due to less inflated final chambers in the last whorl on the umbilical side.

Stratigraphic distribution in the literature: From the *G. falsostuarti* Zone to the *A. mayaroensis* Zone (CHRONOS Portal).

Genus *Globotruncana* CUSHMAN, 1927

Type species: *Pulvinulina arca* CUSHMAN, 1926

Globotruncana aegyptiaca NAKKADY, 1950

Plate 26, Figs. 1-5.

1950 *Globotruncana aegyptiaca* NAKKADY, pl. 80, fig. 20.

1984 *Globotruncana aegyptiaca* NAKKADY- Robaszynski *et al*., pl. 2, figs. 1-6; pl. 3, figs. 1-4.

1998 *Globotruncana aegyptiaca* NAKKADY- Nederbragt, pl. 1, figs. 6, 7.

2002 *Globotruncana aegyptiaca* NAKKADY- Keller, pl. 1, figs. 1-3.

2011 *Globotruncana aegyptiaca* NAKKADY- Korchagin, pl. 5, figs. 3a-c.

Description & Remarks:

Globotruncana aegyptiaca is characterized by very low to flat spiral side, rapidly increasing 3 to 5 chambers in the last whorl, first globular, then petaloid and finally crescentic chambers which creates a ‘’cross’’ shape test, and two keels on all chambers equally developed and separated by imperforate peripheral band. Width of this band may differ from one specimen to another.

In our study *Globotruncana aegyptiaca* was commonly but sporadically found throughout the Maastrichtian *P. hantkeninoides* Zone.

Stratigraphic distribution in the literature: From the *G. aegyptiaca* Zone to the *A. mayaroensis* Zone (CHRONOS Portal).

***Globotruncana arca* CUSHMAN, 1926**

Plate 26, Figs. 6-9; Plate 36, Figs. 10-11.

1926 *Pulvinulina arca* CUSHMAN, pl.3, fig.1.

1984 *Globotruncana arca* CUSHMAN- Robaszynski *et al*., pl. 4, fig. 1-3.

2003 *Globotruncana arca* CUSHMAN- Abramovich *et al*., pl. 5, figs. 1-2.

2004 *Globotruncana arca* CUSHMAN- Premoli Silva and Verga, pl. 10, figs. 11-15; pl. 11, figs. 1-4.

2017 *Globotruncana arca* CUSHMAN- Petrizzo *et al*., fig. 12 (1a-c).

Description & Remarks:

Globotruncana arca is distinguished by having moderately high trochospiral test, 5.5 to 8 but generally 6 to 7 chambers in the last whorl, slowly to moderately increasing chamber size, raised and beaded spiral sutures joining the spiral suture at acute angles, a characteristic horseshoe shape pattern in the umbilical side resulted from combination of adumbilical and sutural ridges. In the lateral view, it has generally more convex spiral side, distinct two keels separated by an imperforate peripheral band tilted towards to the umbilical side. Practically in the lateral view, *G. arca* looks like ‘’parenthesis’’ shape on which spiral side to the left, umbilical side to the right.

It differs from:

G. orientalis by having more robust and thicker test, more prominent, raised and beaded sutures on the spiral side, well developed and wider imperforate peripheral band, and two keels on all chambers.

G. mariei by having more robust and larger test, more chambers, larger peripheral keel and slower increase of chambers in the last whorl.

G. falsostuarti by having two keels on all chambers, and stationary peripheral keel, namely peripheral band do not get closer in the middle of each chamber.

In our samples, *G. arca* generally has 5, 5.5 to 6 chambers in its last whorl. It was common and abundant throughout the Maastrichtian *P. hantkeninoides* Zone.

Stratigraphic distribution in the literature: Santonian-Maastrichtian. From the *D. asymetrica* Zone to the *A. mayaroensis* Zone (CHRONOS Portal).

Globotruncana bulloides VOGLER, 1941

1941 *Globotruncana linnei* (d'ORBIGNY) subsp. *bulloides* VOGLER, pl. 23, figs. 32-39.

1984 *Globotruncana bulloides* VOGLER- Robaszynski *et al*. pl. 6, figs. 1-4.

2003 *Globotruncana bulloides* VOGLER- Abramovich *et al*., pl. 5, fig. 6.

2004 *Globotruncana bulloides* VOGLER- Premoli Silva and Verga, pl. 11, figs. 5-12.

Description & Remarks:

Globotruncana bulloides is distinguished by having almost flat trochospiral test with 6 to 7 chambers in the last whorl. On the spiral side, it has semi-circular to crescent shape inflated and slowly increasing chambers with raised and beaded sutures which join the spiral suture first acute then right angles. It has two equally developed keels parallel or slightly tilted towards to the axis of coiling.

Globotruncana bulloides has characteristic well-developed 'flower' like chamber pattern on the spiral side because of slowly increasing first 3-4 chambers of the last whorl.

It differs from:

Globotruncana arca by having slowly increasing chambers on the last whorl, flat trochospiral test, bi-convex profile and almost parallel imperforate peripheral band, more semi-circular and inflated chamber rather than flat and petaloid as in *G. arca.*

In our study, *Globotruncana bulloides* was found only in two samples (UH-39 and UH-49). Due to its stratigraphic range and poor presence in our samples, these specimens were considered as reworked individuals.

Stratigraphic distribution in the literature: From upper part of Santonian to lower part of Maastrichtian. From *D. asymetrica* Zone to *G. falsostuarti* Zone (Robaszynski et al. 1984). It is important to note that according to Robaszynski et al. (1984), *Globotruncana falsostuarti* Interval Range Zone corresponds to first biozone of Maastrichtian. It starts at the Campanian-Maastrichtian boundary (slightly before the FAD of *G. falsostuarti*) ends with first appearance datum (FAD) of *Gansserina gansseri*.

***Globotruncana dupeublei* CARON, GONZALEZ DONOSO, ROBASZYNSKI and WONDERS, 1984**

Plate 27, Figs. 1-3.

1984 *Globotruncana dupeublei* CARON *et al*., pl. 7, fig. 1.

1984 *Globotruncana dupeublei* CARON *et al*.- Robaszynski *et al*., pl. 7, fig. 1-2.

2004 *Globotruncana dupeublei* CARON *et al*.- Premoli-Silva and Verga, pl. 36, fig. 1, 2.

2011 *Globotruncana dupeublei* CARON *et al*.- Keller *et al*., pl. 2, figs. 9-10.

Description & Remarks:

Globotruncana dupeublei is characterized by large test with 7 to 9 slowly increasing chambers in the last whorl. On the spiral side, it has petaloid chambers with smooth and flat surface and raised - beaded sutures join the spiral suture at almost right angle. In the lateral view, it has bi-convex appearance and one peripheral keel.

It differs from:

Globotruncana esnehensis and *Globotruncanita insignis* by having larger test, more but slowly increasing chambers in the last whorl.

Globotruncanita conica by having convex umbilical side rather than flat, and umbilical system composed of tegilla.

In our study, *Globotruncana dupeublei* was uncommon and sporadically found throughout the Maastrichtian *P. hantkeninoides* Zone.

Stratigraphic distribution in the literature: Campanian-Maastrichtian. From the *G. gansseri* Zone to the *A. mayaroensis* Zone (CHRONOS Portal).

Globotruncana esnehensis* NAKKADY, *1950

Plate 27, Figs. 4-7; Plate 36, Figs. 4-5.

1950 *Globotruncana arca* CUSHMAN var. *esnehensis* NAKKADY, pl. 90, figs. 23-26.

1984 *Globotruncana esnehensis* NAKKADY- Robaszynski *et al*., pl. 9, figs. 1-4. pl. 9, fig. 1-4.

2004 *Globotruncana esnehensis* NAKKADY- Premoli Silva and Verga, pl. 36, figs. 3, 4.

Description & Remarks:

Globotruncana esnehensis is characterized by having a moderate trochospiral test with only one peripheral keel and 5 to 6 moderately increasing chambers in the last whorl. On the spiral side, chambers are petaloid shape with smooth surfaces and sutures join the spiral suture at almost right angles. In lateral view, it has asymmetrical profile where the spiral side is more convex and the umbilical side is very slightly convex.

It differs from:

Globotruncana dupeublei by having smaller test, more rapidly increasing but smaller number of chambers in the last whorl.

Globotruncanita conica by having more convex spiral side, rapidly increasing and more petaloid chambers, and umbilical system composed of tegilla.

Globotruncanita insignis by having more convex spiral side and less convex umbilical side rather than highly convex umbilical side as in *G. insignis*.

In our study, *Globotruncana esnehensis* was commonly found and abundant throughout the Maastrichtian *P. hantkeninoides* Zone.

Stratigraphic distribution in the literature: Campanian-Maastrichtian. From the *G. falsostuarti* Zone through the *A. mayaroensis* Zone (CHRONOS Portal).

***Globotruncana falsostuarti* SIGAL, 1952**

Plate 27, Figs. 8-9; Plate 36, Fig. 9.

1952 *Globotruncana falsostuarti* SIGAL, p. 43, text fig. 46.

1984 *Globotruncana falsostuarti* SIGAL- Robaszynski *et al*., pl. 10, figs. 1-3.

2004 *Globotruncana falsostuarti* SIGAL- Premoli Silva and Verga, pl. 11, figs. 13-15; pl. 12, figs. 1-6.

Description & Remarks:

Globotruncana falsostuarti has highly characteristic test where two keels get closer to each other in the middle of chambers. Namely, its keels are pinched in the middle of the chambers and two keels often absent on the last chambers. In addition to that it has 7 to 8 slowly increasing chambers in the last whorl, flat and smooth chamber surface, moderately high trochospiral test and horse-shoe shaped pattern on the umbilical side.

This species highly looks like *Globotruncana arca*, yet it differs from by having more petaloid and slowly increasing chambers, bending of the keels in the middle of the chambers and absence of two keels through the last chambers of the final whorl.

It also differs from:

Globotruncana esnehensis and *Globotruncana falsostuarti* simply by having two keels.

Globotruncana orientalis by larger test, slower increase in chambers and pinched keels in the middle of the chambers.

Globotruncana rosetta by having larger test, more numerous petaloid and slowly increasing chambers in the last whorl.

In our study, *Globotruncana falsostuarti* is common yet spasmodically present throughout the Maastrichtian in *P. hantkeninoides* Zone.

Stratigraphic distribution in the literature: From the *G. ventricosa* Zone through the *A. mayaroensis* Zone (CHRONOS Portal).

***Globotruncana lapparenti* BROTZEN, 1936; emended PESSAGNO, 1967**

Plate 28, Fig. 3.

1936 *Globotruncana lapparenti* BROTZEN, p. 175-176.

1967 *Globotruncana lapparenti* BROTZEN- Pessagno, pl. 2.

1985 *Globotruncana lapparenti* BROTZEN- Caron, figs. 20.3-4.

2004 *Globotruncana lapparenti* BROTZEN- Premoli Silva and Verga, pl. 13, figs. 2-5.

2011 *Globotruncana neotricarinata* PETRIZZO, FALZONI & PREMOLI SILVA- figs. 3 (1, 2, 4-10).

Description & Remarks:

Globotruncana lapparenti has moderate trochospiral test with 5.5 to 7 chambers in its last whorl, sub-circular to petaloid chambers, raised and beaded sutures on the spiral side, and well developed two keels. This form highly looks like *Globotruncana arca* and *Globotruncana linneiana* and possibly be an intermediate form between these two species.

It differs from:

Globotruncana linneiana by having less raised keels and a narrower imperforate peripheral band.

Globotruncana arca by having more sub-circular chambers and again narrower imperforate peripheral band.

In our samples *Globotruncana lapparenti* was found only in one sample (UH-33). This individual is likely to be a reworked specimen.

Stratigraphic distribution in the literature: Santonian-Maastrichtian. From the *D. asymetrica* Zone through the *A. mayaroensis* Zone (CHRONOS Portal).

Globotruncana linneiana D'ORBIGNY, 1839

1839 *Rosalina linneiana* D'ORBIGNY, pl. 5, figs. 10-12.

1956 *Globotruncana linneiana* D'ORBIGNY- Brönnimann and Brown, pl. 20, figs. 10-12.

1984 *Globotruncana linneiana* D'ORBIGNY- Robaszynski *et al*., pl. 13, figs. 1-4; pl. 14, figs. 1-5.

2004 *Globotruncana linneiana* D'ORBIGNY- Premoli Silva and Verga, pl. 13, figs. 6-13.

2017 *Globotruncana linneiana* D'ORBIGNY- Petrizzo *et al*., fig. 9 (5a-c).

Description & Remarks:

Globotruncana linneiana has highly characteristic almost flat trochospiral test with ''car tyre'' shaped well-developed two keels parallel to the axis of coiling and sometimes offset from one chamber to another. It also has 5 to 7 commonly 6 petaloid to crescent shaped chambers in the last whorl with smooth chamber surface. In umbilical view, spiral and adumbilical sutures create horse-shoe shape pattern. In lateral view, it has symmetrical profile with almost flat spiral and umbilical side.

It differs from:

Globotruncana bulloides by having flat chamber surfaces rather than inflated and more petaloid to crescentic shape chambers rather than sub-circular, and well-developed and wider imperforate peripheral band.

In our study, three *Globotruncana linneiana* individuals were found in one sample (UH-38) and these specimens are possibly reworked forms.

Stratigraphic distribution in the literature: Santonian-Maastrichtian. From the *D. asymetrica* Zone to the *R. fructicosa* Zone (CHRONOS Portal).

Globotruncana hilli PESSAGNO, 1967

Plate 28, Figs. 1-2; Plate 36, Figs. 2-3.

1967 *Globotruncana hilli* PESSAGNO, pl. 64, figs. 9-14.

2004 *Globotruncana hilli* PESSAGNO- Premoli Silva and Verga, pl. 37, figs. 3, 4; pl. 12, figs. 7-12.

2013 *Globotruncana hilli* PESSAGNO- Sarı, pl. 1, fig. 16.

Description & Remarks:

Globotruncana hilli is characterized by almost flat trochospiral and small test with 5 (or 4.5 to 5.5) chambers in the last whorl covered by fine spines. It has *G. linneiana* type wide double keel. Chambers on spiral side are globular then slightly petaloid on final stage. Practically, it has 'tire' shape in lateral view with or without spines on which imperforate peripheral band sometimes may curve slightly towards umbilical side.

It highly resembles *Globotruncana linneiana* but differs from by having globular initial chambers on the final whorl and less developed adumbilical ridges.

In our study, *Globotruncana hilli* was uncommon and sporadic throughout the Maastrichtian *P. hantkeninoides* Zone.

Stratigraphic distribution in the literature: Campanian-Maastrichtian. From the *Globotruncana ventricosa* Zone through the *Abathomphalus mayaroensis* Zone (CHRONOS Portal).

Globotruncana mariei BANNER and BLOW, 1960

Plate 28, Figs. 4-8; Plate 36, Figs. 7-8.

1960 *Globotruncana mariei* BANNER and BLOW, pl. 11, fig. 6.

1984 *Globotruncana mariei* BANNER and BLOW- Robaszynski et al., pl. 15, figs. 1-6.

2004 *Globotruncana mariei* BANNER and BLOW- Premoli Silva and Verga, pl. 13, figs. 14-15; pl. 14, fig. 1.

Description & Remarks:

Globotruncana mariei is characterized by having a moderate trochospiral test with biconvex lateral view, 4-5 rapidly increasing chambers in the last whorl and double keel on the periphery of the chambers. Keel band slightly inclined towards to umbilical side in early chambers of the last whorl.

It differs from:

Globotruncana arca by having smaller size, less numerous but more rapidly increasing chambers in the final whorl and narrower keel band.

Globotruncana rosetta by having well-developed double keel on all chambers of the final whorl, less convex umbilical side and more petaloid chambers.

Globotruncana linneiana by having narrower keel band, more convex spiral side rather than flat trochospiral test, and more rapidly increasing chambers.

In our study, *Globotruncana mariei* was highly common and consistently found throughout the Maastrichtian *P. hantkeninoides* Zone.

Stratigraphic distribution in the literature: Campanian-Maastrichtian. From the *G. elevata* Zone through the *G. gansseri* Zone (CHRONOS Portal). In contrast to what has been pronounced on the CHRONOS Portal, *Globotruncana mariei* has been consistently found in our study until 15 cm below the K-Pg boundary through the *P. hantkeninoides* Zone.

***Globotruncana orientalis* EL NAGGAR, 1966**

Plate 29, Figs. 1-3, Plate 36, Fig. 6.

1966 *Globotruncana orientalis* EL NAGGAR, pl. 12, fig. 4.

1984 *Globotruncana orientalis* EL NAGGAR- Robaszynski *et al*., pl. 16, figs. 1-3; pl. 17, figs. 1-4.

2004 *Globotruncana orientalis* EL NAGGAR- Premoli Silva and Verga, pl. 14, figs. 2-9.

Description & Remarks:

Globotruncana orientalis is characterized by moderate trochospiral test with 5 to 7 chambers in the last whorl. Keel band tilted towards to umbilical side and two keels on the periphery become narrower or even absent on the final chambers of the last whorl.

Globotruncana orientalis highly looks like *Globotruncana arca* yet it differs by having less developed keel band, less robust chambers with less raised and beaded sutures on the spiral side, and two keels become narrower into one.

In our study, *Globotruncana orientalis* was common and consistently found throughout the Maastrichtian *P. hantkeninoides* Zone.

Stratigraphic distribution in the literature: Campanian-Maastrichtian. From the *G. elevata* Zone through the *G. gansseri* Zone (CHRONOS Portal). Different from the literature, *Globotruncana orientalis* has been consistently found through the *P. hantkeninoides* Zone until the K-Pg boundary.

Globotruncana rosetta CARSEY, 1926

Plate 29, Figs. 4-6.

1926 *Globigerina rosetta* CARSEY, pl. 5, figs. 3a-b.

1984 *Globotruncana rosetta* CARSEY- Robaszynski et al., pl. 18, figs. 1-5.

2004 *Globotruncana rosetta* CARSEY- Premoli Silva and Verga, pl. 14, figs. 10-15; pl. 15, figs. 1-3.

Description & Remarks:

Globotruncana rosetta is characterized by having a test with highly convex umbilical and slightly convex spiral side, 4 to 6 rapidly increasing crescent-shaped chambers in the last whorl. Also, it has two keels become absent in the final chambers of the last whorl.

It differs from:

Globotruncana insignis by having two keels at least a couple of initial chambers of the final whorl, more rapidly increasing crescent-shaped chambers.

Globotruncana mariei by having less developed two keels which turn into one keel, more convex umbilical side, and asymmetrical profile in lateral view.

In our study, *Globotruncana rosetta* was sporadically present and became more abundant starting from the middle of the samples (from UH-36).

Stratigraphic distribution in the literature: Campanian-Maastrichtian. From the G. *ventricosa* Zone trough the *A. mayaroensis* Zone (CHRONOS Portal).

***Globotruncana ventricosa* WHITE, 1928**

Plate 29, Figs. 7-9.

1928 *Globotruncana canaliculata* (REUSS) var. *ventricosa* WHITE, pl. 38, figs. 5a-c.

1984 *Globotruncana ventricosa* WHITE- Robaszynski *et al*., pl. 20, figs. 1-3.

2004 *Globotruncana ventricosa* WHITE- Premoli Silva and Verga, pl. 15, figs. 4-15.

2011 *Globotruncana ventricosa* WHITE-Petrizzo *et al*., figs. 2 (1-15a-c).

Description & Remarks:

Globotruncana ventricosa is characterized by very low trochospiral test, 6 to 7 (exceptionally 5, 5.5 or 8) slowly increasing chambers in the last whorl, pronounced-raised sutures with flat chamber surface and slowly increasing chambers on spiral side. In the lateral view, it has asymmetrical profile with flat spiral side and convex umbilical side on which chambers have triangular outline and their sizes double during its ontogeny.

Globotruncana ventricosa differs from:

Globotruncana linneiana by having more and slowly increasing chambers in the last whorl, triangular shape chambers which are more pronounced on the last chambers, more convex umbilical side and narrower keel band.

Globotruncana rosetta by having equally developed double keel on all chambers, more and slowly increasing chambers, flatter spiral side and larger umbilicus.

In our study, *Globotruncana ventricosa* was uncommon and sporadic throughout the Maastrichtian *P. hantkeninoides* Zone.

Stratigraphic distribution in the literature: Campanian-Maastrichtian. From the *G. ventricosa* Zone through the *A. mayaroensis* Zone (CHRONOS Portal).

Genus *Globotruncanita* REISS, 1957

Type species: *Rosalina stuarti* DE LAPPARENT, 1918

Globotruncanita angulata TILEV, 1951

Plate 30, Figs. 1-3.

1951 *Globotruncanita lugeoni* TILEV var. *angulata* TILEV, pl. 3, figs. 1, 13.
1984 *Globotruncanita angulata* TILEV- Robaszynski et al., pl. 23, figs. 1-5.
2004 *Globotruncanita angulata* TILEV- Premoli Silva and Verga, pl. 17, figs. 1-5.

Description & Remarks:

Globotruncanita angulata is characterized by having strongly asymmetrical test with flat to slightly convex spiral side to strongly convex umbilical side, slowly increasing 5 to 6 chambers in the last whorl. Chambers are crescent-shaped to triangular then trapezoidal through the ontogeny.

It differs from:

Gansserina gansseri by having well developed adumbilical ridges and lacking pustulose chamber surface on the umbilical side, straight sutures join the spiral suture at almost 90 degrees at the end of last whorl, and triangular to trapezoidal chambers on the spiral side.

Globotruncanita stuartiformis by having almost flat trochospiral test, rapidly increasing and less numerous chambers on the spiral side.

Globotruncanita pettersi by having slower increase in chamber size, larger test, more trapezoidal chambers and semi-spherical profile in lateral view (chambers join the periphery at right angles).

In our study, *Globotruncanita angulata* was common through initial samples of the quantitative study (UH-30 to UH-39), and almost absent after UH-39.

Specimen in Plate 30, Fig. 3 was considered as ‘’affinity’’ since it has slightly convex spiral side rather than flat.

Stratigraphic distribution in the literature: From top of the *G. falsostuarti* Zone through the *A. mayaroensis* Zone (CHRONOS Portal).

***Globotruncanita conica* WHITE, 1928**

Plate 30, Figs. 4-6; Plate 36, Fig. 23.

1928 *Globotruncana conica* WHITE, pl. 38, fig. 7.
1984 *Globotruncanita conica* WHITE- Robaszynski *et al*., pl. 26, figs. 1-3.
2004 *Globotruncanita conica* WHITE- Premoli Silva and Verga, pl. 17, figs. 7-13.

Description & Remarks:

Globotruncanita conica is distinguished by having a large and highly asymmetrical test which has very convex spiral and flat umbilical side. It has 6 to 9 very slowly increasing chambers in the last whorl.

It differs from:

Globotruncana dupeublei by having larger test with flat umbilical side.

In our study, *Globotruncanita conica* was uncommon and sporadically present throughout the Maastrichtian *P. hantkeninoides* Zone.

Stratigraphic distribution in the literature: From the *G. gansseri* Zone to the *A.* mayaroensis Zone (Robaszynksi et al. 1984).

Globotruncanita insignis GANDOLFI, 1955

Plate 30, Figs. 7-9; Plate 36, Fig. 18.

1955 *Globotruncana (Globotruncana) rosetta* CARSEY subsp. *insignis* GANDOLFI, pl. 67, figs. 2a-c.

1984 *Globotruncana*? *insignis* GANDOLFI- Robaszynski *et al*., pl. 11, figs. 1-3.

2004 *Globotruncana insignis* GANDOLFI- Premoli Silva and Verga, pl. 12, figs. 13-15; pl. 13, fig. 1.

Description & Remarks:

Globotruncanita insignis is characterized by having slightly convex to flat spiral and strongly convex umbilical side, 5 to 7 sometimes 8 crescentic to petaloid shape slowly increasing chambers in the final whorl with smooth surface, and small umbilicus. Some individuals may have ornamentations on the sutures of the spiral side which look like small spines.

It differs from:

Globotruncana rosetta by lacking two keels on the early chambers of the final whorl and having slowly increasing and more chambers on the final whorl and very high convex umbilical but slightly convex spiral side.

Stratigraphic distribution in the literature: From the *G. ventricosa* Zone through the *A. mayaroensis* Zone (CHRONOS Portal).

Globotruncanita pettersi GANDOLFI, 1955

Plate 31, Figs. 1-3.

1955 *Globotruncana (Globotruncana) rosetta* CARSEY subsp. *pettersi* GANDOLFI, pl.6, fig. 3a-c.

1984 *Globotruncanita pettersi* GANDOLFI- Robaszynski *et al*., pl. 29, fig. 1-5.

2004 *Globotruncanita pettersi* GANDOLFI- Premoli Silva and Verga, pl. 18, figs. 11-12.

2013 *Globotruncanita pettersi* GANDOLFI- Sarı, pl. 2, fig. 26.

Description & Remarks:

Globotruncanita pettersi has relatively smaller test with rapidly increasing 4 to 5 crescentic chambers on the last whorl. It has conical profile in lateral view with flat to slightly convex spiral side and strongly convex umbilical side.

It differs from:

Globotruncanita insignis by having smaller test, fewer and rapidly increasing chambers.

Gansserina gansseri by having adumbilical ridges and raised sutural ridges between first chambers of the umbilical side.

In our study, *Globotruncanita pettersi* was highly common and consistent throughout Maastrichtian *P. hantkeninoides* Zone.

Stratigraphic distribution in the literature: Campanian-Maastrichtian. From the *G. gansseri* Zone through the *A. mayaroensis* Zone (CHRONOS Portal).

Globotruncanita stuarti de LAPPARENT, 1918

Plate 31, Figs. 4-6; Plate 36, Figs. 19-22.

1918 *Rosalina stuarti* de LAPPARENT, text fig. 4, lower 3 figures.
1984 *Globotruncanita stuarti* de LAPPARENT- Robaszynski *et al*., pl. 30, figs. 1-3; pl. 31, figs. 1-3.
2004 *Globotruncana stuarti* de LAPPARENT- Robaszynski *et al*., pl. 18, figs. 13-15; pl. 19, figs. 1-7.
2013 *Globotruncana stuarti* de LAPPARENT- Sarı, pl. 2, fig. 25.

Description & Remarks:

Globotruncanita stuarti is characterized by having trapezoidal to quadrangle, slowly increasing 7 to 9 chambers in the last whorl. It has moderately high trochospiral test with more or less symmetrical profile at which both sides are convex.

It differs from:

Globotruncanita stuartiformis by having more circular spiral outline, slowly increasing and larger number of chambers with subrectangular or quadrangular shape, and more convex spiral and umbilical side.

In our study, *Globotruncanita stuarti* was sporadically present through Maastrichtian *P. hantkeninoides* Zone.

Stratigraphic distribution in the literature: Campanian-Maastrichtian. From the *G. gansseri* Zone to the *A. mayaroensis* Zone (CHRONOS Portal).

***Globotruncanita stuartiformis* DALBIEZ, 1955**

Plate 31, Figs. 7-9; Plate 36, Figs. 14-16.

1955 *Globotruncana (Globotruncana) elevata* BROTZEN subsp. *stuartiformis* DALBIEZ, text fig 10.

1984 *Globotruncanita stuartiformis* DALBIEZ- Robaszynski *et al*., pl. 32, figs. 1-4.

2004 *Globotruncanita stuartiformis* DALBIEZ- Premoli Silva and Verga, pl. 19, figs. 8-15.

Description & Remarks:

Globotruncanita stuartiformis is characterized by highly characteristic triangular shape 5 to 7 slowly increasing chambers on the last whorl. Straight sutures join the spiral suture at very acute angles.

It differs from:

Globotruncanita stuarti by having rougher and non-circular spiral outline, triangular shape chambers with sutures join at very acute angles, and generally less convex spiral side.

In our study, *Globotruncanita stuartiformis* was consistently found throughout the Maastrichtian *P. hantkeninoides* Zone.

Stratigraphic distribution in the literature: Santonian-Maastrichtian. From the *D. asymetrica* Zone to the *P. hariaensis* Zone (CHRONOS Portal).

Genus *Contusotruncana* KORCHAGIN, 1982

Type species: *Pulvinulina arca* var. *contusa* CUSHMAN, 1926

***Contusotruncana contusa* CUSHMAN, 1926**

Plate 32, Figs. 1-3.

1926 *Pulvinulina arca* CUSHMAN var. *contusa* CUSHMAN, p. 23, no type specimen given.

1984 *Rosita contusa* CUSHMAN, Robaszynski *et al*., pl. 36, figs. 1-2, pl. 37, figs. 1-3.

2004 *Contusotruncana contusa* CUSHMAN- Premoli Silva and Verga, pl. 3, figs. 1-12.

Description & Remarks:

Contusotruncana contusa is characterized by very high trochospiral test with pyramid-shaped spiral side and flat to concave umbilical side with 4 to 5 slowly increasing chambers on the last whorl. It has closely spaced double keel strongly tilted towards to umbilical side which become perpendicular to coiling axis. Chamber surfaces are undulated on the spiral side.

It differs from:

Globotruncanita conica by having two keels and undulated chamber surface on the spiral side.

Contusotruncana walfischensis by having conical spiral side with undulated chambers surface and lacking rounded dome shape spiral side with flattened apex.

Contusotruncana patelliformis by having larger size and higher trochospire.

In our study, *Contusotruncana contusa* was very rare in the Maastrichtian *P. hantkeninoides* Zone.

Stratigraphic distribution in the literature: Middle and upper parts of the Maastrichtian. From the *G. gansseri* Zone to the *A. mayaroensis* Zone (Robaszynski et al. 1984).

Contusotruncana patelliformis GANDOLFI, 1955

Plate 32, Fig. 4; Plate 36, Fig. 12.

1955 *Contusotruncana (Globotruncana) contusa* (CUSHMAN) subsp. *patelliformis* GANDOLFI, pl. 4, figs. 2a-c.

1984 *Rosita patelliformis* GANDOLFI- Robaszynski *et al*., pl. 39, figs. 1-3.

2004 *Contusotruncana patelliformis* GANDOLFI- Premoli Silva and Verga, pl. 4, figs. 10-13.

Description & Remarks:

Contusotruncana patelliformis highly looks like *Contusotruncana contusa* but it differs by having smaller test with lower trochospire.

In our study, *Contusotruncana patelliformis* was rare and sporadically found throughout the Maastrichtian *P. hantkeninoides* Zone.

Stratigraphic distribution in the literature: Campanian-Maastrichtian. From the *G. ventricosa* Zone through the *A. mayaroensis* Zone (CHRONOS Portal).

Contusotruncana plicata WHITE, 1928

Plate 32, Fig. 5.

1928 *Globotruncana conica* WHITE var. *plicata* WHITE, pl. 38.

1984 *Rosita plicata* WHITE- Robaszynski *et al*., pl. 40, figs. 1-2.

2004 *Contusotruncana plicata* WHITE- Premoli Silva and Verga, pl. 10, figs. 1-2.

Description & Remarks:

Contusotruncana plicata is distinguished by having characteristic fluted test, 4 to 6 chambers on the last whorl. Chambers are initially globular then crescentic, elongated, and inflated. It has very high trochospiral test with very asymmetrical profile where spiral side is strongly convex. Two closely spaced keels decrease into one keel on the last two or three chambers and the keel band prominently lean towards the umbilical side.

It differs from:

Contusotruncana contusa by having inflated and larger chambers with bell-shape general appearance.

Contusotruncana walfischensis by having inflated and less convex spiral side.

Contusotruncana patelliformis by having higher trochospiral test, fluted spiral side, and lobate outline.

The specimen in Plate 32, Fig. 5 was considered as ‘’affinity’’ because of having less inflated and less fluted chambers on the spiral side and less polygonal test.

Stratigraphic distribution in the literature: From the *G. gansseri* Zone to the *A. mayaroensis* Zone (Robaszynski et al. 1984).

***Contusotruncana walfischensis* TODD, 1970**

Plate 32, Fig. 6; Plate 36, Fig. 13.

1970 *Globotruncana walfishensis* TODD, pl. 5, fig. 8.
1984 *Rosita walfishensis* TODD- Robaszynski *et al*., pl. 42, figs. 1-4.
2004 *Contusotruncana walfischensis* TODD- Premoli Silva and Verga, pl. 5, figs. 1-3.

Description & Remarks:

Contusotruncana walfischensis is characterized by having very high trochospiral test with rounded dome shape spiral side with flattened apex and slightly concave umbilical side. 4.5 to 5 chambers slowly increase on the last whorl. It has rounded circular shape in spiral view. Two keels strongly tilted towards to the umbilical side becoming perpendicular to the coiling axis.

It differs from:

Contusotruncana contusa by having rounded spiral outline, globular chambers lacking undulated surface, and less prominent keels.

In our study, *Contusotruncana walfischensis* was very rare throughout the Maastrichtian *P. hantkeninoides* Zone.

Stratigraphic distribution in the literature: Maastrichtian. From *R. fructicosa* Zone through the *P. hantkeninoides* Zone (CHRONOS Portal).

CHAPTER 6

DISCUSSION AND CONCLUSIONS

In this study, the K-Pg boundary in the Haymana Basin was identified and quantitative analysis were carried out on planktonic foraminiferal assemblages in 63-150 μm and >150 μm size fractions across late Maastrichtian and early Danian time interval.

To do this, two sections were measured: UH and UKHB sections. The UH section (9.70 m in total) covers uppermost part of the Maastrichtian, crosses the K-Pg boundary and ends in lowermost Danian. In total 51 samples were collected and quantitative analyses correspond to top 3.90 m of the UH section (covering Maastrichtian and Danian samples). UKHB section (5.14 cm in total), on the other hand, covers a few centimeters of the Maastrichtian, crosses the K-Pg boundary and goes through upper levels in the Danian. 38 samples were collected from the UKHB section.

Three biozones were established within the scope of this study: *Plummerita hantkeninoides* Zone, P0 Zone and Pα Zone. This thesis is the first study in Turkey which demonstrates *Plummerita hantkeninoides* Zone for the latest Maastrichtian. The *P. hantkeninoides* Zone in our study corresponds to whole Maastrichtian samples (9.55 m) from UH-1 to the K-Pg boundary. P0 (*G. cretacea*) Zone, on the other hand, spans 25 cm from the K-Pg boundary to UKHB-4 (UH-52) where Pα Zone starts. The top of the Pα Zone was not identified because it is beyond the scope of this study.

Figure 47 summarizes the relative abundance patterns of key groups and species diversities of in both fractions.

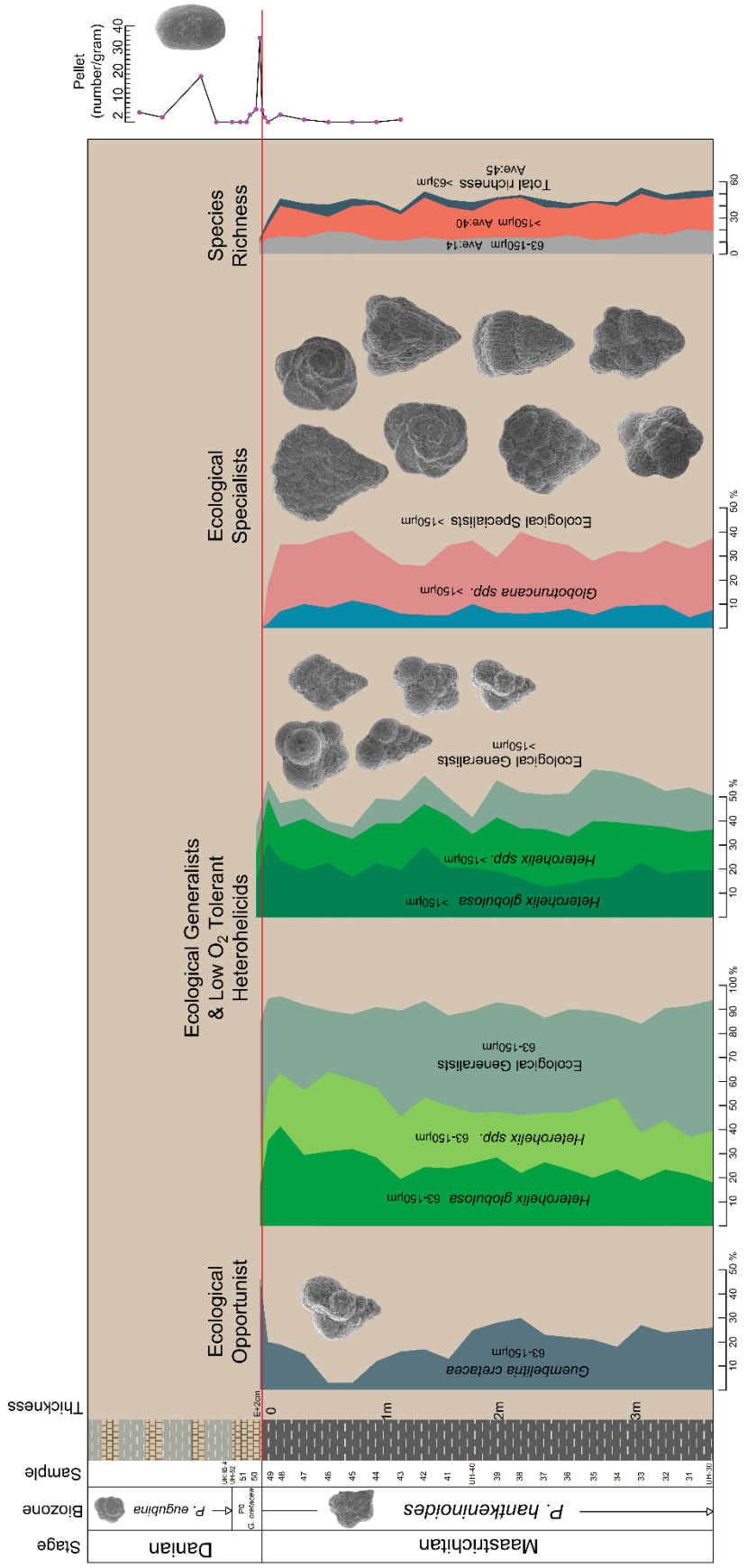

Figure 47. Summary of relative abundance patterns of key groups and species diversities in 63-150 µm and >150 µm fractions. Please note the opportunistic bloom of *Guembelitria cretacea* and echinoid pellet peak right after the K-Pg boundary (red line).

In 63-150 μm fraction, an average of 380 individuals were counted for each sample. Population is composed of small, delicate r-strategists (ecological generalists) (ave. 87%) and almost no large-ornamented K-strategists (ecological specialists) (Fig. 47). Low oxygen tolerant heterohelicids (ave. 54%) coupled with *Guembelitria cretacea* (ave. 20%) dominate this assemblage (Fig. 47). Ecological generalists are tolerant to environmental variations such as, temperature, oxygen, nutrient and salinity (Keller et al. 2002). Therefore, as a result of being composed of resistant ecological generalists, the species diversity in 63-150 μm fraction does not fluctuate markedly but declines very lightly through up-section (Fig. 47).

Right after the K-Pg boundary relative abundance of *Guembelitria cretacea* rapidly increases as other groups such as heterohelicids sharply drops (Fig. 47). This study for the first time in Turkey represents relative abundance patterns of *Guembelitria cretacea* throughout Maastrichtian and its ‘’bloom’’ right after the K-Pg boundary.

Similar to 63-150 μm, population in >150 μm fraction is largely composed of r-strategists (ave. 51% before the K-Pg) with smaller number of K-strategists (ave. 33% before K-Pg) (Fig. 47). Heterohelicids (~40%) are the most dominant group similar to 63-150 μm fraction. As relative abundance values in two size fractions indicate that low-oxygen-tolerant heterohelicids are the most dominant group among the Maastrichtian planktonic foraminifera community in the Haymana Basin. High low-oxygen-tolerant heterohelicid abundance indicate that there were an expanded Oxygen Minimum Zone (OMZ) in the basin prevailed through Maastrichtian *P. hantkeninoides* Zone.

On the other hand, species diversity in >150 μm fraction largely declines throughout the Maastrichtian. In fact, the diversity decreased by 54% from UH-30 to UH-49 (5 cm before the K-Pg boundary) in 3.75 m interval. This decrease trend before the boundary may indicate environmental stress prior to the K-Pg mass extinction.

A couple of speculations can be made germane to the cause of this pre-boundary stress. First of all, this stress might have caused either by ongoing Deccan volcanism, fore-arc setting of the Haymana Basin (and associated subduction and submarine volcanism) or both. The subduction of the Northern Branch of NeoTethys beneath the Eurasian Plate would have created paleo-highs which may have accelerated

terrigenous influx to the basin. Flysch deposits of the Haymana Formation and 9.55 m-thick *P. hantkeninoides* Zone indicate high sediment accumulation in the basin (~3 cm/1000 yr). In consequence of high terrigenous input and eventually high nutrient influx might have resulted in *Guembelitria cretacea* blooms during late Maastrichtian. Similarly, Keller and Pardo (2004b) claim that the most intense *Guembelitria* blooms (>60%) happened in shallow continental shelf localities, shelf/slope margins, and volcanic provinces in Indian Ocean which have common in high nutrient influx (eutrophication) either from continental runoff, upwelling through continental margins or volcanic input.

In our study, the K-Pg boundary is characterized by 2-3 mm thick reddish layer which corresponds to abrupt extinction of Cretaceous planktonic foraminifera. All large, robust, ornamented tropical-subtropical species, such as globotruncanids, planoglobulinids, and rugoglobigerinids went extinct sharply at the K-Pg boundary. Only small, less ornamented r-strategists, such as guembelitrids, heterohelicids and globigerinelloids survived into Danian.

On the other hand, in our section, the K-Pg boundary itself (2-3 mm thick reddish layer) is devoid of planktonic foraminifera with exceptions of a spot of *Hedbergella*, *Heterohelix*, *Guembelitria,* and *Globigerinelloides* species and a small number of benthic foraminifera which was also observed by Smit (2004) in Gredero section (Spain).

Survivor species were recognized by their consistent and abundant presence in Danian sediments while reworked ones represent differential preservation (e.g. discolor, broken test) and inconsistent occurrence. Given these criteria, 13 out of 28 species were considered as survivors (%46 survival rate) which are: *Guembelitria cretacea*, *Heterohelix globulosa*, *Heterohelix navarroensis*, *Heterohelix planata*, *Heterohelix punctulata*, *Laeviheterohelix dentata*, *Laeviheterohelix glabrans*, *Hedbergella holmdelensis*, *Hedbergella monmouthensis*, *Globigerinelloides subcarinatus*, *Globigerinelloides asperum*, *Globigerinelloides prairiehillensis*, and *Globigerinelloides alvarezi*.

Starting from the boundary itself, number of echinoid fecal pellets abruptly increase, peak at 2 cm above the boundary and rapidly turn back to background values through up-section. Our findings support the idea of Miller (2010) who claimed that sharp increase in the amount of echinoid fecal pellets immediately after the boundary can be used as an auxiliary marker for the correlation of the K-Pg boundary.

Additionally, right after the boundary there is a surge in the number of calcareous spherical forms which cover almost all background area of the thin sections. These spheres are relicts of calcareous dinoflagellate cysts belong to *Thoracospharea* species. *Thoracosphaera* acme right after the K-Pg boundary has long been known by various studies (Romein 1979, Pospsichal and Wise 1990, Eshet et al. 1992, Gardin and Monechi 1998, Keller et al. 2001, Smit 2004, Lamolda et al. 2005, 2015). In fact, Tantawy (2003) demonstrated that the K-Pg boundary is characterized by this *Thoracosphaera* acme. Having found *Thoracosphaera* acme right after the K-Pg boundary and 9.55 m-thick *P. hantkeninoides* Zone indicate that our section is complete without any hiatus. *Thoracosphaera* acme immediately after the K-Pg boundary was found for the first time in Turkey by this study.

Moreover, some spherules were recovered from washed residue of the boundary layer (2-3 mm thick reddish layer corresponding the K-Pg boundary). We encountered with these spherules only between 63-150 μm size fraction. They were divided into two group according to their color types and surface textures: black ones generally have smooth surfaces, and amber to yellow color and translucent ones commonly have characteristic texture on their surfaces. EDX analyses have shown that both spherule groups are made up of Ca with minor amount of Si. Two postulations can be made about their genesis: They are either genuine impact induced spherules and their silica altered to calcium under high pH conditions (Belza et al. 2015), or they are inner molds of highly large *Thoracosphaera* forms. Being present only within the K-Pg boundary layer makes these spherules highly enigmatic. No spherule was found at any level below or above the K-Pg boundary.

Paleobathymetry of the depositional area was calculated by using planktonic-benthic ratios. Depth formula of Van der Zwaan (1990) gave an average of 380 m depth, while that of De Rijk et al. (1999) yielded average 490 m. Overall, these two depth formulas

revealed approximately 400 m paleodepth corresponding upper bathyal zone. Finding deep-water dweller planktonic foraminifera, such as *Abathomphalus mayaroensis*, *Heterohelix rajagopalani*, *Gublerina cuvillieri* and *Planoglobulina multicamerata* in our samples corroborates the paleobathymetric estimation. Additionally, heterohelicid and *Guembelitria cretacea* dominance through the Maastrichtian may indicate an upwelling zone in our study area which may be substantiated by upper bathyal setting of the depositional area

A rapid change in the sedimentation was observed in our section after the K-Pg boundary. Maastrichtian deposits are characterized by monotonous mudstones. Right after the boundary these mudstone deposits turn into marl and calcareous mudstone alternations through the Danian. In fact, a prominent ~30 cm-thick marl bed directly overlies the 2-3 mm thick reddish layer (the K-Pg boundary). Similarly, Açıkalın et al. (2015) demonstrated a limestone bed immediately overlying the K-Pg boundary clay in the Mudurnu-Göynük Basin. They claim that this bed has been seen by various outer neritic-upper bathyal sections, such as Agost (Spain), Caravaca (Spain) and Bjala (Bulgaria). Keller (2004) revealed that chalk and limestone deposits in Mishor Rotem section (southern Israel) is a function of low surface productivity. So, the limestone/marl bed immediately following the boundary might represent diminished surface productivity after the K-Pg mass extinction.

Similar to Haymana Basin, Açıkalın et al. (2015) demonstrated that in Mudurnu-Göynük Basin, late Maastrichtian mudstones rapidly change after the K-Pg boundary to limestone-mudstone alternations in early Danian (Fig. 48). Sedimentation styles of the Haymana and the Mudurnu-Göynük basins indicate that these two basins might have connected with each other during Maastrichtian-Danian time interval (Fig. 48).

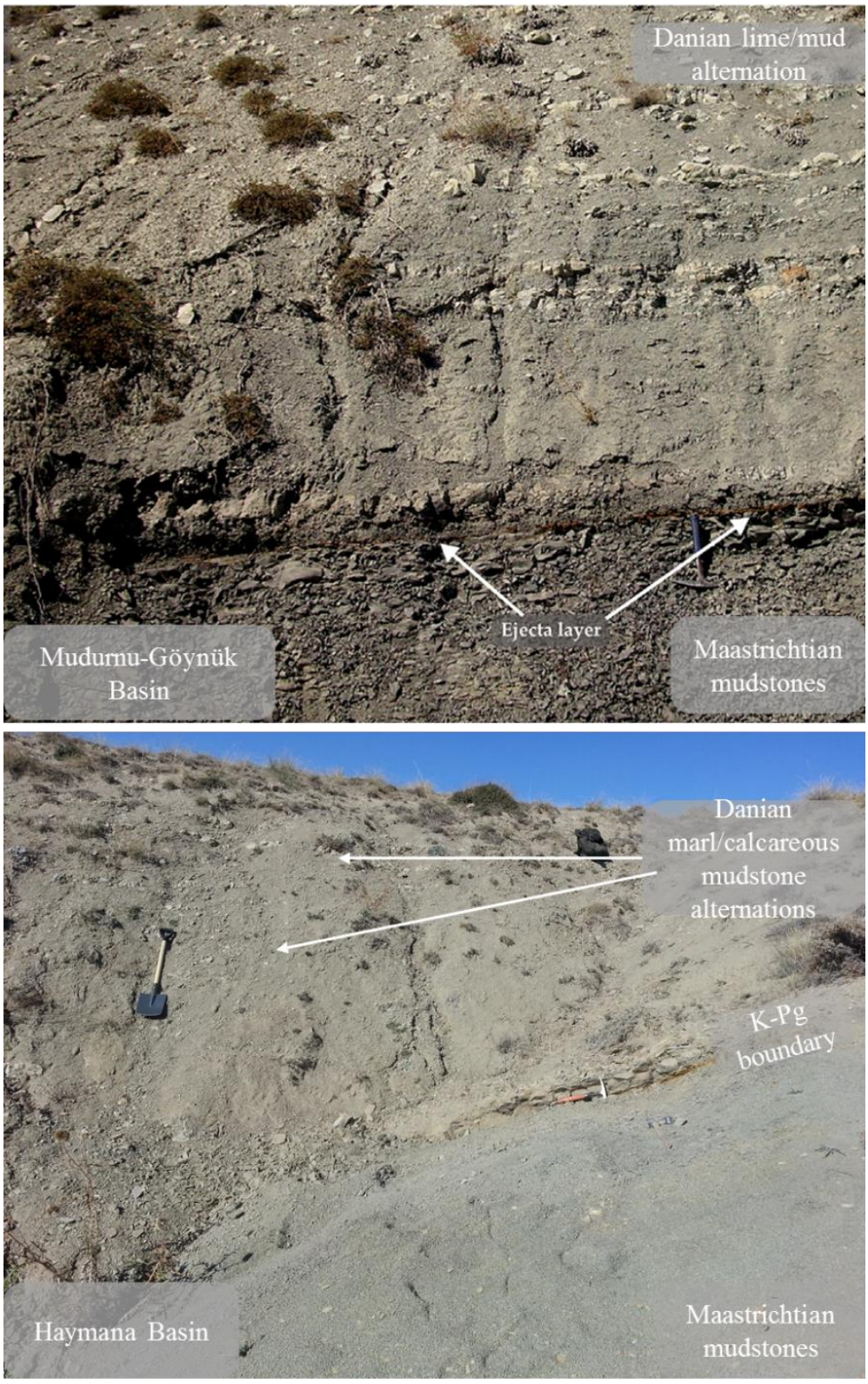

Figure 48. Deposition similarity between Haymana and Mudurnu-Göynük basins indicate that these two basins once connected with each other during Maastrichtian-Danian time interval. Image of the Mudurnu-Göynük Basin was taken and modified after Açıkalın et al. (2015).

All in all, this thesis is the most comprehensive quantitative study on late Cretaceous-early Danian planktonic foraminifera in Turkey thus far. Based on our findings, a general panorama of the Haymana Basin during late Maastrichtian-early Danian interval would be the following:

As a result of tectonically active Haymana Basin, there were high terrigenous runoff which would have yielded high sediment and nutrient influx to the basin. A combination of the Deccan Trap activity (Keller 2014) and subduction-related submarine volcanism (Okay and Altıner 2016) coupled with high nutrient input would have created eutrophication and eventually *Guembelitria cretacea* blooms throughout the Maastrichtian. Additionally, heterohelicid domination in the populations of both fractions indicate expanded oxygen minimum zone (Pardo and Keller 2008) within the basin.

The K-Pg boundary is catastrophic and sharp. Although there has been progressive decline in the species diversity, the boundary is responsible for 54% extinction of the late Cretaceous planktonic foraminifera.

After the boundary, disaster opportunistic *Guembelitria cretacea* blooms rapidly and dominate the planktonic foraminifera population (49% relative abundance). At the same level *Thoracosphaera* blooms prevail and echinoid fecal pellets peak in their number. Through up-section as environmental recovery take place, these *Thoracospharea* blooms diminish and newly-evolved Danian planktonic foraminifera replace the niches.

Additional works will be done for further analysis across the K-Pg boundary, such as Ir and Platinum Group Element (PGEs) composition and oxygen and carbon isotope geochemistry.

REFERENCES

Abramovich, S., Keller, G., 2002, High stress late Maastrichtian paleoenvironment: inference from planktonic foraminifera in Tunisia, Palaeogeogr. Palaeoclimatol. Palaeoecol., 178, p. 145-164.

Abramovich, S., Keller, G., Adatte, T., Stinnesbeck, W., Hottinger, L., Stueben, D., Berner, Z., Ramanivosoa, B., Randriamanantenasoa, A., 2002, Age and paleoenvironment of the Maastrichtian to Paleocene of the Mahajanga Basin, Madagascar: a multidisciplinary approach, Marine Micropaleontology, 47, p. 17-70.

Abramovich, S., Keller, G., Stüben, D., Berner, Z., 2003. Characterization of late Campanian and Maastrichtian planktic foraminiferal depth habitats and vital activities based on stable isotopes, Palaeogeogr. Palaeoclimatol. Palaeoecol., 202, p. 1-29.

Abramovich, S., Yovel-Corem, S., Almogi-Labin, A., Benjamini, C., 2010, Global climate change and planktonic foraminiferal response in the Maastrichtian, Paleoceanography, 25, doi:10.1029/2009PA001843.

Açikalin, S., Vellekoop, J., Ocakoglu, F., Yılmaz, I. Ö., Smit, J., Altiner, S. O., Goderis, S., Vonhof, H., Speiker, R. P., Woelders, L., Fornaciari, E., and Brinkhuis, H., 2015, Geochemical and paleontological characterization of a new K–Pg Boundary locality from the Northern branch of the Neo-Tethys: Mudurnu-Göynük Basin, NW Turkey, Cretaceous Research, 52, p. 251-267.

Akarsu, İ., 1971, II. Bölge AR/TPO/747 nolu sahanın terk raporu. Pet. İş. Gen. Md., Ankara.

Alroy, J., Aberhan, M., Bottjer, D. J., Foote, M., Fürsich, F. T., Harries, P. J., Hendy, A. J. W., Holland, S. M., Ivany, L. C., Kiessling, W., Kosnik, M. A., Marshall, C. R., McGowan, A. J., Miller, A. I., Olszewski, T. D., Patzkowsky, M. E., Peters, S. E., Villier, L., Wagner, P. J., Bonuso, N., Borkow, P. S., Brenneis, B., Clapham, M. E.,

Fall, L. M., Ferguson, C. A., Hanson, V. L., Krug, A. Z., Layou, K. M., Leckey, E. H., Nürnberg, S., Powers, C. M., Sessa, J. A., Simpson, C., Tomašových, A., and Visaggi, C. C., 2008, Phanerozoic trends in the global diversity of marine invertebrates: Science, v. 321, p. 97–100, doi: 10.1126/science.1156963.

Alvarez, L. W., Alvarez, W., Asaro, F., Michel, H. V., 1980, Extraterrestrial cause for the Cretaceous–Tertiary extinction. Science, 208, p. 1095–1108.

Amirov, E., 2008, Planktonic Foraminiferal Biostratigraphy, Sequence Stratigraphy and Foraminiferal Response to Sedimentary Cyclicity in the Upper Cretaceous-Paleocene of the Haymana Basin (Central Anatolia, Turkey), M.Sc. Thesis, Middle East Technical University, 213 p.

Arawaka, Y., Li, X., Ebihara, M., Meriç, E., Tansel, İ., Bargu, S., Koral, H., Matsumaru, K., 2003, Element profiles and Ir concentration of Cretaceous-Tertiary (K-T) boundary layers at Medetli, Gölpazari, northwestern Turkey. Geochemical Journal, 37, p. 681-693.

Arenillas, I., and Arz, J. A., 2013, New evidence on the origin of non-spinose pitted-cancellate species of the early Danian planktonic foraminifera, Geologica Carpthica, 64, p. 237-251.

Arenillas, I., Arz, J. A., 2016, Benthic origin and earliest evolution of the first planktonic foraminifera after the Cretaceous/Palaeogene boundary mass extinction, Historical Biology, 29, p. 25-42.

Arenillas, I., Arz, J. A., Molina, E., 2004, A new high-resolution planktic foraminiferal zonation and subzonation for the lower Danian. Lethaia, 37, p. 79–95.

Arenillas, I., Arz, J. A., Molina, E., Dupuis, C., 2000, The Cretaceous/Paleogene (K/P) boundary at Aïn Settara, Tunisia: sudden catastrophic mass extinction in planktic foraminifera, Journal of Foraminiferal Research, 30, p. 202–218.

Arıkan, Y., 1975, Tuzgölü havzas ın ın jeolojisi ve petrol imkanları. MTA Bülteni, 85, p. 17-38.

Arz, J. A., and Molina, E., 2002, Bioestratigrafia y cronoestratigrafia con foraminiferos planctonicos del Campaniense superior y Maastrichtiense de latitudes subtropicales y templadas (Espana, Francia y Tunicia), Neues Jahrbuch fur Geologie und Palaontologie, Abhundlungen, v. 224, p. 161–195.

Ayyıldız, T., Varol, B., Önal M., Tekin, E., Gündoğan İ., 2015, Cretaceous-Tertiary (K-T) boundary evaporites in the Malatya Basin, eastern Turkey, Carbonates and Evaporites, 30, p. 461-476.

Banner, F. T. and Blow, W. H., 1960, Some primary types of species belonging to the Superfamily Globigerinaceae, Contributions from the Cushman Foundation for Foraminiferal Research, 11, p. 1-41.

Barr, F. T., 1966, Upper Cretaceous foraminifera from the Ballydeenlea Chalk, County Kerry, Ireland, Palaeontology, 9, p. 492-510.

Bayhan, E., 2007, Clay mineralogy of the Upper Cretaceous-Lower Tertiary sedimentary sequences of the Kalecik Region (Central Anatolia, Turkey). Yerbilimleri, Hacettepe Üniversitesi Yerbilimleri Uygulama ve Araştırma Merkezi Dergisi, 28/2, p. 127-136.

Belza, J., Goderis, S., Smit, J., Vanhaecke, F., Baert, K., Terryn, H., Claeys, P., 2015, High spatial resolution geochemistry and textural characteristics of 'microtektite' glass spherules in proximal Cretaceous-Paleogene sections: Insights into glass alteration patterns and precursor melt lithologies, Geochimica et Cosmochimica Acta, 152, p. 1-38.

Berggren, W. A. and Miller, K. G., 1989, Cenozoic bathyal and abyssal calcareous benthic foraminiferal zonation, Micropaleontology, 35, p. 308-320.

Berggren, W. A., Pearson, P. N., 2005, A Revised Tropical to Subtropical Paleogene Planktonic Foraminiferal Zonation, Journal of Foraminiferal Research, 35, p. 279-298.

Berggren, W. A., Kent, D. V., Swisher, C. C., Aubry, M. P., 1995, A revised Cenozoic geochronology and chronostratigraphy. SEPM, Special Publication, 54, p. 129-212.

Bergstresser, T. J. and Frerichs, W. E., 1982, Planktonic foraminifera from the Upper Cretaceous Pierre Shale at Red Bird, Wyoming, Journal of Foraminiferal Research, 12, p. 353-361.

Blow, W. H., 1979, The Cainozoic Globigerinida. 3 Vols., Brill, Leiden. 1413 p.

Bozkaya, Ö., Yalçın, H., 1991a, Hekimhan doğu ve güney kesimindeki Üst Kretase-Tersiyer yaşlı sedimanter birimlerin mineralojisi ve jeokimyası. Türkiye Jeoloji Kurultayı Bülteni, 6, p. 234-252.

Bozkaya, Ö., Yalçın, H., 1991b, An approach to the Upper Cretaceous-Tertiary transition by using clay and carbonate mineralogy, Malatya-Hekimhan province, Eastern Turkey. Proc. 7th Euroclay Conf. Dresden, Greifswald, p. 141-146.

Bozkaya, Ö., Yalçın, H., 1992, Hekimhan havzası (Kuzeybatı Malatya) Üst Kretase-Tersiyer istifinin jeolojisi. TPJD Bülteni, 4/I, p. 59-80.

Bramlette, M. N., Martini, E., 1964, The great change in calcareous nanoplankton fossils between Maestrichtian and Danian, Micropaleontology, 10, p. 291-322.

Bronnimann, P., 1952, Globigerinidae from the Upper Cretaceous (Cenomanian-Maestrichtian) of Trinidad, B.W.I. Bull. Am. Paleontol., 34, p. 1-70.

Brönnimann, P., and Brown, N., 1956, Taxonomy of the Globotruncanidae, Eclogae Geol. Helv., 48, p. 503-561.

Brönnimann, P., Brown, N. K. Jr., 1953, Observations on some planktonic Heterohelicidae from the Upper Cretaceous of Cuba. Contributions from the Cushman Foundation for Foraminiferal Research, 4, p. 150-156.

Brotzen, F., 1936, Foraminiferen aus dem Schwedischen, Untersten Senon von Eriksdal in Schonen, Sveriges Geologiska Undersokning Ârsbok, 30, p. 1-69.

Brugger, J., Feulner G., and Petri S., 2016, Baby, it’s cold outside: Climate model simulations of the effects of the asteroid impact at the end of the Cretaceous, Geophysical Research Letters, 44, doi:10.1002/2016GL072241.

Caron, M., 1985, Cretaceous planktic foraminifera, *In* Bolli H. M., Saunders J. B., Perch-Nielsen, K. (eds.). Plankton Stratigraphy. Cambridge University Press, London, 1032 p.

Carsey, D. O., 1926, Foraminifera of the Cretaceous of Central Texas, University of Texas Bulletin, 2612, p. 1-56.

Chaput, E., 1932, Observations géologiques en Asie Mineure: Le Crétacé supérieur dans l'Anatolie Centrale. C. R. A. S., 194, p. 1960-1961.

Chaput, E., 1935a, L'Eocene du plateau de Galatie (Anatolie Centrale). C. R. A. S., 200, p. 767-768.

Chaput, E., 1935b, Les plissements Tertiare de l'Anatolie Centrale. C. R. A. S., 201, p. 1404-1405.

Chaput, E., 1936, Voyages d'études géologiques et géomorphologiques en Turquie. Mém. Inst. Françaiş D'Archaéo. İstanbul, II, 312 p.

Coccioni R., Premoli-Silva I., 2015, Revised Upper Albian-Maastrichtian planktonic foraminiferal biostratigraphy and magneto-stratigraphy of the classical Tethyan Gubbio section (Italy), Newsletters on Stratigraphy, 48, p. 47-90.

Courtillot, V., and Fluteau, F., 2014, A review of the embedded time scales of flood basalt volcanism with special emphasis on dramatically short magmatic pulses, *In* Keller, G., and Kerr, A.C., (eds.), Volcanism, Impacts, and Mass Extinctions: Causes and Effects: Geological Society of America Special Paper 505, doi:10.1130/2014.2505(15).

Cushman, J. A., 1938. Cretaceous species of *Gümbelina* and related genera. Contributions from the Cushman Laboratory for Foraminiferal Research, 14, p. 2–28.

Cushman, J. A., 1926, The foraminifera of the Velasco Shale of the Tampico Embayment. American Association of Petroleum Geologists Bulletin, 10, p. 581-612.

De Rijk, S., Troelstra, S. R., Rohling, E. J., 1999, Benthic Foraminiferal Distribution in the Mediterranean Sea, Journal of Foraminiferal Research, v. 29, p. 93-103.

Dickinson, W. R., and Seely, D. R., 1979, Structure and stratigraphy of fore-arc regions, American Association of Petroleum Geologists Bulletin, 63, p. 2-31.

Dizer, A., 1964, Sur quelques alveolines de l'Eocene de Turquie. Revue de Micropaléontologie, 7, p. 265-279.

Dizer, A., 1968, Etude micropaléntologique du nummulitique de Haymana (Turquie). Revue de Micropaléontologie, 11, p. 13-21.

Dizer, A., Meriç, E., 1981, Kuzeybati Anadolu'da Üst Kretase-Paleosen Biyostratigrafisi. MTA Bülteni, 95-96, p. 149-163.

D'Orbigny, A. D., 1839, Foraminiferes. *In* de la Sagra, R., (ed.), Histoire Physique, Politique et Naturelle de I'He de Cuba, Bertrand (Paris).

Douglas, R. G., Savin, S. M., 1978, Oxygen isotopic evidence for the depth stratification of Tertiary and Cretaceous planktonic foraminifera, Marine Micropaleontology, 3, p. 175-196.

Douglas, R. G,, 1969, Upper Cretaceous Planktonic Foraminifera in Northern California. Part 1 – Systematics, Micropaleontology, 15, p. 151-209.

Egger, J. G., 1899, Foraminiferen und Ostrakoden aus den Kreidemergeln der Oberbayerischen Alpen. Abhandlungen der Mathematisch-Physikalischen Klasse der Königlich Bayerischen Akademie der Wissenschaften, 21, p. 3-230. [published in 1902].

Ehrenberg, C. G., 1841 [1843], Verbreitung und Einflufs des mikroscopischen Le bens in Süd— und Nord- Amerika. Abhandlungen der Königlichen Akademie der Wissenschaften zu Berlin, p. 291-445.

Ehrenberg, C. G., 1854, Mikrogeologie, Leipzig: L. Voss, 374 p.

El Naggar, Z. R., 1966, Stratigraphy and planktonic foraminifera in the Upper Cretaceous-lower Tertiary succession in the Esna-Idfu region, Nile Valley, Egypt, U.A.R. London Br. Mus. (Nat. Hist). Bull. Geol., Suppl., 2, p. 1-291.

El-Nakhal, H. A., 1988, Planktonic foraminifers from the Palestinian Judea Group (Cretaceous) and their biostratigraphic significance, J. Univ. Kuwait (Sci.), 15, p. 359-371.

Erdoğan, B., 1990, İzmir-Ankara Zonu İle Karaburun Kuşağının Tektonik İlişkisi, MTA Dergisi, 110, p. 1-15.

Eshet, Y., Moshkovitz, S., Habib, D., Benjamini, C., Magaritz, M., 1992, Calcareous nannofossil and dinoflagellate stratigraphy across the Cretaceous-Tertiary boundary at Hor Hahar, Israel, Mar. Micropaleontol. 18, p. 199-228.

Esker, G. C., 1968, A new species of *Pseudoguembelina* from the Upper Cretaceous of Texas. Contributions from the Cushman Foundation for Foraminiferal Research, 19, p. 168-169.

Esmeray, S., 2008, Cretaceous/Paleogene Boundary in the Haymana Basin, Central Anatolia, Turkey: Micropaleontological, Mineralogical and Sequence Stratigraphic Approach, M.Sc. Thesis, Middle East Technical University, 271 p.

Esmeray-Senlet, S., Özkan-Altiner, S., Altiner, D., Miller, K. G., 2015, Planktonic foraminiferal biostratigraphy, microfacies analysis and sequence stratigraphy across the Cretaceous/Paleogene boundary in the Haymana Basin, Central Anatolia, Turkey, J. Sediment. Res., 85, p. 489–508, doi:10.2110/jsr.2015.31.

Eternod Olvera, Y., 1959, Foraminiferos del Cretacico superior de la Quenca de Tampico-Tuxpan, Mexico, Boletin de la Asociacion Mexicana de Geologos Petroleros, 11, 63-134.

Falzoni, F., Petrizzo, M. R., Huber, B. T., and MacLeod, K. G., 2014, Insights into the meridional ornamentation of the planktonic foraminiferal genus *Rugoglobigerina* (Late Cretaceous) and implications for taxonomy, Cretaceous Research, v. 47, p. 87–104.

Farouk, S., 2014, Maastrichtian carbon cycle changes and planktonic foraminiferal bioevents at Gebel Matulla, west-central Sinai, Egypt, Cretaceous Research, 50, p. 238-251.

Galeotti, S., Brinkhuis, H., and Huber, M., 2004, Records of post Cretaceous-Tertiary boundary millennial-scale cooling from the western Tethys: A smoking gun for the impact-winter hypothesis? Geology, 32, p. 529–532, doi:10.1130/G20439.1.

Gandolfi, R., 1955, The genus *Globotruncana* in northeastern Colombia. Bull. Am. Paleontol., 36, p. 7-118.

Gardin, S., Monechi, S., 1998, Palaeoecological change in middle to low latitude calcareous nanoplankton at the Cretaceous/Tertiary boundary, Bull. Soc. Geol. France, 169, p. 709-723.

Georgescu, M. D., 2005, On the systematics of rugoglobigerinids (planktonic Foraminifera, Late Cretaceous), Studia Geologica Polonica, 124, p. 87-97.

Georgescu, M. D., 2006, Santonian-Campanian planktonic foraminifera in the New Jersey coastal plain and their distribution related to the relative sea-level changes, Can. J. Earth Sci., 43, p. 101-120.

Georgescu, M. D., 2012, Restudy of the type specimens of Phanerostomum asperum Ehrenberg 1854 (Late Cretaceous, Foraminiferida), Micropaleontology, 58, p. 291-303.

Georgescu, M. D., 2013, Revised evolutionary systematics of the Cretaceous planktic foraminifera described by C.G. Ehrenberg, Micropaleontology, 59, p. 1-49.

Georgescu, M. D., 2014a, Reinstatement of the Cretaceous Planktic Foraminifer *Bronnimannella* Montanaro Gallitelli 1956 As Directional Lineage in Evolutionary Classification, *In* Evolutionary Classification and English-Based Nomenclature in Cretaceous Planktic Foraminifera, Georgescu, M. D., Henderson, C. M., (eds.), New York: Nova Science Publishers, p. 27-38.

Georgescu, M. D., 2014b, New Late Cretaceous (Santonian-Maastrichtian) Heterohelicid Planktic Foraminifera from the Pacific and Indian Oceans and Their Biostratigraphic and Evolutionary Significance, *In* Evolutionary Classification and English-Based Nomenclature in Cretaceous Planktic Foraminifera, Georgescu, M.D., Henderson, C.M., (eds.), New York: Nova Science Publishers, p. 39-72.

Georgescu, M. D., 2014c, Taxonomic Revision of *Planoglobulina* Cushman 1927 As Directional Lineage in Evolutionary Classification, *In* Evolutionary Classification and English-Based Nomenclature in Cretaceous Planktic Foraminifera, Georgescu, M. D., Henderson, C. M., (eds.), New York: Nova Science Publishers, p. 73-92.

Georgescu, M. D., Abramovich, S., 2009, A new Late Cretaceous (Maastrichtian) serial planktic foraminifer (Family Heterohelicidae) with early planispiral coil and revision of *Spiroplecta* Ehrenberg, 1844, Geobios, 42, p. 687-698.

Georgescu, M. D., Arz, J. A., Macauley, R. V., Kukulski, R. B., Arenillas, I., Perez-Rodriguez, I., 2011, Late Cretaceous (Santonian-Maastrichtian) serial foraminifera with pore mounds or pore mound-based ornamentation structures, Revista Española de Micropaleontología, 43, p. 109-139.

Georgescu, M. D., Saupe, E. E., Huber, B. T., 2008, Morphometric and stratophenetic basis for phylogeny and taxonomy in Late Cretaceous gublerinid planktonic foraminifera, Micropaleontology, 54, p. 397-424. (published in 2009)

Gökçen, S. L., 1976, Haymana güneyinin sedimentolojik incelemesi. I. Stratigrafik birimler ve tektonik. Yerbilimleri, 2, p. 161-201.

Görmüş, M., Karaman, E., 1992, Facies changes and new stratigraphical data in the Cretaceous – Tertiary boundary around Söbüdağ (Çünür – Isparta). Geosound, 21, p. 43- 57.

Görür, N., Oktay, F. Y., Seymen, İ., Şengör, A. M. C., 1984. Paleotectonic evolution of the Tuzgölü Basin complex, central Turkey: Sedimentary record of the neo-tethyan closure, *In* Dixon, J., and Robertson, A. H. F., (eds.), The Geological Evolution of the Eastern Mediterranean. Spec. Pub. 17, Geol. Soc. London, p. 467-481.

Govindan, A., 1972, Upper Cretaceous planktonic foraminifera from the Pondicherry area, south India, Micropaleontology, 19, p. 160-193.

Güray, A, 2006, Campanian-Maastrichtian planktonic foraminiferal investigation and biostratigraphy (Kokaksu section, Bartın, NW Anatolia): remarks on the Cretaceous paleoceanography based on quantitative data. M.Sc. Thesis (unpublished), Middle East Technical University, 244 p.

Hallock, P., 1985, Why are larger Foraminifera large?, Paleobiology, v. 11, p. 195–208.

Haynes, S. J., Huber, B. T., MacLeod, K. G., 2015, Evolution and phylogeny of Mid-Cretaceous (Albian-Coniacian) biserial planktic foraminifera, Journal of Foraminiferal Research, 45, p. 42-81.

Hildebrand-Habel, T., Williems, H., Versteegh, G.J.M., 1999, Variations in calcareous dinoflagellate associations from the Maastrichtian to Middle Eocene of the western South Atlantic Ocean (Sâo Paulo Plateau, DSDP Leg 39, Site 356). Rev. Palaeobot. Palynol. 106, p. 57 –87.

Hofker, J., 1958, Les Foraminifères du Crétacé supérieur de Glons, Annales de la Société Géologique de Belgique, 81, p. 467-493.

Hubbard D, Herman J, and Bell P., 1990, Speleogenesis in a travertine scarp: observations of sulphide oxidation in the subsurface, *In* Herman J, Hubbard D, editors: Travertine-marl: Streamdeposits in Virginia. Pub 101. Charlottesville, VA. Virginia Division of Mineral Resources, p. 177-184.

Huber, B. T., 1988a, Upper Campanian-Paleocene foraminifera from the James Ross Island region (Antarctic Peninsula). *In* Feldmann, R. M., and Woodburne, M. O., (eds.), Geology and Paleontology of Seymour Island, Antarctica. Geol. Soc. Am., Mem. Sen, 169, p. 163-251.

Huber, B. T., 1990, Maestrichtian Planktonic Foraminifer Biostratigraphy of the Maud Rise (Weddell Sea, Antarctica): ODP Leg 113 Holes 689B and 690C, Proceedings of the Ocean Drilling Program, Scientific Results, 113, p. 489-513.

Huber, B., MacLeod, K. G., Tur N. A., 2008, Chronostratigraphic Framework for Upper Campanian-Maastrichtian Sediments on the Blake Nose (Subtropical North Atlantic), Journal of Foraminiferal Research, 38, p. 162-182.

Hüseynov, A., 2007, Sedimentary cyclicity in the Upper Cretaceous successions of the Haymana Basin (Turkey): depositional sequences as response to relative sea-level changes. M.Sc. Thesis, Middle East Technical University, 120 p.

İnan, N., Temiz, H., 1992, Niksar (Tokat) yöresinde Kretase/Tersiyer geçişinin litostratigrafik ve biyostratigrafik özellikleri. Türkiye Jeoloji Bülteni, 35, p. 39-47.

İnan, N., 1995, The importance of the genus *Laffitteina* (Foraminifera) at the Cretaceous/Tertiary transition. International Symposium on the Geology of the Black Sea Region, Ankara, p. 109–118.

İnan, N., İnan, S., Kurt, İ., 1999, Doğu Pontidler'de uyumlu bentik K/T geçişi: Tonya formasyonunun (GB Trabzon) Şahinkaya üyesi. Türkiye Jeoloji Bülteni, 42/2, p. 63-67.

İnan., N., Tasli, K., İnan, S., 2005, *Laffitteina* from the Maastrichtian-Paleocene shallow carbonate successions of the Eastern Pontides (NE Turkey): biozonation and microfacies, Journal of Asian Earth Sciences, 25, p. 367-378.

Kaya, M., 1997, Niksar –Tokat yöresindeki Üst Kretase – Paleosen yaşlı Kırandağ ve Düdenyaylası formasyonlarının foraminifer içeriği. Türkiye Jeoloji Bülteni, 40/2, p. 85-100.

Kaya Özer, C., Toker, V., 2009, Akveren Formasyonu'nun Kampaniyen-Maastrihtiyen planktonik foraminifer biyostratigrafisi (Bartın, Batı Karadeniz). Yerbilimleri 30(3), p. 213–233.

Kaya Özer, C., Toker, V., 2012, Calcareous nannoplankton biostratigraphy of the Bartin Province, Western Black Sea, Turkey. Acta Geol Sin Eng Edition 86(6), p. 1434–1446.

Kaya Özer, C., Cakir, K., 2015, Planktonic foraminiferal biostratigraphy of the Campanian-Ypresian in the İzmit Province, Kocaeli Peninsula, Turkey, Arab J. Geosci. 8, p.11203–11237, doi 10.1007/s12517-015-1976-3.

Kaya Özer, C., 2017, Maastrichtian-Selandian planktonic foraminifera biostratigraphy and paleaeoecological interpretation of Akveren Formation in Bartın area (Western Black Sea, Turkey), Bull. Min. Res. Exp., 154, p. 83–107.

Keller, G., 1988, Extinction, survivorship and evolution of planktic foraminifera across the Cretaceous/Tertiary boundary at El Kef Tunisia. Marine Micropaleontology, 13, p. 239–263.

Keller, G., Barrera, E., Schmitz, B., and Mattson, E., 1993, Gradual mass extinction, species survivorship, and long-term environmental changes across the Cretaceous-Tertiary boundary in high latitudes, Geological Society of America Bulletin, 105, p. 979-997.

Keller, G., Li, L., MacLeod N., 1995, The Cretaceous/Tertiary boundary Stratotype section at El Kef, Tunisia: how catastrophic was the mass extinction? Palaeogeogr. Palaeoclimatol. Palaeoecol., 119, p. 221-254.

Keller, G., Adatte, T., Stinnesbeck, W., Stüben, D., Berner, Z., 2001, Age, chemo- and biostratigraphy of Haiti spherule-rich deposits: a multi-event K-T scenario, Can. J. Earth Sci., 38, p. 197-227.

Keller, G., 2002, *Guembelitria*-dominated late Maastrichtian planktic foraminiferal assemblages mimic early Danian in central Egypt, Marine Micropaleontology, 47, p. 71-99.

Keller, G., Adatte, T., Stinnesbeck, W., Luciani, V., Karoui, N., and Zaghbib-Turki, D., 2002a, Paleoecology of the Cretaceous-Tertiary mass extinction in planktic foraminifera, Palaeogeogr. Palaeoclimatol. Palaeoecol., v. 178, p. 257–297, doi:10.1016/S0031-0182(01)00399-6.

Keller, G., Adatte, T., Stinnesbeck, W., Luciani, V., Karoi-Yaakoub, N., Zaghbib-Turki, D., 2002, Paleoecology of the Cretaceous-Tertiary mass extinction in planktonic foraminifera, Palaeogeogr. Palaeoclimatol. Palaeocol., 178, p. 257-297.

Keller G., Pardo, A., 2004b, Disaster opportunist Guembelitrinidae: index for environmental catastrophes, Marine Micropaleontology, 53, p. 83-116.

Keller, G., Abramovich, S., Berner, Z., Adatte, T., 2009, Biotic effects of the Chicxulub impact, K-T catastrophe and sea level change in Texas, Palaeogeogr. Palaeoclimatol. Palaeocol., 271, p. 52-68.

Keller, G., Abramovich, S., Adatte, T., and Berner, Z., 2011, Biostratigraphy, age of Chicxulub impact, and depositional environment of the Brazos River KTB sequences, *In* Keller, G., Adatte, T., (eds.), End-Cretaceous Mass Extinction and the Chicxulub Impact in Texas SEPM Special Publication No. 100, p. 81-122.

Keller, G., Khozyem, H., Adatte, T., Malarkodi, N., Spangenberg, J. E., and Stinnesbeck, W., 2013, Chicxulub impact spherules in the North Atlantic and Caribbean: age constraints and Cretaceous-Tertiary boundary hiatus, Geological Magazine, 150, p. 885-907.

Keller, G., 2014, Deccan volcanism, the Chicxulub impact, and the end-Cretaceous mass extinction: Coincidence? Cause and effect?, *In* Keller, G., and Kerr, A .C., (eds.), Volcanism, Impacts, and Mass Extinctions: Causes and Effects: Geological Society of America Special Paper 505, p. 57–89, doi:10.1130/2014.2505(03).

Keller, G., Punekar J., and Mateo P., 2016, Upheavals during the Late Maastrichtian: Volcanism, climate and faunal events preceding the end-Cretaceous mass extinction, Palaeogeogr. Palaeoclimatol. Palaeocol., 441, 137-151.

Kikoine, J., 1948, Les Heterohelicidae du Cretace superieur pyreneen. Bulletin de le Societe Geologique de France, Serie 5e, 18(1), p. 15-35.

Klasz, I. de, 1953, On the Foraminiferal Genus *Gublerina* Kikoine, Geologica Bavarica, 17, p. 245-251.

Koçyiğit, A., 1991, An example of an accretionary forearc basin from Central Anatolia and its implications for the history of subduction of Neo-Tethys in Turkey. Geological Society of American Bulletin, 103, p. 22-36.

Koçyiğit, A., Özkan, S., Rojay, B., 1988, Examples of the forearc basin remnants at the active margin of northern Neo-Tethys: development and emplacement ages of the Anatolian Nappe, Turkey, Middle East Technical University Journal of Pure and Applied Sciences, 3, p. 183-210.

Korchagin, O. A., 2011, Upper Campanian-Lower Maastrichtian Planktonic Foraminifers and Biostratigraphy of the Moni Formation, Southern Cyprus, Stratigraphy and Geological Correlation, 19, p. 526-544.

Krasheninnikov, V. A., and Basov, I. A., 1983, Stratigraphy of Cretaceous sediments of the Falkland Plateau based on planktonic foraminifers, Deep Sea Drilling Project, Leg 11, *In* Ludwig, W J., Krasheninnikov, V. A., et al., Init. Repts. DSDP, 71, Washington (U.S. Govt. Printing Office), p. 789-820.

Kring, D. A., 2000, Impact-induced hydrothermal activity and potential habitats for thermophilic and hyperthermophilic life, *In* Catastrophic Events and Mass Extinctions: Impact and Beyond, LPI Contribution 1053, p. 106–107. Lunar and Planetary Institute, Houston.

Kring, D. A., 2007, The Chicxulub impact event and its environmental consequences at the Cretaceous-Tertiary boundary. Palaeogeogr. Palaeoclimatol. Palaeoecol., 255 (1-2), p. 4–21.

Kroon, D., Nederbragt, A. J., 1990, Ecology and Paleoecology of Triserial Planktic Foraminifera, Marine Micropaleontology, 16, p. 25-38.

Lamolda, M. A., Melinte, M. C., Kaiho, K., 2005. Nannofloral extinction and survivorship across the K –Pg boundary at Caravaca, southeastern Spain. Palaeogeogr. Palaeoclimatol. Palaeoecol., 224, p. 27 –52.

Lamolda, M. A., Melinte-Dobrinescu, M. C., Kaiho, K., 2015, Calcareous nanoplankton assemblage changes linked to paleoenvironmental deterioration and recovery across the Cretaceous-Paleogene boundary in the Betic Cordillera (Agost, Spain), Palaeogeogr. Palaeoclimatol. Palaeoecol., 441, p. 438-452.

Li, L., Keller, G., 1998a, Maastrichtian climate, productivity and faunal turnovers in planktic foraminifera in South Atlantic DSDP sites 525A and 21. Marine Micropaleontology 33, p. 55-86.

Li, L., Keller, G., 1998b, Maastrichtian climate, productivity and faunal turnovers in planktonic foraminifera in South Atlantic DSDP sites 525A and 21, 33, p. 55-86.

Lirer, F., 2000, A new technique for retrieving calcareous microfossils from lithified lime deposits. Micropaleontology 46, 365–369.

Liu, C., 1993, Uppermost Cretaceous-Lower Paleocene stratigraphy and turnover of planktonic foraminifera across the Cretaceous/ Paleogene boundary, PhD Thesis, Rutgers University, New Brunswick, NJ, USA.

Loeblich Jr., A. R., 1951, Coiling in the Heterohelicidae. Contributions from the Cushman Foundation for Foraminiferal Research, 2, p. 106–110.

Lokman, K., Lahn, D., 1946, Haymana bölgesi jeolojisi. MTA Bülteni, 36, p. 292-300.

Luciani, V., 2001, High-resolution planktonic foraminiferal analysis from the Cretaceous-Tertiary boundary at Ain Settara (Tunisia): evidence of an extended mass extinction, Palaeogeogr. Palaeoclimatol. Palaeocol., 178, p. 299-319.

Luterbacher, H. P., Premoli-Silva, I., 1964, Biostratigrafia del limite cretaceo–terziario nell'Appennino centrale. Rivista Italiana di Paleontologia, 70, p. 67–117.

MacLeod, N., and Keller, G., 1994, Comparative biogeographic analysis of planktic foraminiferal survivorship across the Cretaceous/Tertiary (K/T) boundary, Paleobiology, v. 20, p. 143-177.

MacLeod, N., 2014, The geological extinction record: History, data, biases, and testing, *In* Keller, G., and Kerr, A.C., (eds.), Volcanism, Impacts, and Mass Extinctions: Causes and Effects: Geological Society of America Special Paper 505, p. 1–28, doi:10.1130/2014.2505(01).

Martin, S. E., 1972, Reexamination of the Upper Cretaceous planktonic foraminiferal genera Planoglobulina Cushman and Ventilabrella Cushman. Journal of Foraminiferal Research, 2, p. 73-92.

Masters, B. A., 1976, Planktic foraminifera from the Upper Cretaceous Selma Group, Alabama, Journal of Paleontology, 50, p. 318-330.

Masters, B. A., 1984, Comparison of planktonic foraminifers at the Cretaceous-Tertiary boundary from the El Haria shale (Tunisia) and the Esna shale (Egypt), *In* Proceedings of the 7th Exploration Seminar, March 1984: Cairo, Egyptian General Petroleum Corporation, p. 310-324.

Mateo, P., Keller, G., Adatte, T., Spangenberg, J. E., 2016, Mass wasting and hiatuses during the Cretaceous-Tertiary transitions in the North Atlantic: Relationship to the Chicxulub impact?, Palaeogeogr. Palaeoclimatol. Palaeocol., 441, p. 96-115.

Meilijson, A., Ashckenazi-Polivoda, S., Ron-Yankovich, L., Illner, P., Alsenz, H., Speijer, R. P., Almogi-Labin, A., Feinstein, S., Berner, Z., Püttmann, W.,

Abramovich, S., 2014, Chronostratigraphy of the Upper Cretaceous high productivity sequence of the southern Tethys, Israel, Cretaceous Research, 50, p. 187-213.

Meriç E., and Şengüler İ., 1986, New observations on the stratigraphy of Upper Cretaceous-Paleocene around Göynük (Bolu, northwest Anatolia). Jeoloji Mühendisligi, 29, p. 61-64 [in Turkish].

Meriç, E., İnan., N., 1998, *Sirelina orduensis* (foraminifera) a new genus and species from the Maastrichtian of Northeast Anatolia (Gölköy-Ordu), Micropaleontology, 44, p. 195-200.

Meriç, E., Oktay, F. Y., Toker, V., Tansel, İ., Duru, M., 1987, Adıyaman yöresi Üst Kretase- Eosen istifinin sedimanter jeolojisi ve biyostratigrafisi (foraminifer, nannoplankton ostrakod). Türkiye Jeoloji Bülteni, 30, p. 19-32.

Miller, K. G., Sherrell, R. M., Browning, J. V., Field, M. P., Gallagher, W., Olsson, R. K., Sugarman, P. J., Tuorto, S., and Wahyudi, H., 2010, Relationship between mass extinction and iridium across the Cretaceous-Paleogene boundary in New Jersey, Geology, 38, p. 867-870.

Molina E., Arenillas I., and Arz A. J., 1998, Mass extinction in planktic foraminifera at the Createceous/Tertiary boundary in subtropical and temperate latitudes, Bull. Soc. Geol. France, p. 351-363.

Molina, E., Alegret, L., Arenillas, I., Arz, J. A., Gallala, N., Hardenbol, J., Von Salis, K., Steurbaut, E., Vandenbeghe, N., Zaghbib-Turki, D., 2006, The Global Boundary Stratotype Section and Point for the base of the Danian Stage (Paleocene, Paleogene, "Tertiary," Cenozoic) at El Kef, Tunisia: original definition and revision. Episodes 29(4), p. 263–273.

Molina, E., Arenillas, I., Arz, J. A., 1996, The Cretaceous/Tertiary boundary mass extinction in planktic foraminifera at Agost, Spain. Revue de Micropaleontologie, 39, p. 225– 243.

Nairn S. P., Robertson A H. F., Ünlügenç U. C., Tasli K., Inan N., 2013, Tectonostratigraphic evolution of the Cretaceous-Cenozoic central Anatolian basins:

an integrated study of diachronous ocean closure and continental collision. Geol. Soc. London Spec. Publ., 372, p. 343-384.

Nederbragt, A. J., 1989, Maastrichtian Heterohelicidae (Planktonic Foraminifera) from the Northwest Atlantic, J. micropaleontology, 8, p. 183-206.

Nederbragt, A. J., 1991. Late Cretaceous biostratigraphy and development of Heterohelicidae (planktic foraminifera). Micropaleontology, 37, 4, p. 329 –372.

Nederbragt, A. J., 1998, Quantitative biogeography of late Maastrichtian planktic foraminifera, Micropaleontology, 44, p. 385-412.

Ogg, J. G., Ogg, G. M., Gradstein, F. M., (Coordinators), 2016, A Concise Geologic Time Scale, Elsevier Publishing Company.

Okay, A. I., 1989, Tectonic Units and Sutures in the Pontides, Northern Turkey, *In* Şengör, A. M. C. (ed.) *Tectonic evolution of the Tethyan region.* Kluwer Academic Publications, Dordrecht, p. 109-115.

Okay, A. I., Altıner, D., 2016, Carbonate sedimentation in an extensional active margin: Cretaceous history of the Haymana region, Pontides, International Journal of Earth Sciences, 105 (7), p. 2013-2030.

Olsson, R. K., 1960, Foraminifera of Latest Cretaceous and Earliest Tertiary age in the New Jersey coastal plain, Journal of Paleontology, 34, p. 1-58.

Olsson, R. K., 1964, Late Cretaceous planktonic foraminifera from New Jersey and Delaware, Micropaleontology, 10, p. 157-188.

Olsson, R. K., Hemleben, C., Berggren, W. A., and Huber, B. T., 1999, Atlas of Paleocene planktonic foraminifera. Smithsonian Contributions to Paleobiology, 85, 252 p.

Orabi, O. H., Zahran, E., 2014, Paleotemperatures and paleodepths of the Upper Cretaceous rocks in El Qusaima, Northeastern Sinai, Egypt, Journal of African Earth Sciences, 91, p. 79-88.

Orbigny, A. d', 1840, Mémoire sur les foraminifères de la Craie Blanche du Basin de Paris. Mémoires de la Société Géologique de France, 4, p. 1-51.

Özcan, E., Özkan-Altıner, S., 1997, Late Campanian-Maastrichtian evolution of orbitoid foraminifera in Haymana basin succession (Ankara, Central Turkey). Revue de Paléobiologie, 16/1, p. 271-290.

Özcan, E., Özkan-Altıner, S. 1999, The genus *Lepidorbitoides* and *Orbitoides*: Evolution and stratigraphic significance in some Anatolian basins (Turkey). Geological Journal, 34/3, p. 275-286.

Özcan, Z., Okay, A. I., Özcan, E., Hakyemez, A., Özkan-Altıner, S., 2012, Late Cretaceous-Eocene Geological Evolution of the Pontides Based on New Stratigraphic and Palaeontologic Data Between the Black Sea Coast and Bursa (NW Turkey), Turkish J. Earth Sci., 21, p. 933-960.

Özer, S., Sözbilir, H., Özkar, İ., Toker, V., Sarı, B., 2001, Stratigraphy of Upper Cretaceous – Paleogene sequences in the southern and eastern Menderes Massif (western Turkey). Int. J. Earth Sciences, 89, p. 852-866.

Özkan, S., 1985, Maastrichtian planktonic foraminifera and stratigraphy of Germav Formation, Gercüş area, Southeast Turkey. M.Sc. Thesis, Middle East Technical University, 273 p.

Özkan, S., Altıner, D., 1987, Maastrichtian planktonic foraminifera from the Germav Formation in Gercüş area (SE Anatolia, Turkey), with notes on the suprageneric classification of globotruncanids. Revue de Paléobiologie, 6/2, p. 261–277.

Özkan-Altıner, S., Özcan, E., 1999, Upper Cretaceous planktonic foraminiferal biostratigraphy from NW Turkey: calibration of the stratigraphic ranges of larger benthonic foraminifera. Geological Journal, 34/3, p. 287-301.

Pardo A., Keller G., 2008, Biotic effects of environmental catastrophes at the end of the Cretaceous and early Tertiary: *Guembelitria* and *Heterohelix* blooms, Cretaceous Research, 29, p. 1058-1073.

Pardo, A., Ortiz, N., Keller, G., 1996, Latest Maastrichtian foraminiferal turnover and its environmental implications at Agost, Spain, in MacLeod, N., and Keller, G., (eds.), Cretaceous-Tertiary mass extinction: New York, W.W. Norton and Co., p. 139–172.

Perch-Nielsen, K., McKenzie, J., He, Q., 1982, Biostratigraphy and isotope stratigraphy and the 'catastrophic' extinction of calcareous nanoplankton at the Cretaceous/Tertiary boundary, Geol. Soc. Am. Spec. Pap., 190, p. 353-371.

Pérez-Rodríguez, I., Lees, J. A., Larrasoaña, J. C., Arz, J. A., Arenillas, I., 2012, Planktonic foraminiferal and calcareous nannofossil biostratigraphy and magnetostratigraphy of the uppermost Campanian and Maastrichtian at Zumaia, northern Spain, Cretaceous Research, 37, p. 100-126.

Peryt, D., 1980, Planktic foraminifera zonation of the Upper Cretaceous in the middle Vistula River Valley, Poland, Palaeontologia Polonica, 41, p. 3-101.

Pessagno, E. A. JR., 1960, Stratigraphy and micropaleontology of the Cretaceous and lower Tertiary of Puerto Rico, Micropaleontology, 6, p. 87-110.

Pessagno, E. A. JR.,1962, The Upper Cretaceous stratigraphy and micropaleontology of south-central Puerto Rico, Micropaleontology, 8, p. 349-368.

Pessagno, E. A. Jr., 1967, Upper Cretaceous planktonic foraminifera from the western Gulf coastal plain. Palaeontographica Americana, 5(37), p. 243-445.

Petrizzo, M. R., 2001, Late Cretaceous planktonic foraminifera from Kerguelen Plateau (ODP Leg183): new data to improve the Southern Ocean biozonation, Cretaceous Research, 22, p. 829-855.

Petrizzo, M. R., Berrocoso, A. J., Falzoni, F., Huber, B. T., and Macleod, K. G., 2017, The Coniacian – Santonian sedimentary record in southern (Ruvuma Basin, East Africa): Planktonic foraminiferal evolutionary, geochemical and palaeoceanographic patterns, Sedimentology, 64, p. 252-285.

Petrizzo, M. R., Francesca, F., Premoli Silva, I., 2011, Identification of the base of the lower-to-middle Campanian *Globotruncana ventricosa* Zone: Comments on reliability and global correlations, Cretaceous Research, 32, p. 387-405.

Plummer, H. J., 1926 [1927], Foraminifera of the Midway Formation in Texas. University of Texas Bulletin, 2644, p. 1-2.

Plummer, H. J., 1931, Some Cretaceous foraminifera in Texas, University of Texas Bureau of Economic Geology and Technology Bulletin, 3101, p. 109-203.

Pospichal, J. J., Wise, S. W. Jr., 1990, Paleocene to middle Eocene calcareous nannofossils of ODP Sites 689 and 690, Maud Rise, Weddell Sea. Proceedings of the Ocean Drilling Program, Scientific Results, 113, p. 613-638.

Premoli-Silva, I. and Sliter, W.V., 1995, Cretaceous Planktonic Foraminiferal Biostratigraphy & Evolutionary Trends from the Bottaccione Section, Gubbio, Italy. Palaeontographia Italica, 82, p. 1-89.

Premoli-Silva, I., Verga, D., 2004. Practical manual of Cretaceous Planktonic Foraminifera. International School on Planktonic Foraminifera, 3. Course: Cretaceous. Verga & Rettori (eds.) Universities of Perugia and Milan, Tipografia Pontefelcino, Perugia (Italy), 283 p.

Punekar, J., Keller, G., Khozyem, H. M., Adatte, T., Font, E., Spangenberg, J., 2016, A multi-proxy approach to decode the end-Cretaceous mass extinction, Palaeogeogr. Palaeoclimatol. Palaeocol., 441, p. 116-136.

Punekar, J., Mateo, P., and Keller G., 2014, Effects of Deccan volcanism on paleoenvironment and planktic foraminifera: A global survey, *In* Keller, G., and Kerr, A.C., (eds.), Volcanism, Impacts, and Mass Extinctions: Causes and Effects: Geological Society of America Special Paper 505, p. 1–28, doi:10.1130/2014.2505(01).

Raup, D. M., and Sepkoski, J. J., Jr., 1982, Mass extinctions in the marine fossil record: Science, v. 215, p. 1501–1503, doi: 10. 1126/science .215.4539.1501.

Reckamp, J., U., Özbey, S., 1960, Petroleum geology of Temelli and Kuştepe structures, Polatlı area. Pet. İş. Gen. Md., Ankara.

Renne, P. R., A. L. Deino, F. J. Hilgen, K. F. Kuiper, D. F. Mark, W. S. Mitchell, L. E. Morgan, R. Mundil, and J. Smit, 2013, Time scales of critical events around the Cretaceous-Paleogene boundary, Science, 339, p. 684–687.

Renne, P. R., Sprain, C. J., Richards, M. A., Self, S., Vanderkluysen L., and Pande K., 2015, State shift in Deccan volcanism at the Cretaceous-Paleogene boundary,

possibly induced by impact, Science, 350(6256), p. 76–78, doi:10.1126/science.aac7549.

Rigo de Righi, M., Cortesini, A., 1959, Regional studies in central Anatolian basin. Progress Report 1, Turkish Gulf Oil Co., Pet. İş. Gen. Md., Ankara.

Robaszynski, F., Caron, M., 1995, Foraminiferes planctoniques du Cretace: commentaire de la zonation Europe-Mediterranee, 6, p. 681-692.

Robaszynski, F., Caron, M., Gonzalez Donoso, J. M., Wonders, A. H. & The European Working Group on Planktonic Foraminifera, 1984, Atlas of Late Cretaceous globotruncanids. Revue de Micropaléontologie, 26, p. 145–305.

Robertson, A., Boulton, S. J., Taslı, K., Yıldırım, N., İnan, N., Yıldız, A., Parlak, O., 2015, Late Cretaceous-Miocene sedimentary development of the Arabian continental margin in SE Turkey (Adıyaman Region): implications for regional palaeogeography and the closure history of Southern Neotethys, Journal of Asian Earth Sciences, 115, p. 571-616.

Rojay, B., 2013, Tectonic evolution of the Cretaceous Ankara Ophiolitic Mélange during the Late Cretaceous to pre-Miocene interval in Central Anatolia, Turkey, J Geodyn, 65, p. 66–81.

Romein, A. J. T., 1979. Lineages in early Paleogene calcareous nannoplankton. Utrecht Micropaleontology Bulletin, 22, 231 p.

Saito, T., Van Donk, J., 1974, Oxygen and carbon isotope measurements of Late Cretaceous and Early Tertiary foraminifera, Micropaleontology, v. 20, p. 152-177.

Sarı, B., 2013, Late Maastrichtian-late Palaeocene planktic foraminiferal biostratigraphy of the matrix of the Bornova Flysch Zone around Bornova (Izmir, western Anatolia, Turkey). Turkish Journal of Earth Sciences 22, p. 143-171.

Sarıgül, V., Hakyemez, A., Tüysüz, O., Can Genç, Ş., Yılmaz İ. Ö., Özcan, E., 2017, Maastrichtian-Thanetian planktonic foraminiferal biostratigraphy and remarks on the K-Pg boundary in the southern Kocaeli Peninsula (NW Turkey), Turkish J. Earth Sci., 26, p. 1-29.

Schmidt, G. C., 1960, AR/MEM/365-266-367 sahalarının nihai terk raporu. Pet. İş. Gen. Md., Ankara.

Schulte, P., Alegret, L., Arenillas, I., Arz, J. A., Barton, P., Bown, P., Bralower, T. J., Christeson, G., Claeys, P., And Cockell, C., 2010, The Chicxulub asteroid impact and mass extinction at the Cretaceous–Paleogene boundary: Science, v. 327, p. 1214–1218.

Şengör, A. M. C., Yılmaz, Y., 1981, Tethyan evolution of Turkey: a plate tectonic approach, Tectonophysics, 75, p. 181-241.

Sirel, E., 1975, Polatlı (GB Ankara) güneyinin stratigrafisi. TJK Bülteni, 18/2, p. 181-192.

Sirel, E., 1976a. Polatlı (GB Ankara) güneyinde bulunan *Alveolina, Nummulites, Ranikothalia* ve *Assilina* cinslerinin baz ı türlerinin sistematik inclemeleri. TJK Bülteni, 19/2, p. 89-103.

Sirel, E., 1976b, Description of six new species of the *Alveolina* found in the South of Polatlı (SW Ankara) region. TJK Bülteni, 19, p. 19-22.

Sirel, E., 1976c, Haymana (G Ankara) yöresi İlerdiyen, Küiziyen ve Lütesiyen'deki *Nummulites, Assilina* ve *Alveolina* cinslerinin bazı türlerinin tanımlamaları ve stratigrafik dağılımları. TJK Bülteni, 19, p. 31-44.

Sirel, E., 1998, Foraminiferal description and biostratigraphy of the Paleocene-Lower Eocene shallow-water limestones and discussion on the Cretaceous-Tertiary boundary in Turkey. General Directorate of the Mineral Research and Exploration, Monography Series, 2, 117 p.

Sirel, E., Dağer, Z., Sözeri, B., 1986, Some biostratigraphic and paleogeographic observations on the Cretaceous-Tertiary boundary in the Haymana-Polatlı region (Central Turkey), *In* Walliser, O., (ed.) Global Bioevents. Lecture Notes in Earth Sciences, 8, p. 385-396.

Sliter, W. V., 1968, Upper Cretaceous foraminifera from Southern California and northwestern Baja California, Mexico, The University of Kansas Paleontological Contributions, 49, p. 1-141.

Sliter, W. V., 1972, Upper Cretaceous Planktonic Foraminiferal Zoogeography and Ecology-Eastern Pacific Margin, Palaeogeogr. Palaeoclimatol. Palaeoecol., 12, p. 15-31.

Sliter, W. V., 1977, Cretaceous foraminifera from the southwest Atlantic Ocean, Leg 36, Deep Sea Drilling Project, *In* Barker, P. F., Dalziel, I.W.D., et al., Init. Repts. DSDP, 36: Washington (U.S. Govt. Printing Office), p. 519-573.

Sliter, W. V., 1989, Biostratigraphic zonation for Cretaceous planktonic foraminifers examined in thin section, Journal of Foraminiferal Research, 19, p. 1-19.

Smit, J., 1982, Extinction and evolution of planktonic foraminifera after a major impact at the Cretaceous/Tertiary boundary. Geol. Soc. Am. Spec. Pap., 190, p. 329–352.

Smit, J., 2004, The section of the Barranco del Gredero (Caravaca, SE Spain): a crucial section for the Cretaceous/Tertiary boundary impact extinction hypothesis, Journal of Iberian Geology, 31, p. 179-191.

Smith, C. C. and Pessagno, E. A. Jr., 1973, Planktonic foraminifera and stratigraphy of the Corsicana Formation (Maestrichtian), north-central Texas, Cushman Foundation for Foraminiferal Research, Special Publications, 13, p. 5-68.

Solak C., Taslı, K., Sarı, B., 2015, Stratigraphy and depositional history of the Cretaceous carbonate successions in the Spil Mountain (Manisa, W Turkey), Cretaceous Research, 53, p. 1-18.

Strong, C. P., 2000, Cretaceous-Tertiary foraminiferal succession at Flaxbourne River, Marlborough, New Zealand, New Zealand Journal of Geology & Geophysics, 40, p. 1-20.

Tansel, İ., 1989, Ağva (İstanbul) yöresinde Geç Kretase – Paleosen sınırı ve Paleosen biyostratigrafisi. TPJD Bülteni, 1/3, p. 211-218.

Tantawy, A. A. A. M., 2003. Calcareous nannofossil biostratigraphy and paleoecology of the Cretaceous –Tertiary transition in the central eastern desert of Egypt. Mar. Micropaleontol. 47, p. 323-356.

Tilev, N., 1951, Etude des Rosalines maestrichtiennes (genre *Globotruncana*) du Sud-Est de la Turquie (sondage de Ramandag). Madan. Tetkik Arama Enst. Yayin., Seri. B, 16, p. 1-101.

Todd, R., 1970, Maestrichtian (Late Cretaceous) foraminifera from a deep-sea core off southwestern Africa. Rev. Esp. Micropaleontol, 2, p. 131-154.

Toker, V., 1975, Haymana yöresinin (SW Ankara) planktonik foraminifera ve nannoplanktonlarla biyostratigrafik incelenmesi. PhD. Thesis, Ankara Üniversitesi Fen Fakültesi, p. 1-57.

Toker, V., 1977, Haymana ve Kavak formasyonlarındaki planktonik foraminifera ve nannoplanktonlar. TBTAK VI. Bilim Kongresi, p. 57-70.

Toker, V., 1979, Haymana yöresi (GB Ankara) Üst Kretase planktonik foraminiferaları ve biyostratigrafi incelemesi. TJK Bülteni, 22, p. 121-132.

Toker, V., 1980, Haymana yöresi (GB Ankara) nannoplankton biyostratigrafisi. TJK Bülteni, 23/2, p. 165-178.

Toker, V., Sonel, N., Ayyıldız, T., Albayrak, M., 1993, Akseki Kuzeyi-Üzümdere (Antalya) Civarının Stratigrafisi, Geological Bulletin of Turkey, 36, p. 57-71.

Torsvik, T. H., Van der Voo, R., Preeden, U., Mac Niocaill, C., Steinberger, B., Doubrovine, P. V., van Hinsbergen, J. J., Domeier, M., Gaina, C., Tohver, E., Meert, J. G., McCausland, P. J. A., Cocks, L. R. M., 2012, Phanerozoic Polar Wander, palaeogeography and dynamics, Earth-Science Reviews, 114, p. 325–368.

Ünalan, G., Yüksel, V., Tekeli, T., Gönenç, O., Seyirt, Z., Hüseyin, S., 1976, Haymana-Polatlı yöresinin (Güneybatı Ankara) Üst Kretase-Alt Tersiyer stratigrafisi ve paleocoğrafik evrimi. TJK Bülteni, 19, p. 159-176.

Van der Zwaan, G. J., Jorissen, F. J., De Stigter, H. C., 1990, The depth dependency of planktonic/benthonic foraminiferal ratios: constraints and applications. Marine Geology, 95, p. 1–16.

Van Eijden, A. J. M., and Smit, J., 1991, Eastern Indian Ocean Cretaceous and Paleogene Quantitative Biostratigraphy, Proceedings of the Ocean Drilling Program, Scientific Results, 121, p. 77-125.

Van Hinsbergen, D. J. J., Kouwenhoven, T. J., van der Zwaan, G. J., 2005, Paleobathymetry in the backstripping procedure: Correction for oxygenation effects on depth estimates, Palaeogeogr. Palaeoclimatol. Palaeoecol., 221, p. 245-265.

Vellekoop, J., Sluijs A., Smit J., Schouten S., Weijers J. W. H., Sinninghe Damsté J. S., and Brinkhuis H., 2014, Rapid short-term cooling following the Chicxulub impact at the Cretaceous-Paleogene boundary, Proc. Natl. Acad. Sci. U.S.A., 111(21), p. 7537-7541, doi:10.1073/pnas.1319253111.

Vellekoop, J., Smit J., van de Schootbrugge B., Weijers J. W. H., Galeotti S., Sinninghe Damsté J. S., and Brinkhuis H., 2015, Palynological evidence for prolonged cooling along the Tunisian continental shelf following the K–Pg boundary impact, Paleogeography Paleoclimatology Paleoecology, 426, p. 216-228.

Weiss, W., 1983, Heterohelicidae (seriale planktonische Foraminiferen) der tethyalen Oberkreide (Santon bis Maastricht). Geologisches Jahrbuch, A72, p. 3-93.

White, M. P., 1928, Some index foraminifera of the Tampico Embayment area, Mexico. J. Paleontol., 2:177-215, p. 280-317.

Wright, C. A., and Apthorpe, M., 1976, Planktonic foraminiferids from the Maastrichtian of the northwest shelf, Western Australia, Journal of Foraminiferal Research,6, p. 228-241.

Yalçın, H., Bozkaya, Ö., 1996, A new discovery of the Cretaceous/Tertiary boundary from the Tethyan belt, Hekimhan Basin, Turkey: mineralogical and geochemical evidence. International Geology Review, 38, p. 759-767.

Yalçın, H., İnan, N., 1992a, Tecer formasyonunda (Sivas) Kretase-Tersiyer geçişine paleontolojîk, mineralojik ve jeokimyasal yaklaşımlar. Türkiye Jeoloji Bülteni, 35, p. 95-102.

Yalçın, H., İnan, N., 1992b, Paleontological features and mineralogical – geochemical changes of the Cretaceous/Tertiary transition at Iğdır formation, Koyulhisar – Sivas,

Turkey. Geosound, First International Symposium on Eastern Mediterranean Geology Special Issue, p. 39-55.

Yıldız, A., Toker, V., 1995, Gürün Yöresi (Sivas) Konakpınar formasyonu K/T sınırı. TJK Bülteni, 10, p. 11-24.

Yıldız, A., Gürel, A., 2005, Palaeontological, diagenetic and facies characteristics of Cretaceous/Paleogene boundary sediments in the Ordu, Yavuzlu and Uzunisa areas, Eastern Pontides, NE Turkey, 26, p. 329-341.

Yüksel, S., 1970, Etude géologique de la region d'Haymana (Turquie Centrale). Thèse Fac. Sci. Univ. De Nancy, p. 1-179.

Web Site References:

Chronos.org, Mesozoic and Paleocene Planktonic Foraminiferal Working Groups, Chronos Portal, Foraminiferal Databases, http://portal.chronos.org/gridsphere/gridsphere?cid=res_taxondb, accessed in July 2017.

APPENDIX

Plate 1

1. *Guembelitria cretacea* CUSHMAN, UH-50, 63-150 μm fraction, P0 Zone.

2. *Guembelitria cretacea* CUSHMAN, UH-45, 63-150 μm fraction, *P. hantkeninoides* Zone.

3. *Guembelitria cretacea* CUSHMAN, UH-48, 63-150 μm fraction, *P. hantkeninoides* Zone.

4. *Guembelitria cretacea* CUSHMAN, UH-48, 63-150 μm fraction, *P. hantkeninoides* Zone.

5. *Guembelitria cretacea* CUSHMAN, UH-48, 63-150 μm fraction, *P. hantkeninoides* Zone.

6. *Guembelitria cretacea* CUSHMAN, top view, UH-45, 63-150 μm fraction, *P. hantkeninoides* Zone.

7. *Guembelitria cretacea* CUSHMAN, top view, UH-48, 63-150 μm fraction, *P. hantkeninoides* Zone.

8. *Guembelitria cretacea* CUSHMAN, top view, UH-48, 63-150 μm fraction, *P. hantkeninoides* Zone.

9. *Guembelitria cretacea* CUSHMAN, close-up view of fig. 6, 63-150 μm fraction, P. *hariaensis* Zone.

Plate 1

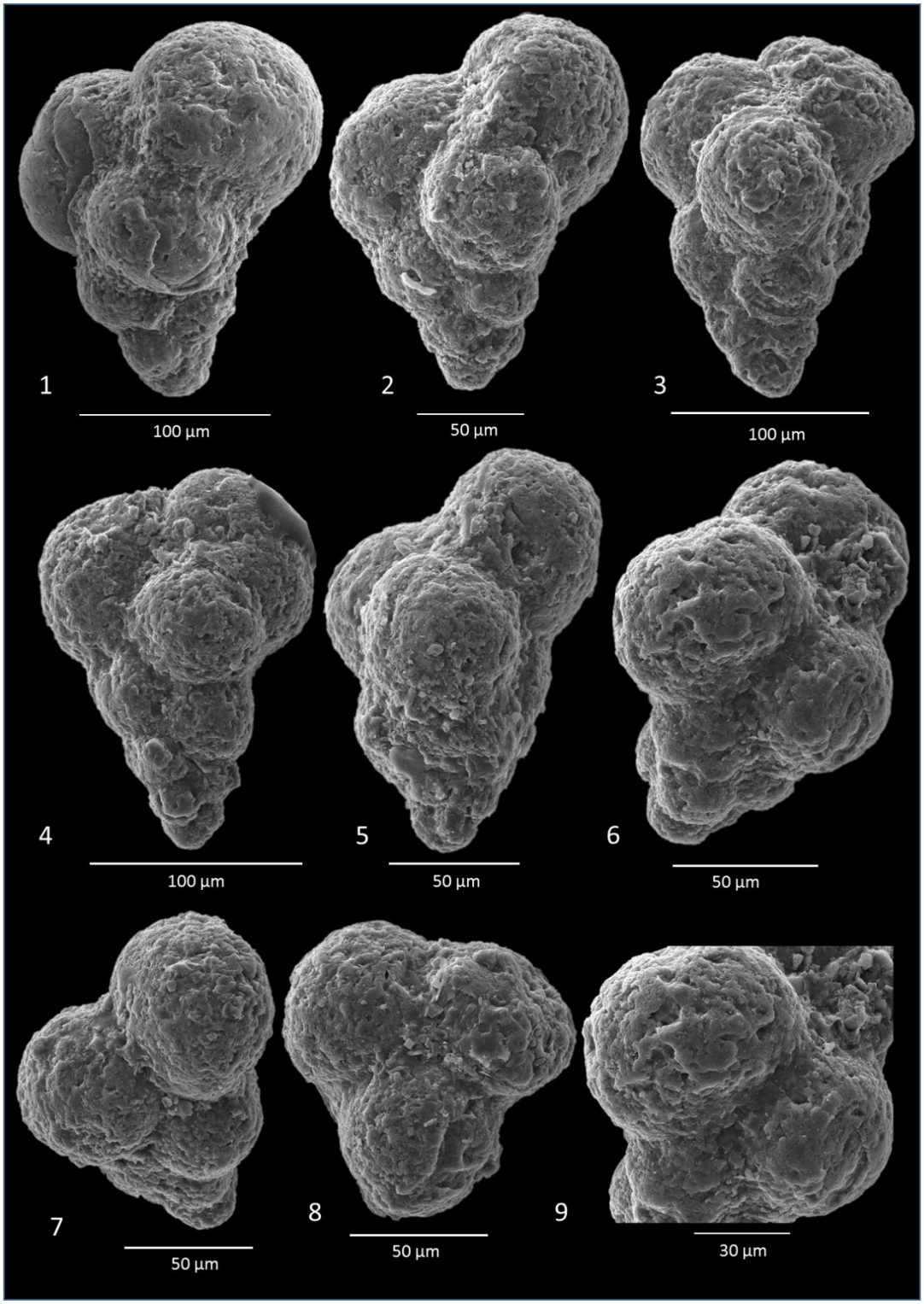

Plate 2

1. *Parvularugoglobigerina eugubina* LUTERBACHER and PREMOLI-SILVA, spiral view, UKHB-4, 63-150 μm fraction, *P. eugubina* Zone.

2. *Parvularugoglobigerina eugubina* LUTERBACHER and PREMOLI-SILVA, spiral view, UKHB-4, 63-150 μm fraction, *P. eugubina* Zone.

3. *Parvularugoglobigerina eugubina* LUTERBACHER and PREMOLI-SILVA, spiral view, UKHB-4, 63-150 μm fraction, *P. eugubina* Zone.

4. *Parvularugoglobigerina eugubina* LUTERBACHER and PREMOLI-SILVA, spiral view, UKHB-5, 63-150 μm fraction, *P. eugubina* Zone.

5. *Parvularugoglobigerina eugubina* LUTERBACHER and PREMOLI-SILVA, spiral view UKHB-4, 63-150 μm fraction, *P. eugubina* Zone.

6. *Parvularugoglobigerina eugubina* LUTERBACHER and PREMOLI-SILVA, spiral view, UKHB-4, 63-150 μm fraction, *P. eugubina* Zone.

7. *Parvularugoglobigerina eugubina* LUTERBACHER and PREMOLI-SILVA, umbilical view, UKHB-4, 63-150 μm fraction, *P. eugubina* Zone.

8. *Parvularugoglobigerina eugubina* LUTERBACHER and PREMOLI-SILVA, umbilical view, UKHB-5, 63-150 μm fraction, *P. eugubina* Zone.

9. *Parvularugoglobigerina eugubina* LUTERBACHER and PREMOLI-SILVA, umbilical view, UKHB-5, 63-150 μm fraction, *P. eugubina* Zone.

Plate 2

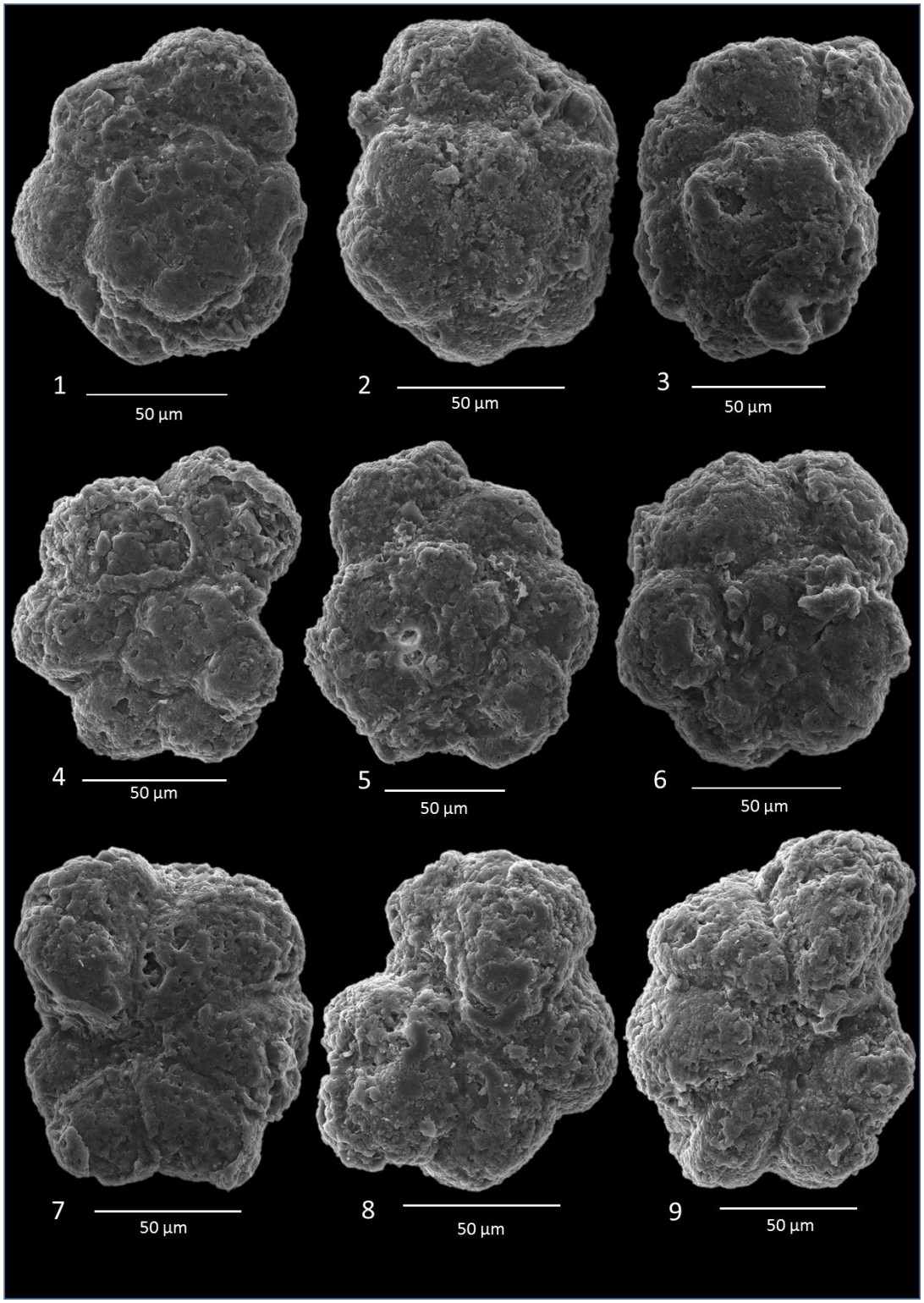

Plate 3

1. *Heterohelix globulosa* EHRENBERG, side view, UH-38, >150 µm fraction, *P. hantkeninoides* Zone.

2. *Heterohelix globulosa* EHRENBERG, side view, UH-33, >150 µm fraction, *P. hantkeninoides* Zone.

3. *Heterohelix globulosa* EHRENBERG, side to edge view, UH-33, >150 µm fraction, *P. hantkeninoides* Zone.

4. *Heterohelix globulosa* EHRENBERG, side view, UH-8, 63-150 µm fraction, *P. hantkeninoides* Zone.

5. *Heterohelix globulosa* EHRENBERG, close-up view of fig. 4., UH-8, 63-150 µm fraction, *P. hantkeninoides* Zone.

6. *Heterohelix labellosa* NEDERBRAGT, side view, UH-33, >150 µm fraction, *P. hantkeninoides* Zone.

7. *Heterohelix navarroensis* LOEBLICH, side view, UH-31, 63-150 µm fraction, *P. hantkeninoides* Zone.

8. *Heterohelix navarroensis* LOEBLICH, side view, UH-42, 63-150 µm fraction, *P. hantkeninoides* Zone.

Plate 3

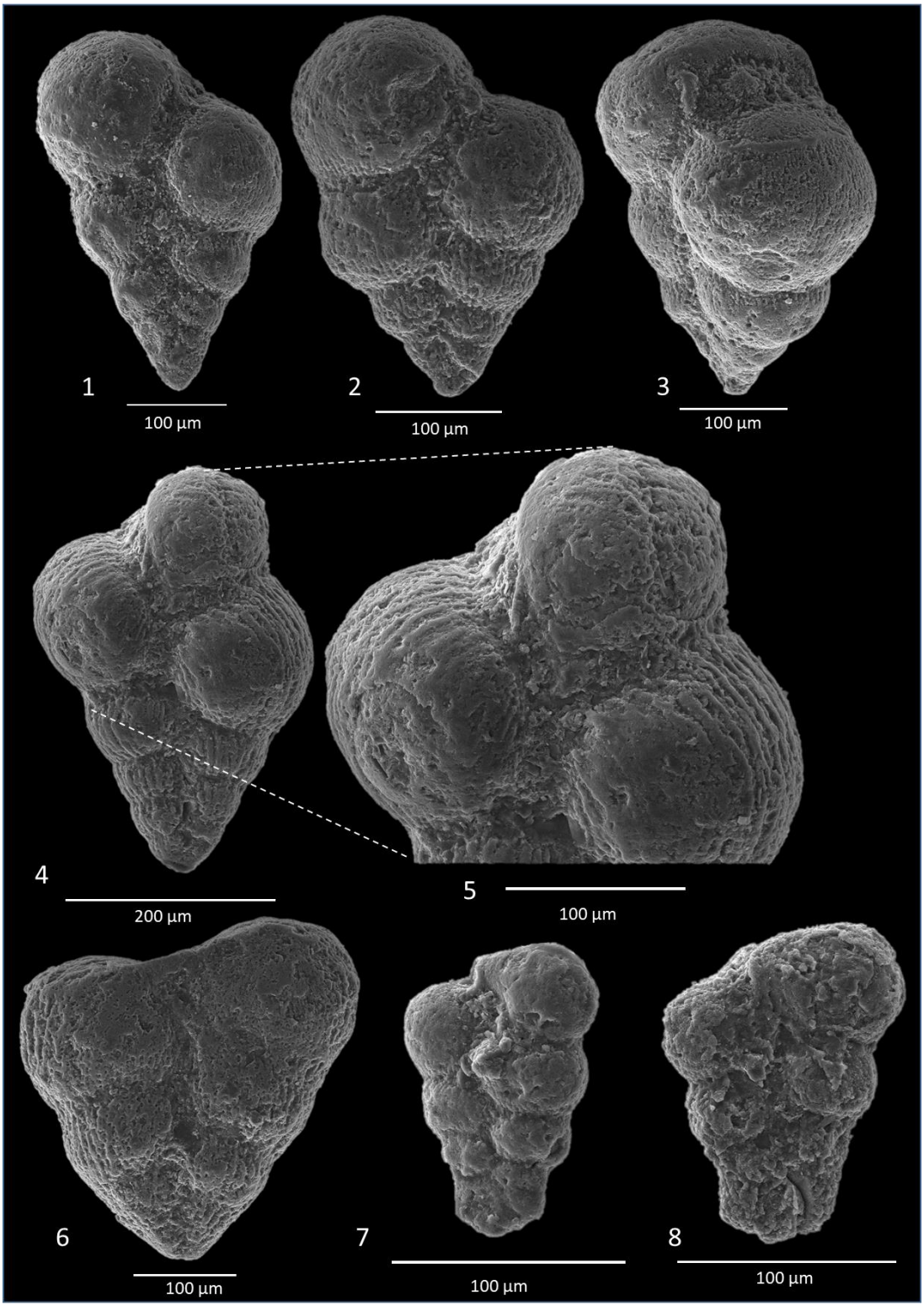

Plate 4

1. *Heterohelix planata* CUSHMAN, side view, UH-35, >150 μm fraction, *P. hantkeninoides* Zone.

2. *Heterohelix planata* CUSHMAN, side view, UH-45, >150 μm fraction, *P. hantkeninoides* Zone.

3. *Heterohelix planata* CUSHMAN, edge view, UH-35, >150 μm fraction, *P. hantkeninoides* Zone.

4. *Heterohelix punctulata* CUSHMAN, side view, UH-48, >150 μm fraction, *P. hantkeninoides* Zone.

5. *Heterohelix punctulata* CUSHMAN, side view, UH-48, 63-150 μm fraction, *P. hantkeninoides* Zone.

6. *Heterohelix punctulata* CUSHMAN, side view, UH-33, >150 μm fraction, *P. hantkeninoides* Zone.

7. *Heterohelix rajagopalani* GOVINDAN, side view, UH-5, >150 μm fraction, *P. hantkeninoides* Zone.

8. *Heterohelix* aff. *rajagopalani* GOVINDAN, side view, UH-14, >150 μm fraction, *P. hantkeninoides* Zone.

Plate 4

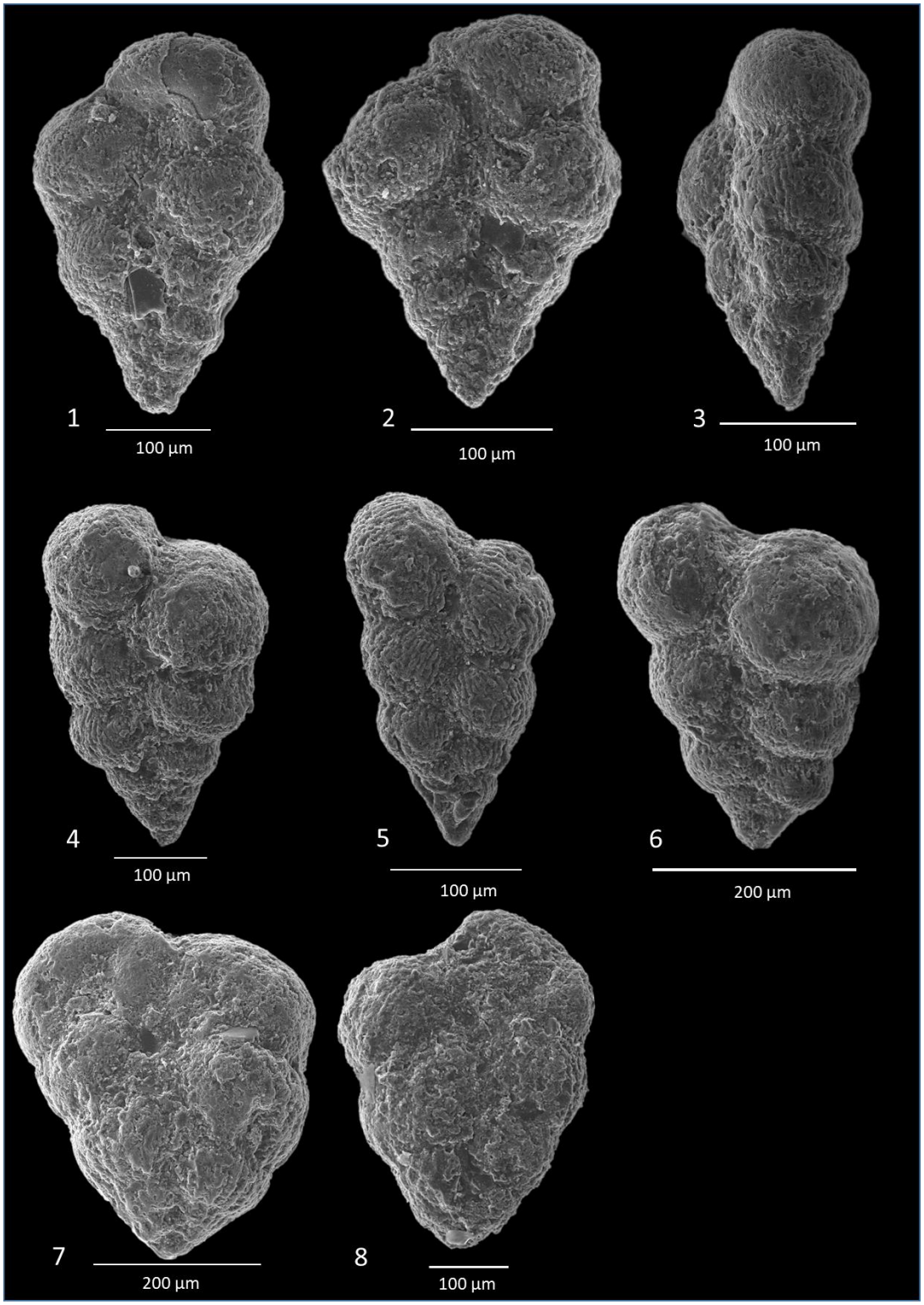

Plate 5

1. *Heterohelix* sp., side view, UH-45, >150 μm fraction, *P. hantkeninoides* Zone.

2. *Heterohelix* sp., side view, UH-38, >150 μm fraction, *P. hantkeninoides* Zone.

3. *Laeviheterohelix dentata* STENESTAD, side view, UH-30, >150 μm fraction, *P. hantkeninoides* Zone.

4. *Laeviheterohelix dentata* STENESTAD, side view, UH-44, 63-150 μm fraction, *P. hantkeninoides* Zone.

5. *Laeviheterohelix dentata* STENESTAD, side view, UH-41, >150 μm fraction, *P. hantkeninoides* Zone.

6. *Laeviheterohelix glabrans* CUSHMAN, side view, UH-35, >150 μm fraction, *P. hantkeninoides* Zone.

7. *Laeviheterohelix glabrans* CUSHMAN, side view, UH-48, >150 μm fraction, *P. hantkeninoides* Zone.

8. *Laeviheterohelix glabrans* CUSHMAN, side view, UH-33, >150 μm fraction, *P. hantkeninoides* Zone.

Plate 5

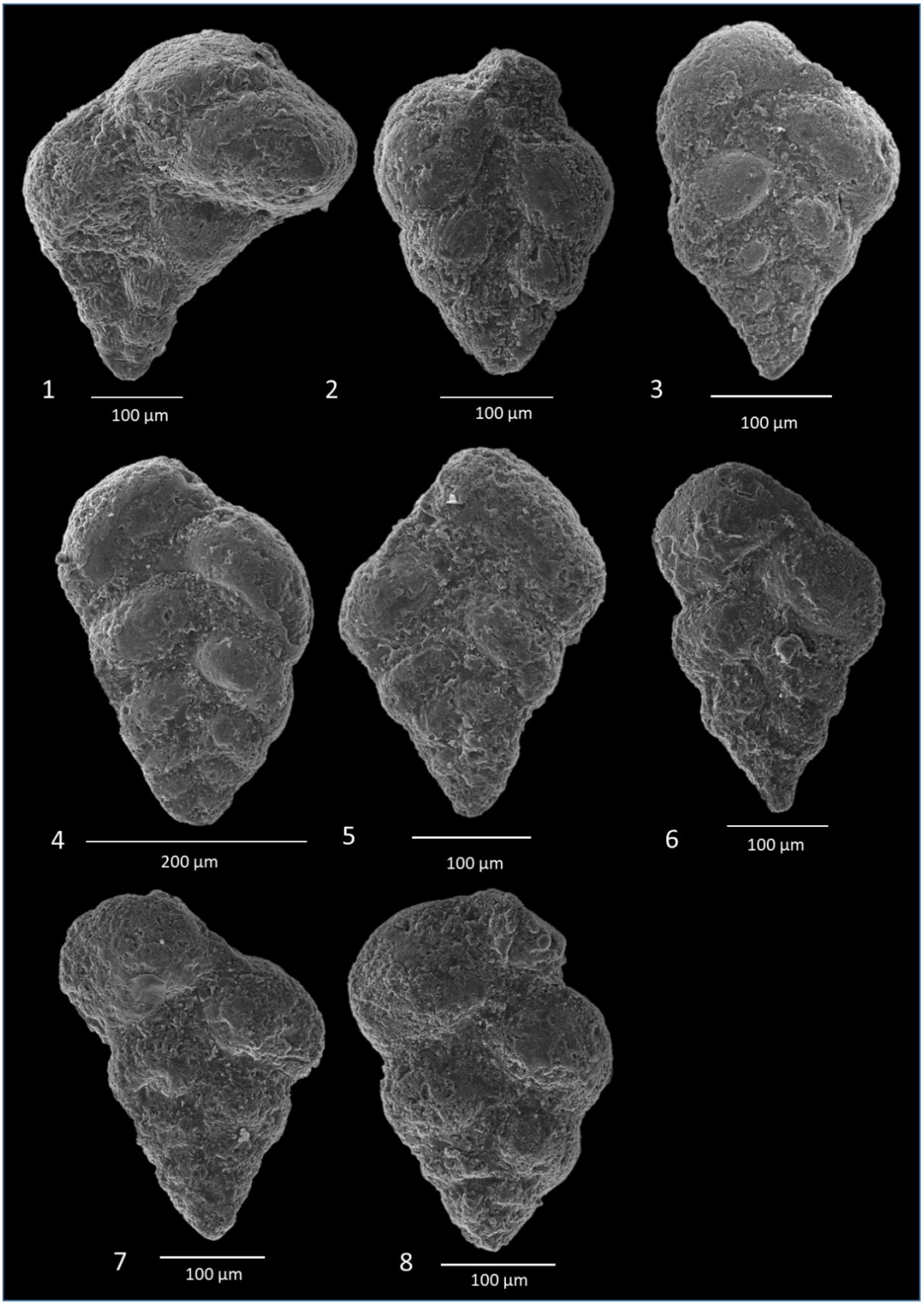

Plate 6

1. *Hartella harti* GEORGESCU & ABRAMOVICH, side view, UH-45, 63-150 μm fraction, *P. hantkeninoides* Zone.

2. *Hartella harti* GEORGESCU & ABRAMOVICH, side view, UH-32, 63-150 μm fraction, *P. hantkeninoides* Zone.

3. *Hartella harti* GEORGESCU & ABRAMOVICH, side view, UH-45, 63-150 μm fraction, *P. hantkeninoides* Zone.

4. *Hartella harti* GEORGESCU & ABRAMOVICH, side view, UH-46, 63-150 μm fraction, *P. hantkeninoides* Zone.

5. *Hartella harti* GEORGESCU & ABRAMOVICH, side view, UH-45, 63-150 μm fraction, *P. hantkeninoides* Zone.

6. *Hartella harti* GEORGESCU & ABRAMOVICH, side view, UH-45, 63-150 μm fraction, *P. hantkeninoides* Zone.

7. *Hartella harti* GEORGESCU & ABRAMOVICH, side view, UH-46, 63-150 μm fraction, *P. hantkeninoides* Zone.

8. *Hartella harti* GEORGESCU & ABRAMOVICH, edge view, UH-45, 63-150 μm fraction, *P. hantkeninoides* Zone.

9. *Hartella harti* GEORGESCU & ABRAMOVICH, edge view, UH-45, 63-150 μm fraction, *P. hantkeninoides* Zone.

Plate 6

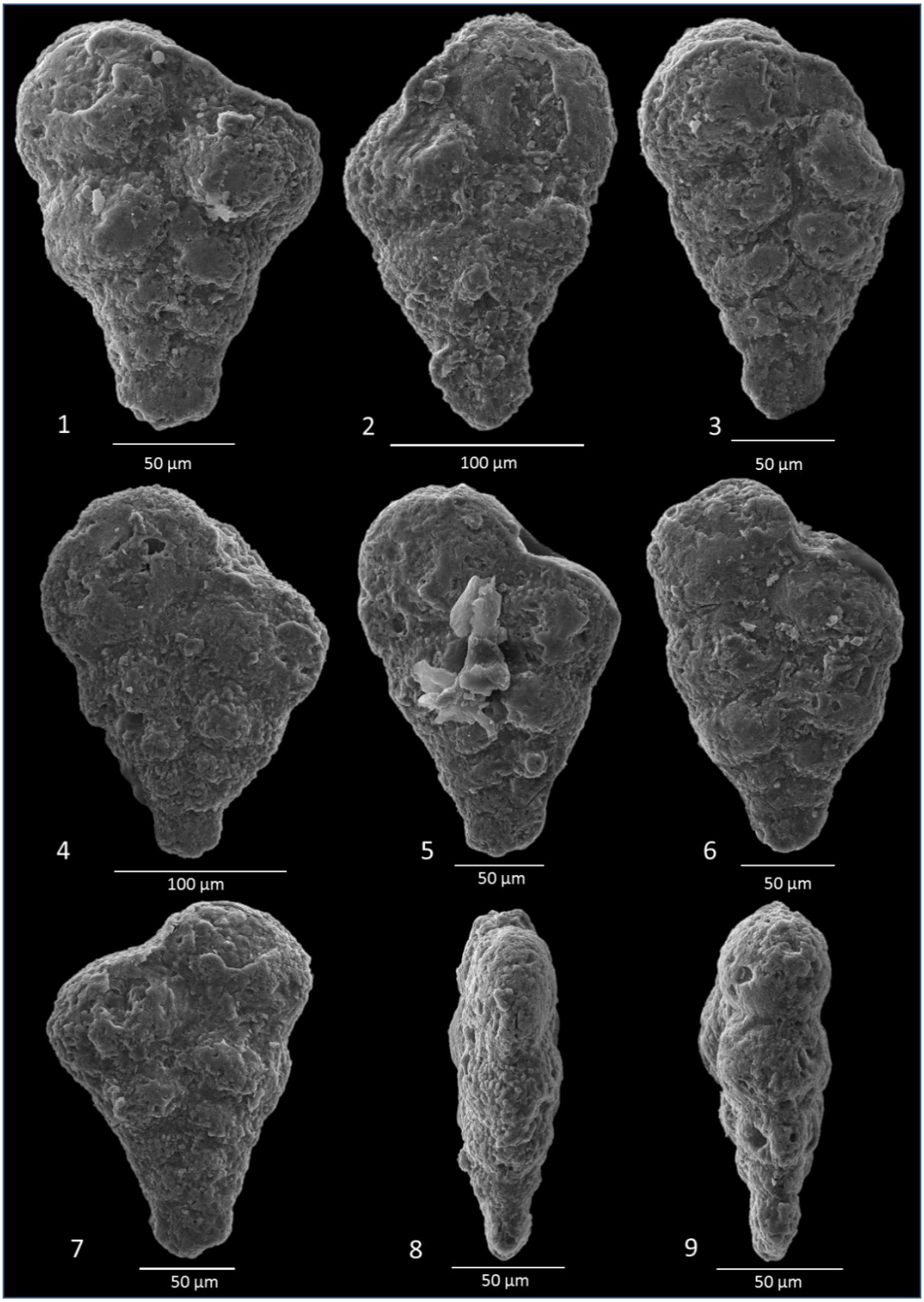

Plate 7

1. *Hartella harti* GEORGESCU & ABRAMOVICH, side view, UH-45, 63-150 μm fraction, *P. hantkeninoides* Zone.

2. *Hartella harti* GEORGESCU & ABRAMOVICH, close-up view of fig. 1.

3. *Hartella harti* GEORGESCU & ABRAMOVICH, close-up view of fig. 1.

4. *Hartella harti* GEORGESCU & ABRAMOVICH, close-up view of fig. 1.

Plate 7

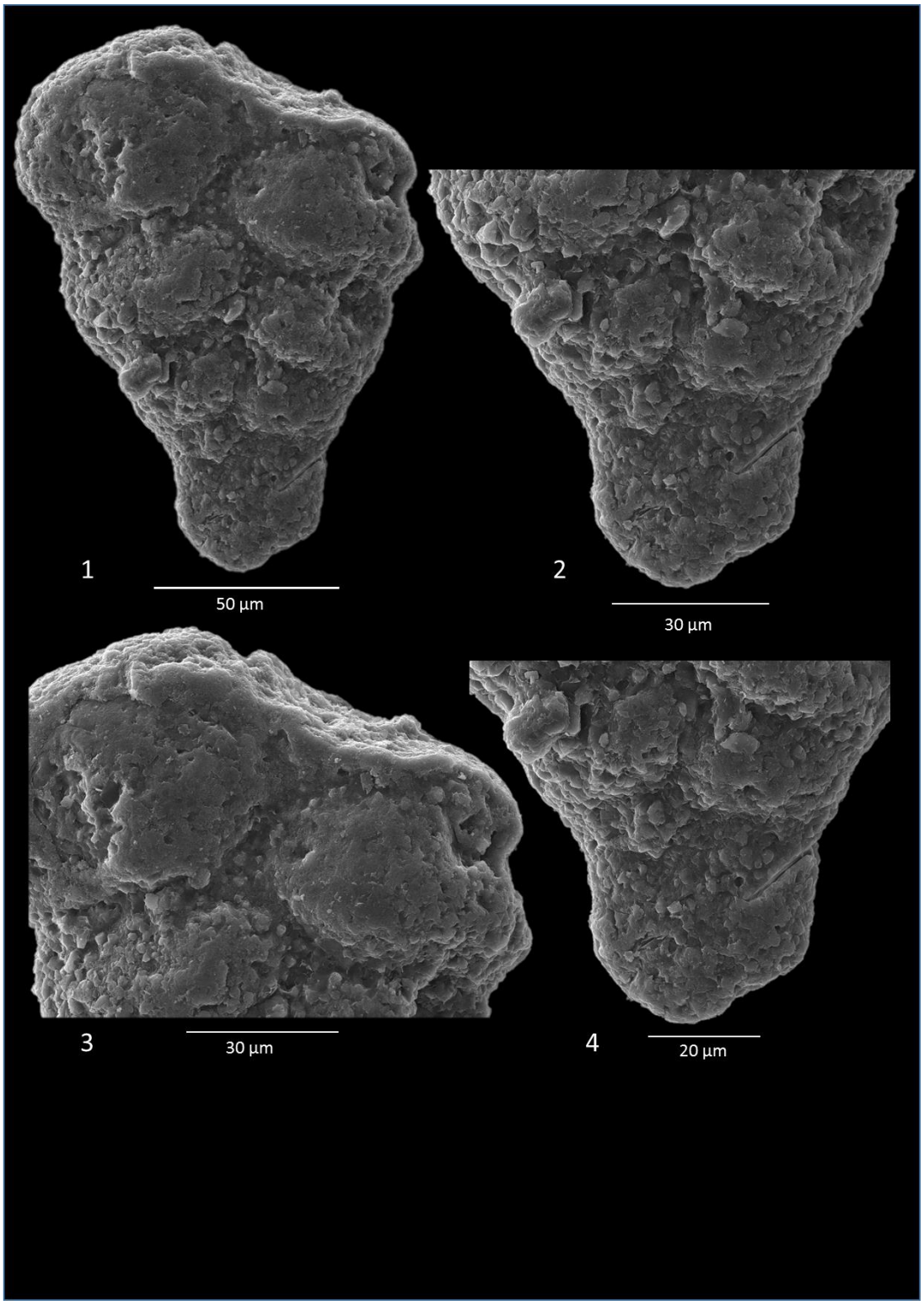

Plate 8

1. *Planoglobulina acervulinoides* EGGER, side view, UH-44, >150 μm fraction, *P. hantkeninoides* Zone.

2. *Planoglobulina acervulinoides* EGGER, side view, UH-45, >150 μm fraction, *P. hantkeninoides* Zone.

3. *Planoglobulina acervulinoides* EGGER, side view, UH-45, >150 μm fraction, *P. hantkeninoides* Zone.

4. *Planoglobulina brazoensis* MARTIN, side view, UH-45, >150 μm fraction, *P. hantkeninoides* Zone.

5. *Planoglobulina brazoensis* MARTIN, side view, UH-45, >150 μm fraction, *P. hantkeninoides* Zone.

6. *Planoglobulina brazoensis* MARTIN, side view, UH-45, >150 μm fraction, *P. hantkeninoides* Zone.

7. *Planoglobulina carseyae* PLUMMER, side view, UH-5, >150 μm fraction, *P. hantkeninoides* Zone.

8. *Planoglobulina carseyae* PLUMMER, close-up view of fig. 7.

Plate 8

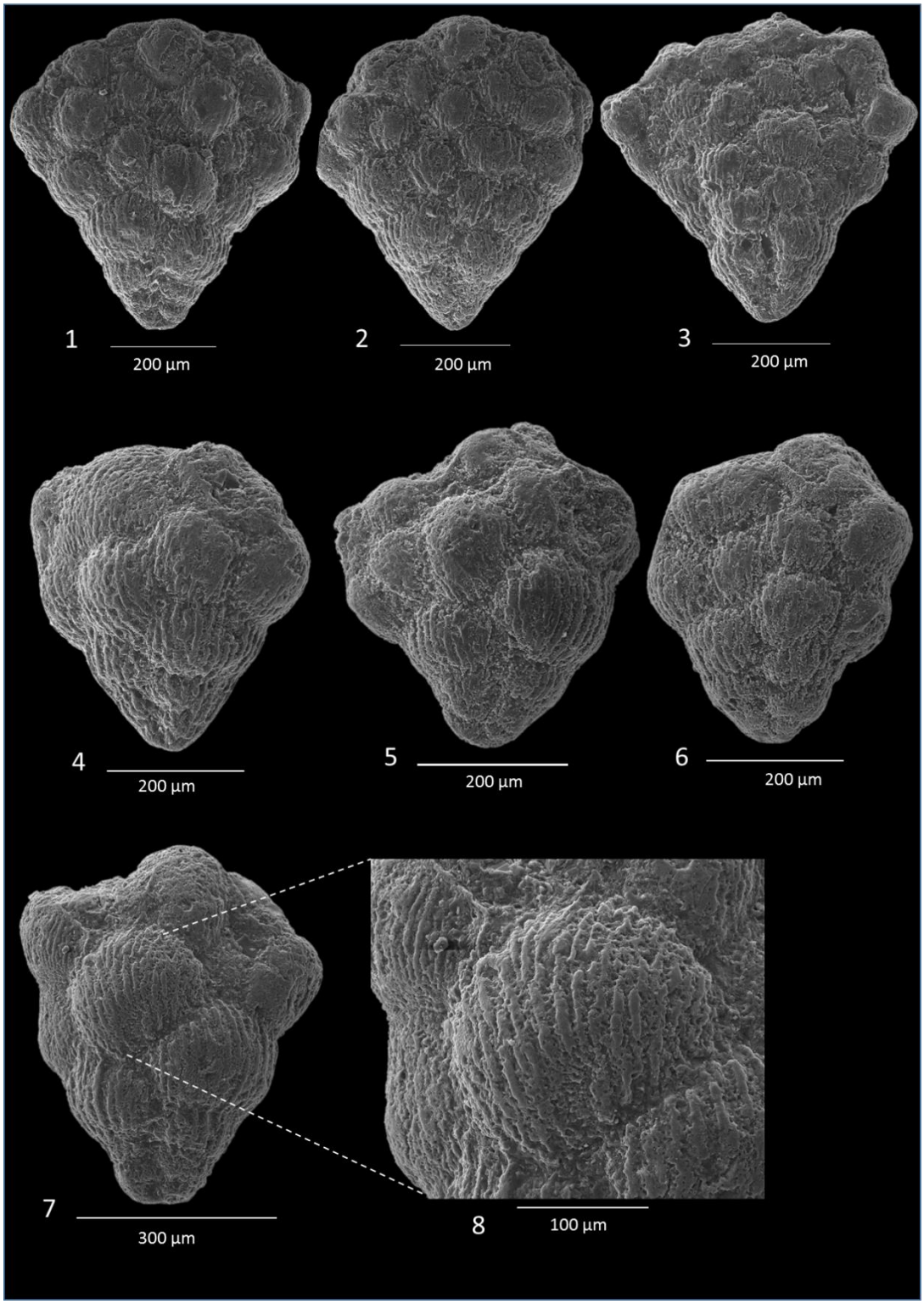

Plate 9

1. *Planoglobulina carseyae* PLUMMER, side view, UH- 44, >150 μm fraction, *P. hantkeninoides* Zone.

2. *Planoglobulina carseyae* PLUMMER, side view, UH-45, >150 μm fraction, *P. hantkeninoides* Zone.

3. *Planoglobulina multicamerata* DE KLASZ, side view, UH-14, >150 μm fraction, *P. hantkeninoides* Zone.

4. *Planoglobulina multicamerata* DE KLASZ, side view, UH-41, >150 μm fraction, *P. hantkeninoides* Zone

5. Intermediate form between *P. acervulinoides* and *P. multicamerata*, side view, UH-48, >150 μm fraction, *P. hantkeninoides* Zone.

6. *Planoglobulina* sp., side view, UH-31, >150 μm fraction, *P. hantkeninoides* Zone.

Plate 9

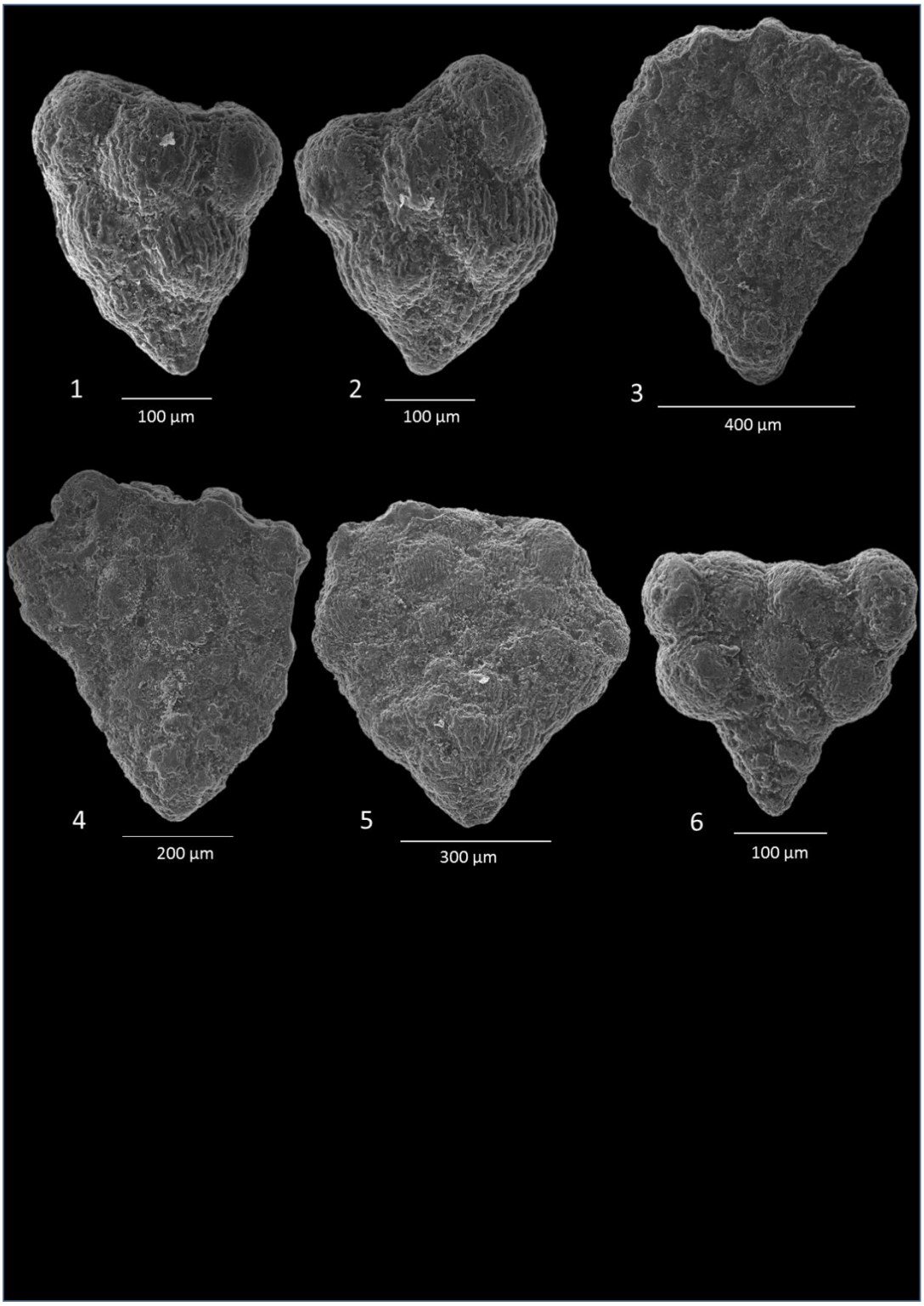

Plate 10

1. *Pseudotextularia elegans* RZEHAK, edge view, UH-32, >150 μm fraction, *P. hantkeninoides* Zone.

2. *Pseudotextularia elegans* RZEHAK, edge view, UH-45, >150 μm fraction, *P. hantkeninoides* Zone.

3. *Pseudotextularia nuttalli* VOORWIJK, edge view, UH-30, >150 μm fraction, *P. hantkeninoides* Zone.

4. *Pseudotextularia nuttalli* VOORWIJK, edge view, UH-30, >150 μm fraction, *P. hantkeninoides* Zone.

5. *Pseudotextularia intermedia* DE KLASZ, edge view, UH-46, >150 μm fraction, *P. hantkeninoides* Zone.

6. *Pseudotextularia intermedia* DE KLASZ, side view, UH-34, >150 μm fraction, *P. hantkeninoides* Zone.

Plate 10

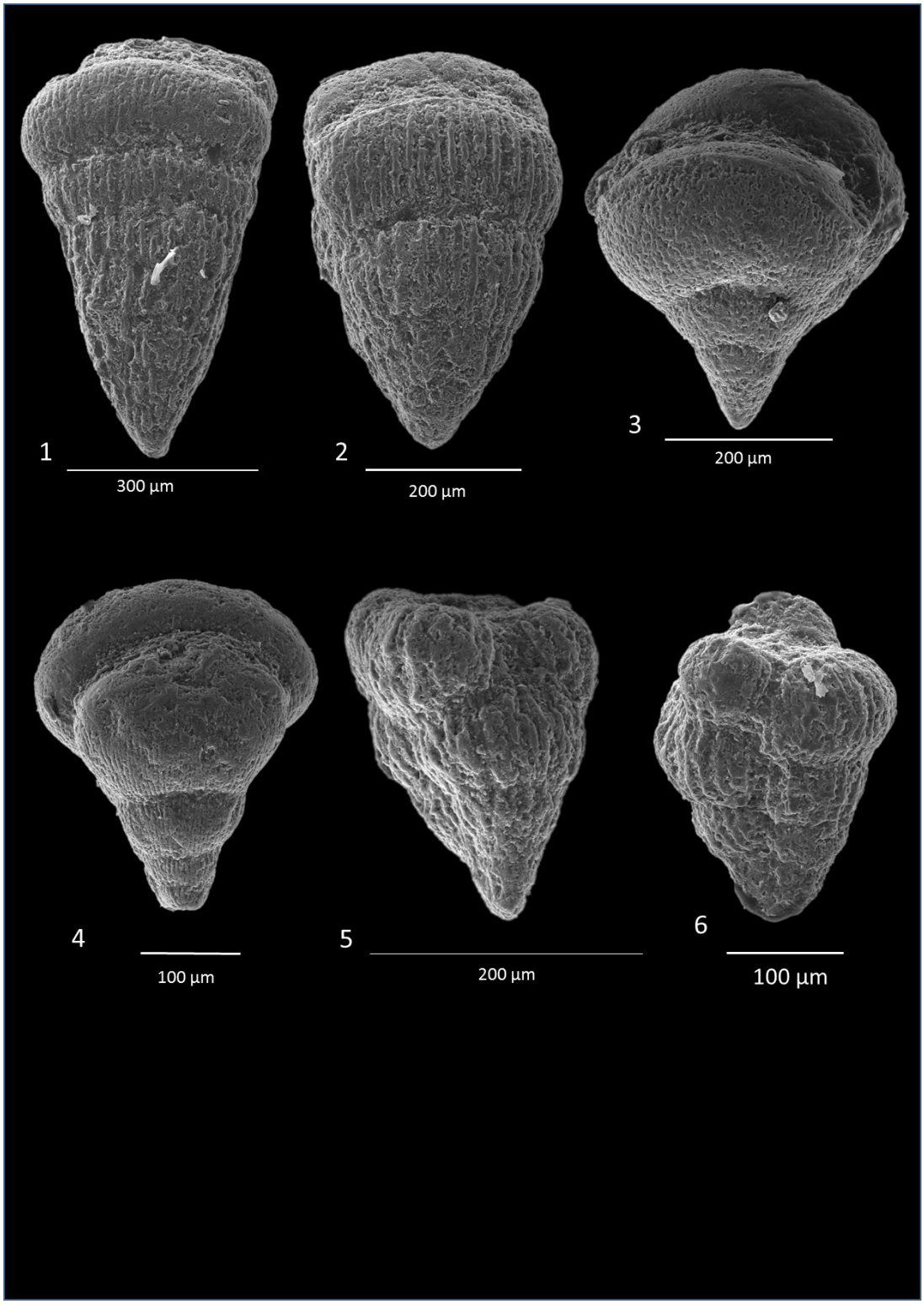

Plate 11

1. *Racemiguembelina fructicosa* EGGER, side view, UH-45, >150 μm fraction, *P. hantkeninoides* Zone.

2. *Racemiguembelina fructicosa* EGGER, side view, UH-45, >150 μm fraction, *P. hantkeninoides* Zone.

3. *Racemiguembelina powelli* SMITH and PESSAGNO, edge view, UH-30, >150 μm fraction, *P. hantkeninoides* Zone.

4. *Racemiguembelina powelli* SMITH and PESSAGNO, side view, UH-38, >150 μm fraction, *P. hantkeninoides* Zone.

5. *Racemiguembelina powelli* SMITH and PESSAGNO, edge view, UH-30, >150 μm fraction, *P. hantkeninoides* Zone.

Plate 11

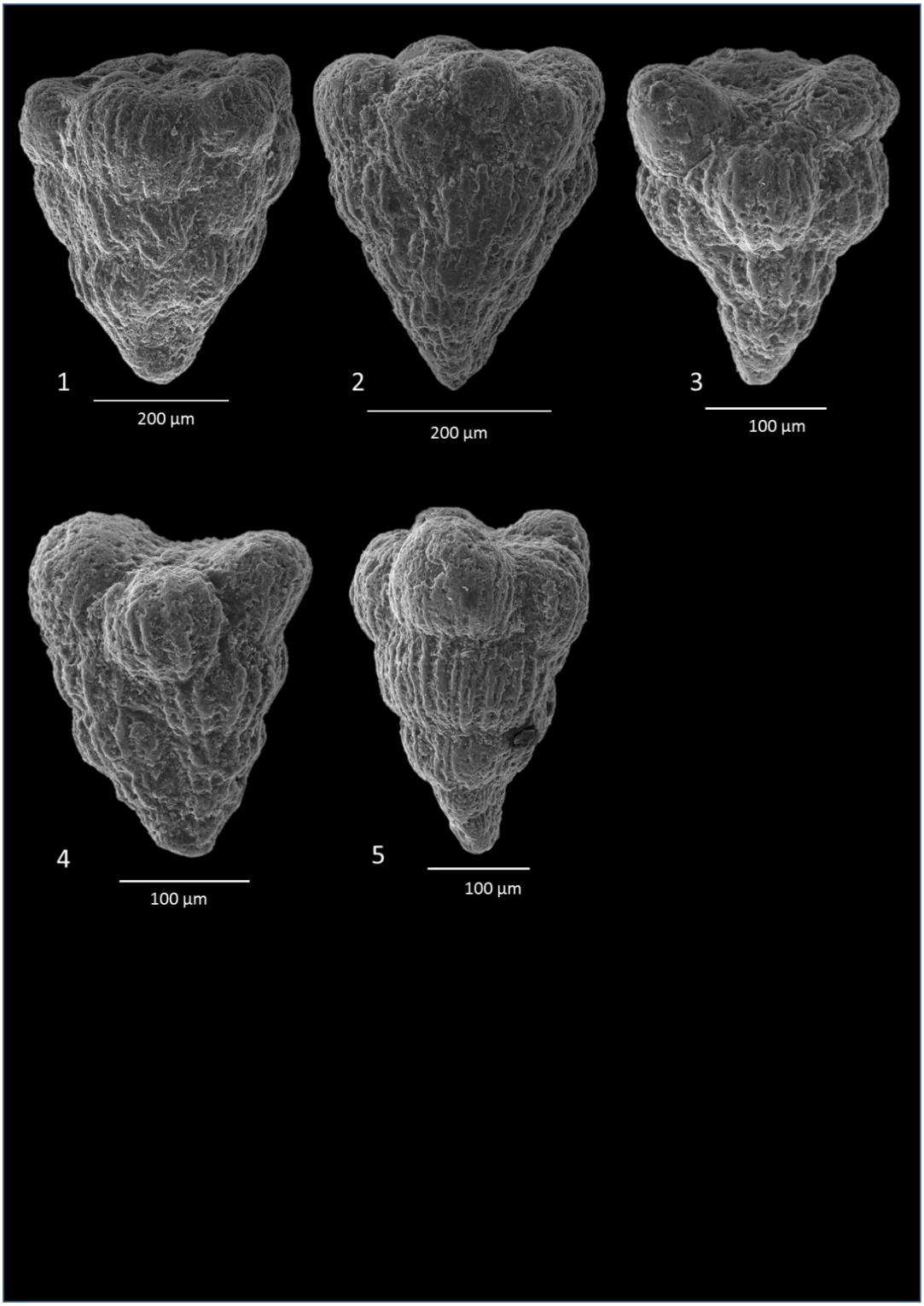

Plate 12

1. *Pseudoguembelina costulata* CUSHMAN, side view, UH-45, >150 μm fraction, *P. hantkeninoides* Zone.

2. *Pseudoguembelina costulata* CUSHMAN, side view, UH-1, >150 μm fraction, P. hantkeninoides Zone.

3. *Pseudoguembelina hariaensis* NEDERBRAGT, side view, UH-47, >150 μm fraction, *P. hantkeninoides* Zone.

4. *Pseudoguembelina hariaensis* NEDERBRAGT, side view, UH-45, >150 μm fraction, *P. hantkeninoides* Zone.

5. *Pseudoguembelina hariaensis* NEDERBRAGT, edge view, UH-34, >150 μm fraction, *P. hantkeninoides* Zone.

6. *Pseudoguembelina hariaensis* NEDERBRAGT, side view, UH-34, >150 μm fraction, *P. hantkeninoides* Zone.

7. *Pseudoguembelina hariaensis* NEDERBRAGT, side view, UH-34, >150 μm fraction, *P. hantkeninoides* Zone.

8. *Pseudoguembelina hariaensis* NEDERBRAGT, top view, UH-31, >150 μm fraction, *P. hantkeninoides* Zone.

9. *Pseudoguembelina palpebra* BRONNIMANN and BROWN, side view, UH-48, >150 μm fraction, *P. hantkeninoides* Zone.

Plate 12

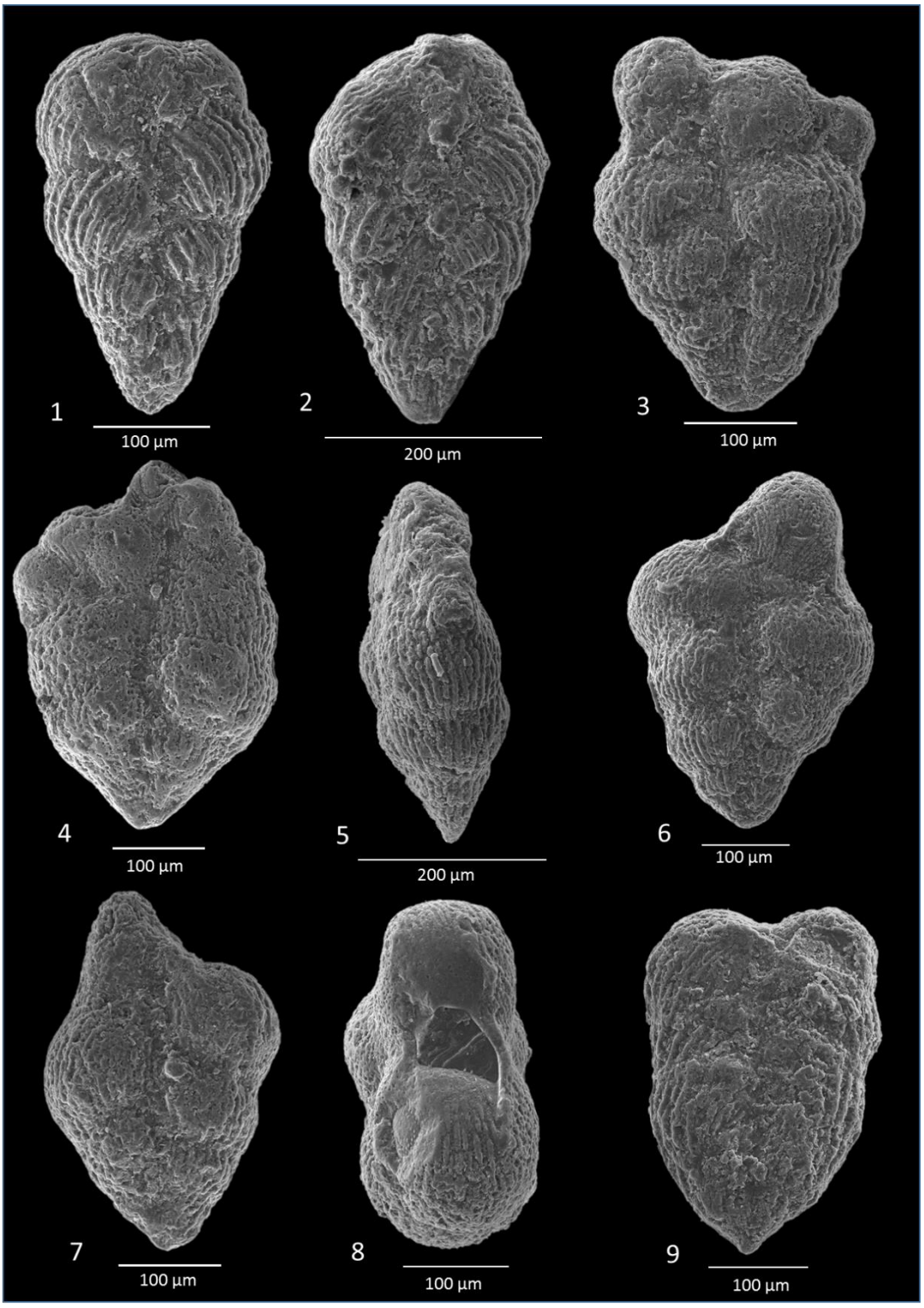
1
100 µm
2
200 µm
3
100 µm
4
100 µm
5
200 µm
6
100 µm
7
100 µm
8
100 µm
9
100 µm

Plate 13

1. *Pseudoguembelina kempensis* ESKER, side view, UH-46, 63-150 μm fraction, *P. hantkeninoides* Zone.

2. *Pseudoguembelina kempensis* ESKER, close-up view of fig. 1.

3. *Pseudoguembelina kempensis* ESKER, close-up view of fig. 1.

4. *Pseudoguembelina kempensis* ESKER, close-up view of fig. 1.

Plate 13

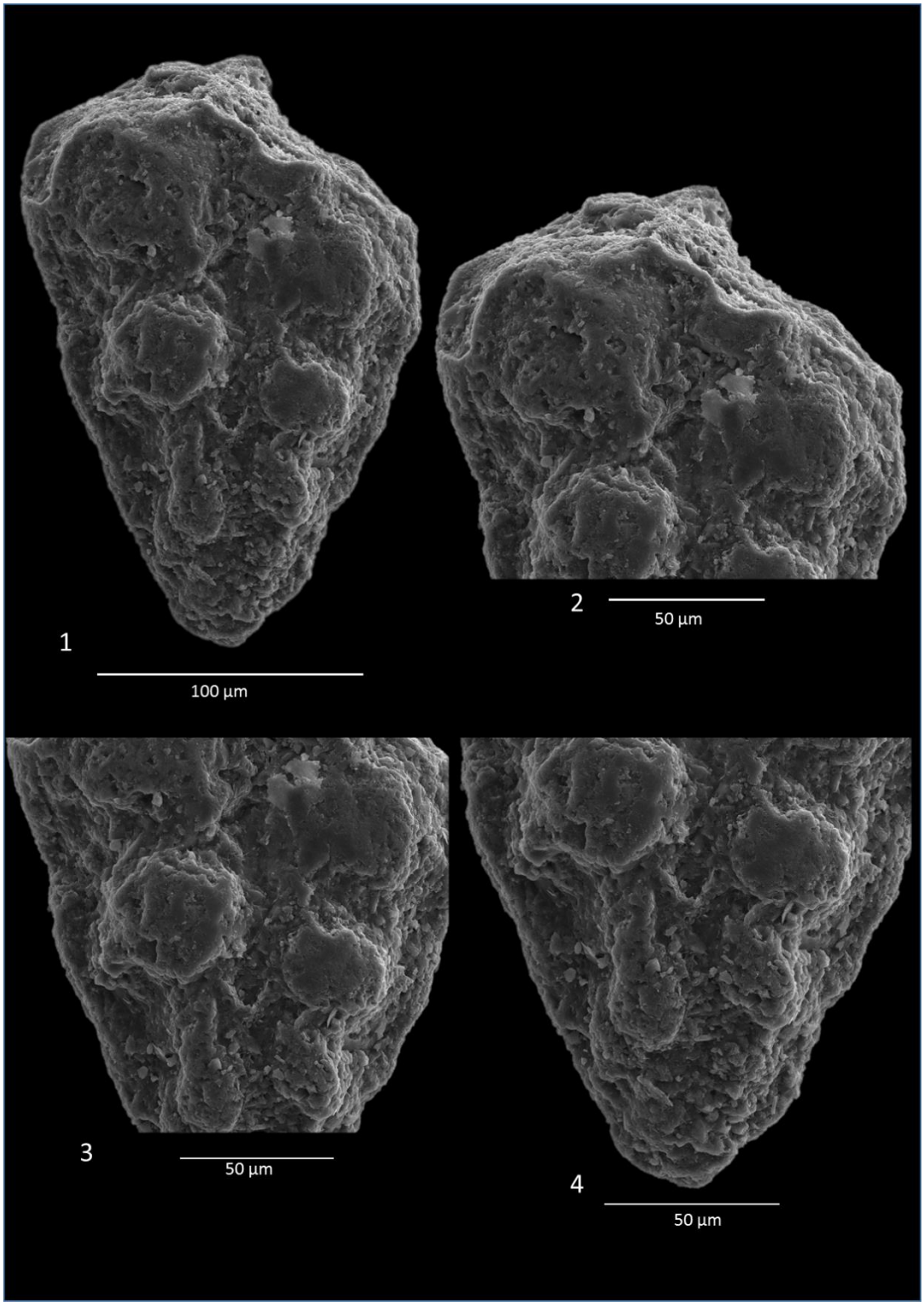

Plate 14

1. *Gublerina acuta* DE KLASZ, side view, UH-31, >150 µm fraction, *P. hantkeninoides* Zone.

2. *Gublerina acuta* DE KLASZ, side view, UH-10, >150 µm fraction, *P. hantkeninoides* Zone.

3. *Gublerina cuvillieri* KIKONE, side view, UH-31, >150 µm fraction, *P. hantkeninoides* Zone.

4. *Gublerina cuvillieri* KIKONE, side view, UH-1, >150 µm fraction, *P. hantkeninoides* Zone.

5. *Gublerina cuvillieri* KIKONE, edge view, UH-33, >150 µm fraction, *P. hantkeninoides* Zone.

6. *Gublerina cuvillieri* KIKONE, side view, UH-45, >150 µm fraction, *P. hantkeninoides* Zone.

7. *Gublerina cuvillieri* KIKONE, side view, UH-45, >150 µm fraction, *P. hantkeninoides* Zone.

Plate 14

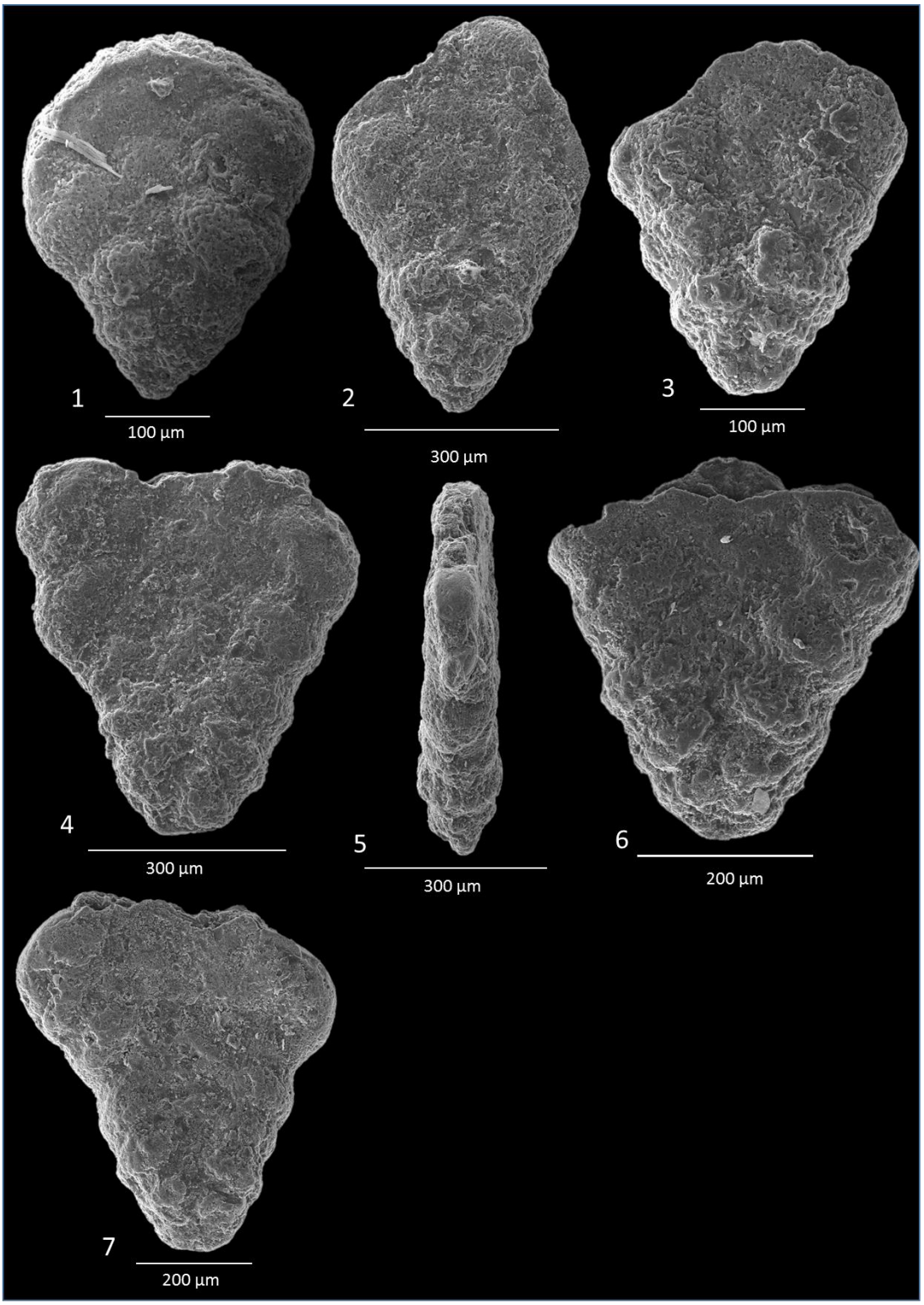

Plate 15

1. *Globigerinelloides alvarezi* ETERNOD OLVERA, side view, UH-45, 63-150 μm fraction, *P. hantkeninoides* Zone.

2. *Globigerinelloides alvarezi* ETERNOD OLVERA, side view, UH-45, 63-150 μm fraction, *P. hantkeninoides* Zone.

3. *Globigerinelloides alvarezi* ETERNOD OLVERA, side view, UH-45, 63-150 μm fraction, *P. hantkeninoides* Zone.

4. *Globigerinelloides alvarezi* ETERNOD OLVERA, side view, UH-45, 63-150 μm fraction, *P. hantkeninoides* Zone.

5. *Globigerinelloides asperum* EHRENBERG, side view, UH-45, 63-150 μm fraction, *P. hantkeninoides* Zone.

6. *Globigerinelloides asperum* EHRENBERG, side view, UH-48, 63-150 μm fraction, *P. hantkeninoides* Zone.

7. *Globigerinelloides multispinus* LALICKER, side view, UH-32, >150 μm fraction, *P. hantkeninoides* Zone.

8. *Globigerinelloides multispinus* LALICKER, edge view, UH-31, >150 μm fraction, *P. hantkeninoides* Zone.

9. *Globigerinelloides multispinus* LALICKER, edge view, UH-45, >150 μm fraction, *P. hantkeninoides* Zone.

Plate 15

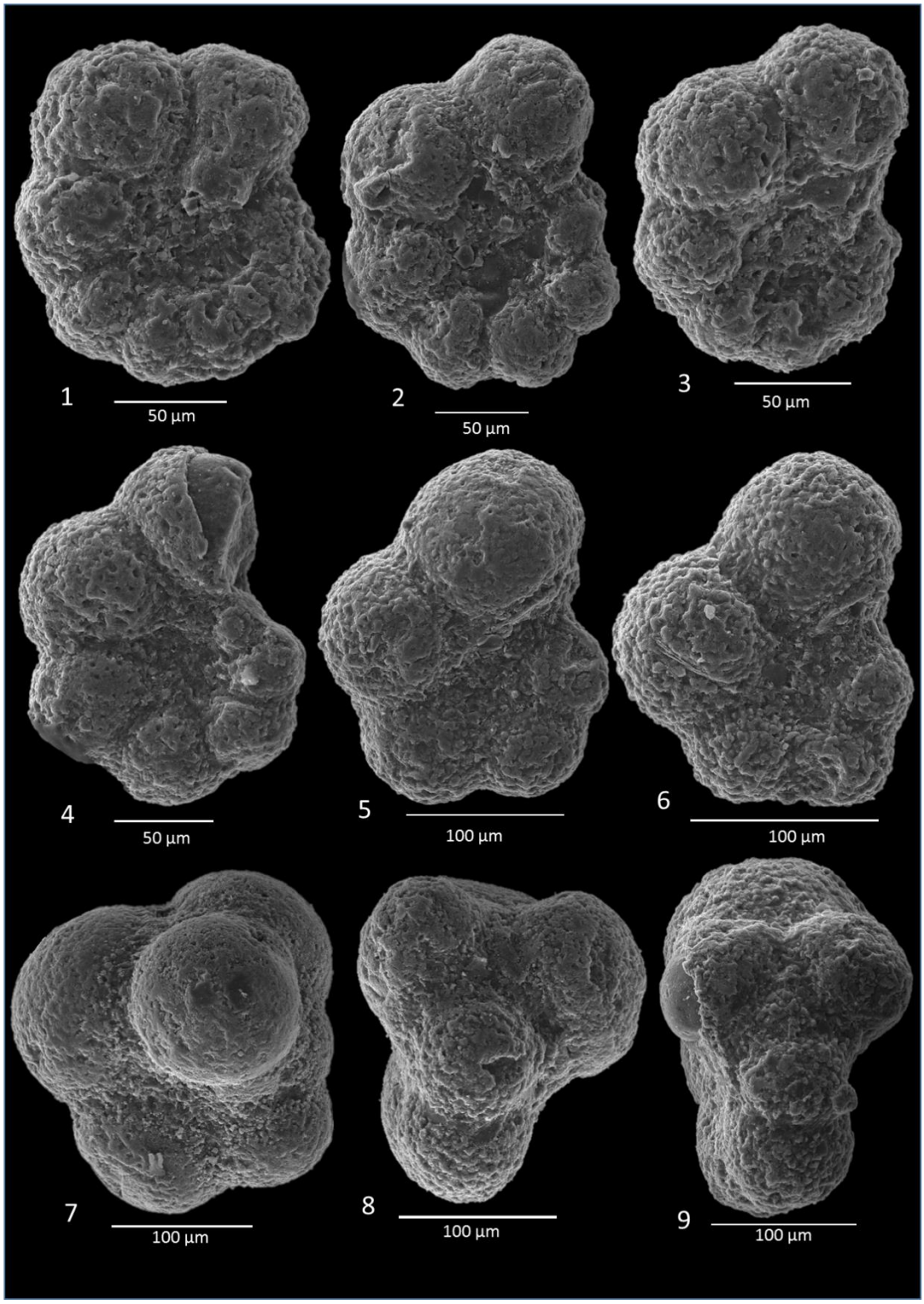
1
50 µm
2
50 µm
3
50 µm
4
50 µm
5
100 µm
6
100 µm
7
100 µm
8
100 µm
9
100 µm

Plate 16

1. *Globigerinelloides* aff. *mendezensis* ETERNOD OLVERA, side view, UH-48, 63-150 μm fraction, *P. hantkeninoides* Zone.

2. *Globigerinelloides* aff. *mendezensis* ETERNOD OLVERA, side view, UH-33, >150 μm fraction, *P. hantkeninoides* Zone.

3. *Globigerinelloides* aff. *mendezensis* ETERNOD OLVERA, side view, UH-46, 63-150 μm fraction, *P. hantkeninoides* Zone.

4. *Globigerinelloides prairiehillensis* PESSAGNO, side view, UH-39, >150 μm fraction, *P. hantkeninoides* Zone.

5. *Globigerinelloides prairiehillensis* PESSAGNO, side to edge view, UH-31, >150 μm fraction, *P. hantkeninoides* Zone.

6. *Globigerinelloides prairiehillensis* PESSAGNO, side view, UH-11, >150 μm fraction, *P. hantkeninoides* Zone.

7. *Globigerinelloides rosebudensis* SMITH and PESSAGNO, side view, UH-30, >150 μm fraction, *P. hantkeninoides* Zone.

8. *Globigerinelloides rosebudensis* SMITH and PESSAGNO, side view, UH-32, >150 μm fraction, *P. hantkeninoides* Zone.

9. *Globigerinelloides rosebudensis* SMITH and PESSAGNO, side view, UH-33, >150 μm fraction, *P. hantkeninoides* Zone.

Plate 16

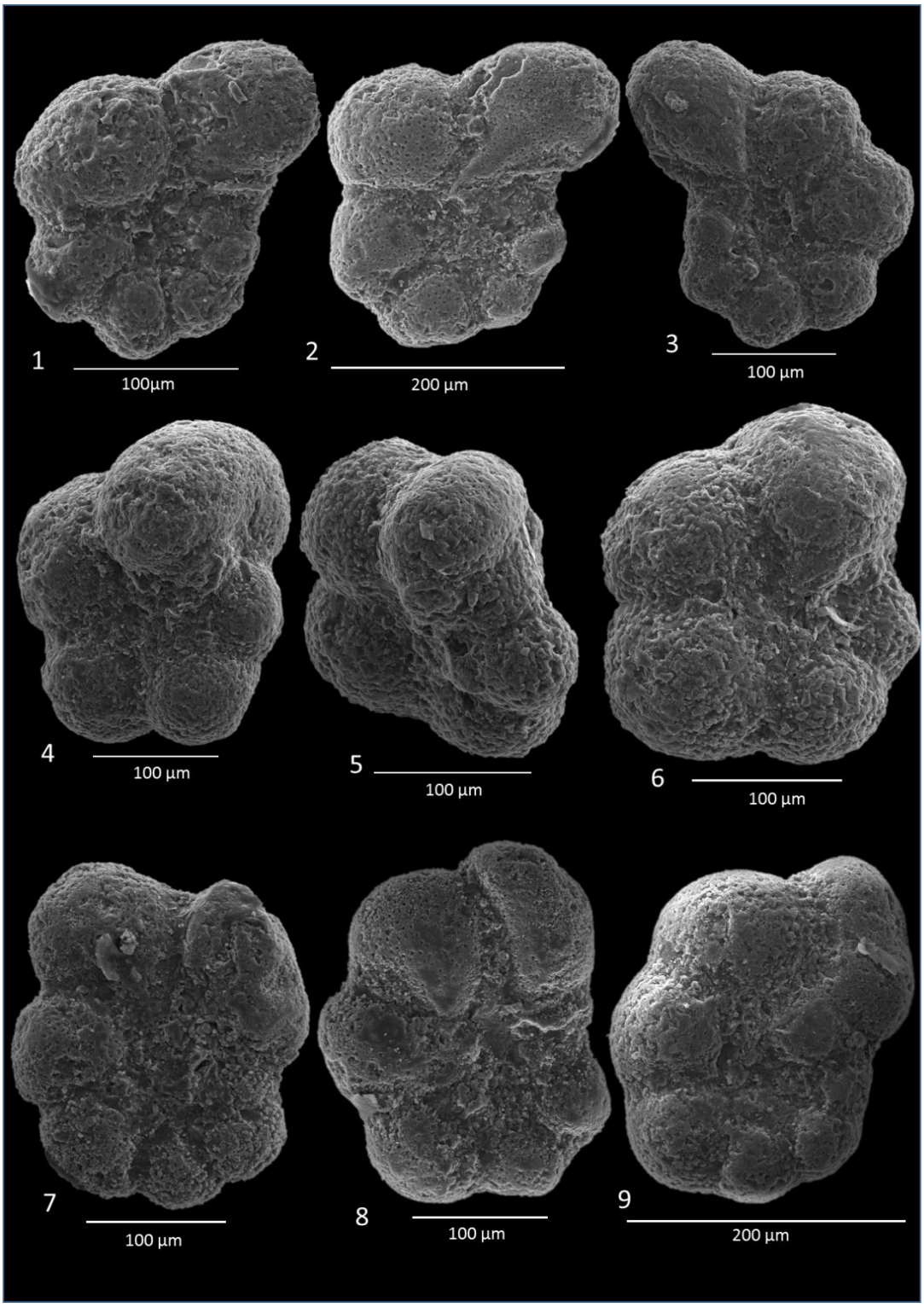
1
100µm
2
200 µm
3
100 µm
4
100 µm
5
100 µm
6
100 µm
7
100 µm
8
100 µm
9
200 µm

Plate 17

1. *Globigerinelloides subcarinatus* BRONNIMANN, side view, UH-45, >150 μm fraction, *P. hantkeninoides* Zone.

2. *Globigerinelloides subcarinatus* BRONNIMANN, side view, UH-45, >150 μm fraction, *P. hantkeninoides* Zone.

3. *Globigerinelloides subcarinatus* BRONNIMANN, side view, UH-31, >150 μm fraction, *P. hantkeninoides* Zone.

4. *Globigerinelloides ultramicrus* SUBBOTINA, side view, UH-1, 63-150 μm fraction, *P. hantkeninoides* Zone.

5. *Globigerinelloides ultramicrus* SUBBOTINA, side view, UH-46, 63-150 μm fraction, *P. hantkeninoides* Zone.

6. *Globigerinelloides ultramicrus* SUBBOTINA, side view, UH-46, 63-150 μm fraction, *P. hantkeninoides* Zone.

Plate 17

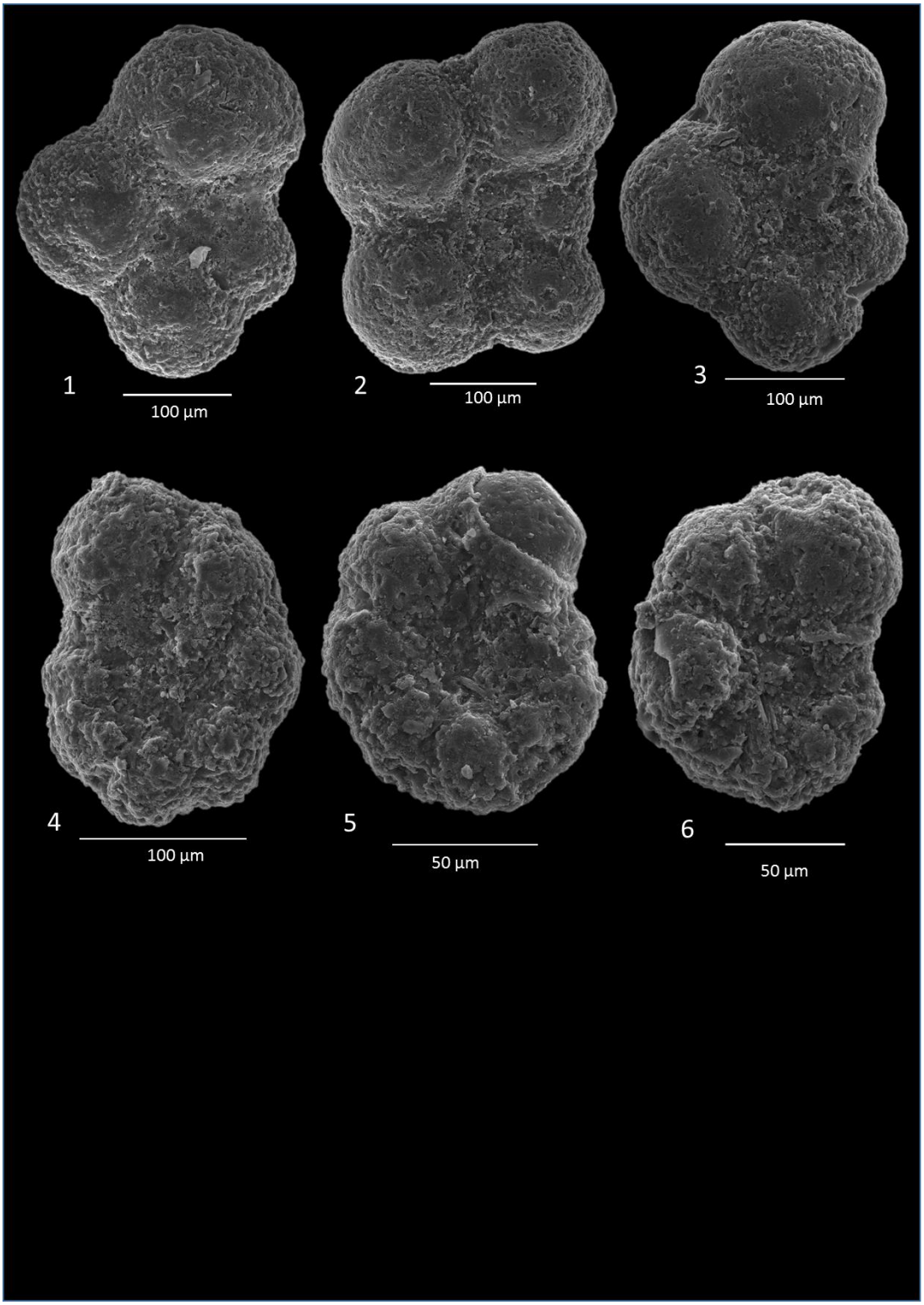

Plate 18

1. *Hedbergella holmdelensis* OLSSON, spiral view, UH-48, 63-150 μm fraction, *P. hantkeninoides* Zone.

2. *Hedbergella holmdelensis* OLSSON, spiral view, UH-39, 63-150 μm fraction, *P. hantkeninoides* Zone.

3. *Hedbergella holmdelensis* OLSSON, spiral view, UH-45, 63-150 μm fraction, *P. hantkeninoides* Zone.

4. *Hedbergella monmouthensis* OLSSON, spiral view, UH-45, 63-150 μm fraction, *P. hantkeninoides* Zone.

5. *Hedbergella monmouthensis* OLSSON, spiral view, UH-37, 63-150 μm fraction, *P. hantkeninoides* Zone.

6. *Hedbergella monmouthensis* OLSSON, spiral view, UH-34, 63-150 μm fraction, *P. hantkeninoides* Zone.

7. *Hedbergella monmouthensis* OLSSON, umbilical view, UH-32, >150 μm fraction, *P. hantkeninoides* Zone.

8. *Hedbergella sliteri* HUBER, umbilical view, UH-46, 63-150 μm fraction, *P. hantkeninoides* Zone.

9. *Hedbergella sliteri* HUBER, umbilical view, UH-40, >150 μm fraction, *P. hantkeninoides* Zone.

Plate 18

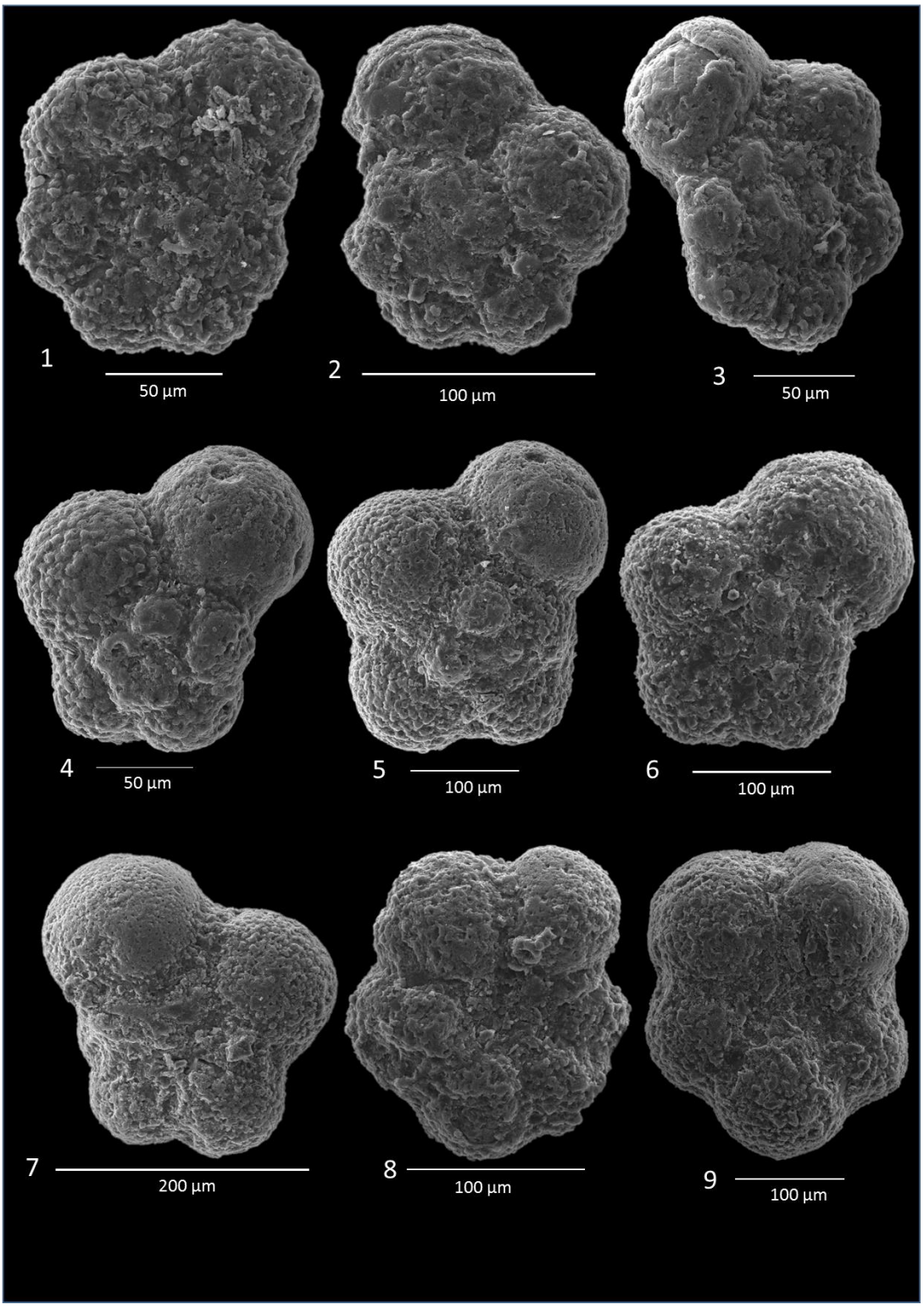
1
50 µm
2
100 µm
3
50 µm
4
50 µm
5
100 µm
6
100 µm
7
200 µm
8
100 µm
9
100 µm

Plate 19

1. *Archaeoglobigerina australis* HUBER, spiral view, UH-45, >150 μm fraction, *P. hantkeninoides* Zone.

2. *Archaeoglobigerina australis* HUBER, spiral view, UH-45, >150 μm fraction, *P. hantkeninoides* Zone.

3. *Archaeoglobigerina australis* HUBER, spiral view, UH-45, >150 μm fraction, *P. hantkeninoides* Zone.

4. *Archaeoglobigerina australis* HUBER, umbilical view, UH-45, >150 μm fraction, *P. hantkeninoides* Zone.

5. *Archaeoglobigerina australis* HUBER, edge view, UH-45, >150 μm fraction, *P. hantkeninoides* Zone.

6. *Archaeoglobigerina blowi* PESSAGNO, spiral view, UH-45, >150 μm fraction, *P. hantkeninoides* Zone.

7. *Archaeoglobigerina blowi* PESSAGNO, spiral view, UH-45, >150 μm fraction, *P. hantkeninoides* Zone.

8. *Archaeoglobigerina blowi* PESSAGNO, spiral view, UH-45, >150 μm fraction, *P. hantkeninoides* Zone.

9. *Archaeoglobigerina* aff. *cretacea* D'ORBIGNY, spiral view, UH-39, >150 μm fraction, *P. hantkeninoides* Zone.

Plate 19

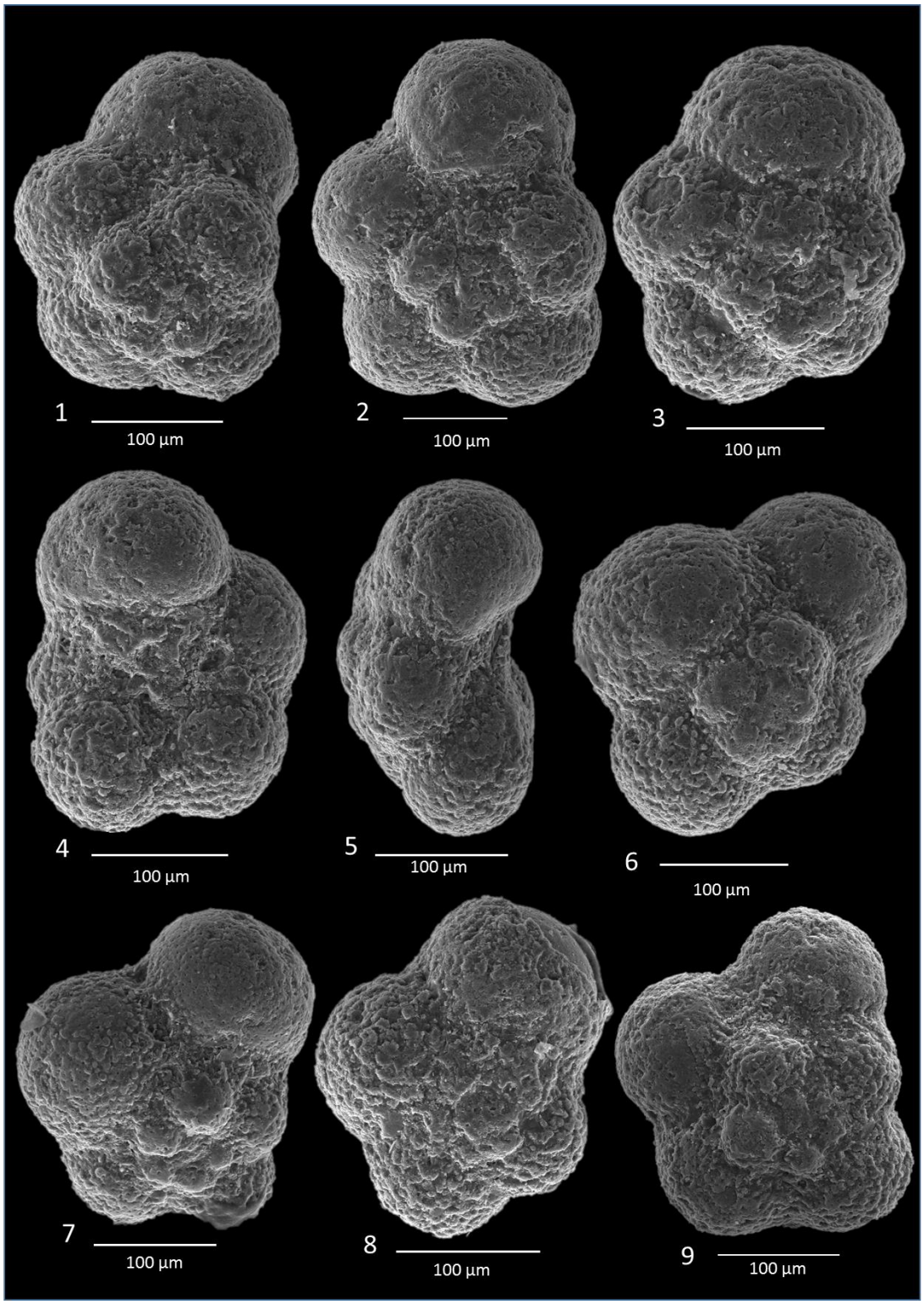
1
100 µm
2
100 µm
3
100 µm
4
100 µm
5
100 µm
6
100 µm
7
100 µm
8
100 µm
9
100 µm

Plate 20

1. *Kuglerina rotundata* BRONNIMANN, spiral view, UH-45, >150 μm fraction, *P. hantkeninoides* Zone.

2. *Rugoglobigerina rugosa* PLUMMER, spiral view, UH-38, >150 μm fraction, *P. hantkeninoides* Zone.

3. *Rugoglobigerina rugosa* PLUMMER, spiral view, UH-30, >150 μm fraction, *P. hantkeninoides* Zone.

4. *Rugoglobigerina hexacamerata* BRONNIMANN, spiral view, UH-40, >150 μm fraction, *P. hantkeninoides* Zone.

5. *Rugoglobigerina hexacamerata* BRONNIMANN, spiral view, UH-32, >150 μm fraction, *P. hantkeninoides* Zone.

6. *Rugoglobigerina macrocephala* BRONNIMANN, umbilical view, UH-39, >150 μm fraction, *P. hantkeninoides* Zone.

7. *Rugoglobigerina macrocephala* BRONNIMANN, spiral view, UH-31, >150 μm fraction, *P. hantkeninoides* Zone.

8. *Rugoglobigerina* aff. *milamensis* SMITH and PESSAGNO, spiral view, UH-30, >150 μm fraction, *P. hantkeninoides* Zone.

9. *Rugoglobigerina pennyi* BRONNIMANN, spiral view, UH-11, >150 μm fraction, *P. hantkeninoides* Zone.

Plate 20

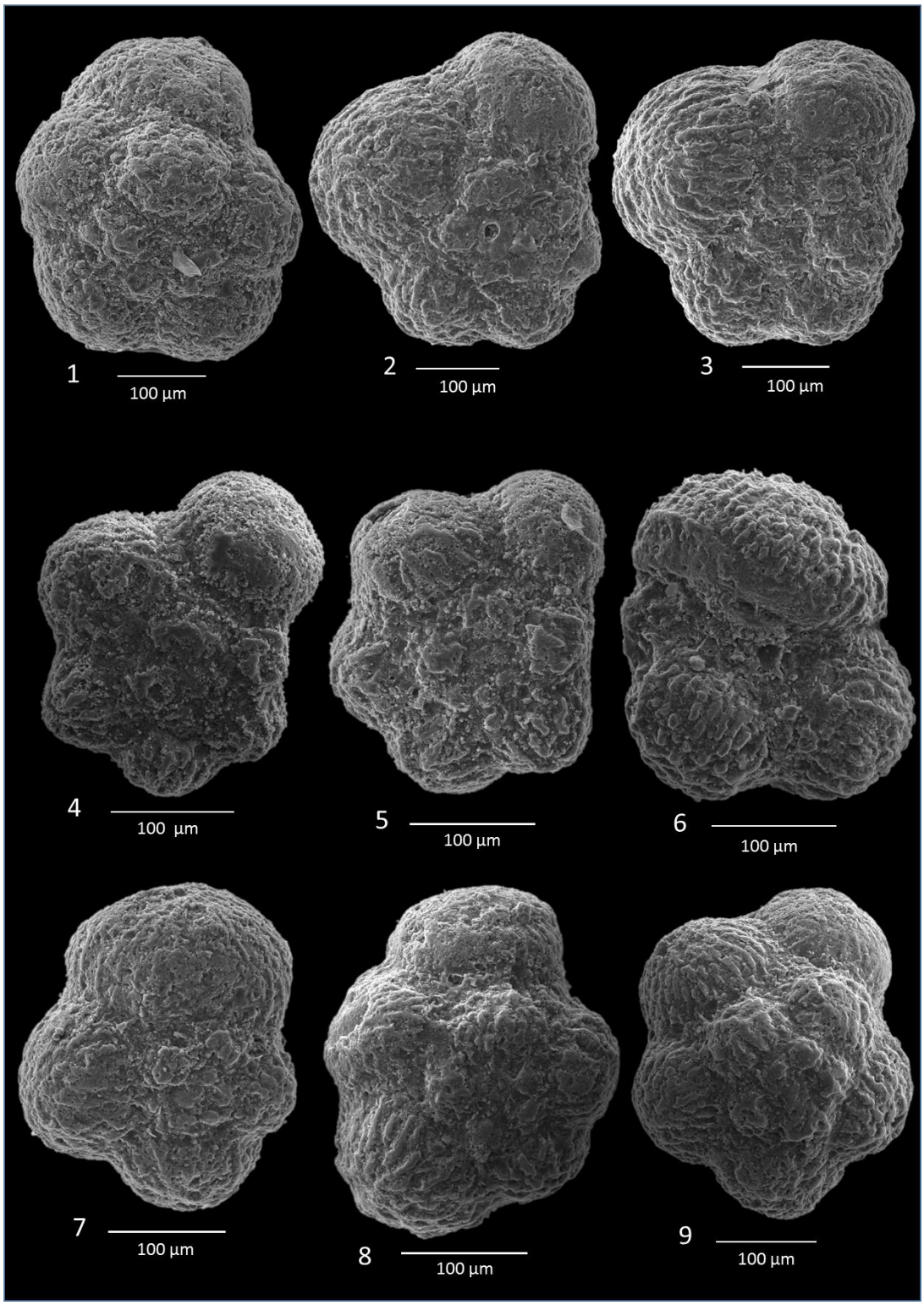
1
100 µm
2
100 µm
3
100 µm
4
100 µm
5
100 µm
6
100 µm
7
100 µm
8
100 µm
9
100 µm

Plate 21

1. *Trinitella scotti* BRONNIMANN, spiral view, UH-33, >150 μm fraction, *P. hantkeninoides* Zone.

2. *Trinitella scotti* BRONNIMANN, edge view, UH-38, >150 μm fraction, *P. hantkeninoides* Zone.

3. *Trinitella scotti* BRONNIMANN, spiral view, UH-45, >150 μm fraction, *P. hantkeninoides* Zone.

4. *Plummerita hantkeninoides* BRONNIMANN, spiral view, UH-1, 63-150 μm fraction, *P. hantkeninoides* Zone.

5. *Plummerita hantkeninoides* BRONNIMANN, umbilical view, UH-31, >150 μm fraction, *P. hantkeninoides* Zone.

6. *Plummerita hantkeninoides* BRONNIMANN, spiral view, UH-30, >150 μm fraction, *P. hantkeninoides* Zone.

7. *Plummerita hantkeninoides* BRONNIMANN, spiral view, UH-45, >150 μm fraction, *P. hantkeninoides* Zone.

8. *Plummerita* aff. *hantkeninoides* BRONNIMANN, spiral view, UH-30, >150 μm fraction, *P. hantkeninoides* Zone.

9. *Plummerita* aff. *reicheli* BRONNIMANN, spiral view, UH-38, >150 μm fraction, *P. hantkeninoides* Zone.

Plate 21

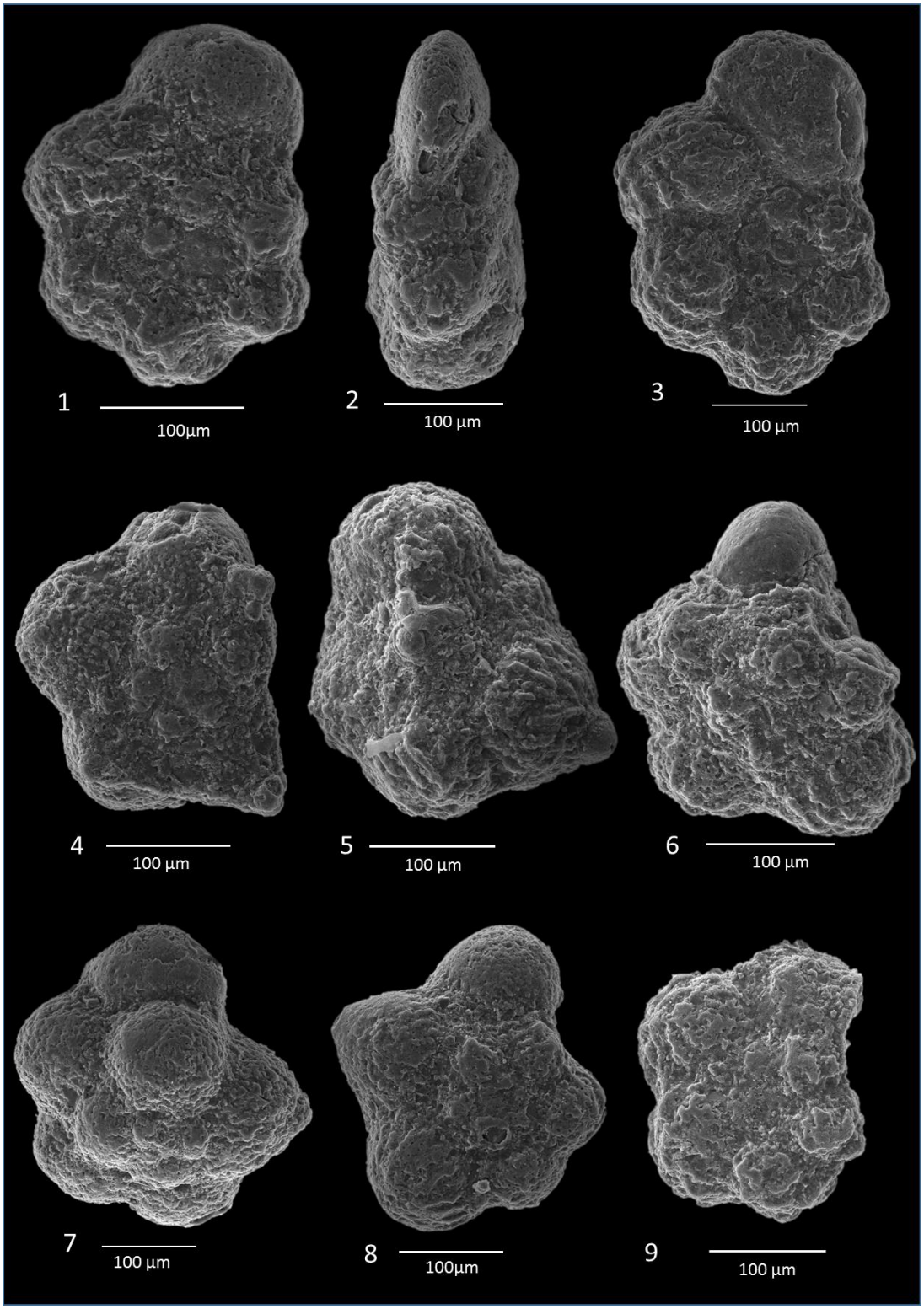
1
100µm
2
100 µm
3
100 µm
4
100 µm
5
100 µm
6
100 µm
7
100 µm
8
100µm
9
100 µm

Plate 22

Figure 1. *Abathomphalus mayaroensis* BOLLI, umbilical view, UH-47, >150 µm fraction, *P. hantkeninoides* Zone.

Figure 2. *Abathomphalus mayaroensis* BOLLI, umbilical view, UH-31, >150 µm fraction, *P. hantkeninoides* Zone.

Figure 3. *Abathomphalus mayaroensis* BOLLI, umbilical view, UH-35, >150 µm fraction, *P. hantkeninoides* Zone.

Figure 4. *Abathomphalus mayaroensis* BOLLI, spiral view, UH-31, >150 µm fraction, *P. hantkeninoides* Zone.

Figure 5. *Abathomphalus mayaroensis* BOLLI, spiral view, UH-31, >150 µm fraction, *P. hantkeninoides* Zone.

Figure 6. *Abathomphalus mayaroensis* BOLLI, edge view, UH-31, >150 µm fraction, *P. hantkeninoides* Zone.

Figure 7. *Abathomphalus* aff. *intermedius* BOLLI, spiral view, UH-45, >150 µm fraction, *P. hantkeninoides* Zone.

Figure 8. *Abathomphalus intermedius* BOLLI, umbilical view, UH-39, >150 µm fraction, *P. hantkeninoides* Zone.

Figure 9. *Abathomphalus* aff. *intermedius* BOLLI, edge view, UH-47, >150 µm fraction, *P. hantkeninoides* Zone.

Plate 22

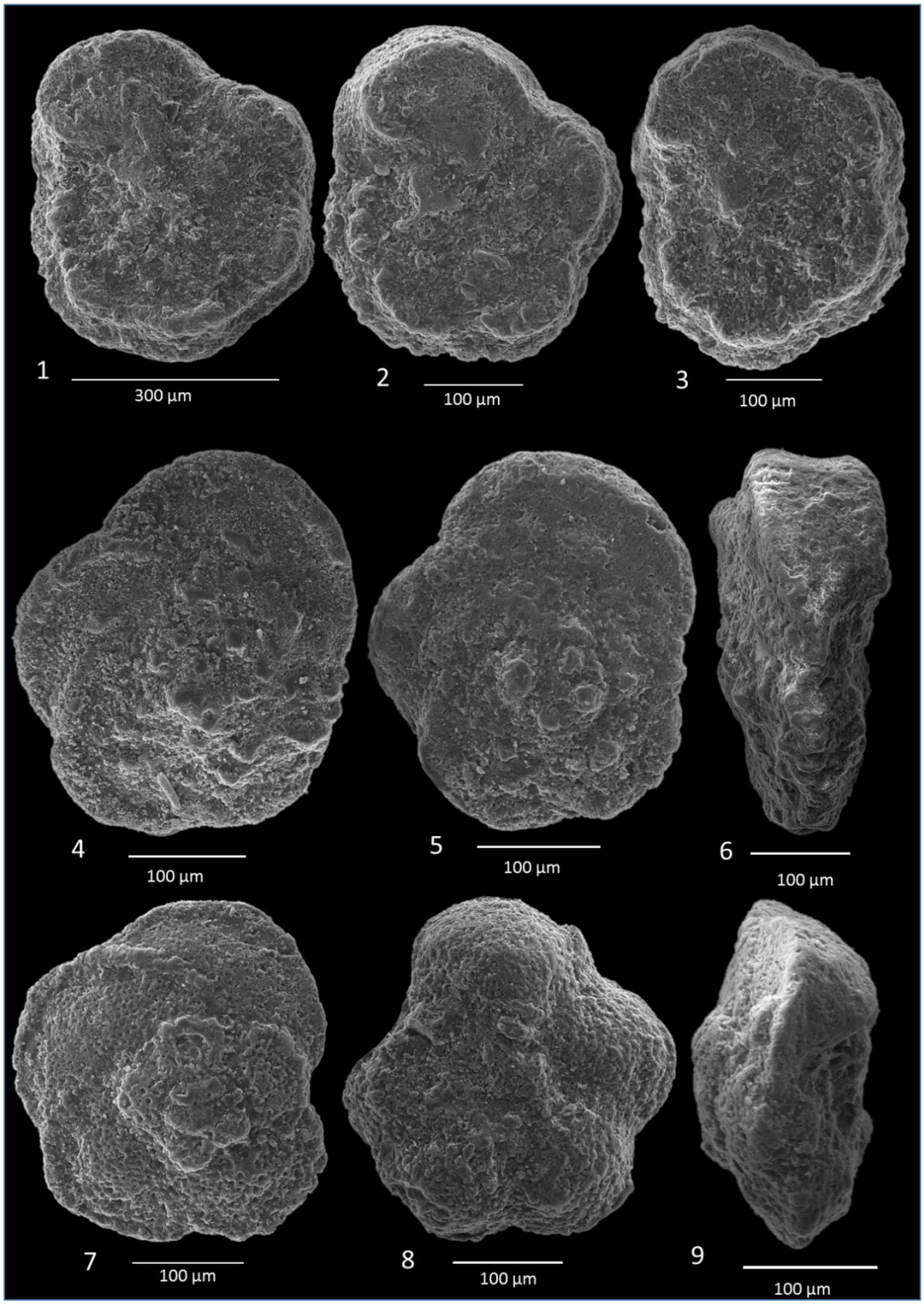
1
300 µm
2
100 µm
3
100 µm
4
100 µm
5
100 µm
6
100 µm
7
100 µm
8
100 µm
9
100 µm

Plate 23

Figure 1. *Globotruncanella petaloidea* GANDOLFI, spiral view, UH-45, >150 μm fraction, *P. hantkeninoides* Zone.

Figure 2. *Globotruncanella petaloidea* GANDOLFI, edge view, UH-45, >150 μm fraction, *P. hantkeninoides* Zone.

Figure 3. *Globotruncanella petaloidea* GANDOLFI, umbilical view, UH-45, >150 μm fraction, *P. hantkeninoides* Zone.

Figure 4. *Globotruncanella havanensis* VOORWIJK, spiral view, UH-37, >150 μm fraction, *P. hantkeninoides* Zone.

Figure 5. *Globotruncanella havanensis* VOORWIJK, edge view, UH-30, >150 μm fraction, *P. hantkeninoides* Zone.

Figure 6. *Globotruncanella havanensis* VOORWIJK, umbilical view, UH-31, >150 μm fraction, *P. hantkeninoides* Zone.

Figure 7. *Globotruncanella havanensis* VOORWIJK, spiral view, UH-31, >150 μm fraction, *P. hantkeninoides* Zone.

Figure 8. *Globotruncanella havanensis* VOORWIJK, umbilical view, UH-31, >150 μm fraction, *P. hantkeninoides* Zone.

Plate 23

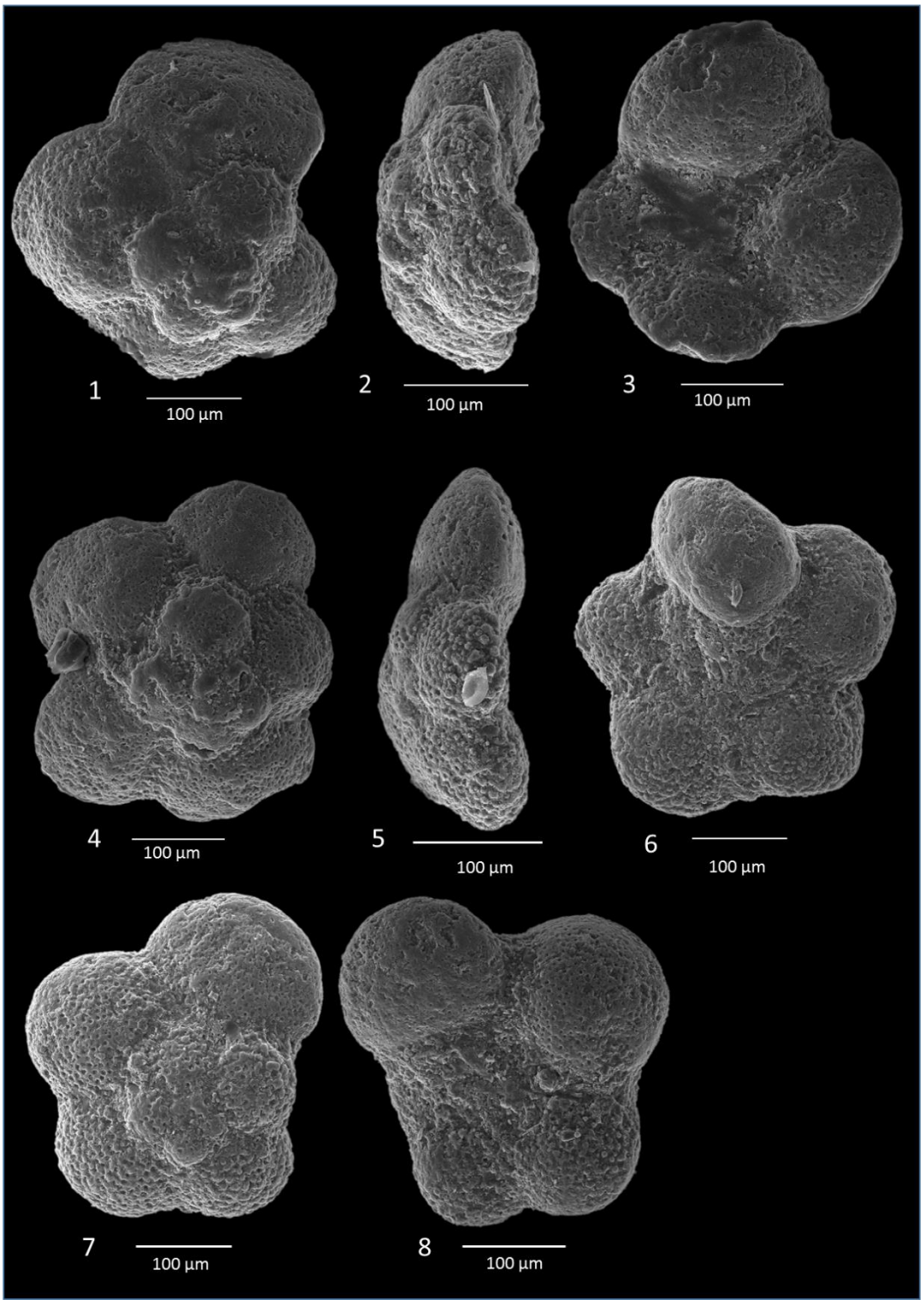

Plate 24

Figure 1. *Globotruncanella pschadae* KELLER, spiral view, UH-36, >150 μm fraction, *P. hantkeninoides* Zone.

Figure 2. *Globotruncanella pschadae* KELLER, edge view, UH-45, >150 μm fraction, *P. hantkeninoides* Zone.

Figure 3. *Globotruncanella pschadae* KELLER, spiral view, UH-38, >150 μm fraction, *P. hantkeninoides* Zone.

Figure 4. *Globotruncanella pschadae* KELLER, edge view, UH-35, >150 μm fraction, *P. hantkeninoides* Zone.

Figure 5. *Globotruncanella pschadae* KELLER, spiral view, UH-10, >150 μm fraction, *P. hantkeninoides* Zone.

Figure 6. *Globotruncanella* aff. *minuta* CARON and GONZALEZ DONOSO, spiral view, UH-47, >150 μm fraction, *P. hantkeninoides* Zone.

Figure 7. *Globotruncanella* aff. *minuta* CARON and GONZALEZ DONOSO, spiral view, UH-46, >150 μm fraction, *P. hantkeninoides* Zone.

Plate 24

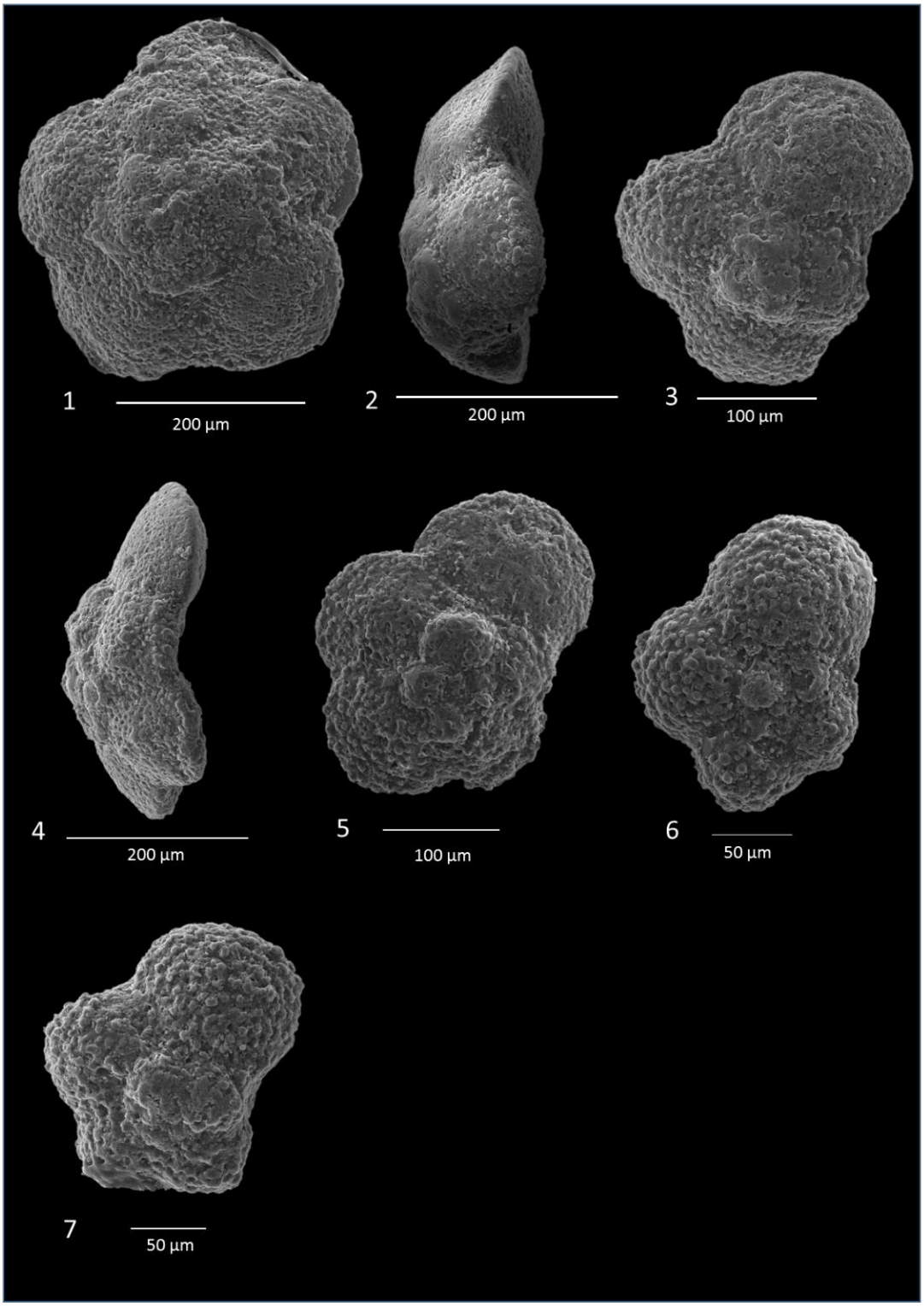

Plate 25

1. *Gansserina* aff. *gansseri* BOLLI, spiral view, UH-33, >150 µm fraction, *P. hantkeninoides* Zone.

2. *Gansserina* aff. *gansseri* BOLLI, umbilical view, UH-33, >150 µm fraction, *P. hantkeninoides* Zone.

3. *Gansserina* aff. *wiedenmayeri* GANDOLFI, umbilical view, UH-33, >150 µm fraction, *P. hantkeninoides* Zone.

4. *Gansserina* aff. *wiedenmayeri* GANDOLFI, edge view, UH-33, >150 µm fraction, *P. hantkeninoides* Zone.

Plate 25

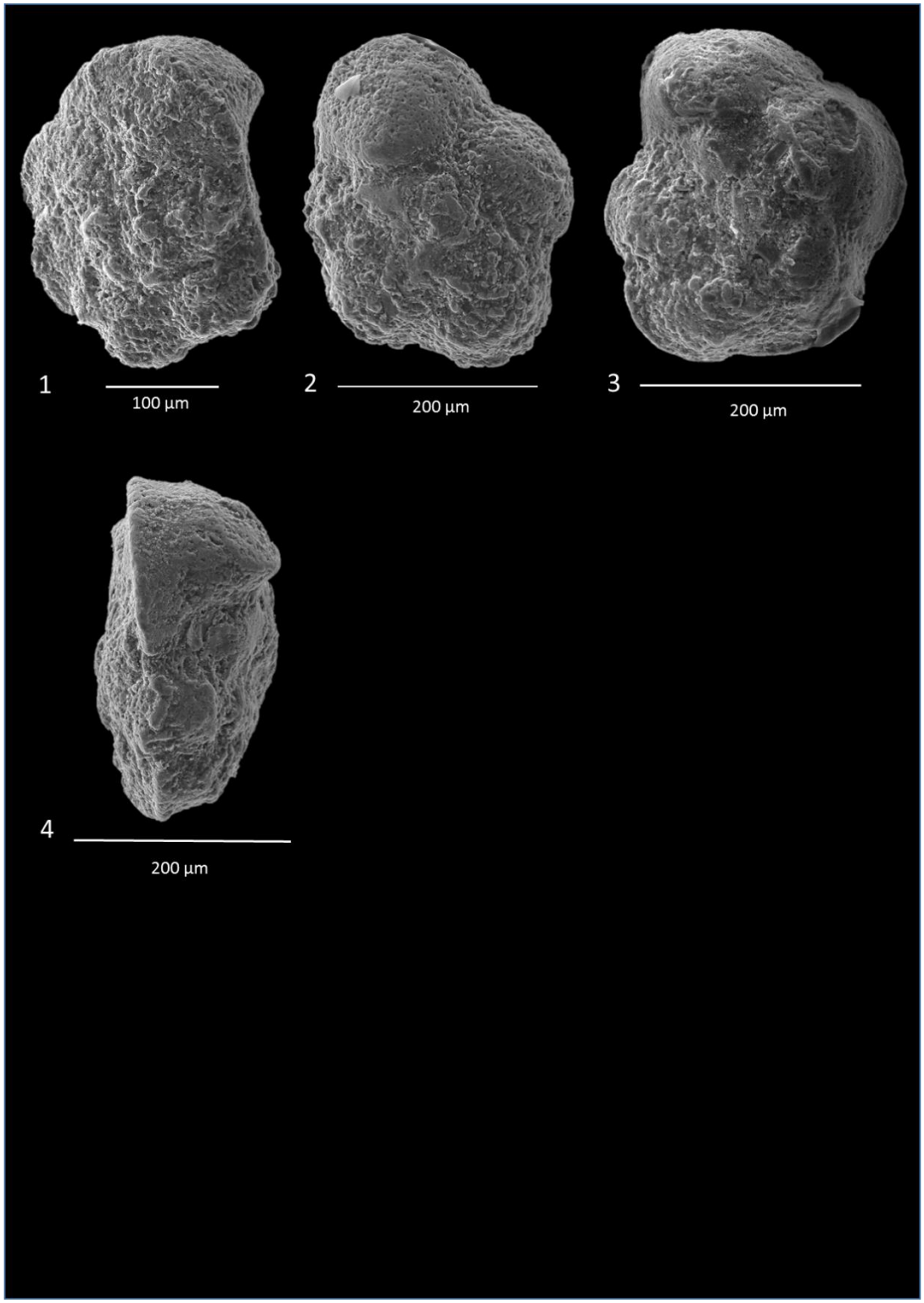

Plate 26

1. *Globotruncana aegyptiaca* NAKKADY, spiral view, UH-47, >150 μm fraction, *P. hantkeninoides* Zone.

2. *Globotruncana aegyptiaca* NAKKADY, spiral view, UH-38, >150 μm fraction, *P. hantkeninoides* Zone.

3. *Globotruncana aegyptiaca* NAKKADY, umbilical view, UH-46, >150 μm fraction, *P. hantkeninoides* Zone.

4. *Globotruncana aegyptiaca* NAKKADY, edge view, UH-31, >150 μm fraction, *P. hantkeninoides* Zone.

5. *Globotruncana aegyptiaca* NAKKADY, edge view, UH-45, >150 μm fraction, *P. hantkeninoides* Zone.

6. *Globotruncana arca* CUSHMAN, spiral view, UH-45, >150 μm fraction, *P. hantkeninoides* Zone.

7. *Globotruncana arca* CUSHMAN, spiral view, UH-32, >150 μm fraction, *P. hantkeninoides* Zone.

8. *Globotruncana arca* CUSHMAN, umbilical view, UH-45, >150 μm fraction, *P. hantkeninoides* Zone.

9. *Globotruncana arca* CUSHMAN, edge view, UH-31, >150 μm fraction, *P. hantkeninoides* Zone.

Plate 26

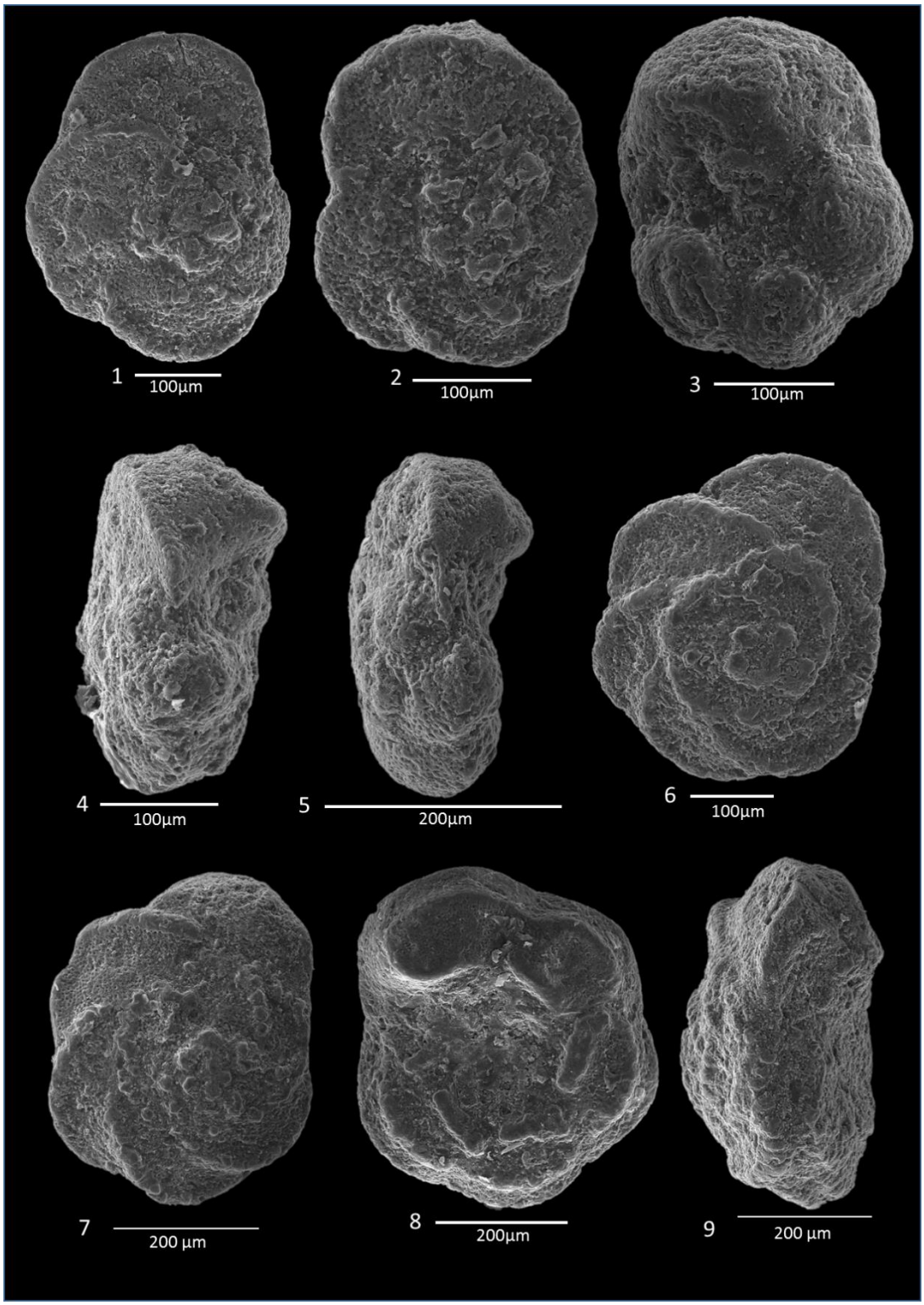
1
100µm
2
100µm
3
100µm
4
100µm
5
200µm
6
100µm
7
200 µm
8
200µm
9
200 µm

Plate 27

1. *Globotruncana dupeublei* CARON *et al*., edge view, UH-32, >150 μm fraction, *P. hantkeninoides* Zone.

2. *Globotruncana dupeublei* CARON *et al*., umbilical view, UH-31, >150 μm fraction, *P. hantkeninoides* Zone.

3. *Globotruncana dupeublei* CARON *et al*., spiral view, UH-33, >150 μm fraction, *P. hantkeninoides* Zone.

4. *Globotruncana esnehensis* NAKKADY, spiral view, UH-38, >150 μm fraction, *P. hantkeninoides* Zone.

5. *Globotruncana esnehensis* NAKKADY, spiral view, UH-45, >150 μm fraction, *P. hantkeninoides* Zone.

6. *Globotruncana esnehensis* NAKKADY, umbilical view, UH-41, >150 μm fraction, *P. hantkeninoides* Zone.

7. *Globotruncana esnehensis* NAKKADY, edge view, UH-38, >150 μm fraction, *P. hantkeninoides* Zone.

8. *Globotruncana falsostuarti* SIGAL, spiral view, UH-45, >150 μm fraction, *P. hantkeninoides* Zone.

9. *Globotruncana falsostuarti* SIGAL, edge view, UH-33, >150 μm fraction, *P. hantkeninoides* Zone.

Plate 27

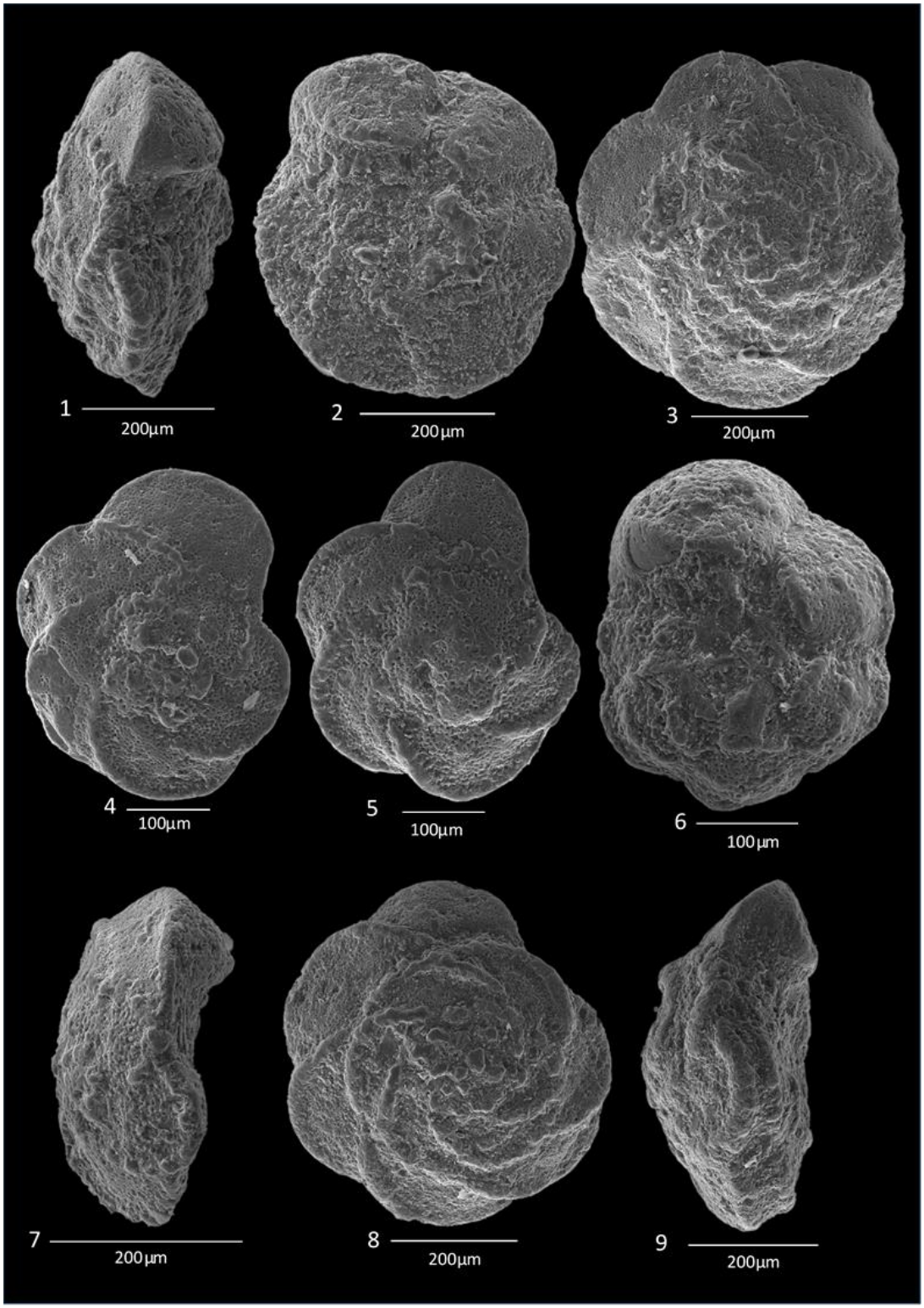
1
200µm
2
200µm
3
200µm
4
100µm
5
100µm
6
100µm
7
200µm
8
200µm
9
200µm

Plate 28

1. *Globotruncana hilli* PESSAGNO, spiral view, UH-3, >150 μm fraction, *P. hantkeninoides* Zone.

2. *Globotruncana hilli* PESSAGNO, edge view, UH-30, >150 μm fraction, *P. hantkeninoides* Zone.

3. *Globotruncana lapparenti* BROTZEN, spiral view, UH-33, >150 μm fraction, *P. hantkeninoides* Zone.

4. *Globotruncana mariei* BANNER and BLOW, spiral view, UH-33, >150 μm fraction, *P. hantkeninoides* Zone.

5. *Globotruncana mariei* BANNER and BLOW, spiral view, UH-45, >150 μm fraction, *P. hantkeninoides* Zone.

6. *Globotruncana mariei* BANNER and BLOW, edge view, UH-45, >150 μm fraction, *P. hantkeninoides* Zone.

7. *Globotruncana mariei* BANNER and BLOW, spiral to edge view, UH-45, >150 μm fraction, *P. hantkeninoides* Zone.

8. *Globotruncana mariei* BANNER and BLOW, umbilical view, UH-45, >150 μm fraction, *P. hantkeninoides* Zone.

Plate 28

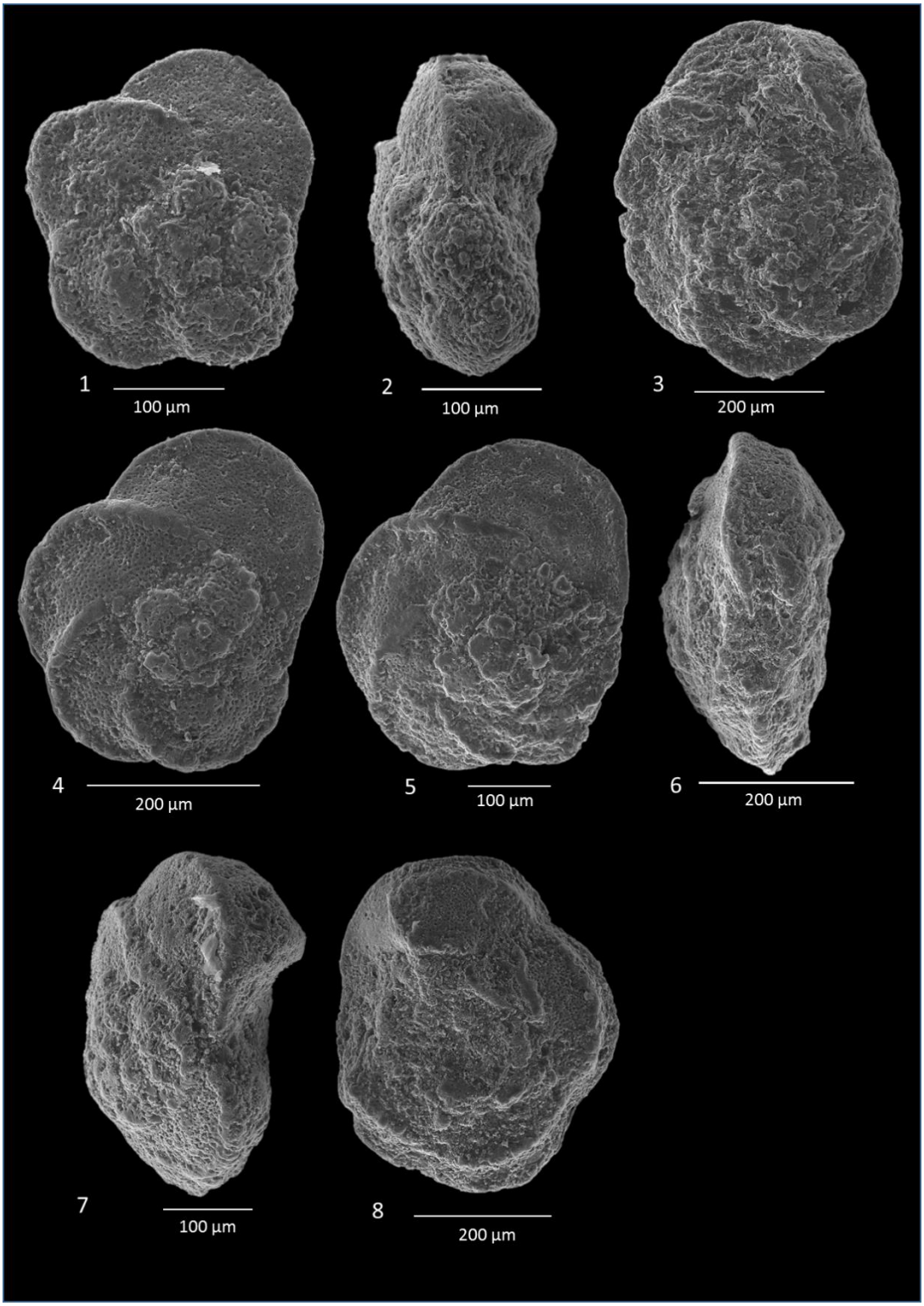

Plate 29

1. *Globotruncana orientalis* EL NAGGAR, spiral view, UH-40, >150 μm fraction, *P. hantkeninoides* Zone.

2. *Globotruncana orientalis* EL NAGGAR, umbilical view, UH-45, >150 μm fraction, *P. hantkeninoides* Zone.

3. *Globotruncana orientalis* EL NAGGAR, edge view, UH-45, >150 μm fraction, *P. hantkeninoides* Zone.

4. *Globotruncana rosetta* CARSEY, spiral view, UH-41, >150 μm fraction, *P. hantkeninoides* Zone.

5. *Globotruncana rosetta* CARSEY, spiral view, UH-48, >150 μm fraction, *P. hantkeninoides* Zone.

6. *Globotruncana rosetta* CARSEY, umbilical view, UH-47, >150 μm fraction, *P. hantkeninoides* Zone.

7. *Globotruncana ventricosa* WHITE, spiral view, UH-44, >150 μm fraction, *P. hantkeninoides* Zone.

8. *Globotruncana ventricosa* WHITE, edge view, UH-44, >150 μm fraction, *P. hantkeninoides* Zone.

9. *Globotruncana ventricosa* WHITE, umbilical view, UH-42, >150 μm fraction, *P. hantkeninoides* Zone.

Plate 29

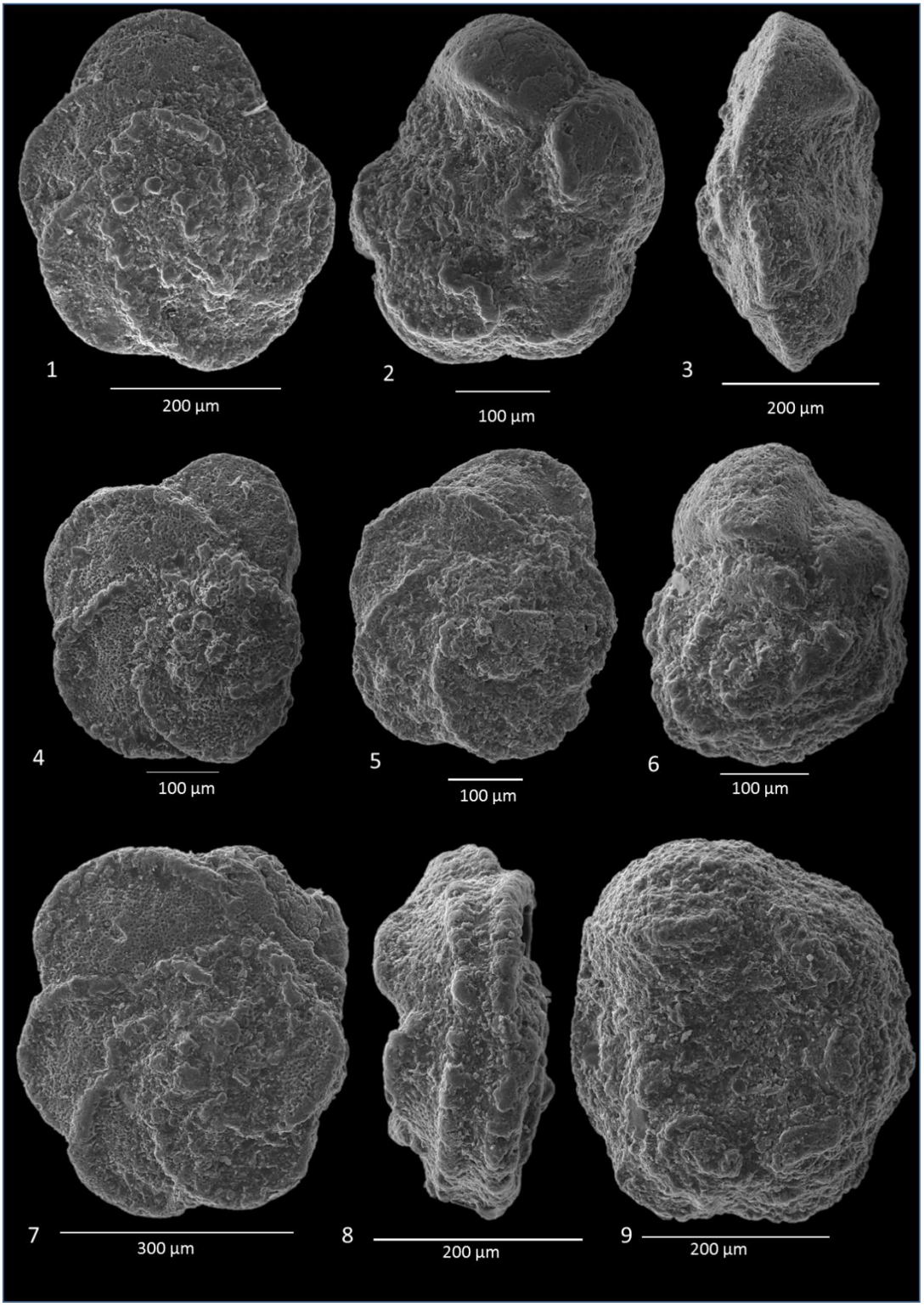
1
200 µm
2
100 µm
3
200 µm
4
100 µm
5
100 µm
6
100 µm
7
300 µm
8
200 µm
9
200 µm

Plate 30

1. *Globotruncanita angulata* TILEV, spiral view, UH-31, >150 μm fraction, *P. hantkeninoides* Zone.

2. *Globotruncanita angulata* TILEV, spiral view, UH-37, >150 μm fraction, *P. hantkeninoides* Zone.

3. *Globotruncanita* aff. *angulata* TILEV, edge view, UH-32, >150 μm fraction, *P. hantkeninoides* Zone.

4. *Globotruncanita conica* WHITE, spiral view, UH-45, >150 μm fraction, *P. hantkeninoides* Zone.

5. *Globotruncanita conica* WHITE, edge view, UH-32, >150 μm fraction, *P. hantkeninoides* Zone.

6. *Globotruncanita conica* WHITE, edge view, UH-47, >150 μm fraction, *P. hantkeninoides* Zone.

7. *Globotruncanita insignis* GANDOLFI, spiral view, UH-45, >150 μm fraction, *P. hantkeninoides* Zone.

8. *Globotruncanita insignis* GANDOLFI, edge view, UH-41, >150 μm fraction, *P. hantkeninoides* Zone.

9. *Globotruncanita insignis* GANDOLFI, umbilical view, UH-33, >150 μm fraction, *P. hantkeninoides* Zone.

Plate 30

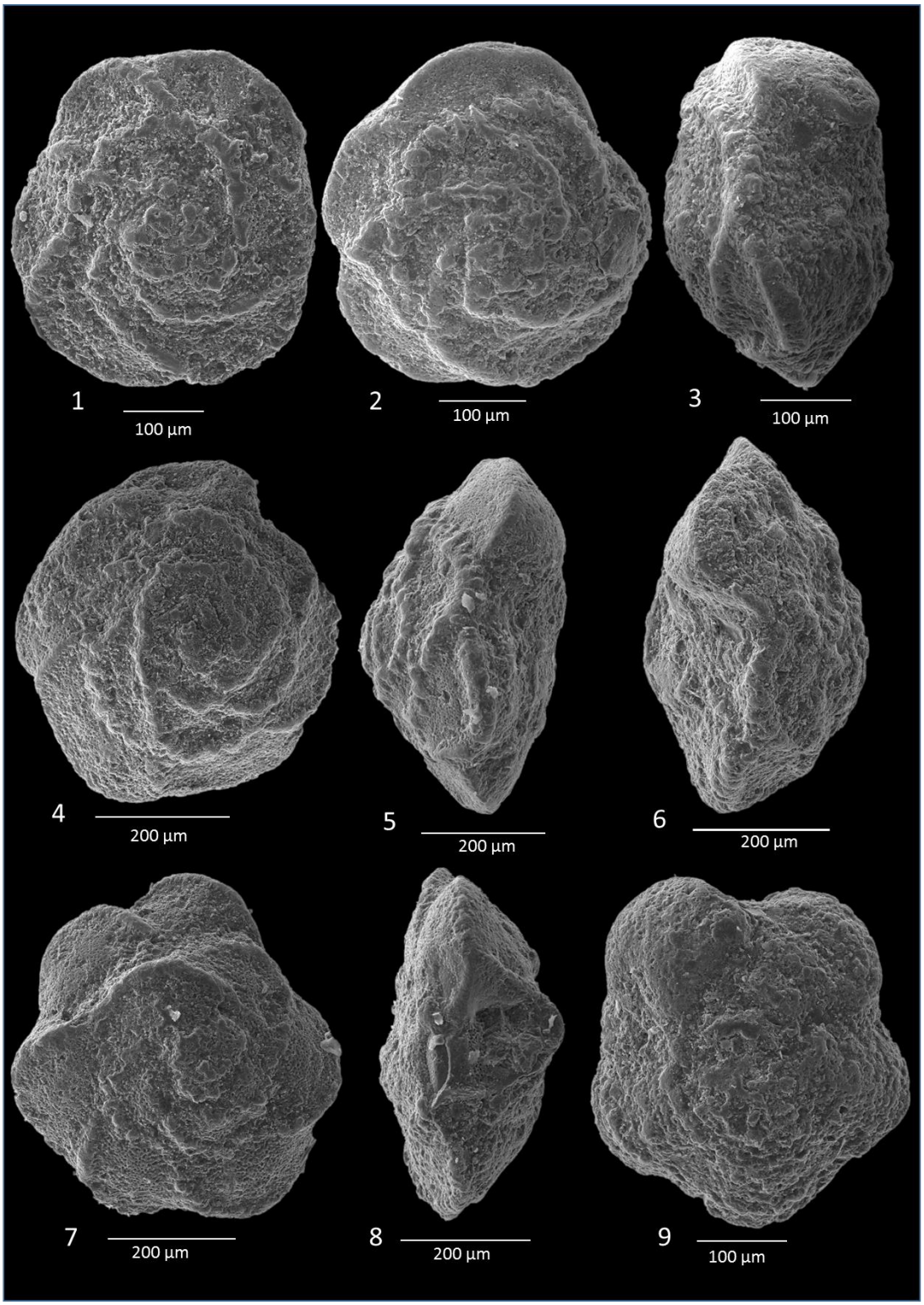
1
100 µm
2
100 µm
3
100 µm
4
200 µm
5
200 µm
6
200 µm
7
200 µm
8
200 µm
9
100 µm

Plate 31

1. *Globotruncanita pettersi* GANDOLFI, spiral view, UH-32, >150 μm fraction, *P. hantkeninoides* Zone.

2. *Globotruncanita pettersi* GANDOLFI, spiral to edge view, UH-46, >150 μm fraction, *P. hantkeninoides* Zone.

3. *Globotruncanita pettersi* GANDOLFI, edge view, UH-46, >150 μm fraction, *P. hantkeninoides* Zone.

4. *Globotruncanita stuarti* de LAPPARENT, spiral view, UH-40, >150 μm fraction, *P. hantkeninoides* Zone.

5. *Globotruncanita stuarti* de LAPPARENT, umbilical view, UH-45, >150 μm fraction, *P. hantkeninoides* Zone.

6. *Globotruncanita stuarti* de LAPPARENT, spiral view, UH-46, >150 μm fraction, *P. hantkeninoides* Zone.

7. *Globotruncanita stuartiformis* DALBIEZ, spiral view, UH-32, >150 μm fraction, *P. hantkeninoides* Zone.

8. *Globotruncanita stuartiformis* DALBIEZ, umbilical view, UH-32, >150 μm fraction, *P. hantkeninoides* Zone.

9. *Globotruncanita stuartiformis* DALBIEZ, spiral view, UH-47, >150 μm fraction, *P. hantkeninoides* Zone.

Plate 31

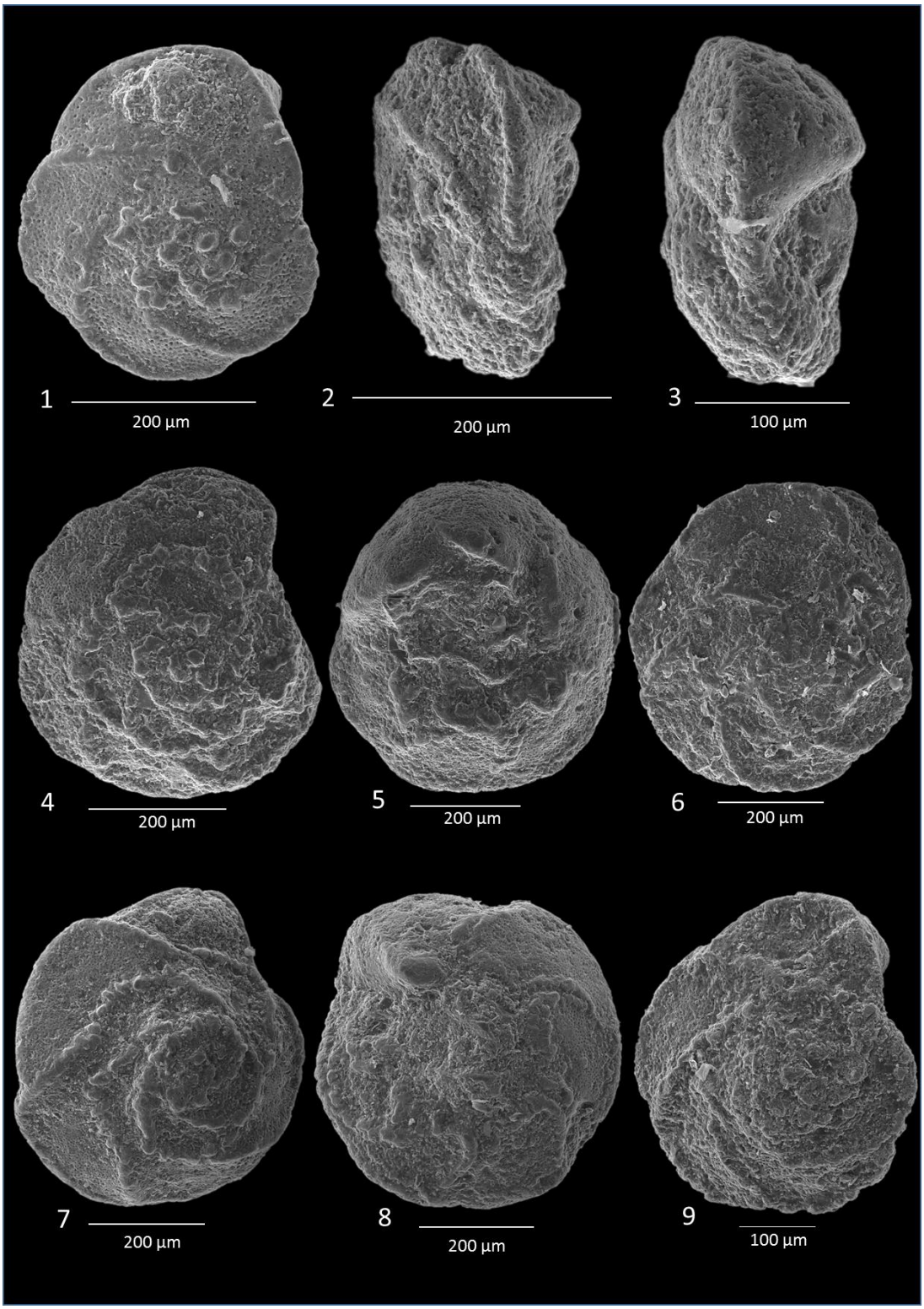
1
200 µm
2
200 µm
3
100 µm
4
200 µm
5
200 µm
6
200 µm
7
200 µm
8
200 µm
9
100 µm

Plate 32

1. *Contusotruncana contusa* CUSHMAN, spiral view, UH-30, >150 μm fraction, *P. hantkeninoides* Zone.

2. *Contusotruncana contusa* CUSHMAN, edge view, UH-49 >150 μm fraction, *P. hantkeninoides* Zone.

3. *Contusotruncana contusa* CUSHMAN, edge view, UH-37, >150 μm fraction, *P. hantkeninoides* Zone.

4. *Contusotruncana patelliformis* GANDOLFI, edge view, UH-37, >150 μm fraction, *P. hantkeninoides* Zone.

5. *Contusotruncana* aff. *plicata* WHITE, spiral view, UH-45, >150 μm fraction, *P. hantkeninoides* Zone.

6. *Contusotruncana walfischensis* TODD, edge view, UH-37, >150 μm fraction, *P. hantkeninoides* Zone.

Plate 32

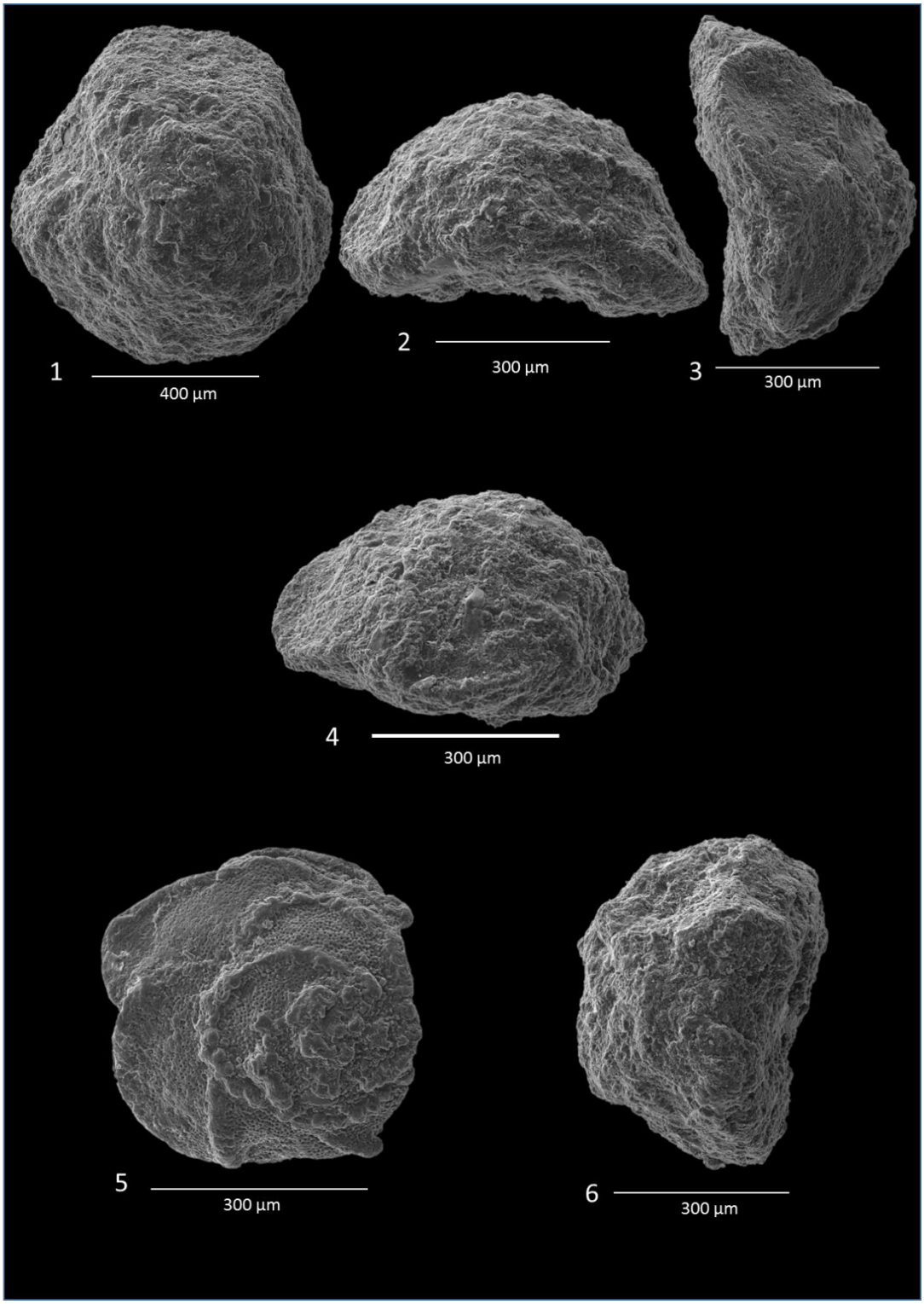

Plate 33

1. *Planoglobulina carseyae* PLUMMER, longitudinal section, UH-43, *P. hantkeninoides* Zone.

2. *Planoglobulina carseyae* PLUMMER, longitudinal section, UH-1, *P. hantkeninoides* Zone.

3. *Planoglobulina carseyae* PLUMMER, longitudinal section, UH-9, *P. hantkeninoides* Zone.

4. *Pseudotextularia intermedia* DE KLASZ, longitudinal section, UH-9, *P. hantkeninoides* Zone.

5. *Pseudotextularia intermedia* DE KLASZ, longitudinal section, UH-22, *P. hantkeninoides* Zone.

6. *Racemiguembelina powelli* SMITH and PESSAGNO, longitudinal section, UH-11, *P. hantkeninoides* Zone.

7. *Planoglobulina acervulinoides* EGGER, longitudinal section, UH-22, *P. hantkeninoides* Zone.

8. *Planoglobulina acervulinoides* EGGER, transverse section, UH-28, *P. hantkeninoides* Zone.

9. *Planoglobulina acervulinoides* EGGER, transverse section, UH-45, *P. hantkeninoides* Zone.

10. *Pseudotextularia intermedia* DE KLASZ, transverse section, UH-20, *P. hantkeninoides* Zone.

11. *Pseudotextularia* sp., transverse section, UH-24, *P. hantkeninoides* Zone.

12. *Pseudotextularia* sp., transverse section, UH-23, *P. hantkeninoides* Zone.

13. *Pseudotextularia elegans* RZEHAK, longitudinal section, UH-47, *P. hantkeninoides* Zone.

14. *Pseudotextularia elegans* RZEHAK, longitudinal section, UH-44, *P. hantkeninoides* Zone.

15. *Pseudotextularia nuttalli* VOORWIJK, longitudinal section, UH-47, *P. hantkeninoides* Zone.

16. *Pseudotextularia nuttalli* VOORWIJK, longitudinal section, UH-3, *P. hantkeninoides* Zone.

Plate 33

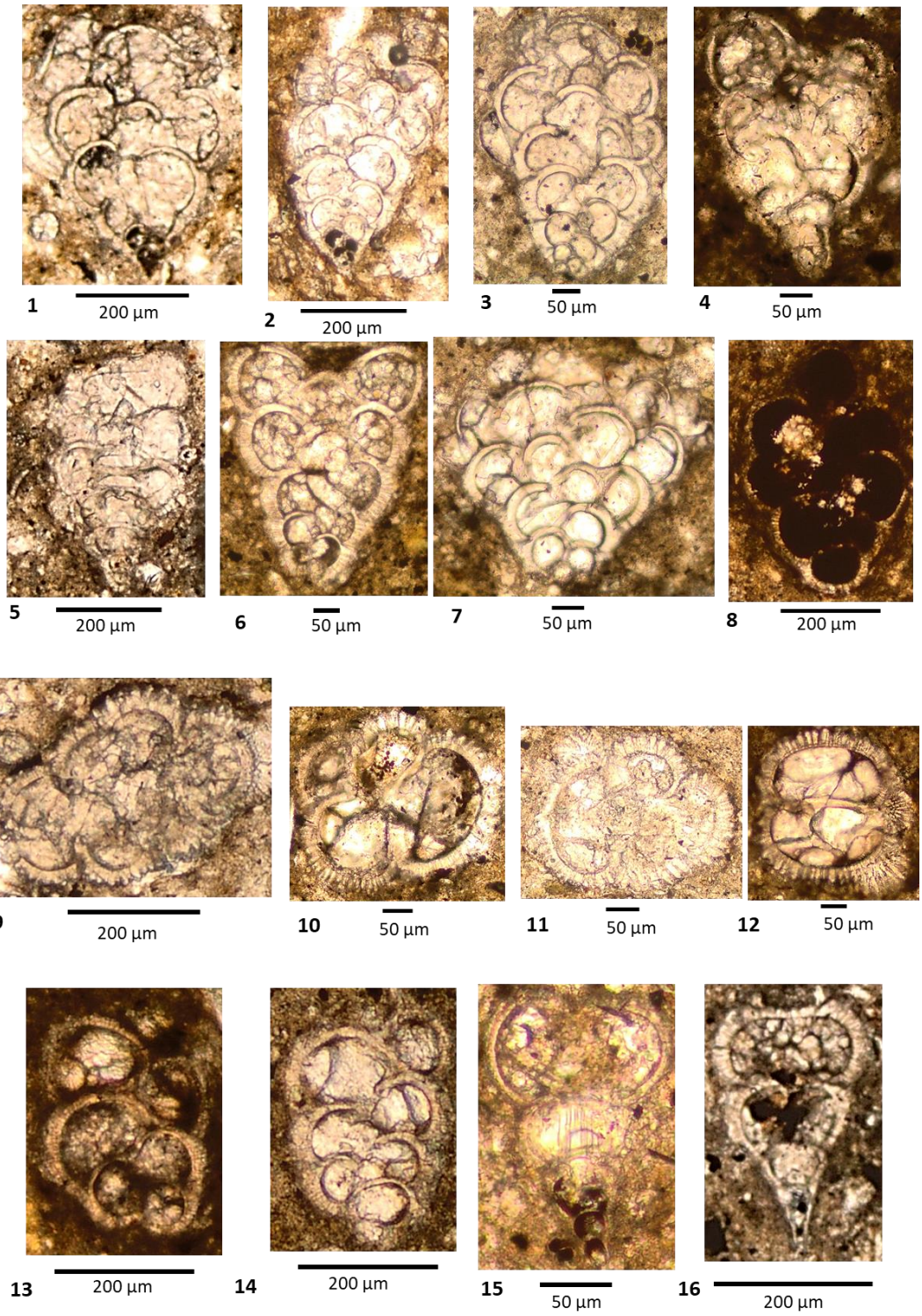
1
200 µm
2
200 µm
3
50 µm
4
50 µm
5
200 µm
6
50 µm
7
50 µm
8
200 µm
9
200 µm
10
50 µm
11
50 µm
12
50 µm
13
200 µm
14
200 µm
15
50 µm
16
200 µm

Plate 34

1. *Heterohelix globulosa* EHRENBERG, longitudinal section, UH-31, *P. hantkeninoides* Zone.

2. *Heterohelix globulosa* EHRENBERG, longitudinal section, UH-41, *P. hantkeninoides* Zone.

3. *Heterohelix globulosa* EHRENBERG, longitudinal section, UH-47, *P. hantkeninoides* Zone.

4. *Heterohelix globulosa* EHRENBERG, longitudinal section, UH-47, *P. hantkeninoides* Zone.

5. *Heterohelix* sp., longitudinal section, UH-38, *P. hantkeninoides* Zone.

6. *Heterohelix planata* CUSHMAN, longitudinal section, UH-41, *P. hantkeninoides* Zone.

7. *Heterohelix navarroensis* LOEBLICH, longitudinal section, UH-47, *P. hantkeninoides* Zone.

8. *Laeviheterohelix dentata* STENESTAD, longitudinal section, UH-32, *P. hantkeninoides* Zone.

9. *Heterohelix* sp., longitudinal section, UH-31, *P. hantkeninoides* Zone.

10. *Guembelitria cretacea* CUSHMAN, transverse section, UH-31, *P. hantkeninoides* Zone.

11. *Guembelitria cretacea* CUSHMAN, transverse section, UH-41, *P. hantkeninoides* Zone.

12. *Guembelitria cretacea* CUSHMAN, transverse section, UH-47, *P. hantkeninoides* Zone.

13. *Guembelitria cretacea* CUSHMAN, transverse section, UH-49, *P. hantkeninoides* Zone.

14. *Globigerinelloides asperum* EHRENBERG, axial section, UH-7, *P. hantkeninoides* Zone.

15. *Globigerinelloides asperum* EHRENBERG, equatorial section, UH-43, *P. hantkeninoides* Zone.

16. *Globigerinelloides asperum* EHRENBERG, equatorial section, UH-24, *P. hantkeninoides* Zone.

17. *Globigerinelloides asperum* EHRENBERG, equatorial section, UH-3, *P. hantkeninoides* Zone.

18. *Globigerinelloides asperum* EHRENBERG, axial section, UH-19, *P. hantkeninoides* Zone.

19. *Globigerinelloides asperum* EHRENBERG, axial section, UH-25, *P. hantkeninoides* Zone.

20. *Globigerinelloides subcarinatus* BRONNIMANN, axial section, UH-43, *P. hantkeninoides* Zone.

21. *Globigerinelloides subcarinatus* BRONNIMANN, axial section, UKHB-1, *P. hantkeninoides* Zone.

22. *Globigerinelloides alvarezi* ETERNOD OLVERA, equatorial section, UH-42, *P. hantkeninoides* Zone.

23. *Globotruncanella havanensis* VOORWIJK, axial section, UH-42, *P. hantkeninoides* Zone.

24. *Parvularugoglobigerina eugubina* LUTERBACHER and PREMOLI-SILVA, equatorial section, UKHB-4, *P. hantkeninoides* Zone.

Plate 34

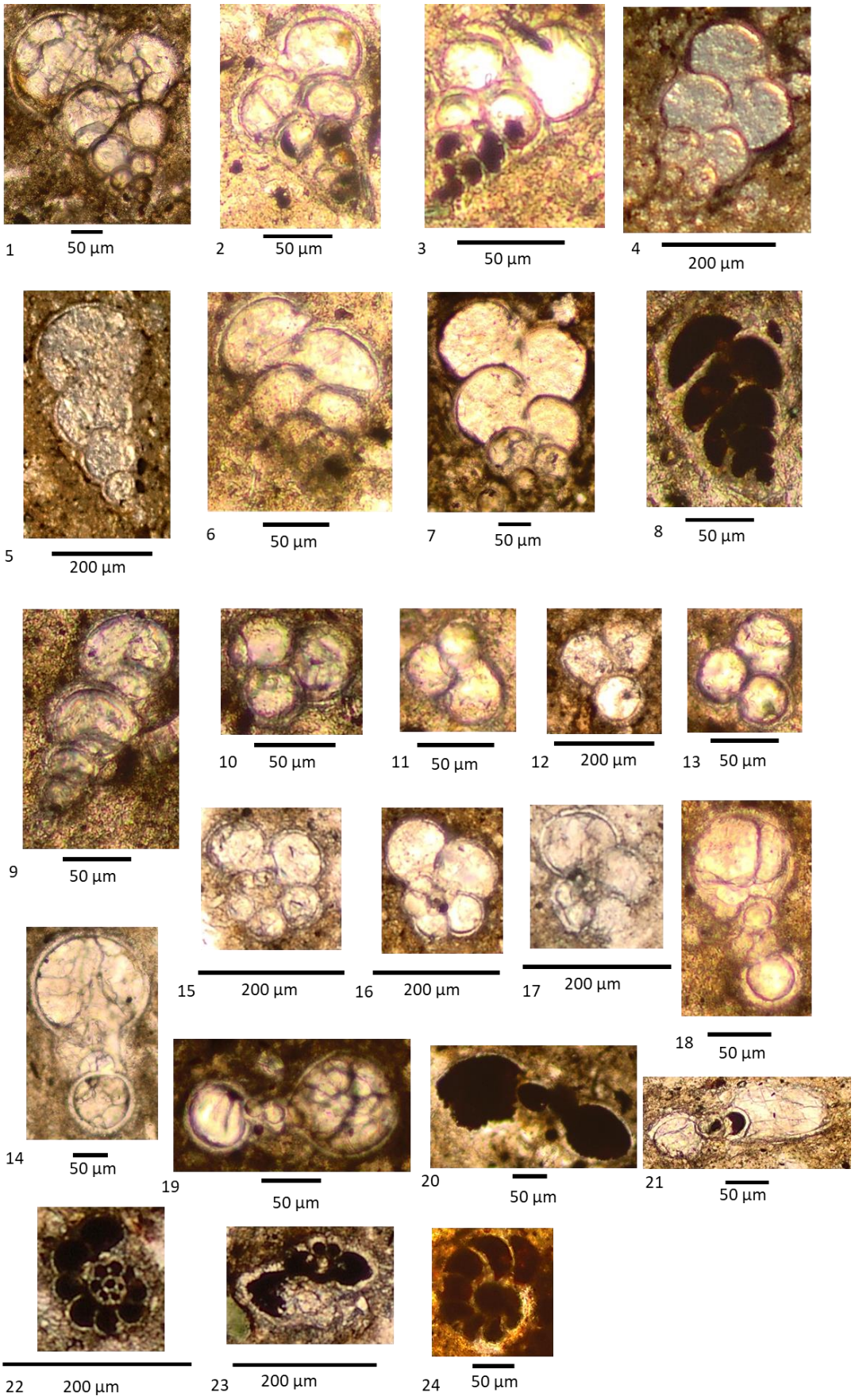
1 50 µm
2 50 µm
3 50 µm
4 200 µm
5 200 µm
6 50 µm
7 50 µm
8 50 µm
9 50 µm
10 50 µm
11 50 µm
12 200 µm
13 50 µm
14 50 µm
15 200 µm
16 200 µm
17 200 µm
18 50 µm
19 50 µm
20 50 µm
21 50 µm
22 200 µm
23 200 µm
24 50 µm

Plate 35

1. *Hedbergella monmouthensis* OLSSON, axial section, UH-11, *P. hantkeninoides* Zone.

2. *Hedbergella monmouthensis* OLSSON**,** axial section, UH-6, *P. hantkeninoides* Zone.

3. *Rugoglobigerina rugosa* PLUMMER, equatorial section, UH-44, *P. hantkeninoides* Zone.

4. *Rugoglobigerina rugosa* PLUMMER, axial section, UH-43, *P. hantkeninoides* Zone.

5. *Rugoglobigerina rugosa* PLUMMER, axial section, UH-11, *P. hantkeninoides* Zone.

6. *Rugoglobigerina macrocephala* PLUMMER, axial section, UH-16, *P. hantkeninoides* Zone.

7. *Rugoglobigerina macrocephala* BRONNIMANN, axial section, UH-16, *P. hantkeninoides* Zone.

8. *Rugoglobigerina macrocephala* BRONNIMANN, tangential section, UH-1, *P. hantkeninoides* Zone.

9. *Rugoglobigerina macrocephala* BRONNIMANN, tangential section, UH-17, *P. hantkeninoides* Zone.

10. *Rugoglobigerina* aff. *milamensis* SMITH and PESSAGNO, axial section, UH-49, *P. hantkeninoides* Zone.

11. *Rugoglobigerina milamensis* SMITH and PESSAGNO, axial section, UH-19, *P. hantkeninoides* Zone.

12. *Rugoglobigerina milamensis* SMITH and PESSAGNO, axial section, UH-3, *P. hantkeninoides* Zone.

Plate 35

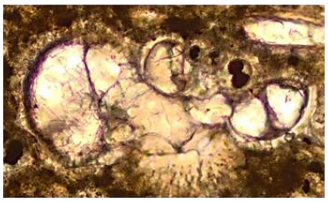

1 50 µm

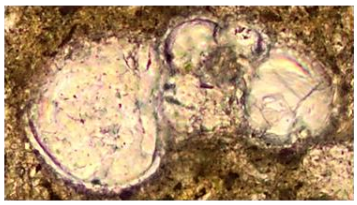

2 50 µm

3 50 µm

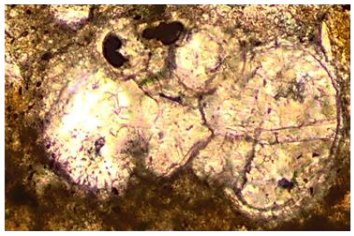

4 50 µm

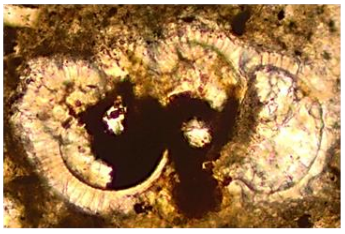

5 50 µm

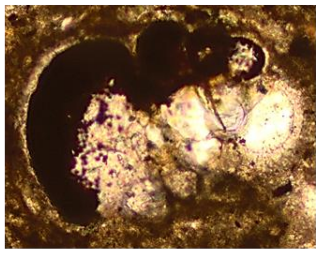

6 50 µm

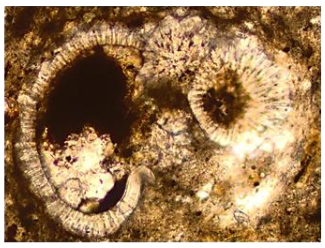

7 50 µm

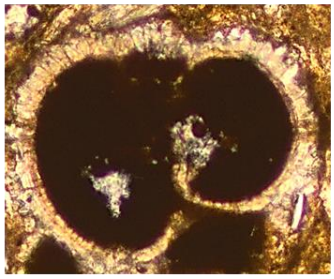

8 50 µm

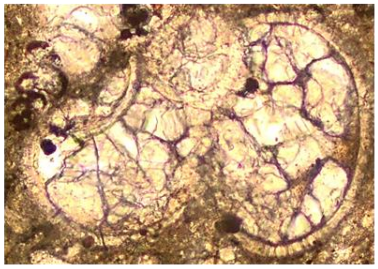

9 50 µm

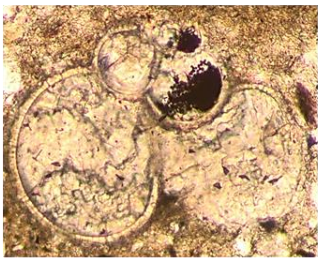

10 50 µm

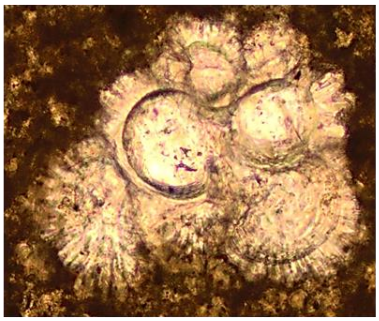

11 50 µm

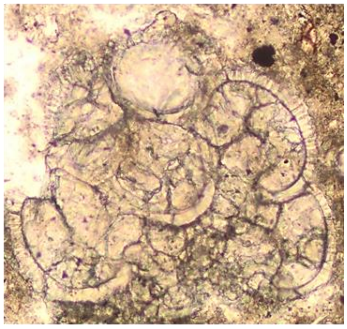

12 50 µm

Plate 36

1. *Gansserina gansseri* BOLLI, axial section, UH-8, *P. hantkeninoides* Zone.

2. *Globotruncana hilli* PESSAGNO, axial section, UH-6, *P. hantkeninoides* Zone.

3. *Globotruncana hilli* PESSAGNO, axial section, UH-22, *P. hantkeninoides* Zone.

4. *Globotruncana esnehensis* NAKKADY, tangential section, UH-17, *P. hantkeninoides* Zone.

5. *Globotruncana esnehensis* NAKKADY, axial section, UH-49, *P. hantkeninoides* Zone.

6. *Globotruncana orientalis* EL NAGGAR, axial section, UH-38, *P. hantkeninoides* Zone

7. *Globotruncana mariei* BANNER and BLOW, axial section, UH-30, *P. hantkeninoides* Zone.

8. *Globotruncana mariei* BANNER and BLOW, axial section, UH-25, *P. hantkeninoides* Zone.

9. *Globotruncana falsostuarti* SIGAL, axial section, UH-46, *P. hantkeninoides* Zone.

10. *Globotruncana arca* CUSHMAN, axial section, UH-18, *P. hantkeninoides* Zone.

11. *Globotruncana arca* CUSHMAN, axial section, UH-47, *P. hantkeninoides* Zone.

12. *Contusotruncana patelliformis* GANDOLFI, axial section, UKHB-1, *P. hantkeninoides* Zone.

13. *Contusotruncana walfischensis* TODD, axial section, UH-44, *P. hantkeninoides* Zone.

14. *Globotruncanita stuartiformis* DALBIEZ, axial section, UH-16, *P. hantkeninoides* Zone.

15. *Globotruncanita stuartiformis* DALBIEZ, axial section, UH-16, *P. hantkeninoides* Zone.

16. *Globotruncanita stuartiformis* DALBIEZ, axial section, UH-10, *P. hantkeninoides* Zone.

17. *Globotruncanita* sp., axial section, UH-3, *P. hantkeninoides* Zone.

18. *Globotruncanita insignis* GANDOLFI, axial section, UH-6, *P. hantkeninoides* Zone.

19. *Globotruncanita stuarti* de LAPPARENT, axial section, UH-43, *P. hantkeninoides* Zone.

20. *Globotruncanita stuarti* de LAPPARENT, axial section, UH-22, *P. hantkeninoides* Zone.

21. *Globotruncanita stuarti* de LAPPARENT, axial section, UH-28, *P. hantkeninoides* Zone.

22. *Globotruncanita stuarti* de LAPPARENT, axial section, UH-18, *P. hantkeninoides* Zone.

23. *Globotruncanita conica* WHITE, axial section, UH-21, *P. hantkeninoides* Zone.

Plate 36

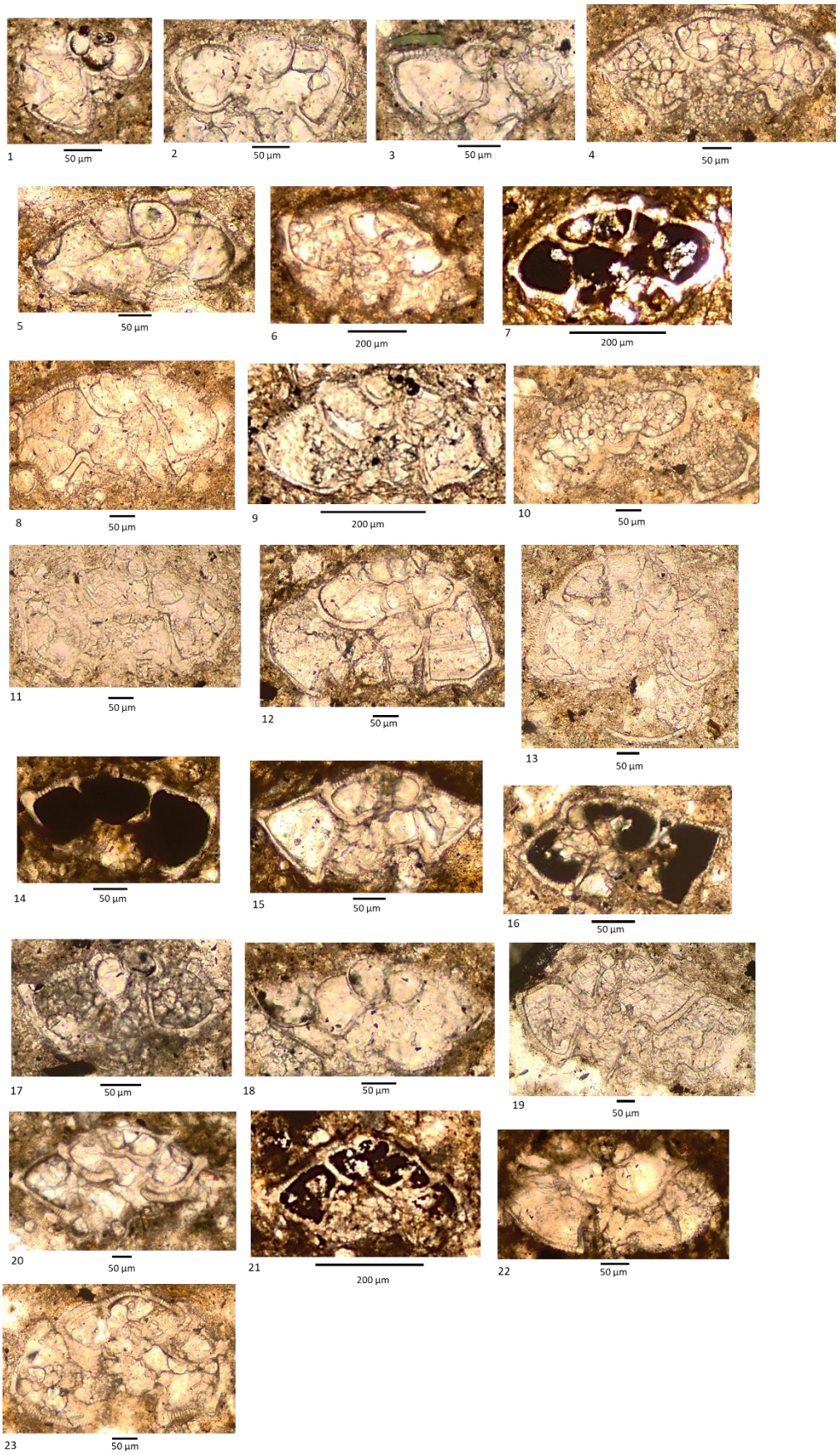
1
50 µm
2
50 µm
3
50 µm
4
50 µm
5
50 µm
6
200 µm
7
200 µm
8
50 µm
9
200 µm
10
50 µm
11
50 µm
12
50 µm
13
50 µm
14
50 µm
15
50 µm
16
50 µm
17
50 µm
18
50 µm
19
50 µm
20
50 µm
21
200 µm
22
50 µm
23
50 µm